University of Nottingham

UK | CHINA | MALAYSIA

Investigation of microplastics in the tilapia found in Lake Victoria, Kenya

Holly Nicholson BVMedSci (Hons)

Thesis submitted to the University of Nottingham for the degree of Master of Research

April 2021

Abstract

Fish play an important role in food and nutritional security around the world. Their consumption offers unique nutritional and health benefits and is considered a key element in a healthy diet. Increased attention is given to fish as a crucial source of protein and other essential nutrients. With a growing global population, the demand for fish is increasing with this increased demand mainly being met from the increased output of aquaculture products, and not from wild sources. Approximately 200 million people in Africa derive high-quality and low-cost proteins from fish. The fisheries and aquaculture sectors in Africa are increasingly contributing to food and nutrition security, foreign exchange and employment. The aquaculture industry on the continent is growing faster than any other part of the world, with countries such as Kenya realising the potential of this industry to provide a sustainable source of affordable protein. The fishery industry faces many challenges, including climate change, and the pollution of aquatic ecosystems. One pollutant of key concern are microplastics, which are causing an environmental crisis by polluting our aquatic environments and threatening the health of fish and humans. The aims of this study were to assess microplastic prevalence in tilapia fish, both wild and farmed, sourced from Lake Victoria, Kenya. The study investigated the prevalence of the five main microplastic types, fragment, foam, film, fibre and bead, by fluorescent light microscopy in both fish muscle and gastrointestinal tract (GIT). In addition, we investigated the presence of a plastisphere and conducted preliminary analyses into the composition of this community, by scanning electron microscopy and polymerase chain reaction.

This study found 48% of the tilapia muscle samples and 100% of the GIT samples analysed to be contaminated with microplastics. The study found variability in microplastic prevalence between the farmed and wild fish. The muscle of wild fish

had a greater prevalence than farmed fish, while the GIT of farmed fish had a greater prevalence than wild fish. Bacterial DNA was isolated from these microplastics and diatoms were also identified, potentially forming part of the plastisphere. Key elements were also identified often associated with the plastics. This study highlights the potential increased risk from ingestion of microplastics through the consumption of farmed (and wild) tilapia sourced from parts of Lake Victoria close to urbanisations and the mouths of key rivers draining into the lake. Further work is needed to identify the specific bacterial species present on the plastisphere and compare these between wild and farmed fish and between locations. This collective knowledge will inform the industry on the importance of monitoring microplastics in the lake and the life it supports as well as highlighting the importance of location for the siting of cages for fish farming. Further research into the potential effects these bacteria and chemicals adsorbed to the plastics may be having on fish and human health is essential.

Acknowledgements

The author would like to thank Professor Tracey Coffey and Dr Sharon Egan for their continuous support and guidance throughout this project. The author would also like extend additional gratitude to Ashley Chishiba and Morena Santi for their invaluable help in the laboratory and to Nicola Weston at the Nanoscale and Microscale Research Centre (nmRC) for her expertise and for analysing the samples on the scanning electron microscope. A special thank you as well to my family and close friends for all their continual encouragement and praise.

Table of contents

Abstract i

Acknowledgements ii

Table of contents iii

1.0 Introduction 1

1.1 Is there a need for sustainable food production? 1

1.2 Fish are a valuable food source 2

1.3 Fisheries industry 3

1.4 Capture fisheries 4

1.4.1 Capture fisheries in Africa 5

1.4.1.1 Future of capture fisheries in Africa 7

1.4.2 Capture fisheries in Kenya 7

1.5 Aquaculture 9

1.5.1 Aquaculture in Africa 10

1.5.2 Aquaculture in Kenya 11

1.5.2.1 Future of Kenyan aquaculture 13

1.6 Lake Victoria 13

1.6.1 Environmental issues facing Lake Victoria 15

1.6.2 Fish species of Lake Victoria 17

1.7 Tilapia in aquaculture 17

1.7.1 Impact of plastics on tilapia 19

1.8 Plastic as a material 20

1.8.1 Plastic additives 21

1.8.1.1 Plasticisers 21

1.8.1.2 Reinforcements 22

1.8.1.3 Fillers 22

1.8.1.4 Stabilizers 22

1.8.1.5 Colourants 23

1.8.2 Plastic as a pollutant 24

1.8.2.1 Plastic pollution in Africa 25

1.8.2.1.1 Plastic pollution in Kenya 26

1.8.2.2 Impact of COVID-19 on plastic pollution 26

1.8.3 Macroplastics 27

1.8.4 Microplastics 28

1.8.4.1 Fragment 30

1.8.4.2 Foam 30

1.8.4.3 Film 30

1.8.4.4 Fibre 31

1.8.4.5 Bead 31

1.8.5 Economic impacts of plastic waste 31

1.8.6 Environmental impacts of plastic pollution 33

1.8.7 Impact of plastic pollution on aquatic life 34

1.8.8 Human health 36

1.9 Persistent organic pollutants 37

1.10 The ‘plastisphere’ 38

1.10.1 Bacteria as a pollutant 40
1.11 Aims and objectives of this study 41
2.0 Methods and materials 43
2.1 Tilapia sampling from Lake Victoria 43
2.1.1 Tilapia sample preparation 47
2.2 Alkaline digestion of fish samples 50
2.2.1 GIT content samples digestion with KOH 51
2.2.2 Whole GIT samples digestion with KOH 51
2.2.3 Tissue samples digestion with KOH 51
2.3 Filtration of digested fish samples 52
2.4 Source of positive controls for plastics 52
2.4.1 Microbeads 52
2.4.2 Fishing Nets 53
2.5 Fluorescent staining 54
2.5.1 Nile red 54
2.5.2 DAPI 55
2.6 Fluorescent microscopic detection 56
2.6.1 Numbered filter paper areas 58
2.7 Extraction of genomic DNA 59
2.7.1 Assessment of the quality and quantity of DNA 59
2.8 Polymerase Chain Reactions 59
2.8.1 Primers for PCR 59
2.8.2 PCR with GoTaq master mix 62
2.8.3 Agarose gel electrophoresis 62
2.9 Cloning 62
2.9.1 Plasmid purification 63
2.9.2 Screening of positive clones using PCR 63
2.10 Scanning electron microscopy 63
2.10.1 Analysis of the SEM 63
2.10.2 Samples analysed by SEM 64
2.10.3 Analysis using the environmental SEM 67
3.0 Results 69
3.1 Analysis of positive controls for plastic 69
3.2 Detection of microplastics in fish muscle 71
3.2.1 Fibre in tilapia muscle 76
3.2.2 Fragment in tilapia muscle 78
3.2.3 Film in tilapia muscle 79
3.2.4 Bead in tilapia muscle 80
3.2.5 Foam in tilapia muscle 81
3.3 Comparison of microplastic presence in caged versus wild tilapia muscle 81
3.4 Detection of microplastics in fish gastrointestinal tract contents 83
3.4.1 Types of microplastic identified 83
3.5 Comparison of microplastic presence in caged versus wild tilapia gastrointestinal tract contents 86

3.6 Detection of microplastics in intact gastrointestinal tracts in fish.....87
3.6.1 Bead in tilapia intact gastrointestinal tract..... 88
3.6.2 Fragment in tilapia intact gastrointestinal tract 89
3.6.3 Film in tilapia intact gastrointestinal tract..... 90

3.7 Comparison of microplastic presence in caged versus wild tilapia intact gastrointestinal tracts 91

3.8 Site location comparison 92
3.8.1 Site location comparison in tilapia muscle 92
3.8.2 Site location comparison in tilapia gastrointestinal tract contents 95
3.8.3 Site location comparison in tilapia intact gastrointestinal tracts.....96

3.9 Comparison of microplastic presence in caged versus wild tilapia samples of muscle, gastrointestinal tract contents and intact gastrointestinal tracts...97
3.9.1 Comparison of microplastic type presence in tilapia muscle versus gastrointestinal tract contents versus intact gastrointestinal tracts..... 99
3.9.2 Comparison of microplastic type presence in caged versus wild tilapia samples of muscle, gastrointestinal tract contents and intact gastrointestinal tracts 100

3.10 Genomic DNA extraction 102

3.11 Polymerase chain reaction 105
3.11.1 Presence of bacterial DNA.....105
3.11.2 Streptococcus uberis.....111
3.11.3 Klebsiella pneumoniae.....111
3.11.4 Escherichia coli 112
3.11.5 Campylobacter coli and Campylobacter jejuni.....112
3.11.6 Lactobacillus 112
3.11.7 Summary of PCR results.....112

3.12 Cloning 115
3.12.1 Screening of colonies isolated 115

3.13 ESEM/EDX screening 117
3.13.1 Screening of control samples 117
3.13.1.1 Filter paper with no reagents 117
3.13.1.2 Filter paper with KOH.....120
3.13.1.3 Filter paper with Nile Red and DAPI stains 122
3.13.1.4 Macroplastic litter and microbeads.....124
3.13.1.5 Macroplastic litter without reagents 126
3.13.2 Screening of the macroplastic 129
3.13.2.1 Presence of diatoms on plastic litter.....129
3.13.3 Screening of the filtered muscle 132
3.13.3.1 Filtered muscle - Ta18 132
3.13.3.2 Filtered muscle – Ta33.....136
3.13.3.3 Filtered muscle – Ta44.....138
3.13.3.4 Filtered muscle – Ta48.....140
3.13.4 Screening of the filtered gastrointestinal tract contents.....143
3.13.4.1 Filtered gastrointestinal tract contents – GI5.....143
3.13.5 Screening of the unfiltered muscle 145
3.13.5.1 Unfiltered muscle – Ta20.....145
3.13.5.1.1 Spectrum 18 and 19 145
3.13.5.1.2 Spectrum 20 and 21 148
3.13.5.1.3 Spectrum 26, 27 and 28 151
3.13.5.1.4 Spectrum 35 154
3.13.5.2 Unfiltered muscle – Ta66.....156

3.13.5.2.1 Spectrum 107 and 108 156
3.13.5.2.2 Spectrum 118 159
3.13.5.3 Unfiltered muscle – Ta69 162
3.13.5.4 Unfiltered muscle – Ta72 164
3.13.5.4.1 Spectrum 100 164
3.13.5.4.2 Spectrum 103 and 104 166
3.13.5.4.3 Spectrum 105 and 106 168
3.13.5.5 Diatom in unfiltered muscle 171
3.13.6 Screening of the unfiltered intact gastrointestinal tract 172
3.13.6.1 Unfiltered intact gastrointestinal tract – GIT20 172
3.13.6.2 Diatoms in the unfiltered intact gastrointestinal tract 174

4.0 Discussion 177

4.1 The importance of tilapia 178
4.1.1 Choice of tissues used for analyses 179
4.1.2 A reproducible and cost-effective method to investigate microplastic presence 179
4.1.2.1 Visualising microplastics 180

4.2 The importance of having controls 181
4.2.1 Microbeads from facewash 181
4.2.2 Macroplastic litter from Lake Victoria 182
4.2.2.1 Diatoms found on macroplastic litter 183

4.3 Is microplastic prevalence greater in wild or farmed fish? 184
4.3.1 Fish muscle from wild fish contains greater numbers of microplastics 184
4.3.2 Is microplastic prevalence greater in the GIT from farmed tilapia? 185

4.4 Microplastics prevalence varies with geographical location 187
4.4.1 Kisumu 187
4.4.2 Northern Winam Gulf 188
4.4.3 Rivers 190
4.4.4 Entrance to the main lake body 190

4.5 Are the bacteria detected from the plastisphere? 191

4.6 Can the plastisphere be visualised? 192

4.7 Can SEM be used to screen for microplastic presence? 195
4.7.1 Microplastic misidentification 195
4.7.2 Determination of microfibre 196
4.7.3 Determination of microbead 197
4.7.4 Determination of fragment 198

4.8 Can microplastics act as a transport vector for harmful chemicals? 199
4.8.1 Barium presence 199
4.8.2 Titanium presence 200
4.8.3 Iron presence 200
4.8.4 Magnesium presence 201
4.8.5 Essential elements in tilapia 202

4.9 Microplastics toxicity risk to fish 203

4.10 Microplastics toxicity risk to humans 204

4.11 Disease level of fish in Lake Victoria 206

4.12 Importance of microplastic monitoring in aquatic systems 207

4.13 Limitations 208
4.14 Future work 209
4.15 Conclusion 210
5.0 References 213
6.0 Appendix 232

1.0 Introduction

1.1 Is there a need for sustainable food production?

The Food and Agriculture Organization (FAO) defines a sustainable food system as 'a food system that delivers food security and nutrition for all in such a way that the economic, social and environmental bases to generate food security and nutrition for future generations are not compromised' (FAO, 2018a). This means that it is must be profitable throughout, and have many broad-based benefits for society, as well as having a positive or neutral impact on the environment (Figure 1.1) (FAO, 2018a).

Food systems are critically considered in the context of rapid population growth, in addition to changing consumption patterns, climate change and the decline in natural resources. Globally, many of these pressures are increasingly impacting societies, with greater demand for all livestock products in order to meet demands from ever growing populations. This is especially apparent in the fishing industry sector. The FAO estimates that 85% of fish stocks are either fully exploited or over fished (WWF, 2020). With over 3 billion people relying on wild-caught and farmed fish as their primary source of protein (WWF, 2020), adaption to this food system is necessary, otherwise we could see a meagre outlook for the availability of nutritional fish to future generations.

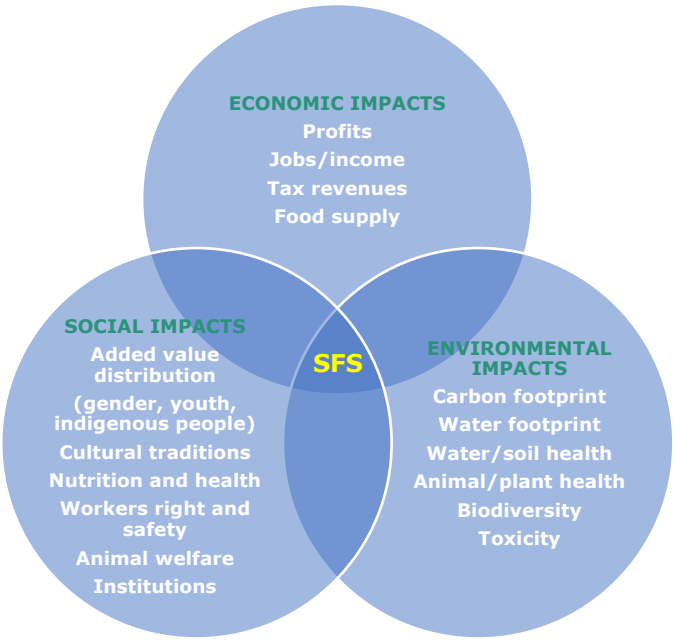

Figure 1.1 Sustainability in food systems. This Venn diagram demonstrates the importance of how the social, economic and environmental impacts must all be appreciated in order to maintain a sustainable food system (SFS). A food system cannot be considered sustainable if any of these components are lacking.

1.2 Fish are a valuable food source

Consumption of fish and their products has high nutritional and health benefits. Fish are rich in essential fatty acids and proteins, vitamins and minerals such as taurine (Lusher, Hollman, et al., 2017). They are particularly important in many low-income populations, or rural areas, as an ideal supplement to nutritionally deficient cereal-based diets. Fish provides more than 1.5 million people, mostly in low and middle income countries (LMICs) with almost 20% of their average intake of animal protein per capita (FAO, 2020a). Today fish remains one of the most traded food commodities worldwide, worth $167 billion (Shahbandeh, 2020).

1.3 Fisheries industry

In 2016, global fish production peaked at around 171 million tonnes (FAO, 2018b). Capture fishing of wild fish stock accounted for 91 million tonnes of this, with aquaculture or fish farming provided 80 million tonnes (Figure 1.2). 151 million tonnes (88%) of the fish produced in both sectors was for direct human consumption (Fisherproject, 2020). Fish consumption has continually increased from the 1960s, and between 1961 and 2016 the annual average of fish consumption (3.2%) globally outpaced population growth (1.6%) and exceeded that of meat (2.8%) (FAO, 2018b). In Africa, the increase has been two-fold, from 4.8kg/capita in 1961 to 9.9kg/capita in 2016 (FAO, 2021). Moreover, there are contrasting amounts consumed within geographical areas. This is significant in the most populated countries of Africa, where per capita fish consumption reached 22.1kg in Egypt, 13.3kg in Nigeria and 0.25kg in Ethiopia in 2013 (Lusher, Hollman, et al., 2017).

Capture fisheries clearly provide a major role in the supply of fish for human consumption. However, their current production is so close to the maximum ecosystem productivity, that they cannot be further increased substantially in the future and could decline if mismanaged (Garcia and Rosenberg, 2010), leaving the world to solve a significant food deficit.

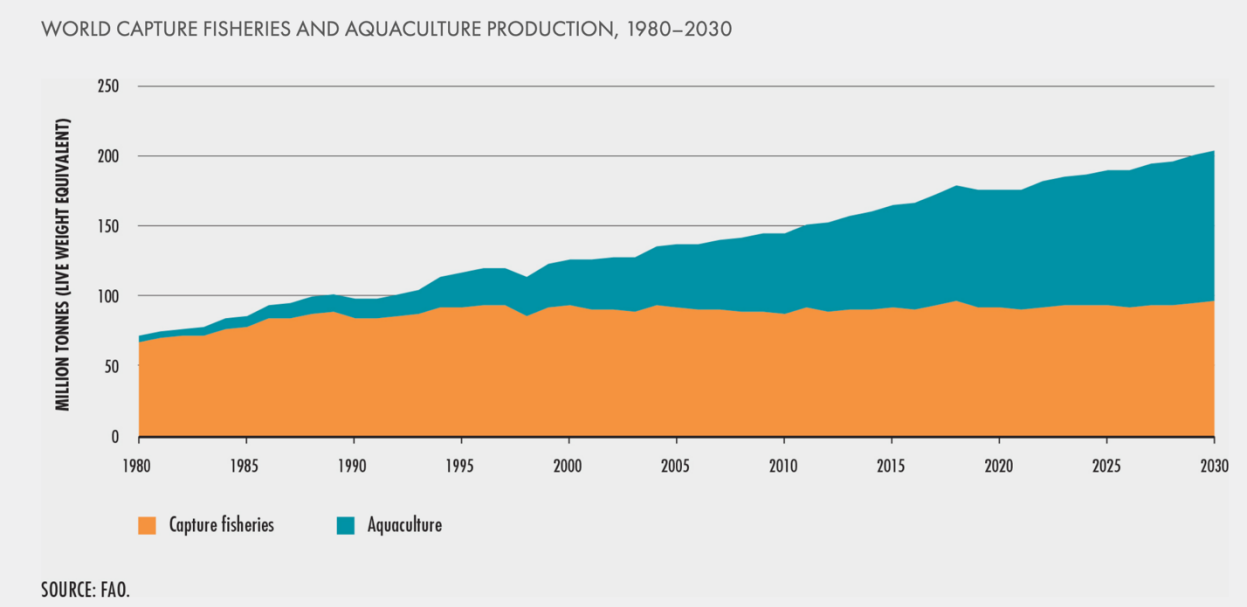

Figure 1.2 Capture fisheries vs aquaculture. Aquaculture has continued to grow since the 1980s, while capture production has increased steadily, but has levelled off in the last 20 years. These trends are set to continue over the next decade (FAO, 2020b).

1.4 Capture fisheries

Wild or capture fisheries refer to harvesting of naturally occurring resources from both marine and freshwater environments. They can be classified as industrial, small-scale and recreational (Garcia and Rosenberg, 2010), with lakes, reservoirs and wetlands providing an ideal rich environment for inland capture fisheries (Welcomme and Lymer, 2012).

World production from inland capture fisheries has grown steadily, in 2016 global capture fisheries production reached 91 million tonnes, with marine capture providing 87.2% of this and aquatic inland waters providing 12.8% of the global total (FAO, 2018b). There has been an 10.5% increase in global catch from inland freshwater since 2005, but this information can be misleading as increases can be from improved data collection at each country level, rather than increased catch volume (FAO, 2018b). Generally, capture fisheries are not increasing at the same

vast rate as aquaculture. Aquaculture production is set for long-term growth, while capture fisheries can expect a moderate recovery at best. This decrease in wild caught fish is the consequence of declining fish stocks from over fishing, along with the introduction of more restrictive fishing policies, which are aiming to ensure sustainable exploitation of fisheries in the future (OECD, 2017). Despite this, 40.3 million farmers were involved in capture fishing in 2016, compared to 19.3 million farmers in aquaculture (FAO, 2018b), with capture fisheries providing millions globally with a source of livelihood and income.

Sixteen countries, mostly in Asia, are accountable for the production of almost 80% of the global inland fishery catch, where they provide an essential food source for many local communities. Additionally, inland catches are an important food source for many African countries, with their inland catches accounting for 25% of global inland catches. (FAO, 2018b).

1.4.1 Capture fisheries in Africa

In 2015, almost 95% of the global catch from inland fisheries was from developing countries (Bartley et al., 2015). A developing country or LMICs is one with less developed industries and a low Human Development Index (HDI) relative to other countries (O'Sullivan and Sheffrin, 2003). Their capture fishery sector is composed of mainly small-scale fishers that depend on the industry for their livelihoods.

In Africa, fish consumption levels remain predominantly low, with a mean of 9.9kg per capita in 2016, and can be as low as 5kg in eastern Africa (FAO, 2018b). This low level of fish consumption is the consequence of the population increasing faster than fish as a food supply. There have been limitations in the expansion of fish production, mainly from the pressure put on capture fisheries resources. Nevertheless, low income levels in these African countries, as well as inadequate

processing infrastructure and storage for the fish and a lack of marketing and distribution channels, have provoked Africa's inability to commercialise these fish products to the wider world, rather than just the local communities where they are caught.

While the rest of the world is seeing a steady level off in capture production, African inland capture fisheries are rising at about 3.7% per year (Welcomme and Lymer, 2012). A variety of fishing gear is used in both small-scale and industrial fisheries. Capture fishery gear usually includes trawl nets (Figure 1.3), surrounding nets, seine nets, lift nets, dredges and hook and lines (GESAMP, 2016), with nets made from plastics, including polypropylene (PP), polyethylene (PE), polyamide (PA), polystyrene (PS), polyvinyl chloride (PVC) and nylon.

Figure 1.3 Capture fishing in Lake Victoria. Fishermen capture fishing near the Ugandan side of Lake Victoria. They have used a plastic trawl net pulled by a boat across the Lake to catch these fish (Michael, 2015).

1.4.1.1 Future of capture fisheries in Africa

The highest growth rates and largest increase in volume produced in capture fisheries are expected in Africa, with Asia being the only continent expecting a decline (OECD, 2020).

Capture fisheries are predicted to see a moderate increase over the next decade, markedly from expectations that improved managements in some regions will continue to pay off, allowing a sustainable increased production of fish stocks. By 2029, it is estimated that 90% of the fish produced will be used for human consumption. Per capita fish consumption is expected to rise in all continents except Africa. (OECD, 2020). This decline is resulting from their population increasing more than their current supply can provide, raising probable nutritional concerns in this area.

1.4.2 Capture fisheries in Kenya

Inland capture fisheries play a significant role in Kenya's economy. The sector has grown rapidly, with fish exports supplying ample income from foreign exchange (Ardjosoediro and Neven, 2008). Today Kenya is responsible for 5.05% of the total capture fishery exports from Africa, catching 124,317 tonnes yearly from their inland waters (Welcomme and Lymer, 2012). There is however widespread opinion that much of the catch from inland fisheries is unrecorded, this is due to the small scale of some individual fisheries, where most of the catch will go directly into domestic local consumption.

Kenya has a total inland water area of 18,029 km^2 (FAO, 2015), with the main water bodies situated in the Rift Valley and Lake Victoria. Freshwater fish landings have always been higher than marine in Kenya, with Lake Victoria mainly accountable for this, supplying around 90% of the fish in the country (FAO, 2015).

Typically, fishermen will use drift nets left overnight, and some will catch fish with baited long lines.

Capture fish levels rose from 1950 until 2001, from the introduction of the Nile perch *(Lates niloticus)*, which was introduced to feed on smaller fish in the lake, thus converting them into a larger fish, reaching higher commercial value (Ogutu-Ohwayo, 1990). However, with the generation of more efficient nets and expansion on processing technologies, the demand pressures on fisheries increased. Since 2001, inland capture fisheries levels have declined (Welcomme and Lymer, 2012), despite the introduction of the Nile tilapia (*Oreochromis niloticus*). The main issues Kenyan capture fisheries have faced are the overexploitation that occurred in Lake Victoria from overfishing (FAO, 2015), environmental degradation and the increased fishing pressures resulting in the introduction of exotic species, which have changed the lake's biodiversity and threatened the sustenance of the lake, on which millions depend on for their livelihoods (Njiru et al., 2008). This has been especially prominent in countries such as Kenya, where a lack of resources and knowledge have led to a failure in adequately incorporating inland fisheries interests into administrative structures (Welcomme and Lymer, 2012).

The numerous threats posed to aquatic ecosystems from human activities has left capture fisheries with a sense of hopelessness for the future. This has led to their neglect as a sector, and priorities have been switched to other sectors. As a result aquaculture has been promoted as the solution to sustain and save catches, against an inevitable continued decline in freshwater fish stocks (FAO, 2018b).

1.5 Aquaculture

Aquaculture is the controlled process of breeding, raising and harvesting fish, shellfish and aquatic plants both marine and freshwater (US Department of Commerce, 2020). As the world's fastest growing food production sector (FAO, 2020), it now produces 82.1 million tonnes globally every year. An increase of 153.4% since 2000 to 2018 (McCarthy, 2020). It also provides huge human benefits, as it employs 26 million workers (FAO, 2020), and provides those in the poorest of countries with access to essential nutrients from fish.

A recent report from the FAO states that a sustainable aquaculture strategy requires 'farmers to earn a fair reward from farming, ensure benefits and costs are shared equitably, promote wealth and job creation, make sure enough food is accessible to all, manage the environment for the benefit of future generations and ensure aquaculture development is orderly, with both authorities and industry well organised' (FAO, 2015).

However, aquaculture is becoming a serious contributor to pollution including of aquatic plastic debris. Unlike ocean plastics, which can get caught up in currents and circulate around the world, plastic accumulating in lakes has nowhere to go (Cosier, 2018). Aquaculture extensively uses plastic for both equipment and packaging, everything from polystyrene foam-filled fish cage collars, to plastic feed sacks and harvest bins (Holmyard, 2019). This in combination with ghost gear (lost or discarded fishing gear) (ASC, 2018), and the likely further advancement of aquaculture production, will only continue to drive the increasing abundance of aquatic plastic debris.

Given that aquaculture already supplies nearly half of the world's fish for human consumption, the industry will inevitably continue to increase over forthcoming decades to meet demand from the rise in the global population (Calich, 2014).

Together with diminishing levels of wild marine and aquatic fish (Holmyard, 2019), there is an increasing need for considerations of the environmental impact of this growing industry. This is essential in order to ensure practices are sustainable for the future of aquaculture.

The ideal warm climate in many LMICs gives them the potential to further increase their aquaculture production, both to support local economy and the food chain but also as a potential export product (Konikoff, 2017). As a result, many LMICs are now global leaders in the exportation of these products, with 76% of the top 10 global exporters being from developing countries (FAO, 2020). African countries, such as Kenya, are examples of LMICs. In Africa the population has increased from 1,182 million people in 2015 to 1,341 million in 2020 and is set to increase exponentially over the forthcoming decades. With increasing populations comes dietary changes, and from 1999 to 2013 the share of animal protein in total protein increased from 21.1% to 23.2%, with fish share of this total protein increasing from 3.8% to 4.5% (FAO, 2020c). Africa has a strong desire to continue to be fish exporters, while providing a cheap and sustainable source of animal protein to a growing population.

1.5.1 Aquaculture in Africa

Aquaculture was first introduced five decades ago to the African continent as an innovation to improve nutritional and economic benefit of its producers, with 5% of its population fully dependent on the sector for their livelihoods (FAO, 2021). Fish in Africa is extremely important, providing the population with 17.4% of their total animal protein intake. It is one of the cheapest and most direct sources of protein for millions of people in Africa (Bene and Heck, 2004). Fish is one of the most traded commodities, with exports of fish increasing by 5.30% since 1981

(Nations, 2017). The major markets for export are Europe (70%), Asia (15%), other African countries (11%) and North America (2%) (FAO, 2020a). However to meet demand, Africa still has to import 4.2 million tonnes of fish products (Brummett et al., 2008), resulting in a continental net loss. With the future of global population set for a further expansion to over 9 billion by 2050, Africa is predicted to have to increase its food production by 300% (Gabriel and Akinrotimi, 2007). It is therefore critical that aquaculture grows in a sustainable way, to enable future populations the access to vital food sources.

One of the major hindrances of aquaculture development is the lack of locally produced high quality fish feed (Gabriel and Akinrotimi, 2007). Fish require high quality nutrition in order to attain market size within the shortest time period. Locally produced feed will reduce production costs and enable the gap to be bridged to commercial investors, showing them that a growing population's demands can be met economically through fish farming with high quality fish feed. The top ten African exporters, include Egypt, Nigeria, Uganda, United Republic of Tanzania, Ghana, Zambia, Madagascar, Tunisia, Kenya and Malawi (FAO, 2020c), and account for 89.5% of the total value of exportation from the continent of fish and their products (Tall, 2015).

1.5.2 Aquaculture in Kenya

Kenya has become one of the fastest growing fish producers in Sub-Saharan Africa (FAO, 2015). In the last six years, their aquaculture production has doubled and is set to grow by 1000% in the next three years (FAO, 2020a). It provides employment for over 500,000 people directly and 2 million indirectly. There is also potential for huge future growth in Kenya, with 1,400,000 hectares of land potentially being available for aquaculture development in the future.

Kenya's aquaculture sector is divided into freshwater aquaculture and mariculture (Munguti et al., 2014), and can take many different forms, ranging from small hand-dug 'kitchen ponds' to dams, all being stocked with fish and harvested periodically (FAO, 2015).

Nile tilapia are the primary focus of Kenyan aquaculture, with an average production of 3 tonnes per hector (FAO, 2015), accounting for ~75% of total production (Munguti et al., 2014). Semi-intensive systems are responsible for their production, with fish held in earthen ponds and cages, utilising pond fertilisation from both chemical and organic fertilizers to enhance natural productivity. To supplement pond productivity, exogenous feeding using cereal bran and other locally available feeds is carried out (FAO, 2015).

The economic benefits of aquaculture development in Kenya are widespread. In towns where aquaculture is practiced, markets have been built to sell the local fish and their products. These markets can now be found in all major towns in Kenya, including most towns in Central, Eastern, Western, Coast, Rift Valley, Nairobi and Nyanza provinces (FAO, 2015), which is providing great economic benefit to these areas. Aquaculture has also allowed many fish farmers who previously farmed at subsistence levels, to transform into commercial smaller-scale fish farmers, earning nearly Kshs 450,000 (£3000) per acre of water surface (FAO, 2015).

The Kenyan government have developed research facilitates across the country to help with aquaculture advancement. Sagana is home to the National Aquaculture Research Development and Training Centre (NARDTC), initiating research aimed at increasing fish growth, greater productivity, higher yield and lower feed conversion ratios (KMFRI, 2018). The Lake's Basin Development Authority (LBDA) is based in Kisumu, and was established to provide a faster more meaningful

development in the Kenyan section of the Lake Victoria basin (LBDA, 2019), as well as the Kenyan Marine Fisheries Research Institute (KMFRI), who are collaborators in this project (KMFRI, 2020).

1.5.2.1 Future of Kenyan aquaculture

The ultimate aspiration of the FAO is for aquaculture to develop to allow more communities to prosper and help people to be healthier. They also hope it will offer more opportunities for improved livelihoods, with increased income and better nutrition, as well as ensuring farmers and women are empowered (FAO, 2020).

In Kenya, the focus is now on encouraging the development of private, commercial, large-scale aquaculture, to increase production (FAO, 2020), making a significant contribution in Kenya in terms of both food security and foreign exchange earnings through export markets.

1.6 Lake Victoria

Bordered by three countries, Kenya, Uganda and Tanzania (Figure 1.4), Lake Victoria is the second largest freshwater lake in the world by surface area. It covers 68,000km^2 in East Arica, with a mean depth of 35m, with 6% of the lake's surface area in Kenya, 43% in Uganda and 51% in Tanzania (Njiru et al., 2018). The Nile, one of the world's most important and longest rivers, eventually feeds into the Lake (Haines, 2019), and flows through Cairo, home to a population of over 20 million (Khan et al., 2018).

Some important rivers feed into the lake, including the rivers Bukora, Mara, Kagera, Katonga, Nyandon and Yale (Figure 1.4). These can carry pollution from

a length of cities, towns and villages that occupy the river's banks, to eventually emptying into the lake's basin. In addition, they and the many other rivers that feed into the lake flow through regions of high agricultural, industrial and mining activity.

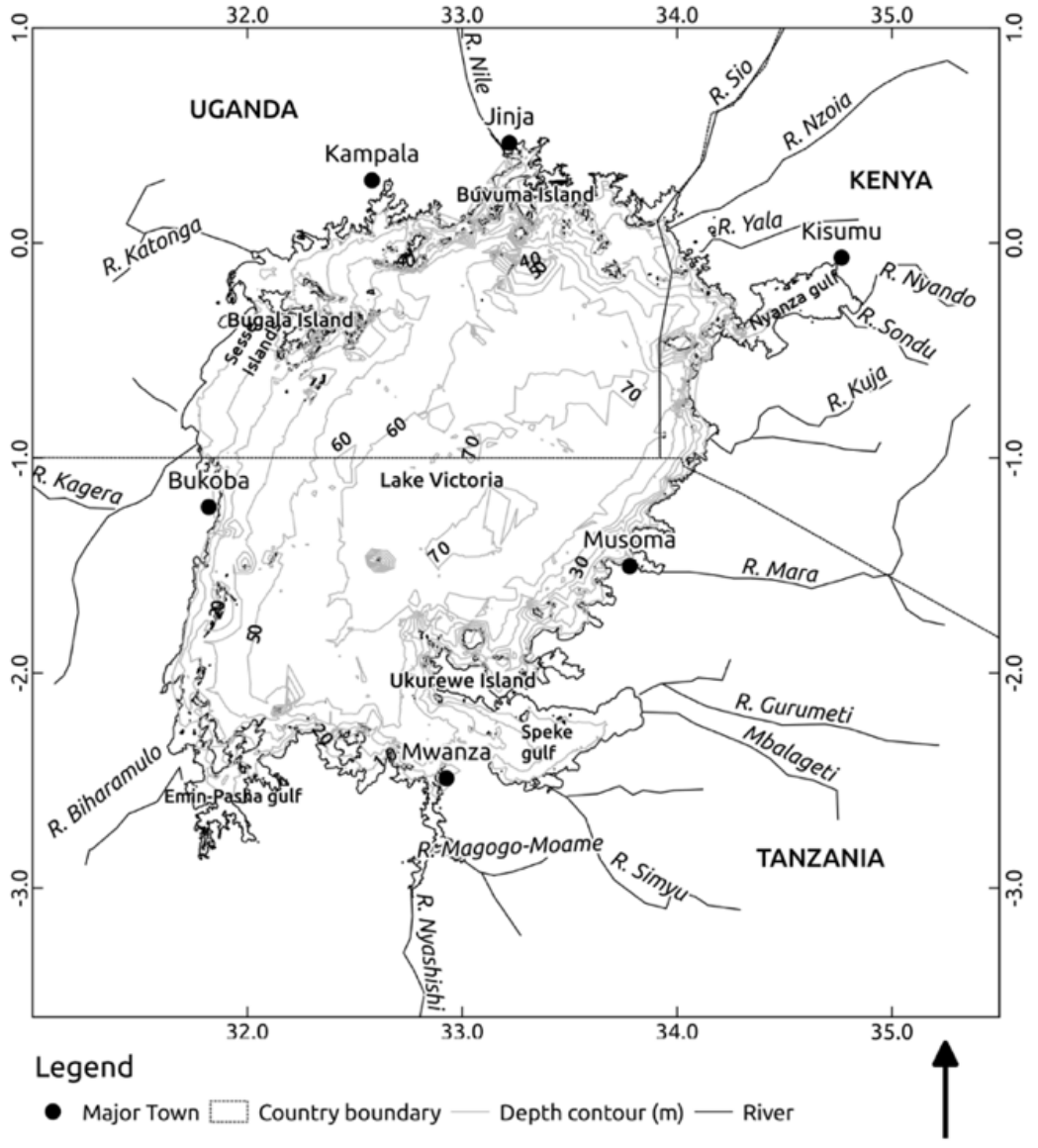

Figure 1.4 Map of Lake Victoria and its major rivers. The 3 countries surrounding Lake Victoria's basin are shown here: Uganda, Tanzania and Kenya. The bathymetry (water depth) is indicated on the sides and major rivers feeding into and out of the lake are labelled (Nyamweya et al., 2016a).

Lake Victoria is one of Africa's most densely populated areas, but its future is being threatened by over fishing and environmental damage from pollution (Britannica, 2019b). Population and economic development are key drivers in the pollution of this water resource and the rivers associated with it (Juma et al., 2014). As they continue to grow, more resources are being used up that the ecosystem cannot sustain. This has led to land development around the basin, where agricultural, urbanization and industrial activities have all expanded, which has driven the degradation of the lake's water quality (Scheren et al., 2000).

To ensure a sufficient nutritional food source is available for future generations, changes to the recycling practices and waste management in the region is critically needed, otherwise the aquatic environment of Lake Victoria will continue to decline.

1.6.1 Environmental issues facing Lake Victoria

An increasing human population with high exploitation rates has imperilled the health of Lake Victoria and its resources. From 1960, the population within 100km from the lake shoreline has increased drastically from 10 to 40 million (Njiru et al., 2018), with their activities causing a detrimental effect on the lake. Towns bordering the lake, such as Kampala in Uganda, Mwanza in Tanzania and Kisumu in Kenya have dumped untreated waste into the lake's waters (Scheren et al., 2000), and while practices are improving there is still an urgent need for further changes. Domestic, industrial and agricultural activities in and around these towns, such as chemical and fertiliser leakage from farms (Facts, 2019) and effluents from mine wastes and tailings (Ngure et al., 2014), all contribute to the pollution. Lack of awareness of good hygiene practices and the consequent

discharge of untreated sewage, storm-water, runoff, animal waste and maritime transport of waste into rivers, directly contributes to the degradation of river and ultimately lake water quality (David et al., 2009).

This has led to a serious decrease in oxygen available for aquatic life and the consequent decrease in fish populations available for human consumption (Scheren et al., 2000). This has increased the demand for the limited oxygen available and caused a significant rise in water-borne pathogens, which has been further exacerbated by run-off and storm water collecting animal and human waste and channelling these into rivers and the lake, creating an ideal environment to support the survival of these pathogens (Schneeberger et al., 2019). These microbes will potentially infect fish, with previous studies of fish harvested from Lake Victoria found to be infected with *Shigella*, *Salmonella* and *Escherichia coli (E.coli)* (Sifuna and Onyango, 2018). They often latch onto vegetation in the lake, such as the highly abundant water hyacinth, or lodge themselves onto the gills and skin surface of the fish (David et al., 2009).

The Winam Gulf (formally the Nyanza gulf, see Figure 1.4), lies wholly within Kenya, and is relatively shallow compared to the main lake basin. It is composed of many bays that receive inflowing water from several key rivers. The vegetated bays and river-mouth areas are an ideal habitat for many fish species (Mwamburi, 2019). However the water hyacinth, an invasive weed, has taken over the whole lakeshores and bays. The plant began to spread in the early 1990s after above normal rainfall during the El Niño washed it into the lake. It infested nearly 200km^2 by 1998 and has continued to persist today (Williams et al., 2007). For fisherman, the water hyacinths have diminished their catch by covering fishing grounds and delaying their access to markets, along with increasing costs from the effort spent in cleaning waterways and the loss of broken or tangled nets (Kateregga and

Sterner, 2009). The weed mats have sealed off nursing, breeding and feeding grounds for inshore fish, and caused further detrimental effects by blocking sunlight, reducing oxygen levels, and allowing hydrogen sulphide and ammonia, both poisonous gases, to accumulate (Kateregga and Sterner, 2009).

1.6.2 Fish species of Lake Victoria

Lake Victoria provides the main income source for populations living around the basin, especially those involved in fishing (CORDIS, 2019), however environmental pressures have put their livelihoods at risk.

Over 14,000 years ago Lake Victoria was home to over 400 species of cichlids (Leah, 2005). However human intervention within the lake and its catchment has resulted in several ecological changes, with dramatic effects on its fish resources. One of the most notable changes is the dramatic reduction and risk of extinction of some fish species (Outa, Yongo, et al., 2020). This led to the introduction of non-native fish species, such as the Nile perch and Nile tilapia (Ogutu-Ohwayo, 1990). As a result of overfishing and competition between species, the lake is now dominated by three fish species. These are commercially fished in the lake and include the Nile perch, the small sardine-like Omena or silver cyprinid (*Rastrineobola argntea*) and the Nile tilapia (Ardjosoediro and Neven, 2008).

1.7 Tilapia in aquaculture

Tilapia fish (Figure 1.5) are not native to Lake Victoria, having been introduced to repopulate after overfishing (Khan et al., 2018). They are now hugely popular in aquaculture, being the third most produced aquatic species globally (Elizabeth Cruz-Suarez et al., 2006). Their tolerance to a high range of salinities and

temperatures, as well as to high ammonia and low dissolved oxygen concentrations in the water (Popma and Masser, 1999), is why they are such a favoured species in aquaculture, with tilapia farming taking place in at least 85 different countries (AGMRC, 2018).

Tilapia are more resistant to bacterial, viral and parasitic diseases than commonly cultured fish (Popma and Masser, 1999). They have a very simple and inexpensive diet, predominantly filter feeding suspended particles in the lake (FAO, 2010) or natural organisms, such as plankton, algae, benthic aquatic invertebrates and decomposing organic matter (Njiru et al., 2004a). This makes them enticing to farmers as they are able to convert low quality feed into higher quality protein. Supplementary feed is determined by the style of farming, which for small-scale tilapia farming is a mix of rice and wheat bran and mustard oil cake (Ahmed, 2009), readily available in local markets. In intensive tilapia farming, they are dependent on industrially manufactured pelleted feed. Feed is given twice a day in both farming systems, with fertilisers also given to maintain tilapia growth, usually consisting of urea, cow dung and triple super phosphate (Ahmed, 2009).

The culture period for tilapia is around 9 months, with the peak season for farming being from April to December. Farmers may harvest tilapia after 4 months, granting them the ability to harvest two crop yields per year (Ahmed, 2009). These attributes, together with the low input costs, have made tilapia such a widely cultured freshwater fish.

Worldwide tilapia demand continues to increase. In the first 6 months of 2017, ~150,000 tonnes of tilapia entered the global market (FAO, 2021). Internationally consumers like the mild flavour and firm flesh of tilapia. In sub-Saharan Africa, where few protein sources are available for communities, tilapia is a favoured dish,

offering high quantities of protein alongside high nutritional benefits. These tropical and subtropical countries also possess favourable temperatures for growth, with their production costs as low as USD 0.55-0.65/kg, which facilitates trade with the USA, the leading importer (FAO, 2010). However, constraints have been reported for tilapia farming, including limited availability and poor quality of feed, lack of technical support and low price in markets (Hussain et al., 2013). Overall, there is a limit in the success of tilapia culture due to poorer farmers with inadequate knowledge and access to high quality of feed. It is imperative that this gap be bridged to provide a sustainable food source of protein to a continually growing population.

Figure 1.5 Tilapia fish. Two tilapia fish are shown here (Jennies Foods, 2021).

1.7.1 Impact of plastics on tilapia

In many African countries plastic recycling procedures are often not established, and even when reuse practices are present, they often lack legal foundation and are only conducted when necessary (Khan et al., 2018). This can lead to illegal

dumping in rivers and lakes, threatening the health of aquatic life. Plastic is physically broken up by weathering in aquatic systems into smaller microplastics and nanoplastics. These pose a huge risk to fish and consumers of fish, as fish can mistake these plastic pieces for food, causing plastic to infiltrate into food chains. A study collecting Nile tilapia from the Nile River found over 75% of the fish contaminated with microplastics in their digestive tracts (Khan et al., 2018).

1.8 Plastic as a material

Our planet has reached an environment crisis, as it is overrun and unable to handle an ever-growing population generating endless amounts of rubbish. One of the most concerning is the ever-increasing amount of plastic, its impact on biodiversity and contribution to climate change. From its first invention in the 1950s (Jambeck et al., 2015), plastic has become a hugely favoured material, replacing conventional materials, such as glass, paper and metal. Its low cost and ability to be versatile, strong but lightweight and the potential to be a transparent material have made it ideal for a range of applications (Andrady, 2011). It can also provide some environmental benefit, by playing a role in maintaining food quality, thus reducing food waste (Eriksen et al., 2014). There are therefore huge complex trade-offs between plastic and its substitutes.

Globally plastic demand is dominated by polypropylene (21%), low-density polyethylene (LDPE) (18%), polyvinyl chloride (17%) and high-density polyethylene (HDPE) (15%) (Hahladakis et al., 2018), which are all used in producing the vast array of plastic packaging products available, from food and drinks containers to car dashboards and bumpers (PlasticEurope, 2008). PP and PE together are collectively known as polyolefins and are primarily used in manufacturing fishing gear (Andrady, 2011). Other common plastic polymers

include polystyrene (8%), polyethylene terephthalate (PET) (7%) and thermosetting plastic polyurethane (PUR) (PlasticEurope, 2008). Plastic polymers are used for common consumer products, but also in the making of synthetic fibres, foams adhesives and sealants, making them applicable in a variety of applications (Hahladakis et al., 2018). However in many plastic products, the polymers are not the only constituent. To meet appropriate properties for the product, the polymer is combined with other ingredients or additives (Britannica, 2019a)

1.8.1 Plastic additives

Plastic additives are chemical compounds that are added to improve the functionality, performance and ageing of the polymer (Hahladakis et al., 2018). They are classed as either plasticisers, reinforces, fillers, stabilizers or colourants, and in almost all cases are not chemically bounded to the polymer (Campanale et al., 2020). Therefore, despite them improving the overall properties of the polymer, many are toxic and have the potential to leach into air, water and food, and potentially human tissue during their use or disposal and consequently expose humans to multiple toxic chemicals.

1.8.1.1 Plasticisers

Plasticisers are added to materials to decrease plasticity and viscosity, and increase workability and performance (Designing Building Wiki, 2020). PVC is a common polymer that plasticisers are used on, converting PVC from a rigid plastic into a flexible and elastic material to use in more applications (Godwin, 2000). Plasticisers can also change the biodegradability, odour, flammability and cost of the final product (Britannica, 2019a). There are five plasticisers of health concern,

di(2-ethylhexyl) phthalate (DEHP), dibutyl phthalate (DBP), diisobutyl phthalate (DIBP) and n-butyl benzyl phthalate (BBP), that have been found to cause adverse endocrine disruption (Koester, 2015), which have the ability to leach into the environment from discarded plastics.

1.8.1.2 Reinforcements

Reinforcements are used to enhance the mechanical properties of plastic (Campanale et al., 2020). Incorporating reinforces such as glass, wood or carbon fibres during the manufacturing of PP and PE can increase their stiffness (Britannica, 2019a). Active magnesium oxide is a reinforcer added to rubber compounds, and its main function is the neutralisation of hydrogen chloride (HCl) that can be released during processing and degrade the plastic material (NikoMag, 2021). Reinforced plastics are becoming the most selected material for building interior and exterior body parts of vehicles and aircrafts, due to their low cost, lightweight and easy parts replacement (Rosato and Rosato, 2004).

1.8.1.3 Fillers

Some plastic resins are blended with fillers to reduce costs, this can also improve the plastic's moldability and stability (Mraz, 2015). They also allow plastic to gain properties not usually associated with it, such as high electrical and thermal conductivity. Carbon black, calcium carbonate and silica are examples of chemicals that can be incorporated as particulate fillers (Britannica, 2019a).

1.8.1.4 Stabilizers

The properties of plastic should change as little as possible over time, in order for it to have a long and useful life in any application. Stabilizers are added to avert

the effects of ageing (Britannica, 2019a), and are also designed to reduce degradation of the plastic by ultra violet (UV) radiation, the ozone and biological agents. Stabilisers of high thermal stability include barium/zinc and potassium/zinc (McKeen, 2019), however these are produced from highly toxic metals. Barium compounds are among the densest used in PVC plastics, despite this their presence has not yet been subject to constraints based on environmental or health grounds (Turner and Filella, 2020a). Metabolic, neurological and kidney diseases, and even breast cancer, are all reported effects of exposure to barium on human health (Campanale et al., 2020).

Additionally to avoid the loss of HCl in PVC during processing temperatures, heat stabilisers are added, such as zinc or calcium, to prevent potential corrosion of equipment (Sastri, 2014). Iron oxides, carbon blacks and barium zirconate are also widely used heat stabilisers in adhesives and sealants (Sastri, 2014).

Nickel plating on plastic is widely implemented in metal finishing industries, its bright metallic appearance is ideal in plating plastic automotive parts and protects against corrosion and wear (SPC, 2020).

1.8.1.5 Colourants

Most consumer plastic products are coloured, turning inexpensive material plastics into more aesthetically pleasing materials to use and are therefore easier to sell (Tolinski, 2015). Compounds to add colour can be added as pigments (insoluble) or dyes (soluble). Popular colour pigments for plastic include carbon (black), titanium oxide and zinc oxide (white) and sometimes inorganic oxides like, chromium and iron (Britannica, 2019a). Iron oxide pigments are used for metallic finishes, where their high transparency gives an attractive finish (SpecialChem,

2018), and leads to a plastic colour change that goes from yellow to red (Campanale et al., 2020).

Titanium oxide is also widely used as it can absorb UV light and therefore increases the weatherability and durability of the plastic product (SpecialChem, 2018), however it has been shown to generate cytotoxicity on human epithelial lung and colon cells (Campanale et al., 2020). Similarly titanium dioxide (TiO_2) is now appearing in PET waste, from the introduction of opaque PET bottles (Matxinandiarena et al., 2019). Studies have shown TiO_2 causes phototoxicity under UV irradiation, and this has induced oxidative DNA damage and lipid peroxidation, eventually causing neuroinflammation in humans (Shah et al., 2017).

1.8.2 Plastic as a pollutant

With limited reuse and recycling options, especially in LMICs, plastics have become the fastest growing component of waste (Figure 1.6). In 2015, 381 million tonnes of plastic was produced globally (Eriksen et al., 2014) and, despite nationwide recycling schemes, the UK only recycles less than a third of its plastic waste (Sewage, 2019). Plastic contributes 10% to all the domestic waste produced worldwide and forms up to 95% of the litter found on beaches, sea floors and the sea surface typically in the form of macroplastics (Galgani et al., 2015).

Each year, 32% of the 78 million tonnes of plastic packaging produced is left to flow into our waters (Pennington, 2016), which is the same as dumping a truck full of plastic litter every minute (Geographic, 2019). In 2025, the predicted ratio of plastic mass to fish in our oceans is estimated to reach 1:3. If this continues, by 2050 plastic weight will be equal to or larger than fish stocks (Güven et al., 2017). Fish are at high risk of plastic pollution exposure as large macroplastic

products are readily broken down into smaller microplastic pieces in the aquatic environment by physical or chemical degradation.

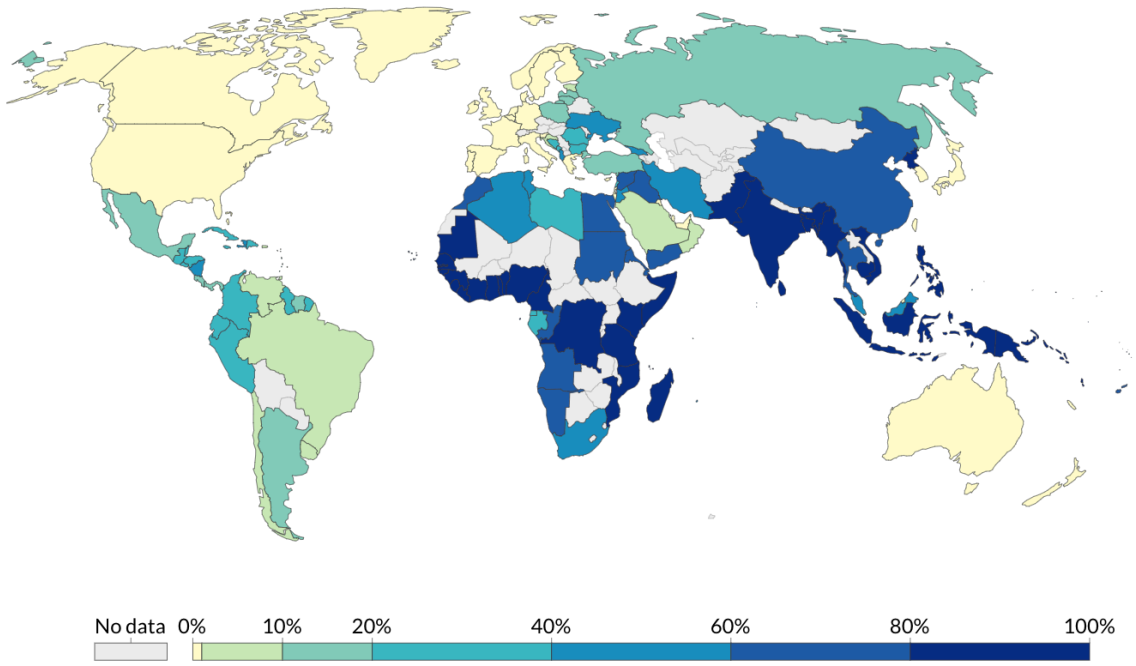

Figure 1.6 Share of plastic waste that is inadequately managed (2010). Inadequately disposed waste includes waste that is not formally managed, and waste disposed in dumps or open uncontrolled landfills, which are not fully contained. This has a high risk of polluting rivers and oceans. Dark blue countries have the most inadequately managed plastic waste, these include many low and middle income countries (Jambeck et al., 2015).

1.8.2.1 Plastic pollution in Africa

Plastic waste poses great environmental and human issues especially in LMICs where they lack nationwide recycling facilities and have a high volume of mismanaged waste (Babayemi et al., 2019). Littering is sadly a part of African culture, often irrespective of socio-economic status. In 2015, the per capita plastic consumption in Africa was 16kg for a population of 1.22 billion (Africa Population, 2021). It was also estimated that each of Africa's countries, including Kenya, used approximately 13.71 mega tonnes (Mt) of plastic in 2015 (Babayemi et al., 2019).

1.8.2.1.1 Plastic pollution in Kenya

Currently, plastic produced in Kenya stands at 400,000 tonnes (Mogoathle, 2019), with 260,000 tonnes of plastic packaging imported annually, and an estimated 174,000 tonnes illegally dumped or left in the environment (Roberts, 2018). In Kenya, rapid urbanisation has exasperated the problem. Most plastic in Africa ends up in dump sites, with frequent open incineration. Littering, lack of segregation at source programmes and indiscriminate dumping along riverbanks are all adding to the crisis.

In 2017, Kenya introduced new laws to address these concerns, and banned the manufacturing, sale and distribution of plastic carrier bags (Waiganjo, 2020). In 2020, they went one step further and banned all single-use plastics, such as water bottles and straws, from its national parks, beaches, forests and other protected areas (AFP, 2020).

1.8.2.2 Impact of COVID-19 on plastic pollution

The COVID-19 pandemic has exacerbated the world's plastic pollution problem. The pandemic has underlined to society that plastic is this irreplaceable material, which provides an inexpensive and widely accessible feedstock in producing medical equipment. Monthly an estimated 129 billion face masks and 65 billion gloves are used globally (Prata et al., 2020) as personal protective equipment (PPE). Masks typically consist of many layers of PP microfibres, PUR and polyacrylonitrile (PAN) (Czigany and Ronkay, 2020). With plastic acting as a vector for the SARS-CoV-2 virus (Prata et al., 2020), and allowing survival on its surface for up to 72 hrs, the recycling and reuse of any of this plastic has been restricted. This coupled with incorrect disposal by the public, has resulted in used masks and

gloves being found littering public spaces and waterways across the globe (Figure 1.7) (Mosely and McMahon, 2020).

Figure 1.7 COVID-19 aquatic plastic pollution. Researchers found surgical gloves, disposable masks and hand sanitiser bottles used for personal protection equipment in the COVID-19 pandemic throughout rivers and seas across Europe (Phys.org, 2020)

1.8.3 Macroplastics

Macroplastics are the largest plastics, typically seen floating in surface waters and littering shorelines (Bråte et al., 2017). Sources include household goods, food and drinks packaging, as well as tourism and construction (Bråte et al., 2017), and many of these are a risk for aquatic life (Figure 1.8). Plastic has a wide range of applications but photodegradation, from prolonged exposure to UV radiation, hydrolysis or physical breakdown (Planet Experts, 2015), breaks them into pieces ranging from micrometres to nanometres (Andrady, 2011).

Figure 1.8 Turtle trapped in plastic ring. Plastic beer holder ring is trapped round the turtle's shell. Debris entanglement can prevent air-breathing aquatic organisms from swimming to surface for air, causing them to drown (Ruiz-Grossman and Dahlen, 2017).

1.8.4 Microplastics

Microplastics are forms of plastic that are <5mm in size (Thompson et al., 2004), and can be split into two main groups, primary and secondary microplastics. Primary microplastics are manufactured at micro size (Picó and Barceló, 2019), and include microbeads from cosmetics and personal care products, and microfibres by abrasion from synthetic textiles in the environment (Hantoro et al., 2019), such as polyester or acrylic fibres (Williams, 2019). A single shower was thought to have sent 100,000 microbeads down the drain and into the ocean. The UK therefore placed a ban on their production and use in products in 2018 (Gove,

2018), however it will be a few decades before we see their presence in the environment fully diminish.

Secondary microplastics are the degradation products of larger macroplastics (Picó and Barceló, 2019), primarily produced for sole domestic functions (plastic bags, fishing nets, plastic bottles and styrofoam products). Degradation can occur by physical or chemical ageing in aquatic systems. Weathering from waves, prolonged exposure to UV radiation and water salinities and temperatures, break macroplastics into smaller micro-sized pieces (Roman Lehner, 2015). There are estimated to be ~5.25 trillion macro- and microplastic pieces floating in our oceans, weighing up to 269,000 tonnes (Eriksen et al., 2014).

Microplastics have been documented in all habitats of open-water (Bråte et al., 2017) and have even been found in locations as isolated as the Arctic (Jambeck et al., 2015). Their small size is similar to food organisms, such as zooplankton (Iwasaki et al., 2017), and are often consumed as a result and therefore transferred through food webs, from environment to organism or prey to predator (Foekema et al., 2013). Fish and bivalves intended for human consumption have been found to contain microplastics (Thiele et al., 2019), with an estimated 11,000 microplastic pieces being ingested by regular seafood consumers (Marine Conservation Society, 2019). This has triggered concerns about the risks of dietary exposure on human health, as well as the implications for aquatic ecosystems and potential economic impacts, especially in coastal towns (Hantoro et al., 2019).

Microplastics demonstrate a huge variation in their physical and chemical properties, such as size, weight, shape, composition and colour (Hidalgo-Ruz et al., 2012). Size is typically based on the longest length of a particle. There are five main categories for shape: fragment, foam, film, fibre and bead (Bråte et al., 2017). These influence the behaviour of the particles within aquatic environments,

affecting their dispersion, adsorption and absorption of contaminants and microbiota (Alexandre et al., 2016).

1.8.4.1 Fragment

Fragments are irregular shaped particles, which can also be termed crystals, fluffs, powder, granules, shavings and flakes (Lusher, Hollman, et al., 2017). They originate from macroplastic breakdown of food and drinks packaging in aquatic environments. Studies have found that fragments tend to absorb less chemicals from their surrounding environment than other microplastic shapes due to their disrupted active sites from their irregular shape (Naqash et al., 2020). They do however have longer gut residence times, meaning they can be persist in fish organs for longer (Hantoro et al., 2019).

1.8.4.2 Foam

Foams originate from the well-known plastic polymer PS. Direct contact with PS has the potential to damage skin, despite this its properties of being lightweight and providing great thermal insulation means it is found in many food packaging and laboratory ware including coffee cup lids, disposable plates and large foam packaging, which by degradation all form foam spheres (Hwang et al., 2020).

1.8.4.3 Film

Films are commonly found on food packaging, but also in agriculture as mulch films that modify soil temperature and moisture. Mulch films are heavily used in agriculture to promote food security, however they are the main source of macro- and microplastics entering agricultural soils (Qi et al., 2020). Soil-contaminated plastics are not recyclable, and the films are often so thin, making their extraction

from the soil at the end of the growing season difficult, this is resulting in a surge in plastic film pollution (Qi et al., 2020).

1.8.4.4 Fibre

Microfibres, also known as filaments, strands or threads, typically come from degradation, including in the washing machine, of clothes and synthetic textiles. Studies have suggested that they are widespread in aquatic ecosystems and can have a negative impact on animal health, having been shown to be linked to respiratory and reproductive changes in fish (Henry et al., 2019), potentially acting as endocrine disruptors (Hu et al., 2020).

1.8.4.5 Bead

Beads are also called grains, spherical microbeads and microspheres. They are used in personal care and cosmetic products and are commonly made of PE, nylon, PP and PET. They are commonly discarded down the drain, allowing them to easily enter waterways (Tanaka and Takada, 2016). Beads have a sphere shape, which makes them more likely to be absorbed by organisms like fish, as their structure mimics their feed (Hantoro et al., 2019).

1.8.5 Economic impacts of plastic waste

Land-origin plastic waste costs the global economy up to $19 billion each year (Consultancy.uk, 2019). Asia currently leaks more waste pollution into waterways and oceans than any other continent, accounting for 82% of global land based plastic pollution and contributing 86% to global plastic costs (Deloitte, 2019). Africa follows as the 3rd highest plastic pollution producing continent. Their clean-

up costs have reached a huge $47.4 billion, leaving them with an average economic loss of $49.8 billion yearly from plastic waste (Deloitte, 2019).

Plastic pollution has been found to result in a $0.3 to $4.3 billion loss of revenue to the fishing and aquaculture sector and a reduction in $0.2 to $2.4 billion to tourist trade (Deloitte, 2019). Grounded plastic along shorelines results in loss of aesthetic value of the environment, an economic cost which takes its form in a decreased value of waterfront real estate. It has negative impacts on tourism, with economic losses coming from decreased tourist revenue, negative impacts on recreational activities and invasive species transport which damage public health (Hardesty et al., 2015). Stranded shoreline plastic also negatively impacts fishing and aquaculture resources, shipping and energy production. The overall estimate of economic impact of plastics on aquatic ecosystems is approximately $13 billion US/year (Sireyjol Trucost et al., 2014). One of the biggest direct cost factors is the clean-up cost required to remove plastic pollution from coastlines and waterways.

Microplastic presence in water bodies has an adverse effect on aquatic biodiversity. It not only impacts local ecosystems and food chains, but also harms fishery reserves, which are the main source of livelihood for the fisheries sector (Gallo et al., 2018). Furthermore, fish larvae are very sensitive to water quality, and therefore have high mortality rates. Microplastic presence can degrade the water quality, creating unfavourable conditions for aquaculture. This can cause huge significant losses to fish farmers, as a single loss of a harvest can bring them to bankruptcy, from the large investment requirements (Deloitte, 2019).

1.8.6 Environmental impacts of plastic pollution

Plastic is one of the most concerning environmental issues, with significant environmental concerns for governments, scientists and members of the public worldwide (Xanthos and Walker, 2017). Globally it has taken over every part of our oceans, rivers and lakes, impairing human health, food safety and tourism (IUCN, 2018). Furthermore, the incineration of plastic waste needed to destroy it is contributing to climate change, from the release of the greenhouse gas carbon dioxide (IUCN, 2018). The production of one tonnes of plastic generates up to 2.5 tonnes of carbon dioxide (Sewage, 2019). Equally as it degrades in aquatic environments, it uses oxygen from the surrounding waters, leaving less available for aquatic life, thereby affecting their survival (Shamseer Mambra, 2019). Plastic pollution in the environment can cause entanglement, ingestion, habitat damage and loss and transport vectors of non-native species through adherence to the plastic's surface (Bråte et al., 2017).

Ingestion of microplastics by aquatic organisms is one of the most deleterious environmental impacts, posing more of a threat than macroplastics. Their small size gives them the potential to travel vast distances, allowing them to be available to many organisms at different trophic levels of the aquatic system. Furthermore, microbeads are often mistaken by surface feeding fish as zooplankton, as they are often similarly opaque in colour (Xanthos and Walker, 2017). Persistent organic pollutants (POPs) can sorb to the microplastics and accumulate at concentrations higher than in ambient water. There is a growing concern that these pollutants are entering the human food chain through ingestion of shellfish, fish and their products (Gallo et al., 2018).

Microplastic contamination in soil has recently become a concern. Many organisms, including humans rely on soil for their survival. Plentiful sources of this

pollution problem have been reported from domestic sewage, fertilisers, biosolids, fibres from clothing and microplastic beads from personal care products, irrigation and wastewater, flooding and illegal dumping (Chae and An, 2018). These particles settle on the soil's surface and then penetrate into subsoils. A study examined whether ingested plastic in the soil transferred pollutants and additives to organisms. They exposed lugworms, a type of sandworm to varying levels of microplastics and demonstrated that microplastics' pollutants and additives were transferred into their gut tissues, causing some harmful biological effects (Browne et al., 2013). This was an important finding, as it showed that microplastics can be transferred in both terrestrial and aquatic systems. These microplastics have the potential to be transferred between organisms and food chains, as well as be retained by the worms and be transported to deeper soil layers and potentially leach to groundwater (Chae and An, 2018).

Unfortunately microplastics are used in many anthropogenic activities, including mining, abrasive air-blasting and antifouling coatings for boats (Botterell et al., 2019). As a result of climate change, the melting of sea ice has been accelerated, releasing high levels of ice bound microplastics back into the marine environment (Obbard et al., 2014), that originated from such anthropogenetic sources. Climate change could also potentially change oceanic currents, which could alter the abundance, distribution and impact of microplastics across aquatic environments (Lusher, Welden, et al., 2017).

1.8.7 Impact of plastic pollution on aquatic life

The most visible and disturbing impacts of plastic pollution are the entanglement (Figure 1.9), ingestion and suffocation of aquatic organisms, causing severe injury and often death (IUCN, 2018). 1 million seabirds are killed yearly by plastic

pollution (Sewage, 2019). University of Plymouth researchers found that over 44,000 animals have become entangled in or swallowed plastic debris across the globe (Merrington, 2015). Marine species such as seabirds, turtles, whales and fish often mistake plastic for their prey, with plastic debris found in 36% of seals, 59% whales and 100% of marine turtles (Sewage, 2019). Most die of starvation as their stomachs are filled with plastic. Additionally, they can suffer from lacerations and internal injuries, leaving them with a reduced ability to swim. Damage to essential internal systems has also been reported, such as the liver and reproductive systems of oysters, which has caused them to produce less eggs (Geographic, 2019).

Microplastics are transferred from environment to organisms and thereby enter the food chains. Zooplankton are the main food source of many marine organisms, such as commercially important fish. Studies have shown microplastics are readily ingested by many zooplankton taxa, with associated negative impacts on their life-span, reproduction and feeding behaviours (Botterell et al., 2019). Zooplankton feed on surface waters, where the abundance of microplastics is highest, and are found in aquatic environments at such a high abundance, that their risk of microplastic ingestion is accelerated.

Additionally, microplastics have a large surface area-to-volume ratio and hydrophobic properties, leading to an accumulation of contaminants on their surface, including heavy metals and chemical pollutants from the aquatic environment (Koelmans et al., 2014). These contaminants, as well as chemical additives that are incorporated during plastic manufacturing, can leach into the biological tissues of aquatic life and potentially cause lethal effects. They also have the ability to accumulate at higher trophic levels of the food web and eventually find their way into human food webs (Koelmans et al., 2016a).

Figure 1.9 Lemon shark with plastic bag trapped round its gills. Taken in the Bahamas, the plastic bag is blocking the shark's gills affecting its ability to breath (Ruiz-Grossman and Dahlen, 2017).

1.8.8 Human health

Consumers of fish and their products are at risk from polluted waters, with ingestion of fish potentially contaminated with plastics (Shamseer Mambra, 2019). Invisible microplastic pieces have even been found in bottled water and beer (IUCN, 2018). A study carried about by the World Health Organisation (WHO) analysed 259 bottles, from 9 different counties and across 11 different brands, and found an average of 325 microplastic particles for every litre of water (WHO, 2019). In a bottle of Nestle Pure Life, concentrations were as high as 10,000 microplastic pieces per litre (Graham Readfearn, 2018).

Despite tourism playing a firm role in economic development in many places, the United Nations Environment Programme estimates that tourists produce 4.8

million tonnes of solid waste each year (Martin, 2018). Furthermore, the aesthetic value of the environment is compromised by mismanaged waste. Plastic debris could cause injuries or harm to human health. This coupled with the unpleasant experience waste brings, results in reduced tourist activity and consequent loss of livelihoods from businesses associated with tourism (Deloitte, 2019). Currently there is insufficient research into the direct and long-term effects of microplastic levels on human health (Williams, 2019). Subsequently, at present more studies around exposure levels to microplastics and their contaminants in humans are being explored.

Potential hazards to humans associated with microplastics include the physical impacts of the particles on the body and chemical and microbial pathogens from the biofilm on the microplastic's surface (EFSA, 2016). The properties of the particle determine the impacts in the body. Size, surface area and shape of the plastic all determine the fate and health impacts following ingestion (WHO, 2019). Despite the plastic polymers being of low toxicity, it is these additives and hydrophobic chemicals sorbed from the environment that are the biggest concern to human health (WHO, 2019), and many health organisations such as WHO are appreciating that this is a huge emerging area of concern (Williams, 2019).

1.9 Persistent organic pollutants

POPs present in aquatic waters are readily picked up by microplastics even at very low concentrations (Andrady, 2011). The hydrophobicity of POPs facilitates their concentration to adhere to microplastics. The contaminated plastics, when ingested by aquatic species, creates a plausible route whereby POPs are able to enter food webs.

With plastics manufactured with POPs as additives (Hahladakis et al., 2018), the leaching of these additives is of greater concern in species with a longer gut retention time, such as fish (Koelmans et al., 2014).

Marine PP pieces were found to have 100,000 to 1 million times higher concentrations of banned POPs than in the surrounding water (Mato et al., 2001). These included DDE (dichloro-diphenyl-dichloroethylene), a POP formed by the loss of HCl and classed as a Group B2, a probable human carcinogen (Bidleman, 1984). In addition, PCBs (polychlorinated biphenyls), which were developed as coolant fluids in electrical apparatus (EPA, 2020), are known to have significant toxic effects in animals, including impacts on reproductive function (Steinberg et al., 2008).

The exposure to living organisms from these pollutants is continually increasing if we consider microplastics interactions as a vector of metals and biota (Campanale et al., 2020). Several variables can influence the interaction of microplastics with compounds, such as increased roughness and alteration of the plastic's surface (Campanale et al., 2020). These accelerate the degradation process, creating more active sites on the plastic's surface for interactions. Other significant variables include pH, salinity, temperature, polymer polarity, photo-oxidative erosion, and the formation of the biofilm.

1.10 The 'plastisphere'

The term 'plastisphere' was first used in 2013 to describe the biofilm or specific microbial community associated with the surface of plastics (Zettler et al., 2013). The impact of plastic debris on aquatic life has been extensively documented, however the interactions between plastics and the plastisphere remains unclear (Schlundt et al., 2019). Layers of inorganic and organic substances rapidly coat

the plastic surface upon entering the aquatic environment. This is followed by swift colonisation from functionally diverse communities of bacteria, protozoa, diatoms (algae) and fungi (Rummel et al., 2017), and collectively forms a thin layer of microbial assemblage on the plastic's surface forming the 'plastisphere' (Figure 1.10).

This development is of particular importance as it determines the fate of plastic in our aquatic systems (Pinto et al., 2019). Colonisation and biofouling are of high concern as they allow the plastic to be changed, thereby altering its buoyancy, allowing it to settle into deeper water, where it can be exposed to even more aquatic species (Andrady, 2011). Plastic litter is functioning as an 'artificial reef' (Zettler et al., 2013), and may cause pathogenic species to be transported over huge distances (Pinto et al., 2019). Furthermore birds and fish heavily rely on chemoreception for food selection, and these biofilms can make plastic smell and taste like their food resulting in greater ingestion (Savoca et al., 2017). The presence of the plastisphere also shields the plastic's surface from abiotic aging by UV radiation, thereby preventing plastic breakdown in the environment.

The physio-chemical properties of the surface of plastic, including roughness, electrostatic interactions, hydrophobicity and charge, have been shown to influence the initial colonisation of the biofilm (Rummel et al., 2017). Weathering from UV radiation and physical breakdown from waves has an influence on this, by determining the condition of the material and its hydrodynamic interactions.

Advanced tools are needed to visualise the distribution of these intact microbial biofilm communities (Schlundt et al., 2019) to determine the subsequent effects on aquatic life and also human health.

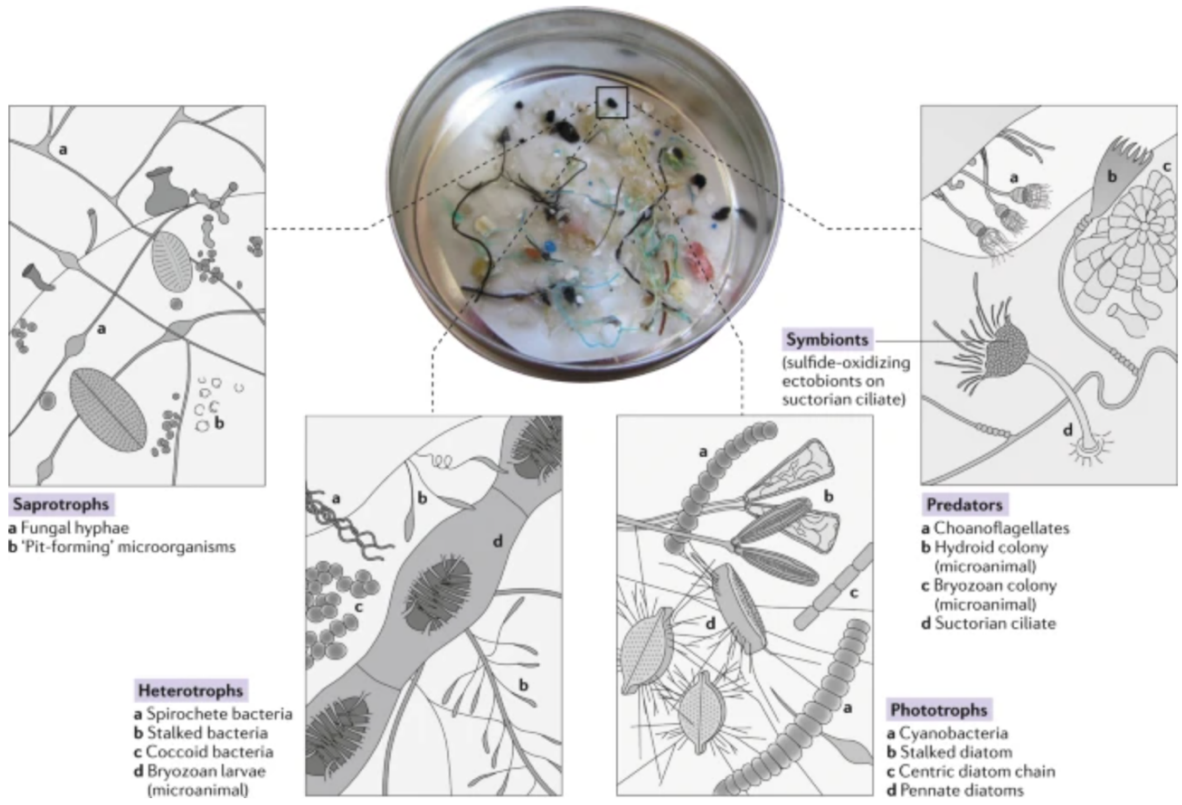

Figure 1.10 The plastisphere community. Conceptual model of the diverse plastisphere that can exist on the surface of plastics, hosting a microbial ecosystem in which members include cyanobacteria and diatoms (Amaral-Zettler et al., 2020).

1.10.1 Bacteria as a pollutant

Recently, microplastics have been recognised as a substrate that can be readily colonised by biofilm-forming microorganisms (Ogonowski et al., 2018). These can propagate on the surface of plastics and contribute to their degradation or distribution amongst aquatic ecosystems. Bacteria are a threat not only by causing disease, but also from the potential increases in levels of antibiotic resistance they may have and be able to pass on (De Tender et al., 2017). Studies have found rich eukaryotic and bacterial communities on PE and PP collected from the North Atlantic ocean (Zettler et al., 2013) and in aquatic environments on PS, of 5 bacterial pathogens including *Flavobacterium columnare, Aeromonas hydrophila,*

Edwardsiella ictaluri, E. tarda, and *E. piscicida* (Cai and Arias, 2017). Potential pathogenic bacteria might be distributed into previously unaffected ecosystems, by hitchhiking on microplastics that could have originated from sewage treatment plants or untreated human and animal waste (Oberbeckmann et al., 2016), threatening aquatic life.

Scanning electron microscopy has been used to explore the microbial diversity on PE, PS and PP particles collected from the North Pacific Gyre, and showed *Bacillus* bacteria and pennate diatoms were abundant on the plastic, with highest abundances on foamed PS (Carson et al., 2013).

The role of microbial plastic colonisation is not fully understood, but potential factors have been found to make biofilm formation on plastic appear appealing for microorganisms (Oberbeckmann et al., 2016). Plastic's surface offers great protection and stability for prokaryotes, creating a favourable environment for microbial biofilm colonisation in various environments. If colonised microplastics are ingested by fish in aquatic environments, and eventually humans, this could result in huge health risks and potential disease infection.

1.11 Aims and objectives of this study

The overall aim of this study was to investigate microplastic prevalence in tilapia fish from Lake Victoria in Kenya, to determine the need for microplastic pollution monitoring in both the aquatic environment and in fish to ensure the sustainability and safety of this important protein source. This was achieved through the following objectives:

1- Compare microplastic prevalence in tilapia muscle versus GIT.

2- Compare microplastic prevalence in wild versus farmed tilapia from key fishing locations in and near the Winam Gulf, Lake Victoria.

3- Detect and visualise the plastisphere present on the identified microplastics, to highlight any bacteria or pollutants that may be present.
4- Investigate some of the bacterial components of this plastisphere.

2.0 Methods and materials

The collection of samples from Lake Victoria was part of a larger study in collaboration with colleagues from the British Geological Society, the KMFRI and the University of Eldoret.

2.1 Tilapia sampling from Lake Victoria

Tilapia samples, both farmed/caged (CT) and wild (WT), were collected from Lake Victoria, Kenya during January 2019 (n=19) and May 2019 (n=63) at different sites (Tables 2.1 and 2.2). The fish were purchased from farmers at point of harvest. For the fish from January, a muscle sample and intact GIT were used as part of this study. For the remaining fish (from May), muscle samples and the contents of the GIT were analysed.

Tilapia were sampled from 18 different sites across the Lake (Figure 2.3). Sites 1 (Dunga), 2 (Maboko Island) and 3 (Asat cages) are situated on the northern shore of the shallow Winam gulf, formerly known as the Nyanza gulf, located only 4.7 miles from Kisumu, the third largest city in Kenya. Site 4 (Uyoma Point) is in the deeper Rusinga channel, between the Gulf and the main body of the lake. Sites 6 (Ngodhe), 7 (Mbeo cages) and 9 (Bridge Island) are near Rusinga Islands where the water is deeper. Site 10 (Kadimo Bay – Anyanga) is where the Nzoia river flows into Winam Gulf, it is Kenya's second biggest river by discharge. Site 11 (Madiany water) is situated in a bay, in the northern shore of the main lake. Site 13 (University of Eldoret pond) is in the narrow channel entrance to the Winam Gulf. Sites 15 (Port Bunyala) and 16 (Mageta Islands) are both located further north in the main body of Lake Victoria. Sites 18 (Sori Bay) is near the mouth of

the River Migori, located in the main body of the lake out of the Winam Gulf, it is also the site closest to the Kenya/Tanzania border.

Site	Location	Fish muscle sample ID	Fish intact GIT ID
1A	Dunga	Ta61, Ta62, Ta63, Ta64	GIT15
1B	Dunga	Ta65, Ta66, Ta67, Ta68	GIT19, GIT20
4	Uyoma Point	Ta69, Ta70, Ta71, Ta72, Ta73, Ta74, Ta75	GIT6, GIT7
7B	Mbeo cages	Ta76, Ta77, Ta78	GIT10
18A	Sori Bay	Ta79, Ta80	GIT13

Table 2.1 Tilapia sampling sites January 2019. This table shows the sites, 1A, 1B, 7B and 18A, where farmed and wild tilapia (Ta) were caught. NFS – no fish sampled. GIT – intact gastrointestinal tract. Ta – muscle.

Site	Location	Fish muscle sample ID	Fish GI content sample ID
1A	Dunga	Ta28, Ta55, Ta56, Ta57	NFS
1B	Dunga	Ta12, Ta13, Ta17, Ta58, Ta59, Ta60	NFS
1C	Dunga	Ta32, Ta34, Ta37	NFS
2	Maboko Islands	NFS	NFS
3	Asat cages	NFS	NFS
3C	Asat cages	Ta54	NFS
4	Uyoma Point	NFS	NFS
4D	Uyoma Point	Ta29, Ta30, Ta31, Ta33, Ta53	NFS
5A	Naya Bay	NFS	NFS
5B	Naya cages	NFS	NFS
6	Off Ngodhe	NFS	NFS
6B	Off Ngodhe	Ta2, Ta41, Ta45, Ta46	NFS
7A	Mbeo cages	Ta50	NFS
7B	Mbeo cages	Ta1, Ta7, Ta8, Ta47	NFS
7C	Mbeo cages	NFS	NFS
7D	Mbeo cages	Ta42, Ta43, Ta44	NFS
8	Mbita West	NFS	NFS
9	Bridge Island	NFS	NFS
9B	Bridge Island	Ta14, Ta15, Ta18, Ta22, Ta52	GI1, GI2, GI3, GI4
9E	Bridge Island	Ta19, Ta23, Ta26	GI5
10	Kadimo Bay (Anyanga)	Ta49, Ta51	NFS
11	Madiany Water Intake	NFS	NFS
11E	Madiany Water Intake	Ta3, Ta4, Ta11	NFS
11F	Madiany Water Intake	Ta5, Ta9, Ta10	NFS
12	Achieng' Oneku (Kunya)	NFS	NFS
13	University of Eldoret pond	NFS	NFS
13B	University of Eldoret pond	Ta6, Ta20, Ta24	NFS
13D	University of Eldoret pond	Ta16, Ta21, Ta25, Ta27	NFS
15	Port Bunyala	NFS	NFS
15B	Port Bunyala	Ta39, Ta40, Ta48	NFS
16B	Mageta Island	Ta35, Ta36, Ta38	NFS

Table 2.2 Tilapia sampling sites May 2019. This table shows the sites, 1C-C, 3C, 4D, 6B, 7A-B, 7D, 9B, 9E, 10, 11E-F, 13B, 13D, 15B and 16B, where farmed and wild tilapia (Ta) were caught from. NFS – no fish sampled. GI – gastrointestinal tract contents. Ta – muscle.

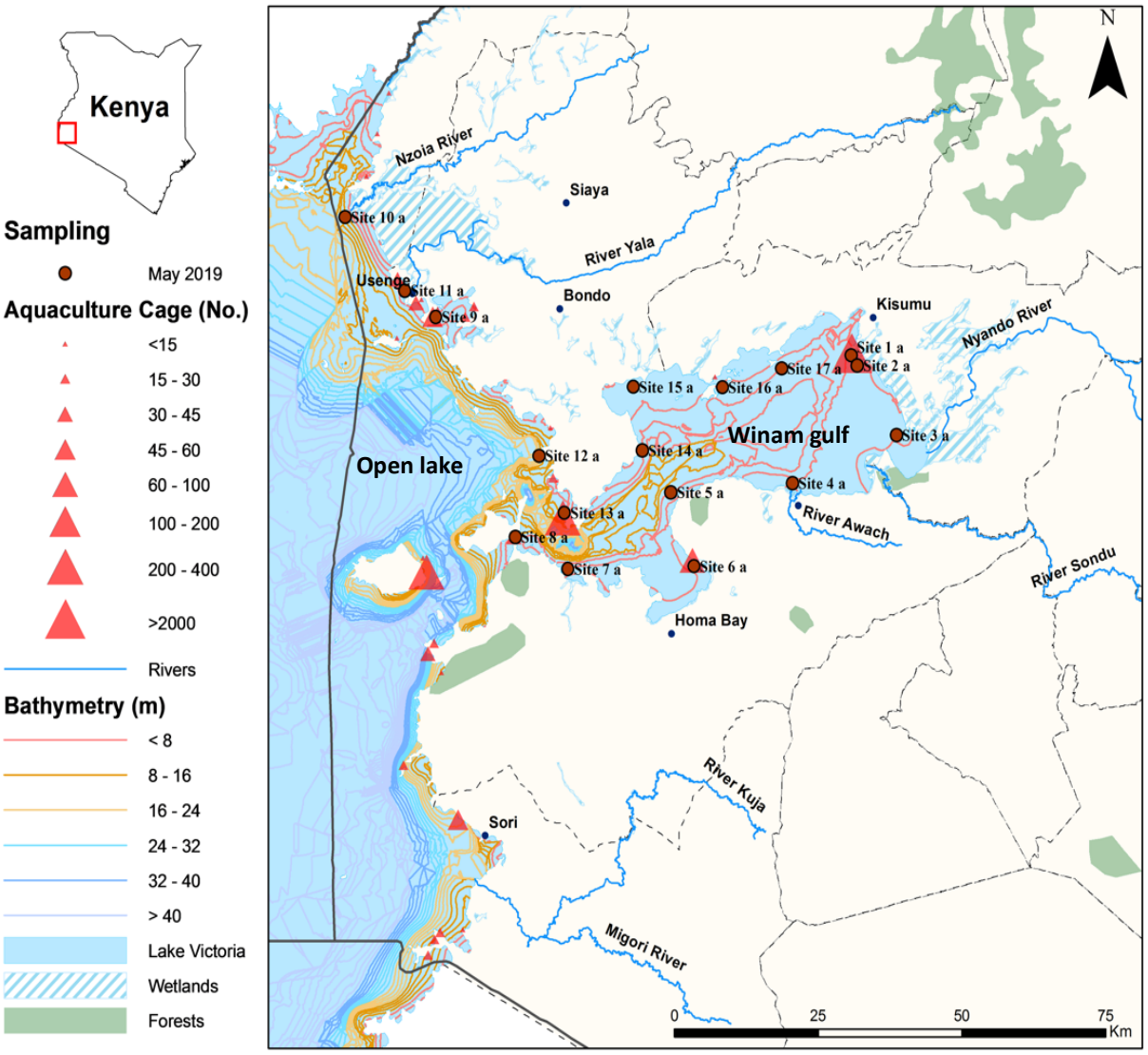

Figure 2.3 Map of sample sites across Lake Victoria. Wild tilapia sample sites are indicated with a red circle. Farmed/caged tilapia sites are indicated with a red triangle. Some sample sites had both wild and farmed tilapia sourced from them. The bathymetry data highlights the shallow nature of the Winam Gulf in comparison to the main body of the Lake. Rivers flowing into the lake, as well as cities around the lake's basin are labelled. Image kindly provided by Dr Andrew Marriott at the BGS.

2.1.1 Tilapia sample preparation

Tilapia tissue muscle samples were prepared by filleting the fish into two, with one fillet cut into smaller pieces prior to being placed into individually labelled bags before freezing. For some fish, the entire GIT (intestines, pyloric ceca, stomach and oesophagus) was located and removed, and the entire contents squeezed into individually labelled bags and subsequently frozen. Some fish samples had the entire GIT removed, with contents intact and frozen straight after to preserve the whole GIT plus contents.

Cut tilapia muscle samples were labelled (Ta), tilapia GIT contents were labelled (GI) and tilapia intact gastrointestinal tracts were labelled (GIT). The site location they were caught from and the date of isolation was recorded, as well as whether they were a farmed/caged (CT) or a wild tilapia (WT) (Tables 2.4 and 2.5).

ID	SITE LOCATION	CAGED (CT) OR WILD (WT)	DATE OF ISOLATION
Ta1	SITE 7B	CT3	May 2019
Ta2	SITE 6B	CT4	May 2019
Ta3	SITE 11E	CT3	May 2019
Ta4	SITE 11E	CT1	May 2019
Ta5	SITE 11F	WT3	May 2019
Ta6	SITE 13B	CT2	May 2019
Ta7	SITE 7B	CT2	May 2019
Ta8	SITE 7B	CT4	May 2019
Ta9	SITE 11F	WT1	May 2019
Ta10	SITE 11F	WT2	May 2019
Ta11	SITE 11E	CT2	May 2019
Ta12	SITE 1B	CT2	May 2019
Ta13	SITE 1B	CT3	May 2019
GI1	SITE 9B	CT1	May 2019
GI2	SITE 9B	CT2	May 2019
GI3	SITE 9B	CT3	May 2019
GI4	SITE 9B	CT4	May 2019
GI5	SITE 9E	WT1	May 2019
Ta14	SITE 9B	CT1	May 2019
Ta15	SITE 9B	CT3	May 2019
Ta16	SITE 13D	WT3	May 2019
Ta17	SITE 1B	CT1	May 2019
Ta18	SITE 9B	CT4	May 2019
Ta19	SITE 9E	WT3	May 2019
Ta20	SITE 13B	CT3	May 2019
Ta21	SITE 13D	WT4	May 2019
Ta22	SITE 9B	CT2	May 2019
Ta23	SITE 9E	WT1	May 2019
Ta24	SITE 13B	CT1	May 2019
Ta25	SITE 13D	WT2	May 2019
Ta26	SITE 9E	WT2	May 2019
Ta27	SITE 13D	WT1	May 2019
Ta28	SITE 1A	WT1	May 2018

Table 2.4 Fish samples analysed (May 2019 and 2018). This table shows the different tilapia samples used in this study. The date, site number and location they were caught from was recorded and whether they were a caged (CT) or a wild tilapia (WT). Tilapia muscle samples used were labelled (Ta) and tilapia gastrointestinal tract contents were labelled (GI). Most samples were collected in May 2019, but some samples from May 2018 were also analysed.

Ta29	SITE 4D	WT1	May 2019
Ta30	SITE 4D	CT1	May 2019
Ta31	SITE 4D	CT2	May 2019
Ta32	SITE 1C	WT2	May 2019
Ta33	SITE 4D	WT3	May 2019
Ta34	SITE 1C	WT3	May 2019
Ta35	SITE 16B	CT2	May 2019
Ta36	SITE 16B	CT3	May 2019
Ta37	SITE 1C	WT1	May 2019
Ta38	SITE 16B	CT1	May 2019
Ta39	SITE 15B	WT3	May 2019
Ta40	SITE 15B	WT1	May 2019
Ta41	SITE 6B	CT2	May 2019
Ta42	SITE 7D	WT1	May 2019
Ta43	SITE 7D	WT2	May 2019
Ta44	SITE 7D	WT3	May 2019
Ta45	SITE 6B	CT1	May 2019
Ta46	SITE 6B	CT3	May 2019
Ta47	SITE 7B	CT1	May 2019
Ta48	SITE 15B	WT2	May 2019
Ta49	SITE 10	CT3	May 2018
Ta50	SITE 7	CT2	May 2018
Ta51	SITE 10	WT1	May 2018
Ta52	SITE 9B	CT3	May 2019
Ta53	SITE 4D	WT2	May 2019
Ta54	SITE 3C	WT2	May 2018
Ta55	SITE 1A	WT1	May 2018
Ta56	SITE 1A	WT2	May 2018
Ta57	SITE 1A	WT3	May 2018
Ta58	SITE 1B	CT2	May 2018
Ta59	SITE 1B	CT3	May 2018
Ta60	SITE 1B	CT1	May 2018

Table 2.4 (continued) Fish samples analysed (May 2019 and 2018). This table shows the different tilapia samples used in this study. The date, site number and location they were caught from was recorded and whether they were a caged (CT) or a wild tilapia (WT). Tilapia muscle samples used were labelled (Ta) and tilapia gastrointestinal tract contents were labelled (GI). Most samples were collected in May 2019, but some samples from May 2018 were also analysed.

ID	SITE LOCATION	CAGED (CT) OR WILD (WT)	DATE OF ISOLATION
GIT6	SITE 4	CT2	Jan 2019
GIT7	SITE 4	WT2	Jan 2019
GIT10	SITE 7B	CT1	Jan 2019
GIT13	SITE 18A	WT1	Jan 2019
GIT15	SITE 1A	WT1	Jan 2019
GIT19	SITE 1B	CT1	Jan 2019
GIT20	SITE 1B	CT2	Jan 2019
Ta61	SITE 1A	WT1	Jan 2019
Ta62	SITE 1A	WT2	Jan 2019
Ta63	SITE 1A	WT3	Jan 2019
Ta64	SITE 1A	WT4	Jan 2019
Ta65	SITE 1B	CT1	Jan 2019
Ta66	SITE 1B	CT2	Jan 2019
Ta67	SITE 1B	CT3	Jan 2019
Ta68	SITE 1B	CT4	Jan 2019
Ta69	SITE 4	CT1	Jan 2019
Ta70	SITE 4	CT2	Jan 2019
Ta71	SITE 4	CT3	Jan 2019
Ta72	SITE 4	WT1	Jan 2019
Ta73	SITE 4	WT2	Jan 2019
Ta74	SITE 4	WT3	Jan 2019
Ta75	SITE 4	WT4	Jan 2019
Ta76	SITE 7B	CT1	Jan 2019
Ta77	SITE 7B	CT2	Jan 2019
Ta78	SITE 7B	CT3	Jan 2019
Ta79	SITE 18A	WT1	Jan 2019
Ta80	SITE 18A	WT2	Jan 2019

Table 2.5 Fish samples analysed (January 2019). This table shows the different tilapia samples used in this study. The date, site number and location were caught from is given and whether they were a caged (CT) or a wild tilapia (WT). Tilapia muscle samples used were labelled (Ta) and tilapia intact gastrointestinal tracts were labelled (GIT). These samples were all collected in January 2019.

2.2 Alkaline digestion of fish samples

Potassium hydroxide (KOH) was chosen as a suitable digestion reagent, at a 10% solution concentration (Thiele et al., 2019). KOH has been shown to be the most viable extraction media, allowing the digestates to be filterable, without polymer

modification. 10g of KOH flakes (Thermo Fisher Scientific) was weighed out and added to 100ml of reverse osmosis (RO) water, this solution was then poured onto either the GIT contents, the whole intact GITs or muscle/tissue samples from each fish sample. These samples were then gently mixed, sealed with parafilm (Bemis) before incubation at 60°C for 19-21 hours (hr) (Alexandre et al., 2016).

2.2.1 GIT content samples digestion with KOH

Each tilapia GIT contents sample was weighed in their individual bags (see Table 2 in appendix), 100ml of RO water was poured into the bag to wash the contents into a labelled conical flask. 10g of KOH flakes (to make a 10% solution) were added to the flask and the empty bag was re-weighed, to determine the original weight of the GIT contents.

2.2.2 Whole GIT samples digestion with KOH

Intact GIT samples were weighed in their individual bags (see Table 2 in appendix), 100ml of RO water was poured into the bag to wash the GIT into a labelled conical flask. A 10% solution of KOH solution was added to the flask. These samples contained more organic content, and digestion at 60°C for 24hr was not sufficient to digest this material. KOH digestion at a lower temperature, 40°C for 12 days (d) and 16d was also tested as an alternative for these samples.

2.2.3 Tissue samples digestion with KOH

Whole tissue/muscle samples were weighed, and their weight recorded. Small 10mm^3 pieces of the tissues were cut, weighed and recorded again (see Table 1 in appendix), before being placed into individually labelled conical flasks, when a

10% solution of KOH solution was added. The remaining tissue sample placed back into the freezer.

2.3 Filtration of digested fish samples

Following 60°C incubation for 19-21hr, conical flasks were removed and left on the bench. Due to their micro size, contamination from atmospheric microplastics poses a risk in producing inaccurate results. To prevent contamination all samples were filtered over Whatman glass microfibre filters, Grade GF/A, 1.6 µm pore size (Sigma-Aldrich), which were folded to sit inside a glass funnel (Pyrex). All glass filter funnels, scalpels, forceps, scissors and weighing scales used were washed with 70% ethanol. Each digested sample was poured onto the filter, with unwanted liquid passing through the filter and collecting in a large media bottle, leaving any non-digested content to collect on the filter paper. Post-filtration, petri dishes (Sigma-Aldrich) were labelled with the samples details and the filter paper was unfolded and placed flat in the petri dish to air dry for 24hr.

2.4 Source of positive controls for plastics

2.4.1 Microbeads

'Clean & Clear' face wash (Johnson & Johnson Limited) (Figure 2.6) used to contain PE blue and white microbeads. Their use was discontinued in 2017 with the microbeads replaced with biodegradable cellulose and jojoba beads, derived from plants (Clean & Clear, 2017). A microbead-containing version of the face wash was used for a source of primary microplastics for a control. Beads were extracted by adding 400ml of RO water to the face wash, followed by centrifugation at 3000g for 15 minutes (min). The resulting solution was filtered using sterile muslin

cloths; this was repeated 4 times. Whatman glass microfiber filters were used to filter the solution, and the filter was left to air dry prior to recovery from the filter.

Figure 2.6 Clean & Clear face wash. This product (from 2017) contained both white and blue microbeads, these were extracted in the initial part of the project. The product composition has now changed and microbeads have been replaced with biodegradable jojoba and cellulose beads, derived from plants (Clean&Clear, 2017).

2.4.2 Fishing Nets

Fishing nets caught from Lake Victoria, abandoned as ghost gear from fishing boats, were split according to colour (Figure 2.7). Blue, yellow, white and green netting were split into singular strands, weighed and length measured (see Table 3 in appendix). These were then individually digested with KOH (10% solution) for 24hr at 60°C. These were then filtered and stained using Nile red (Sigma-Aldrich) and DAPI (Thermo Fisher Scientific). These net pieces were also used in method optimisation, by allowing dye efficacy of both stains to be tested, as well

as investigating if any plastic polymers are degraded at varying temperatures and time lengths of KOH digestion.

Figure 2.7 Fishing net caught from Lake Victoria. The collection of fishing nets was split according to colour – blue, yellow, white and green. These net pieces were classed as plastic microfibres and so were used as positive controls for testing dye efficacy.

2.5 Fluorescent staining

2.5.1 Nile red

Nile red (Sigma-Aldrich) is a lipid soluble fluorescent dye which allows the in-situ staining of lipids, and subsequent visualisation under a microscope. Nile red was diluted with acetone (Thermo Fisher Scientific) to give an optimum concentration of 10µg/ml (Maes et al., 2017). An incubation time of 30min (Joon Shim et al., 2016) was adopted for staining, as incubation times longer than 30 to 60min led to gradual aggregation of unabsorbed dye and stronger background staining of the filters.

An 1/8th of each filter paper was cut (Figure 2.8), placed on a glass side inside a staining box and 200µl of diluted Nile red was covered over the filter paper slice. During the incubation period, the staining box was covered in foil, as the dye is photosensitive.

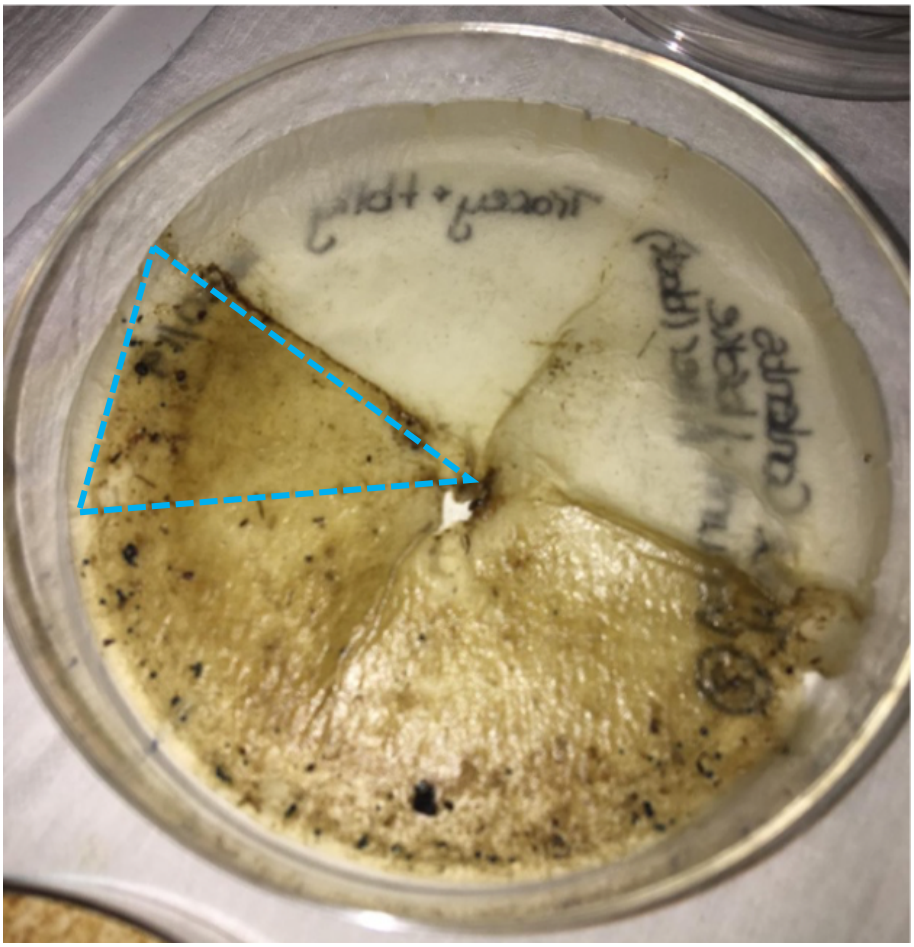

Figure 2.8 Petri dish containing filer paper. This was taken after the digestion and filtration processes were completed (prior to drying) and shows a typical 1/8th cut of filter paper (demonstrated by blue dashed line) used for staining and microscopic analysis.

2.5.2 DAPI

DAPI (4',6-diamidino-2-phenylindole) (Thermo Fisher Scientific) staining solution is a fluorescent stain for labelling DNA and therefore biological material in fluorescent microscopy. DAPI was dissolved in water to give a final concentration

of 0.5µg/ml (Stanton et al., 2019). DAPI staining was performed after all other staining and acts as a counterstain.

Following staining and incubation with Nile red, the same 1/8th of filter paper was covered with 200µl of diluted DAPI solution and placed in the foiled staining box to incubate for 5min (Figure 2.9). The sample was then ready for fluorescent microscopy analysis.

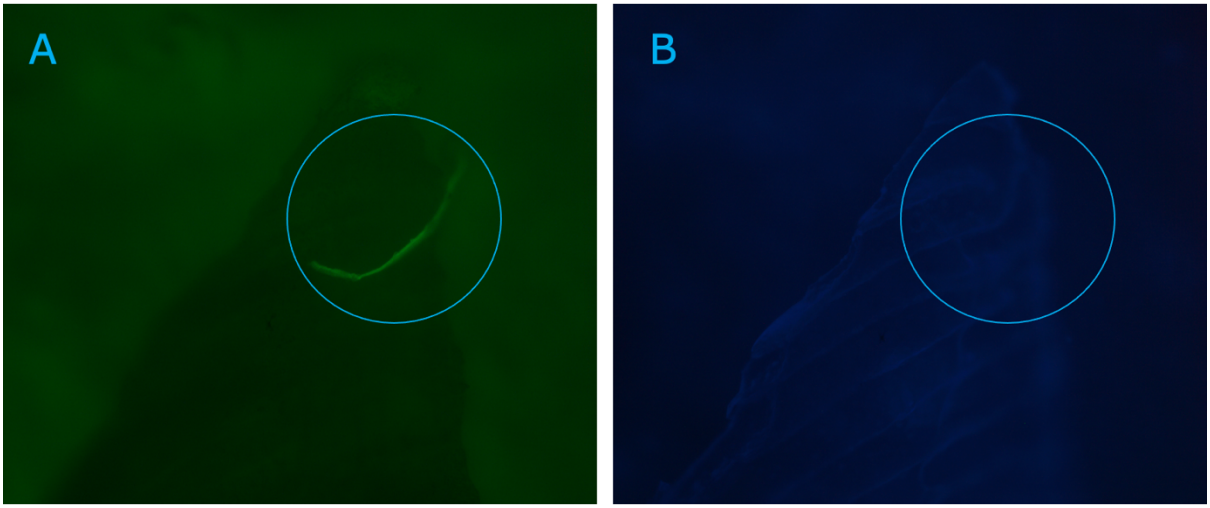

Figure 2.9 Example of staining with Nile red or DAPI stain. This image shows an example of how microplastics fluoresce green when stained with Nile Red (A) and organic material fluoresces blue after using the counterstain DAPI (B). A fibre is identified here from a wild tilapia muscle sample after 30 minutes incubation with Nile Red (A). Image B is after 5 minutes incubation with DAPI, highlighting that this fibre is not an organic material. Image taken from area 14 on the 1/8th of filter paper on the Lecia DFC420 microscope at x40 magnification.

2.6 Fluorescent microscopic detection

Stained samples were viewed under the Lecia DFC420 microscope. For initial fluorescent analysis for the Nile Red stain, a high powered L5 blue light (excitation wavelength, 430−490 nm; emission wavelength, 510−560 nm) was used. This was combined with an orange filter to remove any unwanted background interference. The exposure values used were dependent on the final thickness of

debris on the filter paper, post-digestion. A gamma value of 0.65 and a gain of 2.1 were applied to all samples. A magnification of x40 was used to view all samples and take images. Some images of the smaller micro fragments and beads were taken at a x100 magnification (Figure 2.10). The images taken were labelled to show their sample ID and the presence or lack of microplastics, as well as their location on the filter paper.

Secondary DAPI stain analysis used the same microscope but was observed in blue fluorescence with an A4 FLUO light (excitation wavelength, 355–405 nm; emission wavelength, 420–480 nm). A gamma value of 0.60 and a gain of 1.0 was applied to all samples.

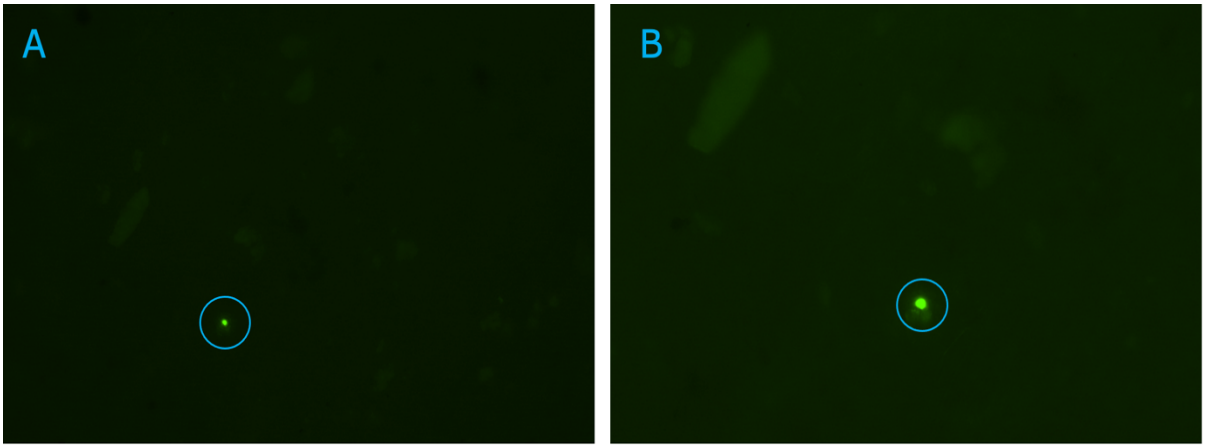

Figure 2.10 Example of X40 magnification or X100 magnification. The image shown is an example of a fluorescent image taken on the Leica DFC420 microscope at X40 magnification (A) and an image taken at a X100 magnification (B). A bead is identified here from a wild tilapia muscle sample after 30 minutes incubation with Nile Red. Images taken from area 30 on the 1/8th of filter paper.

2.6.1 Numbered filter paper areas

Whatman glass microfiber filters were divided into 1/8th pieces for staining and subsequent microscope analysis. This 1/8th was further divided into 5mm^2 boxes, each box was numbered, with numbers ranging from 1 to 38 (Figure 2.11). During microscopic analysis when a microplastic piece was identified, the numbered area where it was identified was recorded.

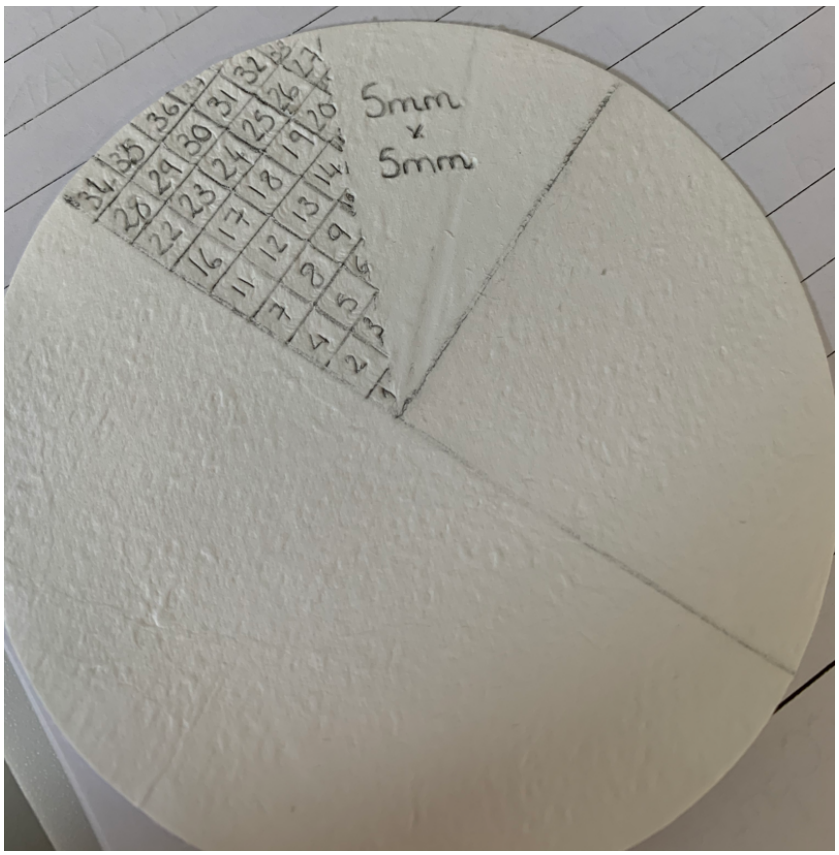

Figure 2.11 Filter paper areas. This shows the 5mm^2 boxes the 1/8th of stained filter paper was divided into. Box numbers ranged from 1 to 38 and this number was recorded when a microplastic was identified.

2.7 Extraction of genomic DNA

The 1/8th of filter paper used for fluorescent microscopy was washed and used to extract genomic DNA from plastispheres present on the microplastics. 440µl of PBS (Thermo Fisher Scientific) was washed over the filter paper and collected in a microcentrifuge tube (Thermo Fisher Scientific). 200µl of buffer AL (Qiagen) and 20µl proteinase K (Qiagen) was added, this was incubated for 3hr at 56°C. Extraction of genomic DNA from this was carried out using the DNeasy Blood and Tissue kit (Qiagen) following the manufacturer's protocol. Genomic DNA was eluted from the spin column with 200µl of buffer AE (Qiagen), incubated (room temperature, 1min) prior to centrifugation (1min, 6000g). Eluted DNA was stored at -20°C.

2.7.1 Assessment of the quality and quantity of DNA

The nanodrop 8000 (Thermo Fisher Scientific) was used to assess the quantity and quality of the extracted genomic DNA.

2.8 Polymerase Chain Reactions

Polymerase chain reaction (PCR) was used to screen for the presence of bacterial DNA and bacterial species-specific DNA using a Genetouch (Bioer) PCR machine.

2.8.1 Primers for PCR

Primer pairs that targeted a range of different bacterial specific genes were used in this study (Table 2.12). The V_3V_6 primer pair (Chakravorty et al., 2007) targets the 16s Ribosomal rRNA and was used to detect the presence of bacterial DNA, potentially from the plastisphere on the microplastic's surface. The remaining primer pairs (Table 2.12) were used to screen for the specific bacterial

genus/species; *carA (Pseudomonas fragi, Pseudomonas putida* and *Pseudomonas lundensis)* (Ercolini et al., 2007), *sub0888 (Streptococcus uberis)* (Leigh et al., 2010), *tyrB* (*Klebsiella pneumoniae)* (Heilbronn et al., 1999), *uspA* (*Escherichia coli)* (Chen and Griffiths, 1998), *uidA* (*Escherichia coli)* (Heijnen and Medema, 2006), *porA* (*Campylobacter coli* and *Campylobacter jejuni*) (Fontanot et al., 2014), *jej* (*Campylobacter coli* and *Campylobacter jejuni*) (Linton et al., 1997) and *lact* (*Lactobacillus*) (Dubernet et al., 2002). These bacteria reflect a small proportion of the bacteria which can be associated with an aquatic environment and/or fish.

Gene Name	Forward primer	Reverse primer	Amplicon size (bp)	Annealing temperature	Reference
V₃V₆	5'ACTYCTACGGRAGGCWGC'3	5'CRRCACCAGCTGACGAC'3	739	58°C	(Chakravorty et al., 2007)
carA	5'CGTCAGCACCGAAAAAGCC'3	5'TGATGRCCSAGGCAGATRCC'3	370	56.6°C	(Ercolini et al., 2007)
carA	5'ATGCTGGTTGCYCGTGGC'3	5'TGATGRCCSAGGCAGATRCC'3	230	56.6°C	(Ercolini et al., 2007)
carA	5'TGTGGCGATTGCAGGCATT'3	5'TGATGRCCSAGGCAGATRCC'3	530	56.6°C	(Ercolini et al., 2007)
sub0888	5'CTTTATGAAAATAGCCAAGCTGAAA'3	5'TGTGAGCCAGTTGGAGGAAG'3	974	56.1°C	(Leigh et al., 2010)

Table 2.12 Table of primers used in this study. This table shows the primer name, sequence, their amplicon size in base pairs (bp) and their annealing temperatures (°C). The *V₃V₆* primer pair (Chakravorty et al., 2007) targets the 16s Ribosomal rRNA and was used to detect the presence of bacterial DNA on the microplastic's surface. The remaining primer pairs were used to screen for the presence of specific bacterial genus/species present; *carA (Pseudomonas fragi, Pseudomonas putida, Pseudomonas lundensis)* (Ercolini et al., 2007), *sub0888 (Streptococcus uberis)* (Leigh et al., 2010).

Gene Name	Forward primer	Reverse primer	Amplicon size (bp)	Annealing temperature	Reference
tyrB	5'GGCTGTACTACAACGATGAC'3	5'TTGAGCAGGTAATCCACTTTG'3	931	54.7°C	(Heilbronn et al., 1999)
uspA	5'CCGATACGCTGCCAATCAGT'3	5'ACGCAGACCGTAGGCCAGAT'3	884	58.9°C	(Chen and Griffiths, 1998)
uida	5'TATGGAATTTCGCCGATTTT'3	5'TGTTTGCCTCCCTGCTGCGG'3	166	52.5°C	(Heijnen and Medema, 2006)
porA	5'TGGTTGGGATGCAACTCTT'3	5'GCCTACACGAACTGTTTCG'3	211	56.1°C	(Fontanot et al., 2014)
jej	5'AATCTAATGGCTTAACCATTA'3	5'GTAACTAGTTTAGTATTCCGG'3	854	50.8°C	(Linton et al., 1997)
lact	5'CTTGTACACACCGCCCGTCA'3	5'CTGAAAACTAAACAAAGTTTC'3	250	51.1°C	(Dubernet et al., 2002)
M13 reverse /T7	5'GTAAAACGACGGCCAG'3	5'CAGGAAACAGCTATGAC'3	178 (without insert)	54.8°C	(Tabor and Richardson, 1987)

Table 2.12 (continued) Table of primers used in this study. This table shows the primer name, sequence, their amplicon size in base pairs (bp) and their annealing temperatures (°C). The remaining primer pairs were used to screen for the presence of specific bacterial genus/species present; *tyrB* (*Klebsiella pneumoniae)* (Heilbronn et al., 1999), *uspA* (*Escherichia coli)* (Chen and Griffiths, 1998), *uidA* (*Escherichia coli)* (Heijnen and Medema, 2006), *porA* (*Campylobacter coli* and *Campylobacter jejuni*) (Fontanot et al., 2014), *jej* (*Campylobacter coli* and *Campylobacter jejuni*) (Linton et al., 1997) and *lact* (*Lactobacillus*) (Dubernet et al., 2002). The *M13/T7* primer pair (Tabor and Richardson, 1987) are used for PCR amplification, to sequence inserts that have been cloned.

2.8.2 PCR with GoTaq master mix

PCRs were run according to the manufacturer's protocol using GoTaq green master mix (Promega). The conditions were an initial incubation for 3min at 95°C. Followed by 30 cycles of denature for 30sec at 98°C, annealing for 30sec at 58°C and extension for 20sec at 72°C. Followed by a final extension for 7min at 72°C.

2.8.3 Agarose gel electrophoresis

PCR products were run on a 1% agarose gel (Invitrogen) using Tris-acetate Ethylenediaminetetraacetic acid (TAE, Thermo Fisher Scientific), containing 2 µl of Gel Red (Invitrogen). Loading dye was already present in the PCR product, so 20µl of PCR product was loaded onto the gel, along with 5µl of 1kb ladder (Promega), prior to electrophoresis (Biorad, 70V, 45min). 5µl of remaining PCR product was frozen at –20°C.

2.9 Cloning

Cloning was carried out using the TOPO TA Cloning Kit (Invitrogen) following the manufacturer's protocol. Nutrient agar plates (Oxoid) containing ampicillin (50µg/ml), were spread with 40µl of 40mg/ml of X-gal. The cloning mix was spread on two plates, 50µl on one and 150µl on the other and both incubated overnight (37°C). White colonies formed were picked and suspended in both 3ml of nutrient broth containing ampicillin (50µg/ml) and 3ml of nutrient both containing kanamycin (50µg/ml) and incubated overnight in the thermo shaker (37°C, 200rpm).

2.9.1 Plasmid purification

The QIAprep spin miniprep kit (Qiagen) was used to extract plasmid DNA, following the manufacturer's protocol. Plasmid DNA was eluted in buffer EB (Qiagen) and stored at -20°C.

2.9.2 Screening of positive clones using PCR

PCR on the purified plasmid DNA from the positive clones was carried out using GoTaq (Promega), with M13 reverse and T7 primers (Table 2.12). The conditions were an initial incubation for 3min at 95°C. Followed by 30 cycles of denature for 30sec at 98°C, annealing for 30sec at 58°C and extension for 20sec at 72°C. Followed by a final extension for 7min at 72°C. The PCR products were run as previously described (see section 2.8.3).

2.10 Scanning electron microscopy

2.10.1 Analysis of the SEM

The Nanoscale and Microscale Research Centre (nmRC) at the University of Nottingham used their Scanning Electron Microscope (SEM) to analyse the samples, and further investigate the potential microplastics observed for the presence of a biofilm. COVID-19 prevented us from analysing the samples ourselves alongside the technical support staff of the nmRC.

A finely focused electron beam was scanned across the samples, generating electron signals, these were amplified and detected to produce an image of the microplastic's surface in the samples. An energy dispersive X-ray microanalysis (X-Max -150 EDX) system was used for high sensitivity chemical analysis to determine the elemental composition of areas in the sample.

2.10.2 Samples analysed by SEM

A section of Whatman microfibre filter paper with no reagents on and a filter paper section with KOH (10% solution), Nile Red and DAPI stains on it, were sent as controls for SEM analysis. Their structure and elemental composition were recorded, as this highlighted any interference that came from the reagents or equipment used and therefore would be considered when screening for microplastics in the tilapia samples.

Macroplastic litter and nets collected from Lake Victoria, as well as extracted microbeads from the 2017 Clean & Clear facewash, were sent as controls of plastics for SEM analysis (Figure 2.13). Their structure and elemental composition were recorded, as this gave microplastic indicators that could be screened for in the tilapia samples.

The same filter paper samples used for fluorescent microscopy were sent for SEM analysis. These samples included four tilapia muscle samples (Ta18, Ta33, Ta44 and Ta48) and one tilapia GIT contents sample (GI5). This filter paper also contained KOH (10% solution) used to digest the organic material, as well as Nile Red and DAPI stains.

Untreated samples were also sent for SEM analysis, consisting of 1cm cubes of tilapia muscle (Figure 2.14), and 1cm sections of intestines from intact tilapia GIT (Figure 2.15). As samples were examined hydrated, there was no preparation required prior to scanning. These samples included four muscle samples (Ta20, Ta66, Ta69, Ta72) and one intact GIT (GIT20).

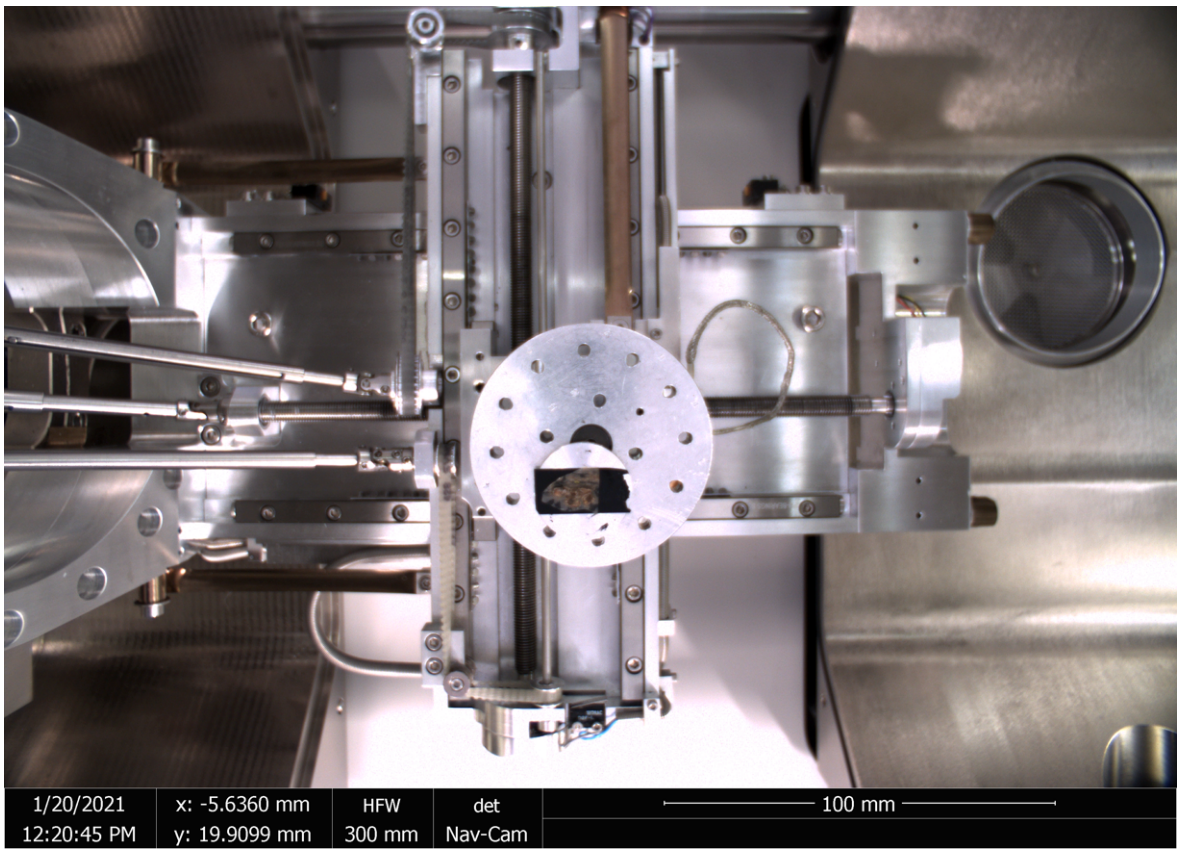

Figure 2.13 Analysis of macroplastic litter collected from Lake Victoria with environmental scanning electron microscope. This image shows a 1cm section of macroplastic litter found in Lake Victoria being analysed by the environmental scanning electron microscope (ESEM) at the Nanoscale and Microscale Research Centre (nmRC) (University of Nottingham). The macroplastic litter here is an item of food packaging and was used as a control for microplastic indicators. Image kindly provided by Nicola Weston at the nmRC.

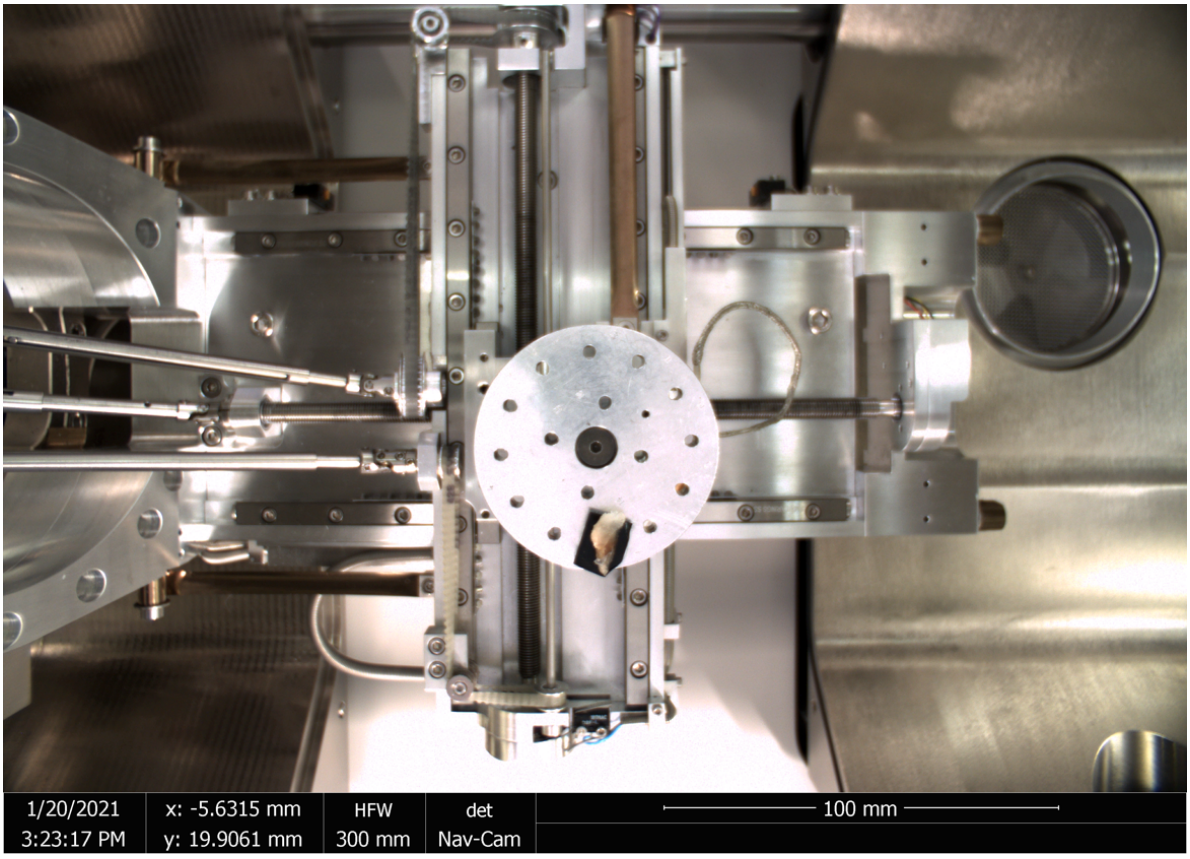

Figure 2.14 Analysis of tilapia muscle sample with environmental scanning electron microscope. This image shows a 1cm cube of tilapia muscle sample (Ta20; caged tilapia, site 13B), being analysed by the environmental scanning electron microscope (ESEM) at the Nanoscale and Microscale Research Centre (nmRC) (University of Nottingham). This muscle sample was untreated and examined hydrated. Image kindly provided by Nicola Weston at the nmRC.

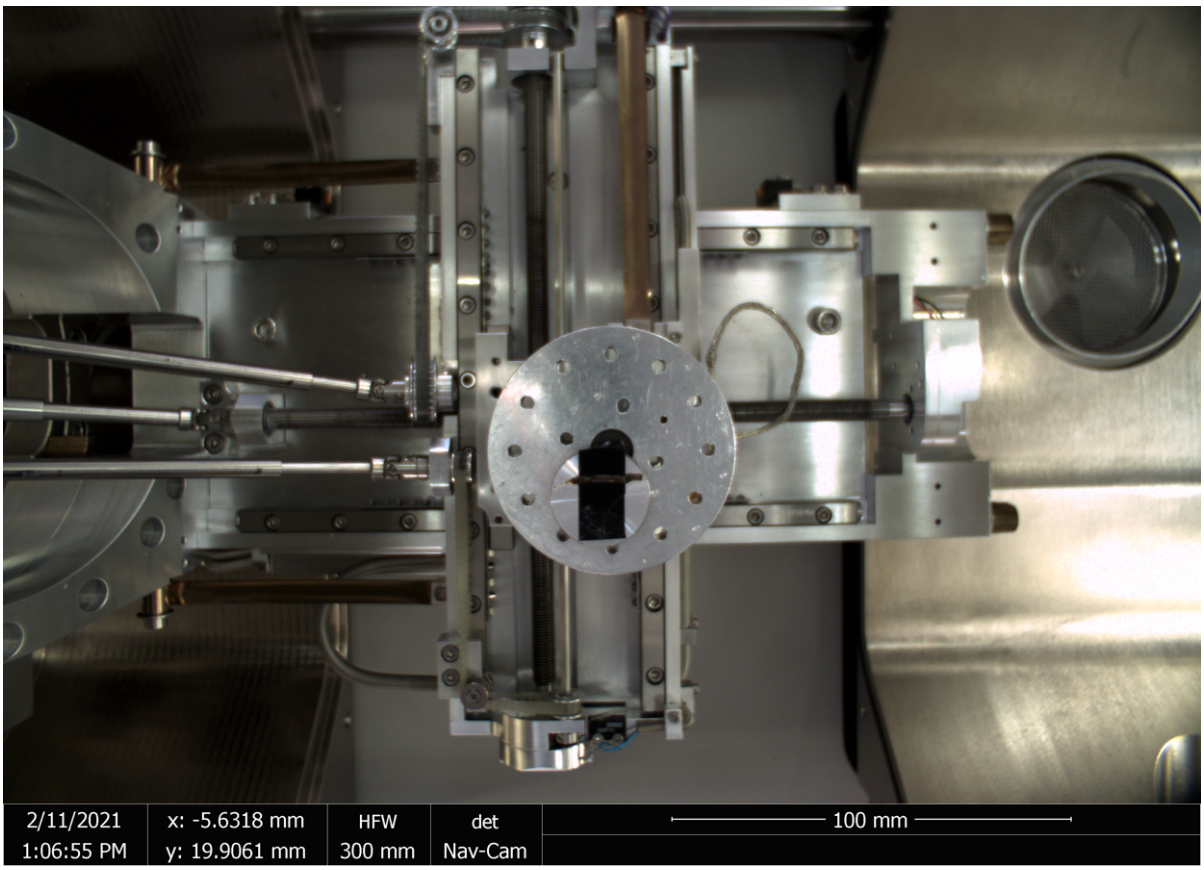

Figure 2.15 Analysis of tilapia intact gastrointestinal tract section sample with environmental scanning electron microscope. This image shows a 1cm section of intestines taken from intact gastrointestinal tract sample GIT20 (caged tilapia, site 1B), being analysed by the environmental scanning electron microscope (ESEM) at the Nanoscale and Microscale Research Centre (nmRC) (University of Nottingham). This GIT sample was untreated and examined hydrated. Image kindly provided by Nicola Weston at the nmRC.

2.10.3 Analysis using the environmental SEM

Environmental SEM (FEI Quanta 650 ESEM) allows for the imaging of samples with minimal preparation and adds variables such as hydration, thermal cycling, and the introduction of gas to characterize in situ dynamic changes. Images were taken in Low Vac mode with water vapour as the imaging gas, and using the Large Field Gaseous Detector (LFD) to obtain topographical images and the Back Scattered Detector (BSE) to obtain compositional images (a higher atomic number

appears brighter). Chamber pressure was in the range of 60 to 70 Pa in most cases (this is displayed in the individual image databar). In this study they were used to examine the fully hydrated samples.

Filter papers were mounted onto subs using carbon adhesive tape, and for the unfiltered frozen samples, a section was cut, thawed and placed on a stub, with any excess water wiped off. All samples were imaged using the same parameters. EDX spectra and maps were obtained using the Oxford Instruments Aztec system. The EDX system determined the elemental composition of areas in the sample. A scale was developed to group detected elements by their concentrations, measured in cps/eV (Table 2.16). A value >100 cps/eV was grouped very high, 60-99 cps/eV was grouped high, 20-59 cps/eV was medium, 10-19 cps/eV was low and <10 was grouped as trace.

Groups	Amount detected (cps/eV)
Very high	>100
High	60-99
Medium	20-59
Low	10-19
Trace	<10

Table 2.16 Groups for cps/eV amounts detected using EDX. This table shows the scale developed to group detected elements by their concentrations, after EDX analysis. Concentrations were measured in cps/eV, a value >100 cps/eV was grouped very high, 1-60-99 cps/eV was grouped high, 20-59 cps/eV was grouped medium, 10-19 cps/eV was grouped low and <10 was grouped as trace.

3.0 Results

3.1 Analysis of positive controls for plastic

To test the reliability of the Nile Red and DAPI stains, a mixture of microbeads from the face wash and different coloured net strands from macroplastic litter from Lake Victoria were digested, filtered and analysed by fluorescent microscopy, following staining with Nile Red and DAPI. The net strands fluoresced highly with Nile Red, and did not fluoresce with the counterstain DAPI. Figure 3.1 shows a yellow net stand fluorescing with Nile Red and not fluorescing with DAPI stain. As these net strands were taken from macroplastic litter, the samples appeared larger than microfibres would appear under the same microscope magnification view.

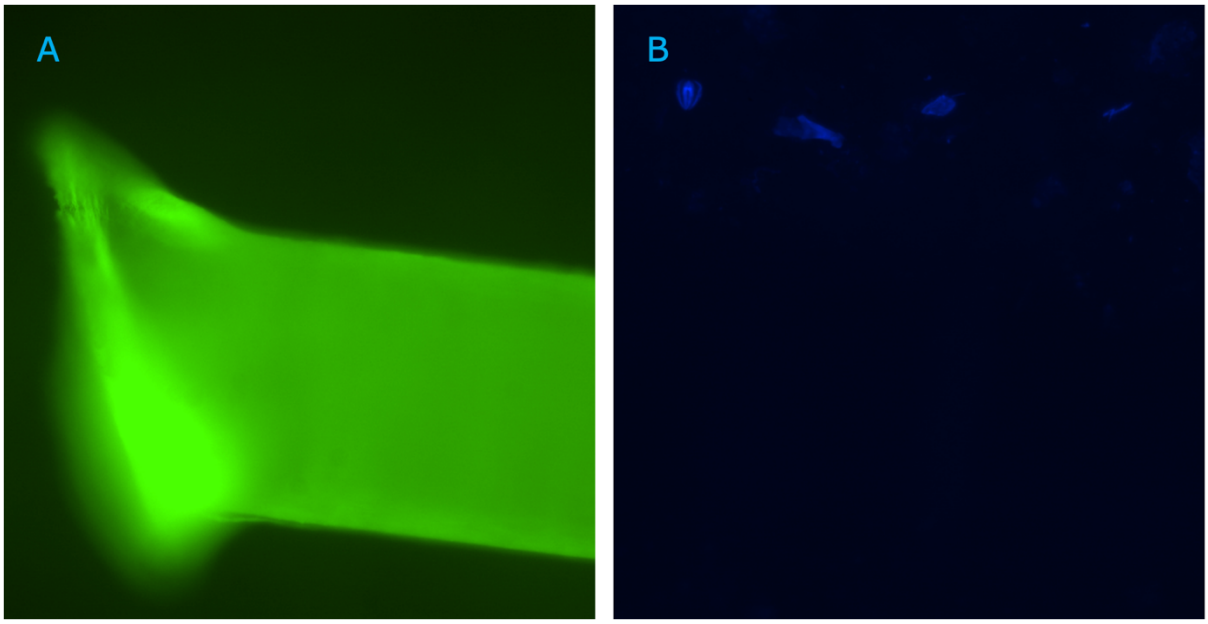

Figure 3.1 Positive control for plastic net. This image shows a yellow macroplastic net strand from Lake Victoria, used as a positive control in this study. Image A is after 30 minutes incubation with Nile Red. Image B is after 5 minutes incubation with DAPI. Image taken on Lecia DFC420 microscope at X40 magnification.

The facewash product used contained two different types of microbeads: smaller white beads and larger blue beads. Upon fluorescent analysis the white beads fluoresced highly and appeared non-uniform in their shapes. Figure 3.2 shows a blue net strand fluorescing highly, surrounded by the smaller fluorescing white microbeads from the facewash.

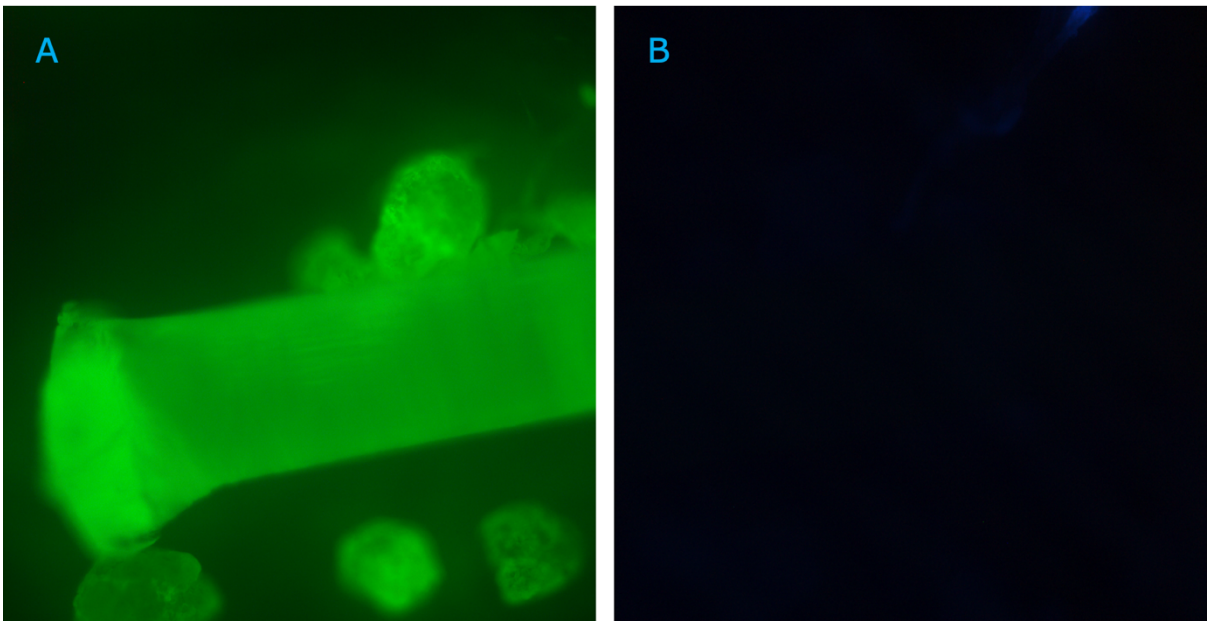

Figure 3.2 Positive control for white microbeads. This image shows a blue macroplastic net strand from Lake Victoria, surrounded by white microbeads from a facewash product, which were both used as positive controls in this study. Image A is after 30 minutes incubation with Nile Red. Image B is after 5 minutes incubation with DAPI. Image taken on Lecia DFC420 microscope at X40 magnification.

Interestingly fluorescent analysis of the larger blue microbeads found them to appear as dark spheres with Nile Red that glowed with DAPI stain. Figure 3.3 shows a larger blue bead appearing as a dark sphere with Nile Red (shown by the blue arrow) and fluorescing with DAPI stain. The smaller white beads can be seen fluorescing around the outside structure of the blue bead.

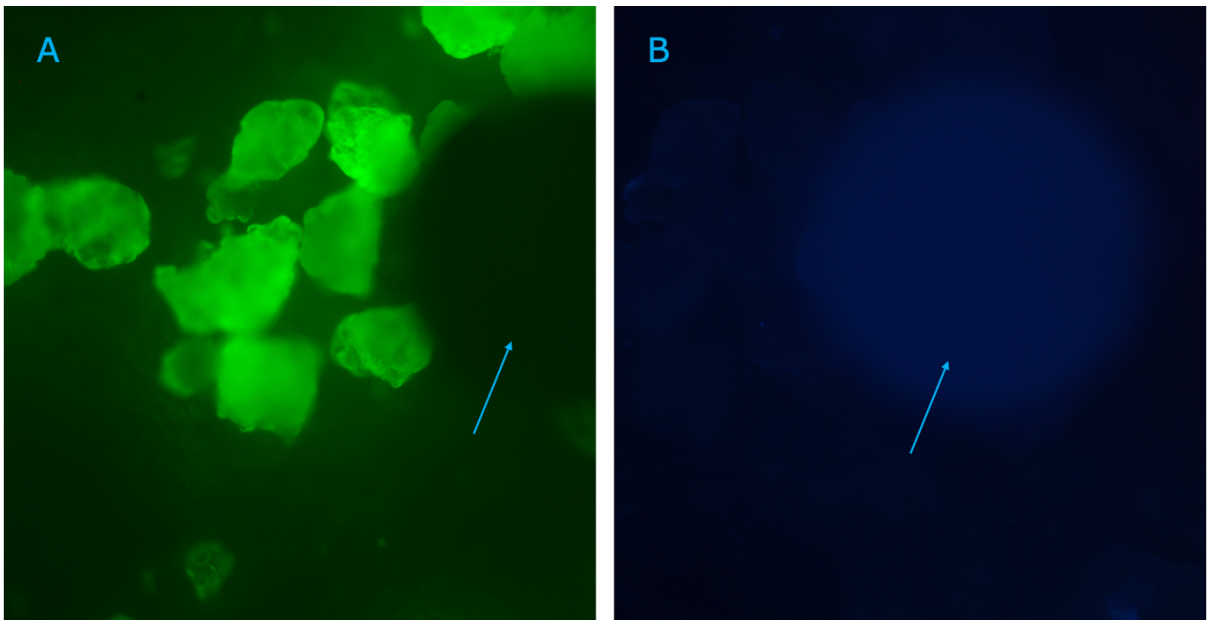

Figure 3.3 Positive control for blue microbeads. This image shows a larger blue microbead (shown by blue arrow), surrounded by smaller white microbeads, both from a facewash product and used as positive controls in this study. Image A is after 30 minutes incubation with Nile Red. Image B is after 5 minutes incubation with DAPI. Image taken on Lecia DFC420 microscope at X40 magnification.

3.2 Detection of microplastics in fish muscle

Eighty digested and filtered tilapia muscle samples (Ta) were analysed by fluorescent microscopy, following staining with Nile Red and DAPI. In total, 81 microplastic pieces were identified from the muscle samples. At least 1 microplastic piece was detected in 38 out of the 80 (48%) Ta, with 25% of samples having more than 1 microplastic piece. The prevalence of microplastics within each sample (see section 2.6.1 for division of filter paper area used) was grouped by

their structural appearance into either fragment, foam, film, fibre or bead (Table 3.4). Forty muscle samples had no identifiable microplastics, and 2 of the samples (Ta8 and Ta49) could not be analysed due to insufficient digestion of organic material in the sample.

ID	MP confirmed filter paper areas	MP type	MP amount
Ta1	-	-	0
Ta2	-	-	0
Ta3	3	Fragment	**1**
Ta4	-	-	0
Ta5	-	-	0
Ta6	-	-	0
Ta7	22 + 14	Film + Fragment	1 + 1 = **2**
Ta8	VOID	VOID	VOID
Ta9	9 + 20	Fibre + Bead	1 + 3 = **4**
Ta10	10	Bead + Film	3 + 1 = **4**
Ta11	-	-	0
Ta12	13	Bead	**2**
Ta13	-	-	0
Ta14	-	-	0
Ta15	14	Film	**2**
Ta16	1	Fragment	**4**
Ta17	-	-	0
Ta18	7	Fibre	**1**
Ta19	-	-	0
Ta20	15	Fragment	**1**
Ta21	-	-	0
Ta22	-	-	0
Ta23	-	-	0
Ta24	-	-	0
Ta25	-	-	0

Table 3.4 Microplastic presence in tilapia muscle samples. This table shows the microplastic (MP) type (fragment, foam, film, fibre and bead), amount present and the numbered filter paper area where it was identified in each tilapia muscle sample, after staining with Nile Red and DAPI and subsequent visualisation under the fluorescent microscope. Some sample's results were 'VOID' due to too much undigested debris present, making the sample unreadable under the microscope.

ID	MP confirmed filter paper areas	MP type	MP amount
Ta26	26	Fragment	**1**
Ta27	14 + 18	Foam + Fibre	1 + 2 = **3**
Ta28	-	-	0
Ta29	10	Film	**1**
Ta30	-	-	0
Ta31	-	-	0
Ta32	-	-	0
Ta33	12 + 13	Fibre	**2**
Ta34	-	-	0
Ta35	10	Fragment	**1**
Ta36	9 + 17	Fibre	**2**
Ta37	-	-	0
Ta38	8	Fibre	**11**
Ta39	13	Fragment	**1**
Ta40	14 + 60	Fragment	**2**
Ta41	-	-	0
Ta42	26	Fibre	**2**
Ta43	-	-	0
Ta44	7 + 8 + 20	Film + Fibre + Fragment	1 + 1 + 1 = **3**
Ta45	9	Fibre	**1**
Ta46	7	Film	**1**
Ta47	12	Fragment	**1**
Ta48	18 + 24	Fragment	4 + 2 = **6**
Ta49	VOID	VOID	VOID
Ta50	15	Fibre	**1**
Ta51	10 + 13	Fibre + Fragment	2 + 1 = **3**
Ta52	-	-	0
Ta53	16 + 18 + 20	Fibre + Film	1 + 2 = **3**
Ta54	-	-	0
Ta55	2	Fragment	**1**
Ta56	-	-	0
Ta57	-	-	0
Ta58	-	-	0
Ta59	-	-	0
Ta60	-	-	0

Table 3.4 (continued) Microplastic presence in tilapia muscle samples. This table shows the microplastic (MP) type (fragment, foam, film, fibre and bead), amount present and the numbered filter paper area where it was identified in each tilapia muscle sample, after staining with Nile Red and DAPI and subsequent visualisation under the fluorescent microscope. Some sample's results were 'VOID' due to too much undigested debris present, making the sample unreadable under the microscope.

ID	MP confirmed filter paper areas	MP type	MP amount
Ta61	30	Fragment	**2**
Ta62	3	Fibre	**1**
Ta63	24	Film	**1**
Ta64	-	-	0
Ta65	12	Fragment	**2**
Ta66	3	Fibre	**1**
Ta67	9	Fibre	**1**
Ta68	22	Fragment	**1**
Ta69	-	-	0
Ta70	-	-	0
Ta71	17	Fibre	**1**
Ta72	-	-	0
Ta73	-	-	0
Ta74	8 + 25	Fibre	**2**
Ta75	-	-	0
Ta76	-	-	0
Ta77	-	-	0
Ta78	9 + 19	Fibre	**2**
Ta79	-	-	0
Ta80	-	-	0

Table 3.4 (continued) Microplastic presence in tilapia muscle samples. This table shows the microplastic (MP) type (fragment, foam, film, fibre and bead), amount present and the numbered filter paper area where it was identified in each tilapia muscle sample, after staining with Nile Red and DAPI and subsequent visualisation under the fluorescent microscope.

Microplastics were found in 48% of the muscle samples. The most common microplastic type was a fibre, found in 21% of the muscle samples, representing 17 fish **(Table 3.5)**. Fragments were observed in 20% of the fish muscle, from 16 fish. Beads were observed in 6% of the fish muscle, from 5 fish. The least common type was foam which was only seen in one fish.

MP Type	Fragment	Foam	Film	Fibre	Bead
Amount in fish muscle	**27**	**1**	**10**	**35**	**8**
% of total MP identified	**34%**	**1%**	**12%**	**43%**	**10%**
% of fish identified	**20%**	**1%**	**10%**	**21%**	**6%**
Samples present	Ta3, Ta7, Ta16, Ta20, Ta26, Ta35, Ta39, Ta40, Ta44, Ta47, Ta48, Ta51, Ta55, Ta61, Ta65, Ta68	Ta27	Ta7, Ta15, Ta27, Ta29, Ta44, Ta46, Ta53, Ta63	Ta9, Ta10, Ta18,Ta33, Ta36, Ta38, Ta42, Ta44, Ta45, Ta50, Ta51, Ta53, Ta66, Ta67, Ta71, Ta74, Ta78	Ta9, Ta10, Ta12, Ta27, Ta62

Table 3.5 Quantitative microplastic analysis. This table shows the total amount of microplastics (MP) identified in digested tilapia muscle samples (Ta) samples after microscopic fluorescent analysis. Microplastics were grouped by the five types: fragment, foam, film, fibre and bead. The sample identity for each MP type present was recorded and the total amount of MPs present in all samples was determined. The percentage (%) of each type compared to the total microplastics content was calculated and the percentage (%) of total fish containing each microplastic type was calculated. The most common microplastic types were fibres and fragments (21% and 20%) respectively, with foam being the least common.

3.2.1 Fibre in tilapia muscle

Fibres were the most commonly identified microplastic with 35 pieces (43%) found in tilapia muscle samples. Fibres were identified in 17 of the fish analysed within the study; Ta9, Ta10, Ta18, Ta33, Ta36, Ta38, Ta42, Ta44, Ta45, Ta50, Ta51, Ta53, Ta66, Ta67, Ta71, Ta74 and Ta78. Sample Ta38 had the most fibres identified in all analysed muscle samples, with 11 fibres identified. Figure 3.6 shows a representative example of microplastic fibre found in the fish muscle following staining with Nile Red.

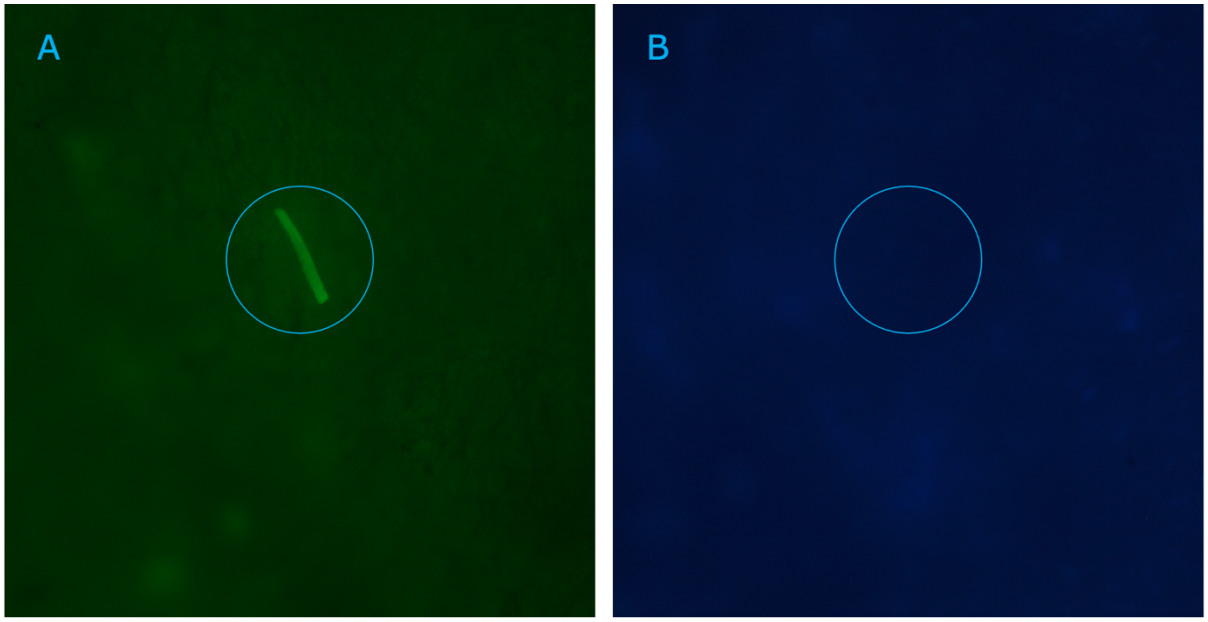

Figure 3.6 Example of microplastic fibre in tilapia muscle. This image shows an example of a fibre in caged tilapia muscle sample Ta36 (Site 16B). Image A is after 30 minutes incubation with Nile Red. Image B is after 5 minutes incubation with DAPI. Image taken from area 17 on the 1/8th of filter paper on Lecia DFC420 microscope at X40 magnification.

Muscle sample Ta38 had the highest volume of microplastics detected out of all muscle samples with 11 potential fibres detected (Figure 3.7).

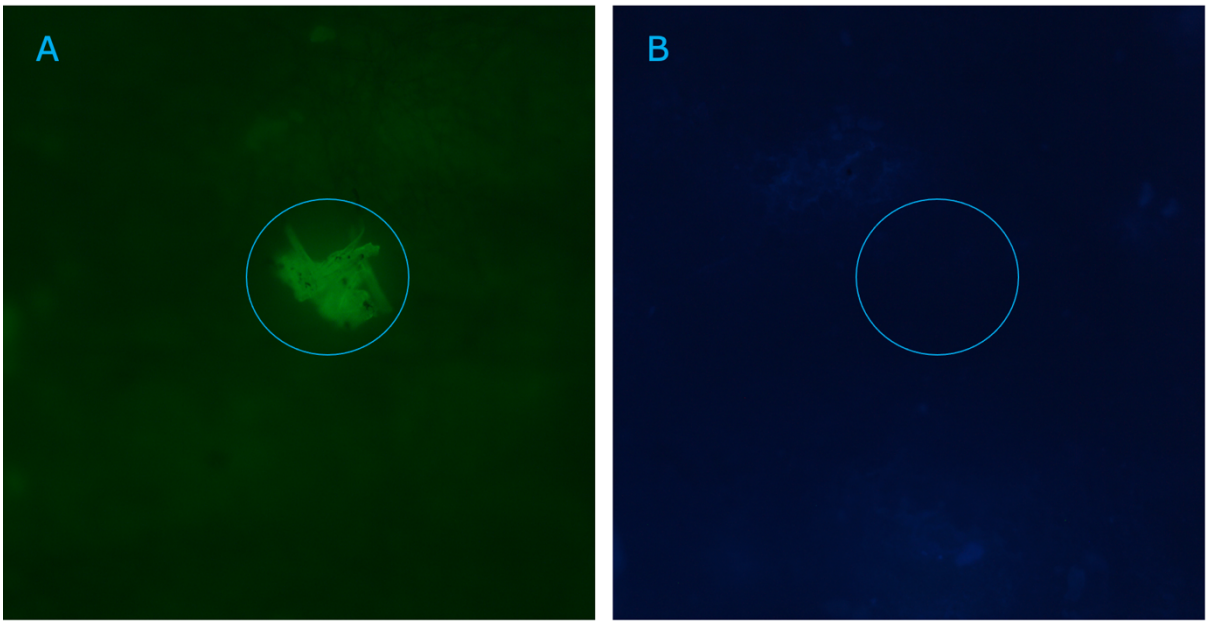

Figure 3.7 Example of multiple fibres in tilapia muscle. This image shows a clump of multiple fibres (n=11) identified in a caged tilapia muscle sample Ta38 (Site 16B). Image A is after 30 minutes incubation with Nile Red. Image B is after 5 minutes incubation with DAPI. Image taken from area 8 on the 1/8th of filter paper on Lecia DFC420 microscope at X40 magnification.

3.2.2 Fragment in tilapia muscle

Twenty-seven fragments (34%) were detected in the muscle samples, observed in 16 fish (Ta3, Ta7, Ta16, Ta20, Ta26, Ta35, Ta39, Ta40, Ta44, Ta47, Ta48, Ta51, Ta55, Ta61, Ta65 and Ta68). Ta16 and Ta48 had the most fragment, with 4 and 6 identified in each respectively (Figure 3.8).

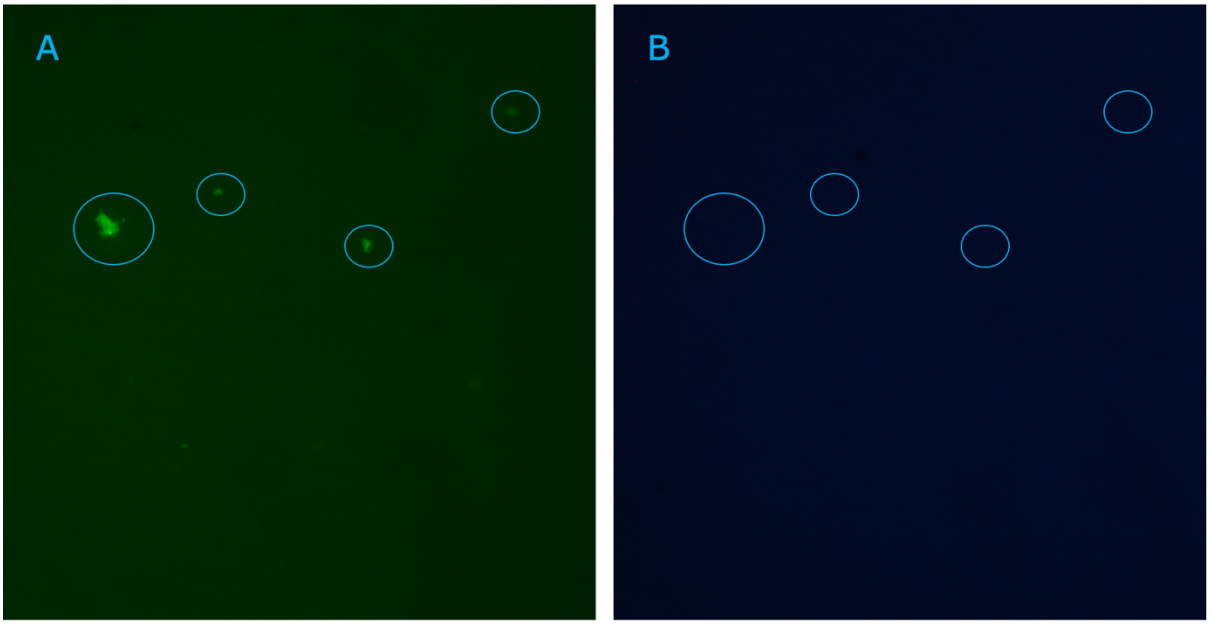

Figure 3.8 Example of microplastic fragments in tilapia muscle. This image shows an example of 4 fragments identified in wild tilapia muscle sample Ta48 (Site 15B). Image A is after 30 minutes incubation with Nile Red. Image B is after 5 minutes incubation with DAPI. Image taken from area 18 on the 1/8th of filter paper on Lecia DFC420 microscope at X40 magnification.

3.2.3 Film in tilapia muscle

Ten films (12%) were identified in the muscle samples, observed in 8 fish (Ta7, Ta15, Ta27, Ta29, Ta44, Ta46, Ta53 and Ta63). Ta15 and Ta53 both had the most films identified in all the muscle samples that were analysed, with 2 films identified in each sample. Figure 3.9 shows a representative example of microplastic film found in the fish muscle following staining with Nile Red.

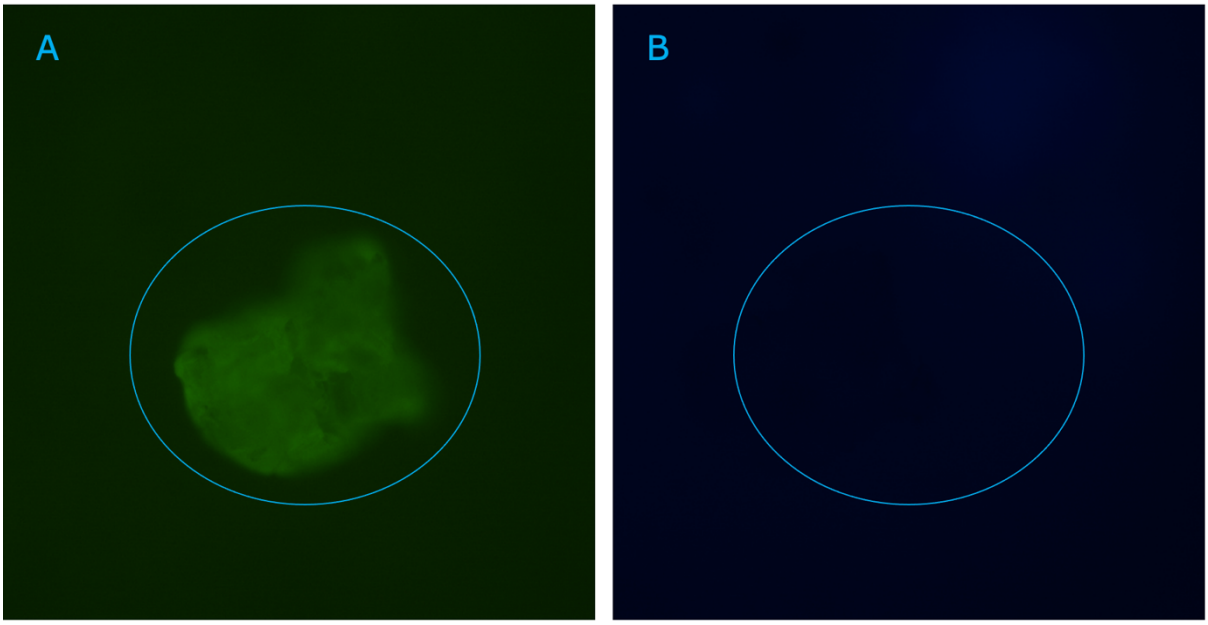

Figure 3.9 Example of microplastic film in tilapia muscle. This image shows an example of a film in wild tilapia muscle sample Ta63 (Site 1A). Image A is after 30 minutes incubation with Nile Red. Image B is after 5 minutes incubation with DAPI. Image taken from area 24 on the 1/8th of filter paper on Lecia DFC420 microscope at X40 magnification.

3.2.4 Bead in tilapia muscle

Eight beads (10%) were detected in 5 tilapia muscle samples from Ta9, Ta10, Ta12, Ta27 and Ta62. Samples Ta9 and Ta10 had the most beads identified in all analysed muscle samples, with 3 beads identified in each. Figure 3.10 shows a representative example of microplastic bead found in the fish muscle following staining with Nile Red.

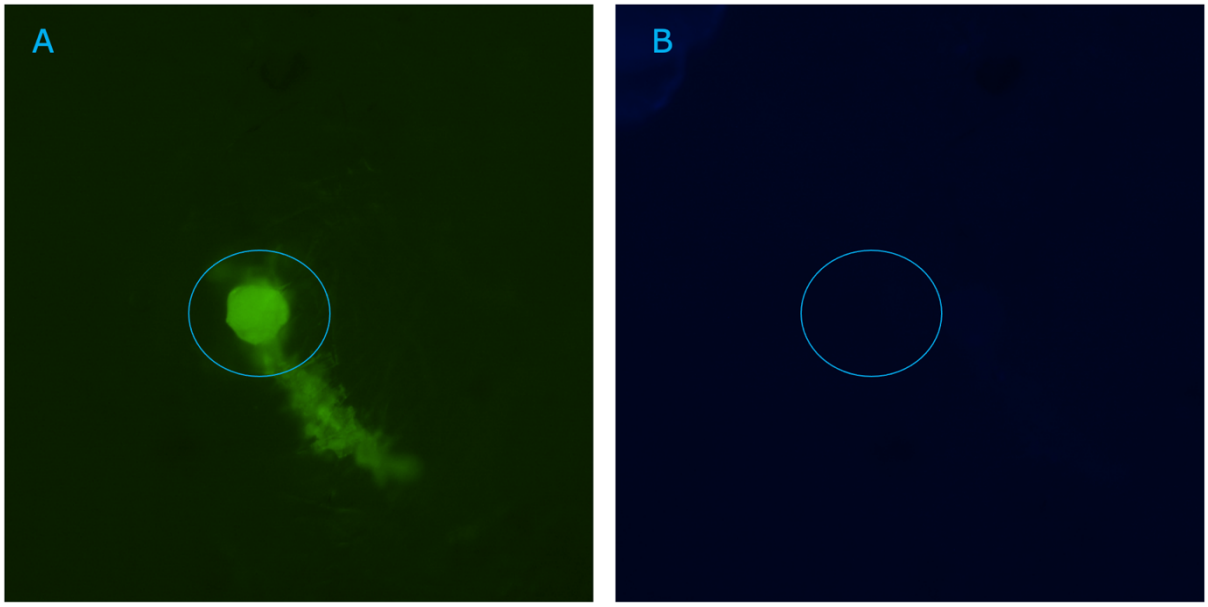

Figure 3.10 Example of microplastic bead in tilapia muscle. This image shows an example of a bead identified in caged tilapia muscle sample Ta62 (Site 1A). Image A was taken at X100 magnification and is after 30 minutes incubation with Nile Red. Image B was taken at X40 magnification and is after 5 minutes incubation with DAPI. Image taken from area 23 on the 1/8th of filter paper on Lecia DFC420 microscope.

3.2.5 Foam in tilapia muscle

Foam was the least prevalent microplastic identified in the muscle samples, with only 1 foam detected (sample Ta27) (Figure 3.11).

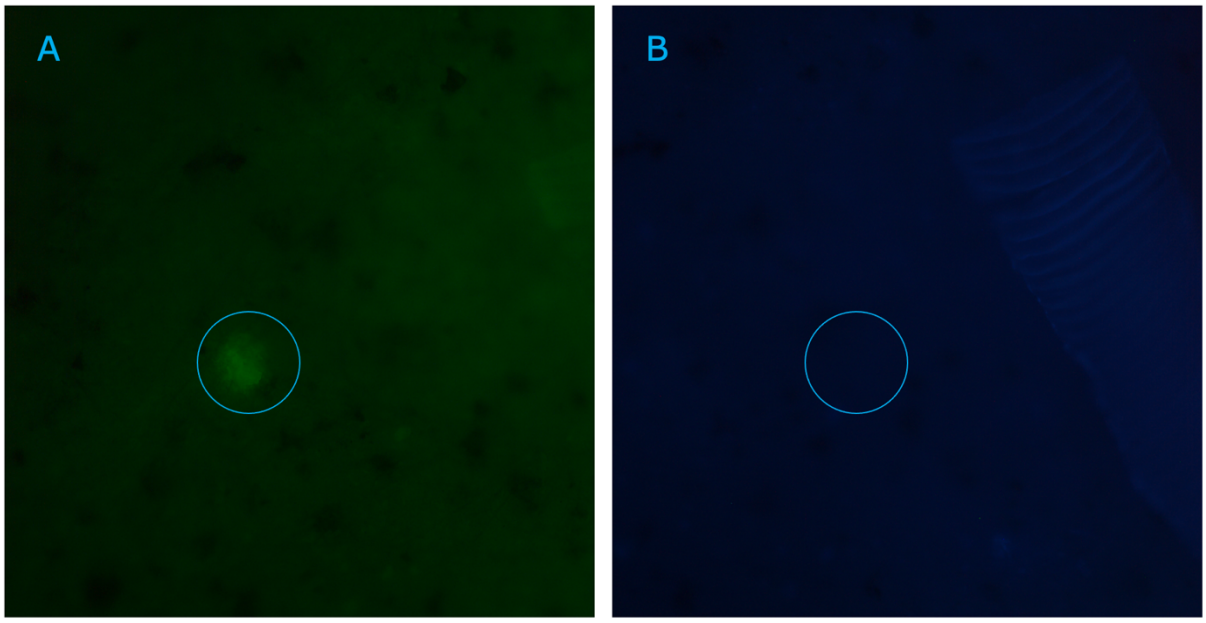

Figure 3.11 Example of microplastic foam in tilapia muscle. This image shows an example of a foam identified in wild tilapia muscle sample Ta27 (Site 13D). Image A is after 30 minutes incubation with Nile Red. Image B is after 5 minutes incubation with DAPI. Image taken from area 14 on the 1/8th of filter paper on Lecia DFC420 microscope at X40 magnification.

3.3 Comparison of microplastic presence in caged versus wild tilapia muscle

Eighty-one microplastic pieces were identified in 31 of the 80 tilapia muscle samples used in this study. Microplastics were more abundant in the wild tilapia muscle samples (WTM) than the farmed/caged tilapia muscle samples (CTM), with 35 microplastic pieces (43%) in the CTM, (n=42) and 46 microplastic pieces (57%) in the WTM, (n=38) (Table 3.12).

More fragments were identified in WTM (19 fragments) than CTM (8 fragments), found in 19 and 8 fish respectively. One foam was identified in WTM (Ta27), while none were identified in CTM. More films were identified in WTM (6 films) compared

to 4 films in CTM, found in 6 and 4 fish respectively. However, CTM had a greater number of fibres (21 fibres) than the WTM (14 fibres), which were found in 21 and 14 fish respectively. There were more beads identified in WTM (6 beads) than CTM (2 beads), and these were seen in 6 and 2 fish respectively.

Fibres were the most prevalent microplastic type identified in CTM (21 fibres), whereas fragments were the most prevalent microplastic type identified in WTM (19 fragments). Foam was the least prevalent microplastic type in both CTM and WTM, with none found in CTM and 1 in the WTM.

	Total MPs	Fragment	Foam	Film	Fibre	Bead
CTM	**35**	8	0	4	21	2
WTM	**46**	19	1	6	14	6
CTM ID		Ta3, Ta7, Ta20, Ta35, Ta47, Ta65, Ta65, Ta68		Ta7, Ta15, Ta15, Ta46	Ta18, Ta36, Ta36, Ta38, Ta38, Ta38, Ta38, Ta38, Ta38, Ta38, Ta38, Ta38, Ta38, Ta45, Ta50, Ta66, Ta67, Ta71, Ta78, Ta78	Ta12, Ta12
WTM ID		Ta16, Ta16, Ta16, Ta16, Ta26, Ta39, Ta40, Ta40, Ta44, Ta48, Ta48, Ta48, Ta48, Ta48, Ta51, Ta55, Ta61, Ta61	Ta27	Ta10, Ta29, Ta44, Ta53, Ta63, Ta63	Ta9, Ta27, Ta27, Ta33, Ta33, Ta42, Ta42, Ta44, Ta51, Ta51, Ta53, Ta62, Ta74, Ta74	Ta9, Ta9, Ta9, Ta10, Ta10, Ta10

Table 3.12 Comparison of microplastic presence in caged vs wild tilapia muscle samples. This table shows a comparison of the microplastic (MP) type and the amount identified in caged tilapia muscle samples (CTM) (n=42) vs wild tilapia muscle samples (WTM) (n=38), after staining with Nile Red and DAPI and subsequent visualisation under the fluorescent microscope. The muscle ID (Ta) is shown here and a sum of the total amount of microplastics identified in CTM vs WTM.

3.4 Detection of microplastics in fish gastrointestinal tract contents

Five digested and filtered tilapia GIT contents were analysed by fluorescent microscopy, following staining with Nile Red and DAPI. Five microplastic pieces were identified during microscopy of the GIT contents, present in all four fish samples that could be visualised under the microscope (Table 3.13). No results were obtained from GI1 as there was too much undigested debris, making it unreadable under the microscope.

ID	MP confirmed filter paper areas	MP type	MP amount
GI1	VOID	VOID	VOID
GI2	25	Bead	**1**
GI3	1	Fibre	**1**
GI4	2	Fragment	**1**
GI5	4 + 34	Fibre + Bead	1 + 1 = **2**

Table 3.13 Microplastic presence in tilapia gastrointestinal tract contents. This table shows the microplastic (MP) type, amount present and the numbered filter paper area where it was identified in each tilapia gastrointestinal tract contents sample (GI), after staining with Nile Red and DAPI and subsequent visualisation under the fluorescent microscope. GI1 results were 'VOID' due to too much undigested debris present, making the sample unreadable under the microscope.

3.4.1 Types of microplastic identified

A single bead was identified in both samples GI2 and GI5 (Figure 3.14). Interestingly, beads identified in the GIT contents fluoresced at a greater intensity than other microplastics. A single bead was found in GI2 and GI5, with a fibre found in GI3 (Figure 3.15) and GI5, and a fragment in GI4 (Figure 3.16). No films or foams were identified in any of the GIT contents samples.

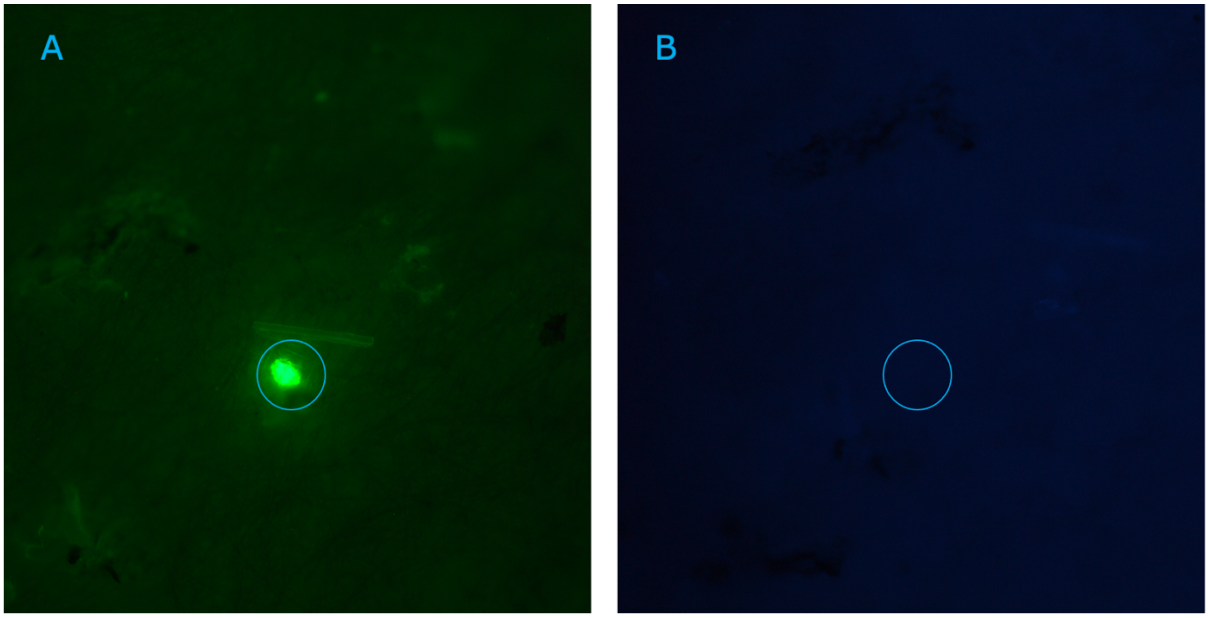

Figure 3.14 Example of bead in tilapia gastrointestinal tract contents. This image shows an example of a bead in gastrointestinal tract contents sample GI5 (Site 9E). Image A is after 30 minutes incubation with Nile Red. Image B is after 5 minutes incubation with DAPI. Image taken from area 34 on the 1/8th of filter paper on Lecia DFC420 microscope at X40 magnification.

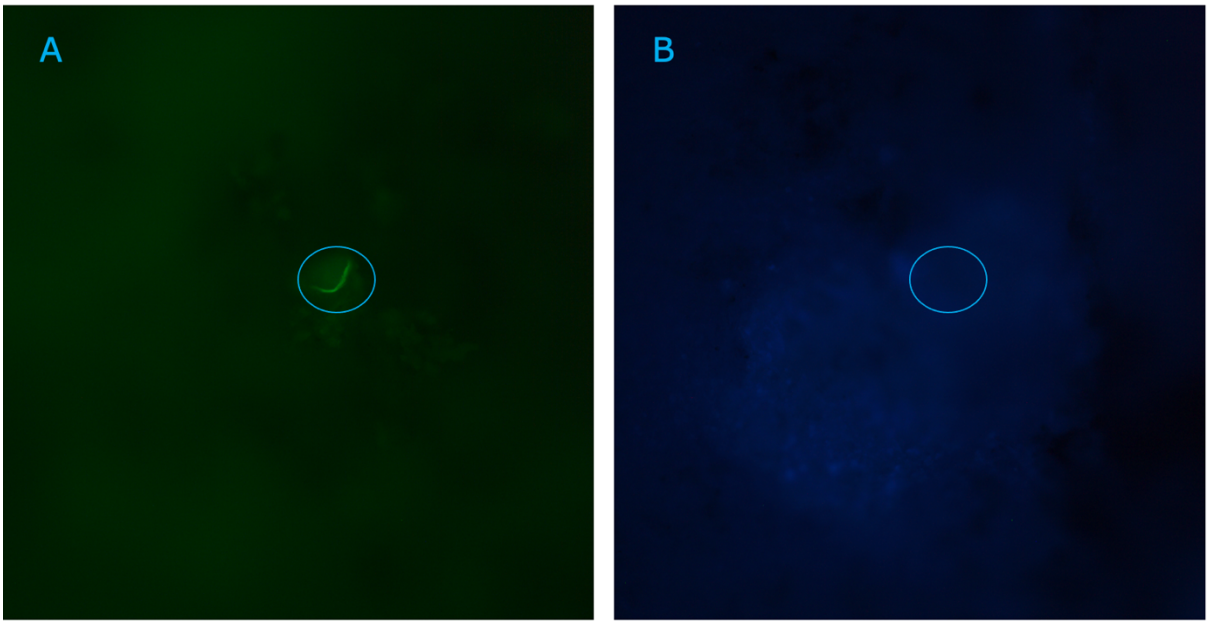

Figure 3.15 Example of fibre in tilapia gastrointestinal tract contents. This image shows an example of a fibre in gastrointestinal tract contents sample GI3 (Site 9B). Image A is after 30 minutes incubation with Nile Red. Image B is after 5 minutes incubation with DAPI. Image taken from area 1 on the 1/8th of filter paper on Lecia DFC420 microscope at X40 magnification.

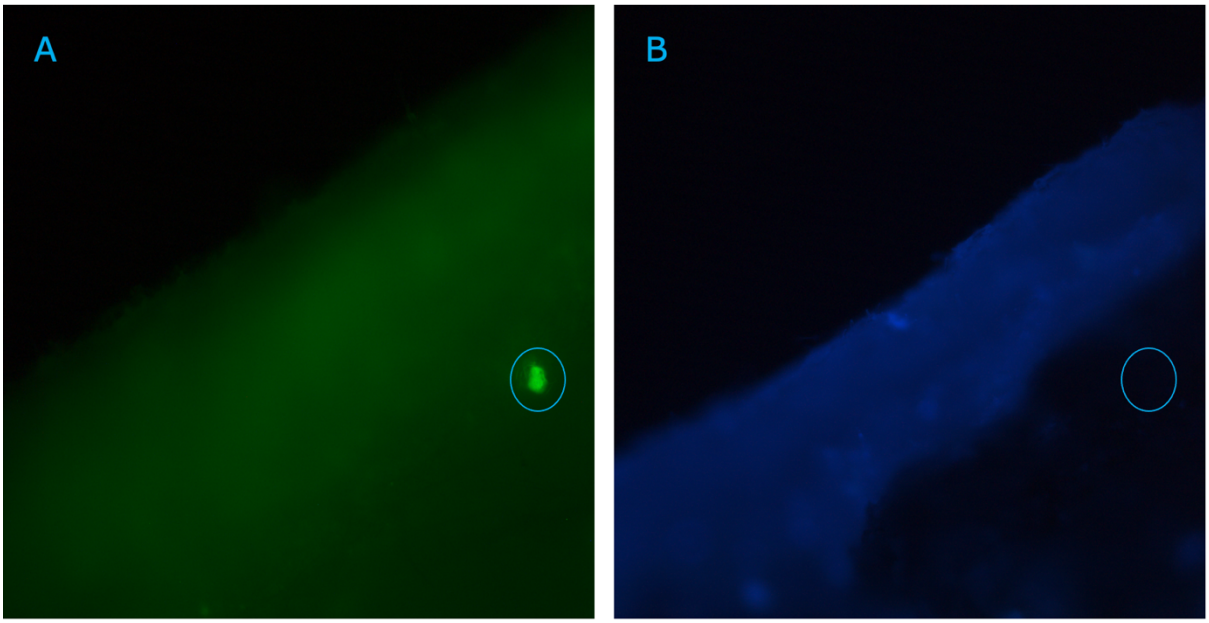

Figure 3.16 Example of fragment in tilapia gastrointestinal tract contents. This image shows an example of a fragment in gastrointestinal tract contents sample GI4 (Site 9B). Image A is after 30 minutes incubation with Nile Red. Image B is after 5 minutes incubation with DAPI. Image taken from area 2 on the 1/8th of filter paper on Lecia DFC420 microscope at X40 magnification.

3.5 Comparison of microplastic presence in caged versus wild tilapia gastrointestinal tract contents

Five microplastics were identified in all 4 of the 5 GIT contents samples that could be analysed under the microscope. Three microplastic pieces were identified in farmed/caged tilapia GIT contents samples (CTGI) (n=4). Two microplastic pieces were identified in the wild tilapia GIT contents sample (WTGI) (n=1), however the CTGI had marginally more microplastics identified than the WTGI (Table 3.17). Equal amounts of fibres and beads were identified in both CTGI and WTGI, but CTGI sample GI4 also contained a fragment. No foams or films were detected in either CTGI or WTGI samples.

	Total MPs	Fragment	Foam	Film	Fibre	Bead
CTGI	**3**	1	0	0	1	1
WTGI	**2**	0	0	0	1	1
CTGI ID		GI4	-	-	GI3	GI2
WTGI ID		-	-	-	GI5	GI5

Table 3.17 Comparison of microplastic presence in caged vs wild tilapia gastrointestinal tract contents. This table shows a comparison of the microplastic (MP) type and the amount identified in caged tilapia gastrointestinal tract contents (CTGI) (n=4) vs wild tilapia gastrointestinal tract contents (WTGI) (n=1), after staining with Nile Red and DAPI and subsequent visualisation under the fluorescent microscope. The gastrointestinal tract contents ID (GI) is shown here and a sum of the total amount of microplastics identified in CTGI vs WTGI.

3.6 Detection of microplastics in intact gastrointestinal tracts in fish

Six digested and filtered tilapia intact GITs were analysed by fluorescent microscopy, following staining with Nile Red and DAPI. Twenty-eight microplastic pieces were identified during microscopy (Table 3.18), with the most common microplastic type being a bead which was found in five of the six samples analysed. A film and a fragment were observed in one of the six samples, GIT13 and GIT15 respectively, with no foams or fibres identified in any of the GIT samples.

ID	MP confirmed filter paper areas	MP type	MP amount
GIT6	26 + 32	Bead	3 + 3 = **6**
GIT7	12	Bead	**3**
GIT10	6 + 14 + 23	Bead	2 + 3 + 2 = **7**
GIT13		Film + Bead	1 + 1 + 1 = **3**
GIT15	23	Bead + Fragment	1 + 1 + 1 = **3**
GIT19	32	Fragment	**6**

Table 3.18 Microplastic presence in tilapia intact gastrointestinal tracts. This table shows the microplastic (MP) type, amount present and the numbered filter paper area where it was identified in each tilapia intact gastrointestinal tract (GIT) sample, after staining with Nile Red and DAPI and subsequent visualisation under the fluorescent microscope.

3.6.1 Bead in tilapia intact gastrointestinal tract

Bead was the most prevalent microplastic type identified in the GITs, with 20 identified which were present in 5 of the samples. Sample GIT10 had the highest microplastic content with 7 beads identified (Figure 3.19).

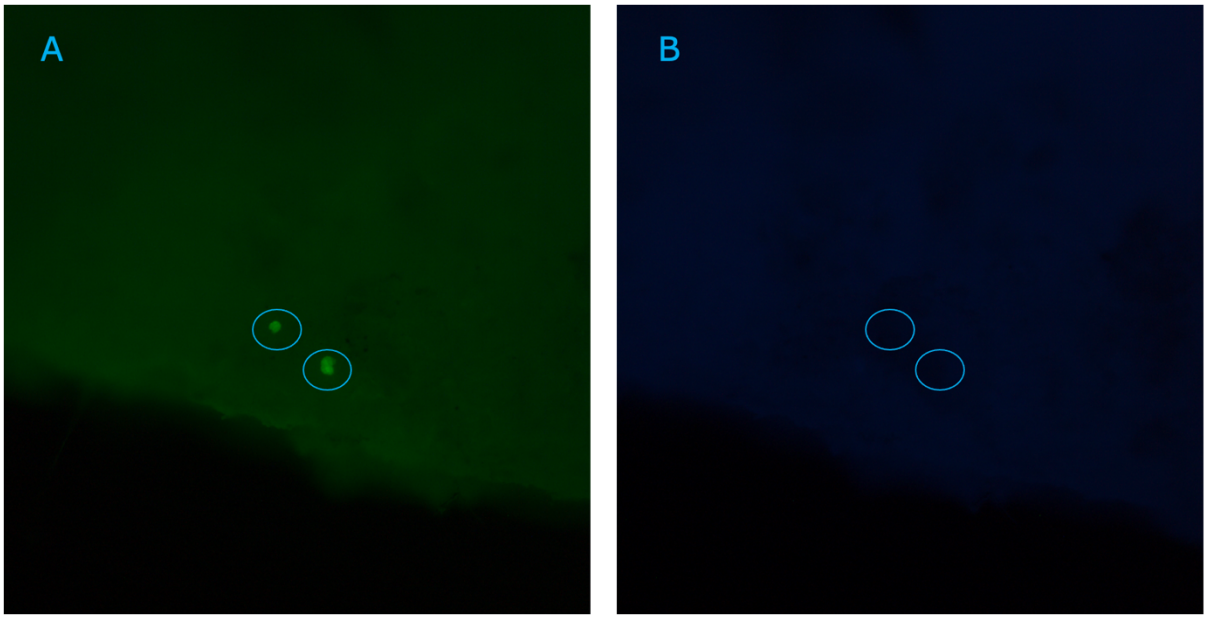

Figure 3.19 Example of beads in tilapia intact gastrointestinal tract. This image shows an example of 2 beads in intact gastrointestinal tract sample GIT10 (Site 7B). Image A is after 30 minutes incubation with Nile Red. Image B is after 5 minutes incubation with DAPI. Image taken from area 6 on the 1/8th of filter paper on Lecia DFC420 microscope at X40 magnification.

3.6.2 Fragment in tilapia intact gastrointestinal tract

Seven fragments were identified in all the GITs, of these 6 were identified in sample GIT19 and 1 fragment in sample GIT15 (Figure 3.20). The fragments fluoresced at a greater intensity than the other microplastic types in the GITs.

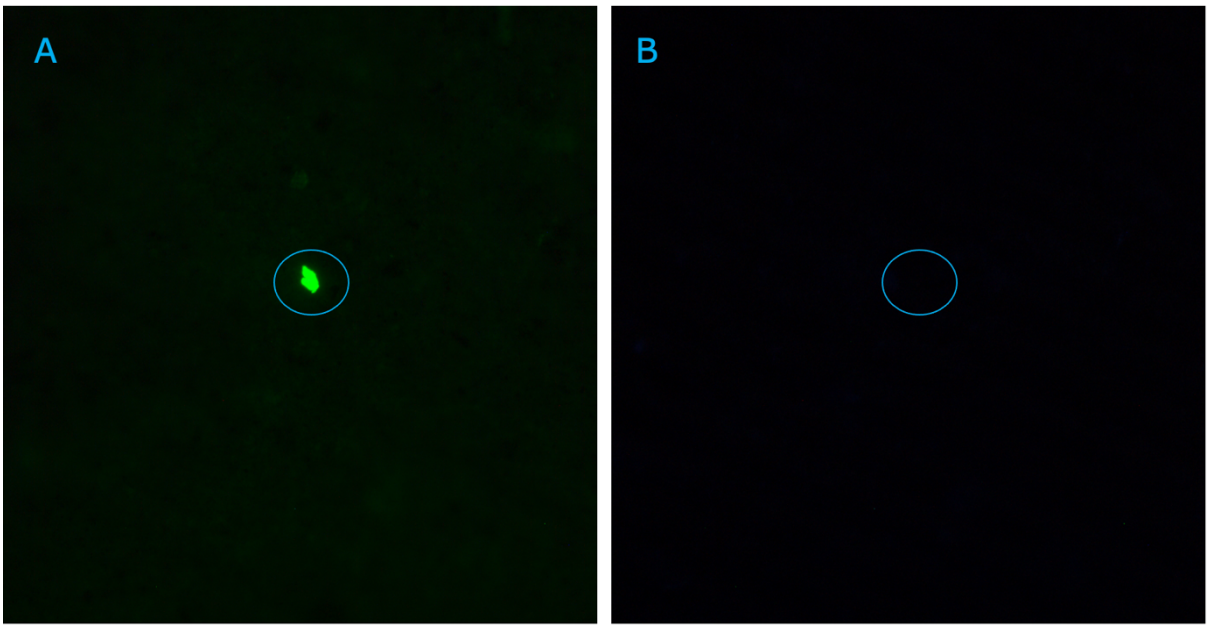

Figure 3.20 Example of fragment in tilapia intact gastrointestinal tract. This image shows an example of a fragment in intact gastrointestinal tract sample GIT15 (Site 1A). Image A is after 30 minutes incubation with Nile Red. Image B is after 5 minutes incubation with DAPI. Image taken from area 23 on the 1/8th of filter paper on Lecia DFC420 microscope at X40 magnification.

3.6.3 Film in tilapia intact gastrointestinal tract

Of the six samples analysed, film was only observed in 1 of the samples, GIT13 (Figure 3.21).

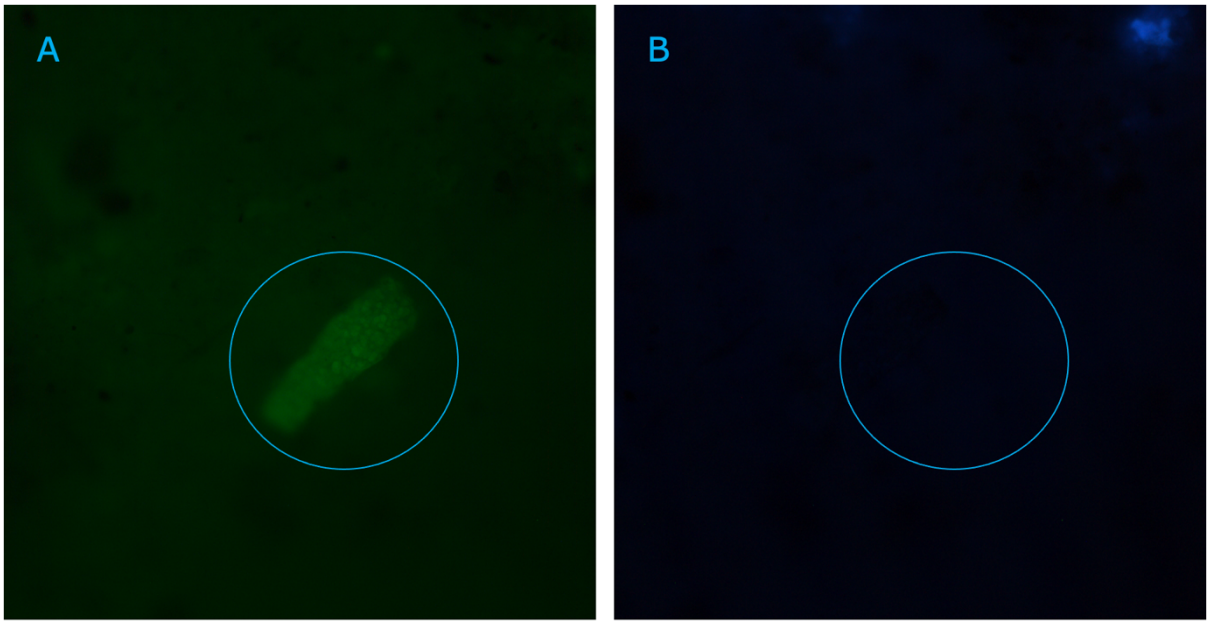

Figure 3.21 Example of film in tilapia intact gastrointestinal tract. This image shows an example of a film in intact gastrointestinal tract (GIT) sample GIT13 (Site 18A). Image A is after 30 minutes incubation with Nile Red. Image B is after 5 minutes incubation with DAPI. Image taken from area 9 on the 1/8th of filter paper on Lecia DFC420 microscope at X40 magnification.

3.7 Comparison of microplastic presence in caged versus wild tilapia intact gastrointestinal tracts

Twenty-eight microplastics were identified in all 6 GIT samples. Nineteen (68%) microplastic pieces were identified in farmed/caged tilapia GIT samples (CTGIT) (n=3), whilst 9 (32%) were identified in wild tilapia GIT samples (WTGIT) (n=3) (Table 3.22).

Bead was the microplastic type most identified in both CTGIT and WTGIT. A greater number of fragments were identified in CTGIT compared to WTGIT. No foams or fibres were identified in any of the CTGIT or WTGIT samples.

	Total MPs	Fragment	Foam	Film	Fibre	Bead
CTGIT	**19**	6	0	0	0	13
WTGIT	**9**	1	0	1	0	7
CTGIT ID		GIT19, GIT19, GIT19, GIT19, GIT19, GIT19	-	-	-	GIT6, GIT6, GIT6, GIT6, GIT6, GIT6, GIT10, GIT10, GIT10, GIT10, GIT10, GIT10, GIT10
WTGIT ID		GIT15	-	GIT13	-	GIT7, GIT7, GIT7, GIT13, GIT13, GIT15, GIT15

Table 3.22 Comparison of microplastic presence in caged vs wild tilapia intact gastrointestinal tracts. This table shows a comparison of the microplastic (MP) type and the amount identified in caged tilapia intact gastrointestinal tracts (CTGIT) (n=3) vs wild tilapia intact gastrointestinal tracts (WTGIT) (n=3), after staining with Nile Red and DAPI and subsequent visualisation under the fluorescent microscope. The intact gastrointestinal tract ID (GIT) is shown here and a sum of the total amount of microplastics identified in CTGIT vs WTGIT.

3.8 Site location comparison

Tilapia were collected from 18 different site locations across Lake Victoria (Figure 2.3), with fish from sites 1A, 1B, 1C, 3C, 4, 4D, 6B, 7A, 7B, 7D, 9B, 9E, 10, 11E, 11F, 13B, 13D, 15B, 16B and 18A used in this study. No microplastics were found in fish from sites 1C, 3C and 7C. Fish from all the other sites (1A, 1B, 4, 4D, 5A, 6B, 7A, 7B, 7D, 9B, 9E, 10, 11E, 11F, 13B, 13D, 15B, 16B and 18A) were found to contain microplastics.

3.8.1 Site location comparison in tilapia muscle

Site 16B (Mageta Island), where 3 of the caged fish (Ta35, Ta36 and Ta38) originated, had the greatest amount of microplastics (n=14) identified when comparing all the fish from all sites (Table 3.23). All samples contained microplastics, but the majority were found in 1 fish (Ta38), where 11 fibres were identified.

Sites 1A (Dunga) and 1B (Dunga) had the greatest number of fish analysed. Eight WT were from site 1A (Dunga), and a total of 6 microplastics were identified in 4 of these (Ta55, Ta61, Ta62 and Ta63). 10 CT were from Site 1B (Dunga), and a total of 7 microplastics were identified in the muscle from 5 of these (Ta12, Ta65, Ta66, Ta67 and Ta68).

In the four WT from site 4 (Uyoma point), only 1 microplastic piece was identified in 1 fish (Ta74). Of the 3 CT from site 4 (Uyoma point), 2 microplastics were identified in 1 of the fish (Ta71). Of the two CT from Site 4D (Uyoma point), none were found to contain microplastics. However in the 3 WT from the same site (site 4D, Uyoma point) all contained microplastics, with a total of 5 microplastics identified.

In the four CT from site 6B (Off Ngodhe), 2 microplastics were identified in 2 of the fish (Ta45 and Ta46). In the one CT from site 7A (Mbeo cages), 1 microplastic was identified in this fish (Ta50). Of the 7 CT from site 7B (Mbeo cages), 5 microplastics were identified in 3 of the fish (Ta7, Ta47 and Ta78). Three WT were from site 7D (Mbeo cages), and a total of 5 microplastics were identified in 2 of the fish (Ta42 and Ta44).

In the five CT from site 9B (Bridge Island), 3 microplastics were identified in 2 of the fish (Ta15 and Ta18). Of the three WT from site 9E (Bridge Island), 1 microplastic was identified in 1 of the fish (Ta26).

In the one CT from site 10 (Kadimo Bay – Anyanga), no microplastics were identified. In the one WT from site 10 (Kadimo Bay – Anyanga), 3 microplastics were identified in this fish (Ta51). In the three CT from site 11E (Madiany water intake), 1 microplastic piece was identified in 1 of the fish (Ta3). Of the three WT from site 11F (Madiany water intake), 8 microplastic pieces were identified in 2 of the fish (Ta9 and Ta10).

In the three CT from site 13B (University of Eldoret pond), 1 microplastic was identified in 1 of the fish (Ta20). Of the four WT from site 13D (University of Eldoret pond), 7 microplastics were identified in 2 of the fish (Ta16 and Ta27).

In the three WT from site 15B (Port Bunyala), 9 microplastics were identified in all 3 of the fish (Ta35, Ta36 and Ta38). Fish sourced from sites 1C (Dunga), 3C (Asat cages) and 18A (Sori Bay) had no detectable microplastics.

A total 46 microplastic pieces (57%) were identified at sites where WT were harvested, with a total 35 microplastic pieces (43%) from those sites where CT were harvested. Sites where WT were harvested had 14% more microplastics in the fish, than in the fish at sites where CT were harvested.

Site	Total number of fish sourced from site	Sample IDs with MPs identified	Fragment	Foam	Film	Fibre	Bead	Total number of MPs identified at site
1A	8	Ta55, Ta61, Ta62, Ta63	3	0	2	1	0	**6**
1B	10	Ta12, Ta65, Ta66, Ta67, Ta68	3	0	0	2	2	**7**
1C	3	-	0	0	0	0	0	**0**
3C	1	-	0	0	0	0	0	**0**
4	3	Ta71	0	0	0	1	0	**1**
4	4	Ta74	0	0	0	2	0	**2**
4D	2	-	0	0	0	0	0	**0**
4D	3	Ta29, Ta33, Ta53	0	0	2	3	0	**5**
6B	4	Ta45, Ta46	0	0	1	1	0	**2**
7A	1	Ta50	0	0	0	1	0	**1**
7B	7	Ta7, Ta47, Ta78	2	0	1	2	0	**5**
7D	3	Ta42, Ta44	1	0	1	3	0	**5**
9B	5	Ta15, Ta18	0	0	2	1	0	**3**
9E	3	Ta26	1	0	0	0	0	**1**
10	1	-	0	0	0	0	0	**0**
10	1	Ta51	1	0	0	2	0	**3**
11E	3	Ta3	1	0	0	0	0	**1**
11F	3	Ta9, Ta10	0	0	1	1	6	**8**
13B	3	Ta20	1	0	0	0	0	**1**
13D	4	Ta16, Ta27	4	1	0	2	0	**7**
15B	3	Ta39, Ta40, Ta48	9	0	0	0	0	**9**
16B	3	Ta35, Ta36, Ta38	1	0	0	13	0	**14**
18A	2	-	0	0	0	0	0	**0**

Table 3.23 Site location comparison of microplastics in tilapia muscle. This table shows the presence of different microplastic (MP) types at each site location where caged tilapia muscle (Ta) samples (n=42) and wild tilapia muscle samples (n=38) were analysed in this study. The site locations in blue (site 1B) are where caged tilapia were analysed in this study and the locations in green (site 1A) are where wild tilapia were analysed. The total number of fish sourced from each site and the sample IDs (Ta) containing microplastics is shown. Fish at sites 1C, 3C and 18A had no detectable microplastics.

3.8.2 Site location comparison in tilapia gastrointestinal tract contents

Samples were sourced from site 9 (Bridge Island), with CTGI from site 9E and WTGI from site 9B. Bead and fibre were found in fish from both sites, with a microplastic fragment seen in the GIT contents from a CT in site 9E (Table 3.24). In the 4 CT from site 9B (Bridge Island), their GIT contents contained a total of 3 microplastics, found in in 3 of the 4 fish (GI2, GI3 and GI4). In the 1 WT from site 9E (Bridge Island), 2 microplastics were identified in this sample (GI5).

A total 4 microplastic pieces (75%) were identified in the CT from site 9B, with only 1 microplastic (25%) identified in the WT from site 9E. The GIT contents sourced from the site where caged fish were analysed contained more microplastics than fish sourced from the site where wild fish were sourced, but more CT (n=4) were analysed compared to only 1 WT.

Site	Total number of fish sourced from site	Sample IDs with MPs identified	Fragment	Foam	Film	Fibre	Bead	Total number of MPs identified at sites
9B	4	GI2, GI3, GI4	1	0	0	1	1	**3**
9E	1	GI5	0	0	0	1	1	**2**

Table 3.24 Site location comparison with microplastic presence in tilapia gastrointestinal tract contents. This table shows the presence of the different microplastic (MP) types at each site location where caged tilapia gastrointestinal tract contents samples (n=4) and wild tilapia gastrointestinal tract contents samples (n=1) were analysed in this study. The site location in blue (site 9B) is where caged tilapia were analysed and the location in green (site 9E) is where wild tilapia were analysed. The total number of fish sourced from each site and the sample IDs (GI) containing microplastics is shown.

3.8.3 Site location comparison in tilapia intact gastrointestinal tracts

GIT samples were sourced from fish from sites 1A and 1B (Dunga), 4 (Uyoma point), 7B (Mbeo cages) and 18A (Sori Bay), with all fish analysed at these sites found to contain microplastics (Table 3.25). In the one WT from site 1A (Dunga), 3 microplastics were identified in this sample (GIT15). In the one CT from site 1B (Dunga), 6 microplastics were identified in this sample (GIT19).

In the one CT from site 4 (Uyoma point), 6 microplastics were identified in this sample (GIT6). In the one WT from site 4 (Uyoma point), 3 microplastics were identified in this sample (GIT7). In the one CT from site 7B (Mbeo cages), 7 microplastics were identified in this sample (GIT10). In the one WT from site 18A (Sori Bay), 2 microplastics were identified in this sample (GIT13).

The bead was the most prevalent microplastic type among the sites, with 20 beads out of the total of 28 microplastics identified overall. Beads were most common in fish at site 4, with a total of 9 beads identified in both CT and WT harvested from here. A total of 19 microplastics were identified in the CT, compared to a total of 9 microplastics identified in the WT. The GIT samples sourced from the sites where caged fish were analysed contained more microplastics than fish sourced from the sites where wild fish were sourced.

Site	Total number of fish sourced from site	Sample IDs with MPs identified	Fragment	Foam	Film	Fibre	Bead	Total number of MPs identified at sites
1A	1	GIT15	1	0	0	0	2	**3**
1B	1	GIT19	6	0	0	0	0	**6**
4	1	GIT6	0	0	0	0	6	**6**
4	1	GIT7	0	0	0	0	3	**3**
7B	1	GIT10	0	0	0	0	7	**7**
18A	1	GIT13	0	0	1	0	2	**3**

Table 3.25 Site location comparison with microplastic presence in tilapia intact gastrointestinal tracts. This table shows the presence of the different microplastic (MP) types at each site location where caged tilapia intact gastrointestinal tract samples (n=3) and wild tilapia intact gastrointestinal tract samples (n=3) were analysed in this study. The site locations in blue (site 1B) are where caged tilapia were analysed and the locations in green (site 1A) are where wild tilapia were analysed. The total number of fish sourced from each site and the sample IDs (GIT) containing microplastics is shown.

3.9 Comparison of microplastic presence in caged versus wild tilapia samples of muscle, gastrointestinal tract contents and intact gastrointestinal tracts

Of the 81 microplastic pieces found in 38 (48%) of the 80 tilapia muscles analysed in this study, 35 (43%) of these were found in CT (n=42) and 46 (57%) microplastics were found in WT (n=38) **(**Figure 3.26).

Five microplastic pieces were identified in 4 analysed tilapia GIT contents. Three of these microplastics were found in CT (n=4) and 2 were found in WT (n=1).

Twenty-eight microplastic pieces were identified in all 6 of the analysed tilapia intact GITs, with 19 (68%) found in CT (n=3) and 9 (32%) in WT (n=3).

A greater number of microplastics were found in the muscle of wild tilapia than farmed/caged, however more microplastics were found in the GIT (contents and intact) of caged tilapia than wild ones.

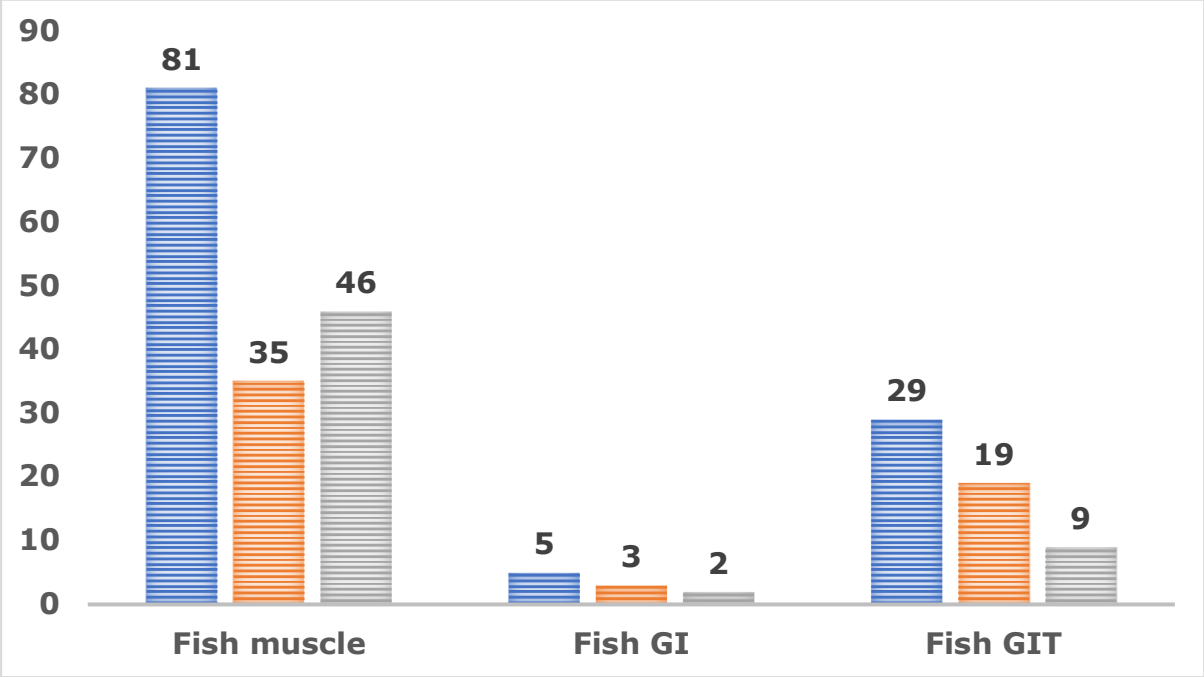

Figure 3.26 Comparison of microplastic content in caged vs wild tilapia samples. The graph shows a comparison of microplastic content in caged vs wild tilapia samples of the 3 different tilapia parts analysed (muscle, gastrointestinal tract contents (GI) and intact gastrointestinal tracts (GIT)). Total amount of microplastics (MP) identified in both caged (CT) and wild tilapia (WT) (shown in blue), vs total amount of MP found in CT (shown in orange), vs total amount of MP found in WT (shown in grey). X axis, categories used to show the 3 different tilapia parts analysed (fish muscle (n=80), fish GI (n=5) and fish GIT (n=6)). Y axis, shows the number of microplastics identified.

3.9.1 Comparison of microplastic type presence in tilapia muscle versus gastrointestinal tract contents versus intact gastrointestinal tracts

In the muscle samples, fibre (n=35) was the most identified microplastic type (Figure 3.27), with foam (n=1) as the least identified type. Fragments (n=27), films (n=10) and beads (n=8) were also identified. In the GIT contents, both fibre (n=2) and bead (n=2) were the most identified microplastic type, one fragment was identified, and no foam or film (n=0) were identified. In the intact GITs, bead (n=20) was the most identified microplastic type, with fragment (n=7) and film (n=1) also identified, and no foam or fibre (n=0).

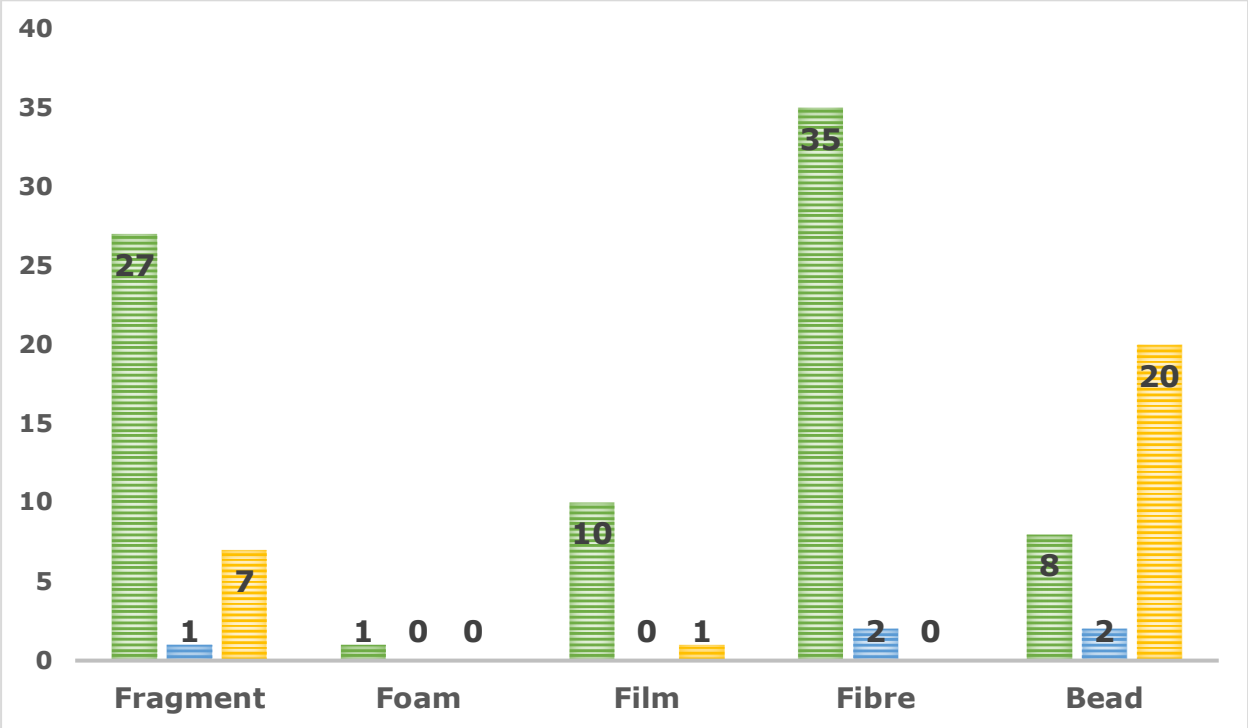

Figure 3.27 Comparison of microplastic types present in tilapia muscle vs gastrointestinal tract contents vs intact gastrointestinal tracts. This graph shows a comparison of the total amount of each microplastic type identified in tilapia muscle (n=80) (shown in green) vs tilapia gastrointestinal tract contents (n=5) (shown in blue) vs tilapia intact gastrointestinal tracts (n=6) (shown in yellow). X axis, categories used to show the 5 different structural types of microplastic identified (fragment, foam, film, fibre and bead). Y axis, shows the number of microplastics identified.

3.9.2 Comparison of microplastic type presence in caged versus wild tilapia samples of muscle, gastrointestinal tract contents and intact gastrointestinal tracts

In the muscle samples, of the 35 fibres identified, 21 were identified in CT, while 14 were identified in WT. Of the 27 fragments identified, 8 were identified in CT, while 19 were identified in WT (Figure 3.28). Of the 10 films identified, 4 were identified in CT, while 6 were identified in WT. Of the 8 beads identified, 2 were identified in CT, while 6 were identified in WT. No foams were identified in CT, while the one identified was in WT. Fibre was identified more in the muscle of CT than WT, while fragment, bead, film and foam were identified more in the muscle of WT than CT.

In the GIT contents samples, of the 2 beads identified, 1 was identified in CT and 1 was identified in WT. Of the 2 fibres identified, 1 was identified in CT and 1 was identified in WT. The one fragment identified was in CT, while none were identified in WT. No foams or films were identified in the GIT contents of CT or WT. Fibre and bead were the most identified types in the GIT contents of both CT and WT, but an additional fragment was found in the CT than WT.

In the intact GIT samples, of the 20 beads identified, 13 were identified in CT, while 7 were identified in WT. Of the 7 fragments identified, 6 were identified in CT, while 1 was identified in WT. No films were identified in CT, while the 1 identified was in WT. No foams or fibres were identified in the GIT of CT or WT. Bead and fragment were identified more in the intact GIT of CT than WT, while film was identified more in the intact GIT of WT than CT.

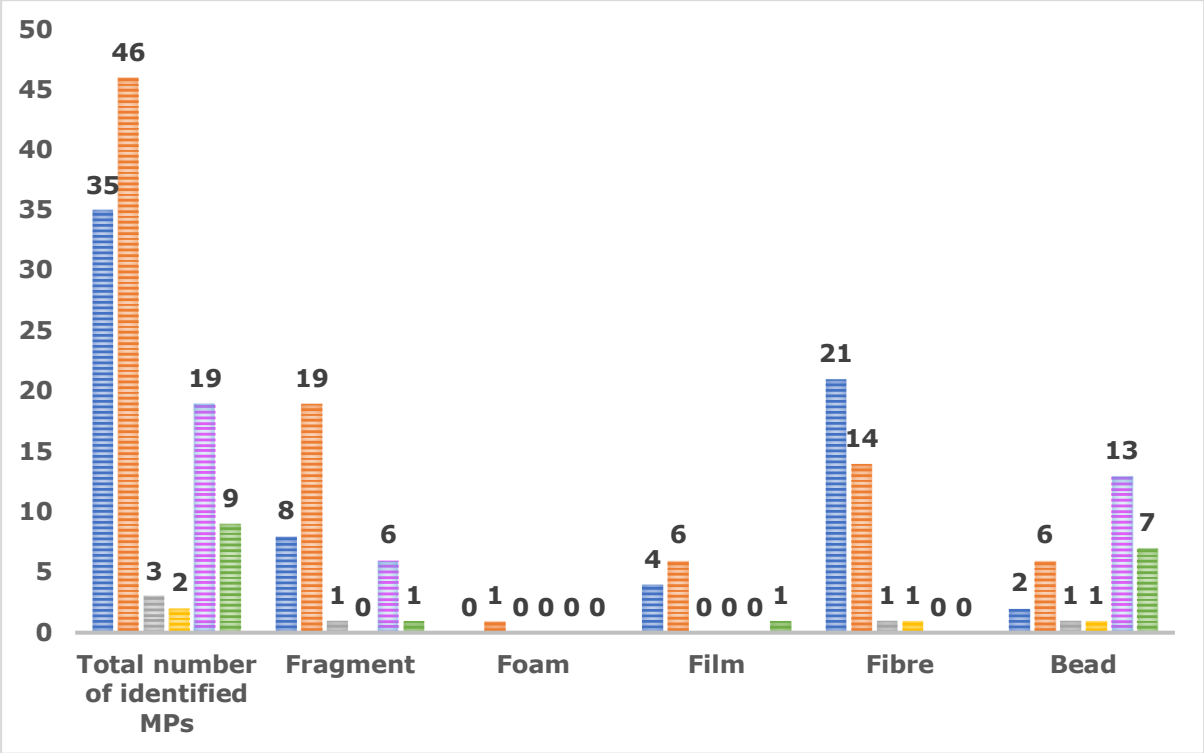

Figure 3.28 Comparison of microplastic type presence in caged vs wild tilapia samples of muscle, gastrointestinal tract contents and intact gastrointestinal tracts. This graph shows a comparison between caged and wild tilapia samples of muscle (n=80), gastrointestinal tract (GIT) contents (n=5) and intact GITs (n=6) analysed in this study and their presence for the different microplastic (MP) types (fragment, foam, film, fibre and bead). Results for caged tilapia muscle are shown in blue, wild tilapia muscle are shown in orange, caged tilapia GIT contents are shown in grey, wild tilapia GIT contents are shown in yellow, caged tilapia intact GITs are shown in purple and wild tilapia intact GITs are shown in green. X axis, categories used to show the 5 different structural types of microplastics identified (fragment, foam, film, fibre and bead), and a sum of the total number of MPs identified. Y axis, shows the number of microplastics identified.

3.10 Genomic DNA extraction

Genomic DNA was extracted from the plastisphere on the surface of the microplastics identified in the tilapia samples (Table 3.29) and from the plastic macrolitter collected from Lake Victoria (Tables 3.30 and 3.31). DNA was assessed for its quality (260/280 and 260/230) and the quantity (ng/µl). Any samples with a negative value for the 260/230 ratios were noted as a low or seemingly negative ratio, which may be the result of a contaminant absorbing at 230 nm or less.

Recovered DNA concentrations from the remaining samples were low, ranging from 1.77-13.54ng/µl in the fish samples and 6.708-19.93ng/µl from the macroplastic litter. The quality of the DNA was variable (0.86-3.48 for 260/280 and -2.55-2.03 for 260/230), with low ratios at both 260/280 and 260/230 ratio suggesting a contaminant absorbing at 280 nm or less and 230 nm or less respectively.

Sample ID	260/280	260/230	ng/µl
Ta7 DNA 1	1.87	1.35	3.303
Ta7 DNA 2	1.77	1.99	2.429
Ta18 DNA 1	1.34	-0.99	3.389
Ta18 DNA 2	1.46	-1.04	2.736
Ta20 DNA 1	1.87	-2.55	2.385
Ta20 DNA 2	1.72	0.58	4.465
Ta33 DNA 1	1.77	2.03	13.54
Ta33 DNA 2	1.87	-2.26	6.784
Ta44 DNA 1	1.88	-0.62	1.962
Ta44 DNA 2	0.86	-0.99	2.244
Ta48 DNA 1	1.42	-0.25	3.082
Ta48 DNA 2	2.18	-0.43	3.668
Ta61 DNA 1	1.79	-0.56	3.329
Ta61 DNA 2	1.39	-0.89	3.377
Ta66 DNA 1	1.35	-0.62	2.651
Ta66 DNA 2	2.93	0.56	3.944
Ta69 DNA 1	1.19	2.34	4.215
Ta69 DNA 2	3.48	0.31	5.448
Ta72 DNA 1	1.59	-0.36	2.547
Ta72 DNA 2	1.01	-0.28	2.216
GI5 DNA 1	2.1	-0.16	1.814
GI5 DNA 2	1.58	-0.17	1.77
GIT13 DNA 1	1.62	1.35	4.442
GIT13 DNA 2	1.45	0.32	5.554

Table 3.29 Quality and quantity of genomic DNA from microplastics in tilapia muscle, gastrointestinal tract contents and intact gastrointestinal tracts. The table shows the quality (260/280 & 260/230 ratios) and quantity (ng/µl) values for the chosen 6 tilapia muscle (Ta), 1 gastrointestinal tract contents (GI) and 1 intact gastrointestinal tract sample (GIT). Two microplastics in each sample were chosen and their plastispheres were extracted independently and then assessed, resulting in 2 DNA extractions per sample (DNA 1 and DNA 2). The genomic DNA was assessed using a Nanodrop 8000. Samples with a seemingly negative 260/230 ratio were indicative of contaminant absorbing at 230 nm or less.

Sample ID	260/280	260/230	ng/µl
Blue net DNA 1	1.62	1.34	9.698
Blue net DNA 2	1.57	0.79	10.67
Green net DNA 1	1.81	0.94	6.708
Green net DNA 2	1.76	0.58	6.876
Yellow net DNA 1	1.99	1.05	10.49
Yellow net DNA 2	1.52	0.63	10.16
Sandwich bag DNA 1	1.61	2.59	13
Sandwich bag DNA 2	1.83	1.53	14.52

Table 3.30 Quality and quantity of genomic DNA from macroplastic litter collected from Lake Victoria. The table shows the quality (260/280 & 260/230 ratios) and quantity (ng/µl) values for the chosen 3 different coloured fishing net strands and 1 sandwich bag litter collected from Lake Victoria. Two DNA samples were extracted and assessed per litter sample (DNA 1 and DNA 2). The genomic DNA was assessed using a Nanodrop 8000.

Sample ID	260/280	260/230	ng/µl
Blue net DNA 1	1.73	0.74	10.93
Blue net DNA 2	1.64	0.58	12.91
Green net DNA 1	1.52	0.61	11.45
Green net DNA 2	1.66	0.73	9.919
Yellow net DNA 1	1.81	0.84	9.594
Yellow net DNA 2	1.58	0.46	7.183
Sandwich bag DNA 1	1.62	0.70	19.93
Sandwich bag DNA 2	1.68	1.06	14.75

Table 3.31 Quality and quantity of genomic DNA from plastic litter collected from Lake Victoria – 2nd extraction. The table shows the quality (260/280 & 260/230 ratios) and quantity (ng/µl) values for the chosen 3 different coloured fishing net strands and 1 sandwich bag litter collected from Lake Victoria. DNA extraction was repeated on another piece of the same sample. Two DNA samples were extracted and assessed per litter sample (DNA 1 and DNA 2). The genomic DNA was assessed using a Nanodrop 8000.

3.11 Polymerase chain reaction

PCR was carried out on all extracted genomic DNA. This included using primers to the 16S Ribosomal rRNA gene (Chakravorty et al., 2007), which aimed to determine if there was bacterial DNA present. In addition, several bacterial species-specific primer pairs were used to screen for presence or absence of key bacterial species.

3.11.1 Presence of bacterial DNA

Of the genomic DNA extracted from microplastics found in the 12 tilapia samples, Ta7, Ta20 and Ta48, were all positive for bacterial DNA presence using V_3V_6. Bands of the expected size (739bp) were present but were very faint, suggesting the level of bacterial DNA was detectable but low.

All of the 8 extracted genomic DNA samples from the plastic litter collected from Lake Victoria also produced a band of the expected size using primers. Images of successful V_3V_6 PCRs are shown for samples of blue net (Figure 3.32), yellow net (Figure 3.33), green net (Figure 3.34), sandwich bag (Figure 3.35), Ta7 (Figure 3.36) and Ta48 (Figure 3.37).

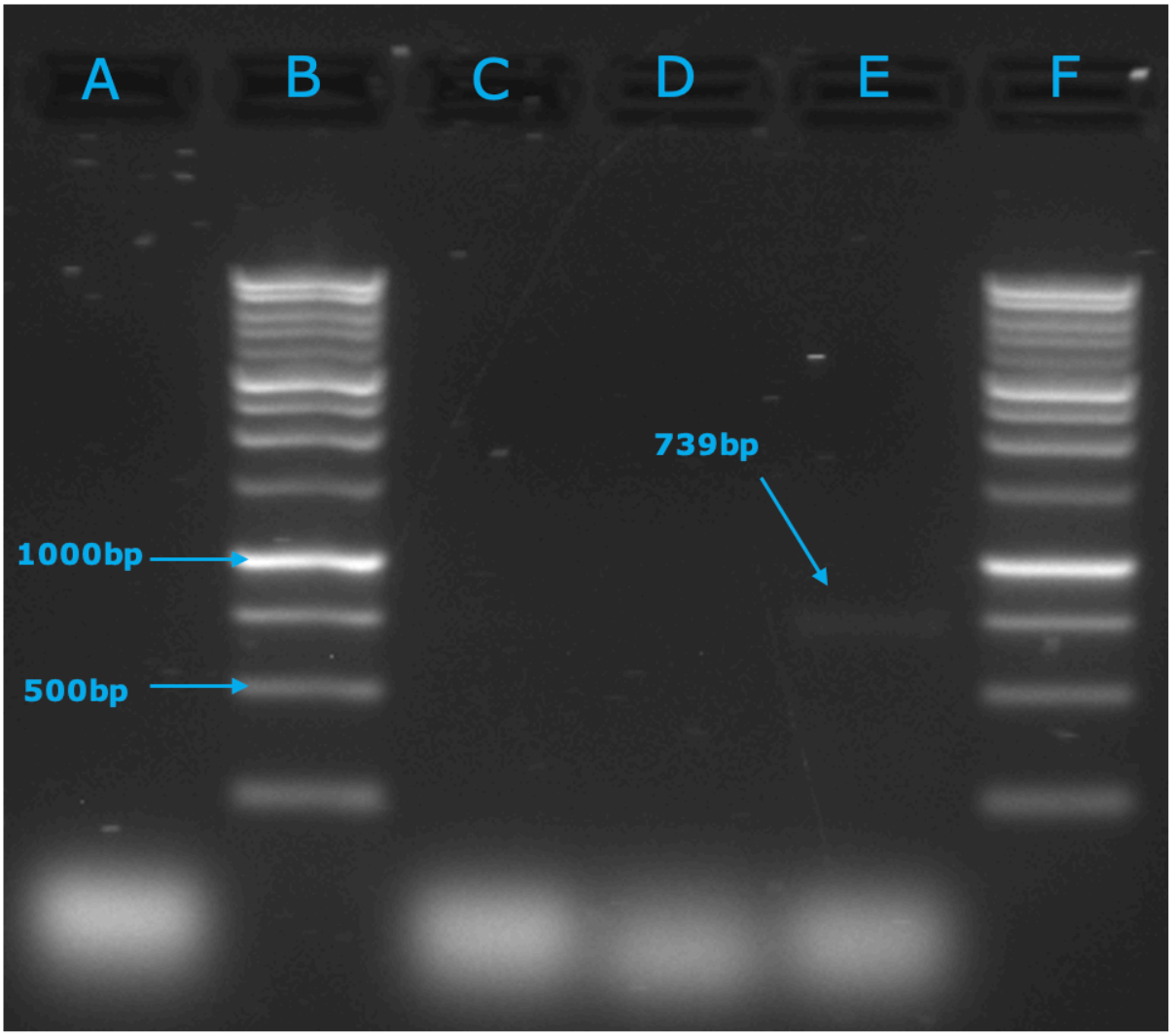

Figure 3.32 A typical image of a positive V_3V_6 PCR of blue net DNA 1 (1st batch). This is a typical image of a positive result with the expected band size of 739bp for bacterial DNA presence in lane E of blue net DNA 1 sample. V_3V_6 primers (Chakravorty et al., 2007) were used, at an annealing temperature of 58°C. Lane A is the negative control and lanes B and F are 1kb ladder (Promega).

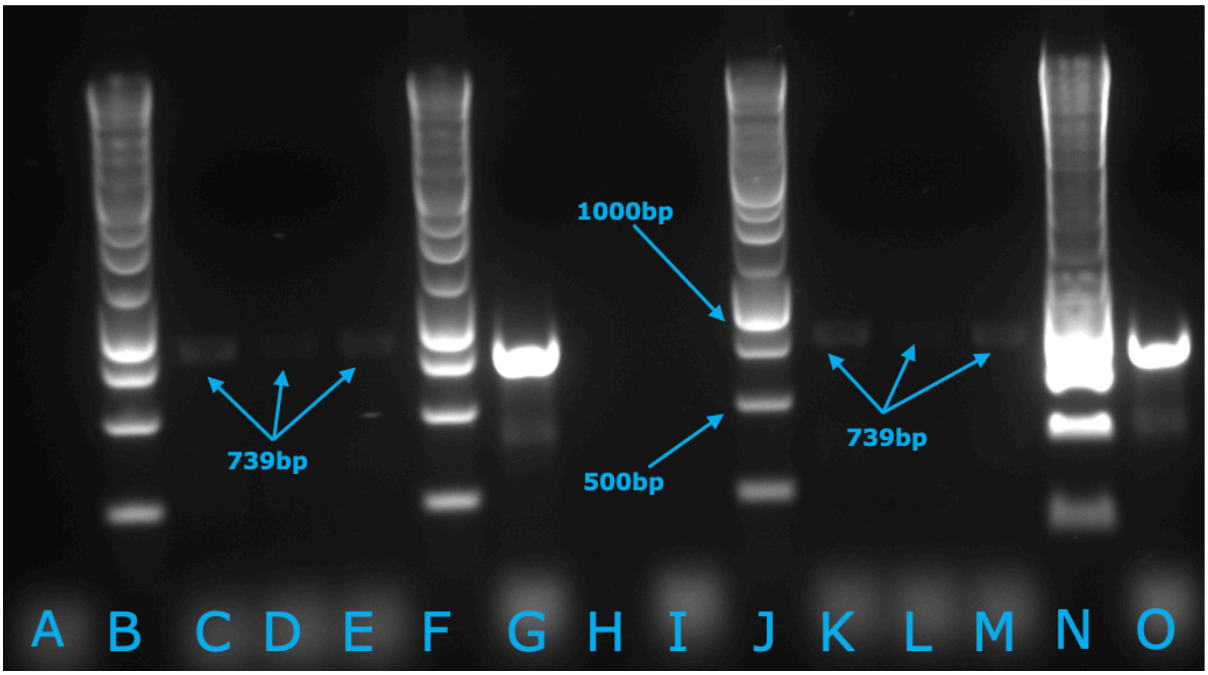

Figure 3.33 Positive V_3V_6 PCR of yellow net DNA 1 and 2 (2nd batch). This image shows two PCRs – yellow net DNA 1 *(left)* and yellow net DNA 2 *(right)*. There are positive results with the expected band size of 739bp for bacterial DNA presence in lanes C, D and E of yellow net DNA 1 *(left)* and lanes K, L and M of yellow DNA 2 *(right)*. *V_3V_6* primers (Chakravorty et al., 2007) were used, at an annealing temperature of 58°C. Lanes A and I are negative controls and lanes G and O are positive controls using *Streptococcus uberis* DNA. Lanes B, F, J and N are 1kb ladder (Promega).

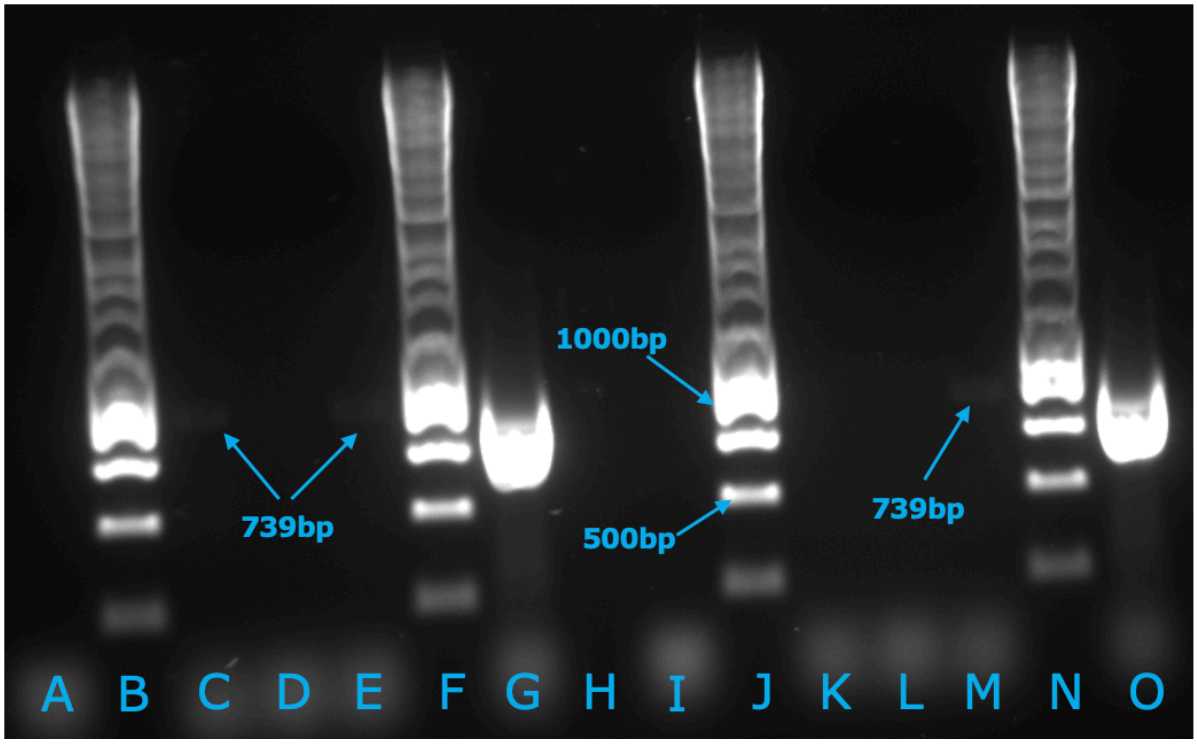

Figure 3.34 Positive V_3V_6 PCR of green net DNA 1 and 2 (2nd batch). This image shows two PCRs – green net DNA 1 *(left)* and green net DNA 2 *(right)*. There are positive results with the expected band size of 739bp for bacterial DNA presence in lanes C and E of yellow net DNA 1 *(left)* and lane M of yellow net DNA 2 *(right)*. V_3V_6 primers (Chakravorty et al., 2007) were used, at an annealing temperature of 58°C. Lanes A and I are negative controls and lanes G and O are positive controls using *Streptococcus uberis* DNA. Lanes B, F, J and N are 1kb ladder (Promega).

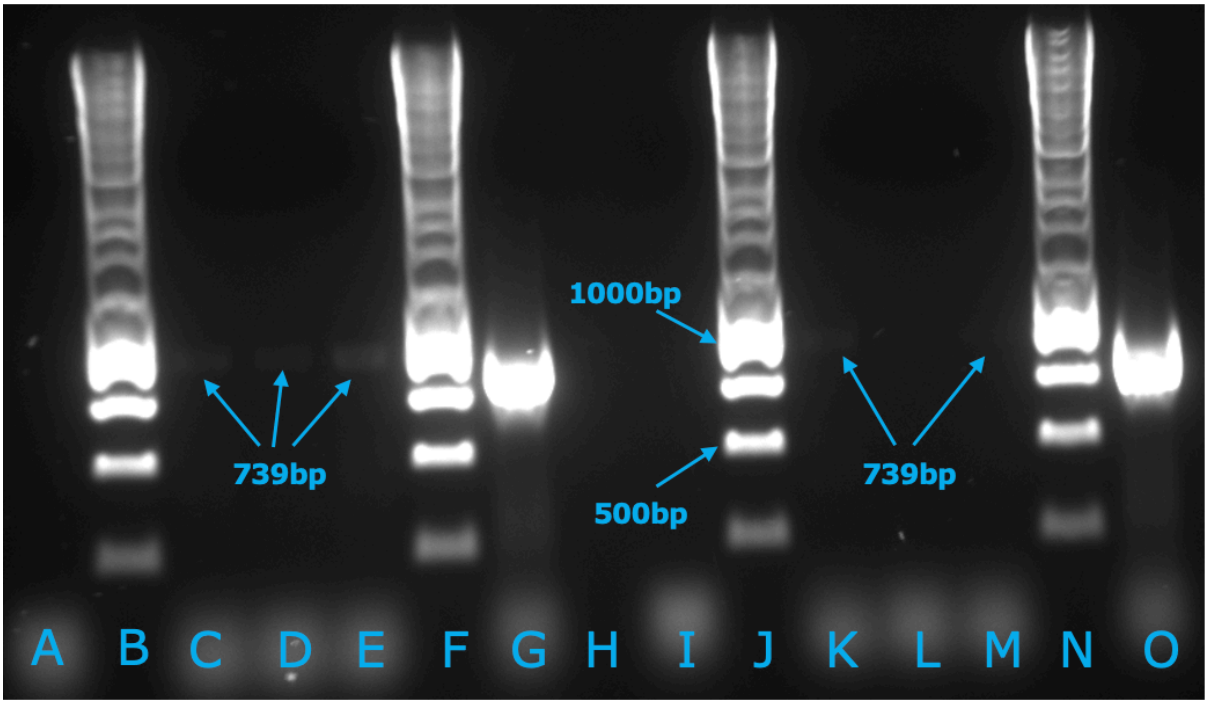

Figure 3.35 Positive V_3V_6 PCR of sandwich bag DNA 1 and 2 (2nd batch). This image shows two PCRs – sandwich bag DNA 1 *(left)* and sandwich bag DNA 2 *(right)*. There are positive results with the expected band size of 739bp for bacterial DNA presence in lanes C, D and E of sandwich bag DNA 1 *(left)* and lanes K and M of sandwich bag DNA 2 *(right)*. *V_3V_6* primers (Chakravorty et al., 2007) were used, at an annealing temperature of 58°C. Lanes A and I are negative controls and lanes G and O are positive controls using *Streptococcus uberis* DNA. Lanes B, F, J and N are 1kb ladder (Promega).

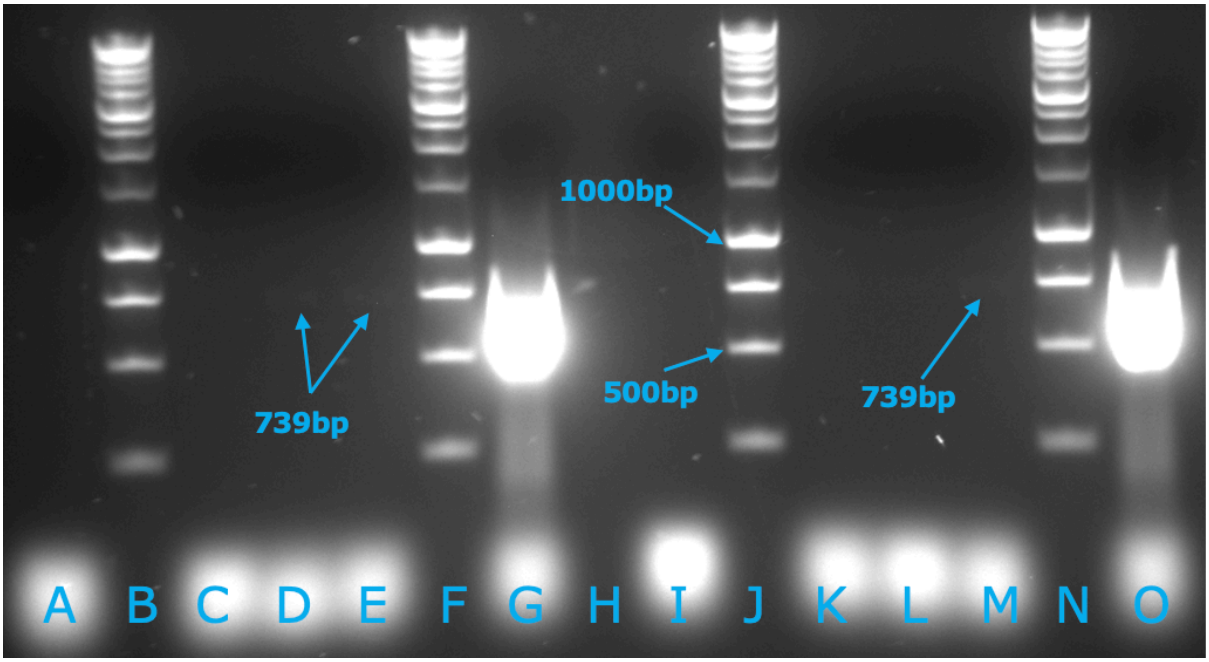

Figure 3.36 Positive V_3V_6 PCR of tilapia muscle Ta7 DNA 1 and 2 (2nd batch). This image shows two PCRs – Ta7 DNA 1 *(left)* and Ta7 DNA 2 *(right)*. There are positive results with the expected band size of 739bp for bacterial DNA presence in lanes D and E of Ta7 DNA 1 *(left)* and lane M of Ta7 DNA 2 *(right)*. *V_3V_6* primers (Chakravorty et al., 2007) were used, at an annealing temperature of 58°C. Lanes A and I are negative controls and lanes G and O are positive controls using *Streptococcus uberis* DNA. Lanes B, F, J and N are 1kb ladder (Promega).

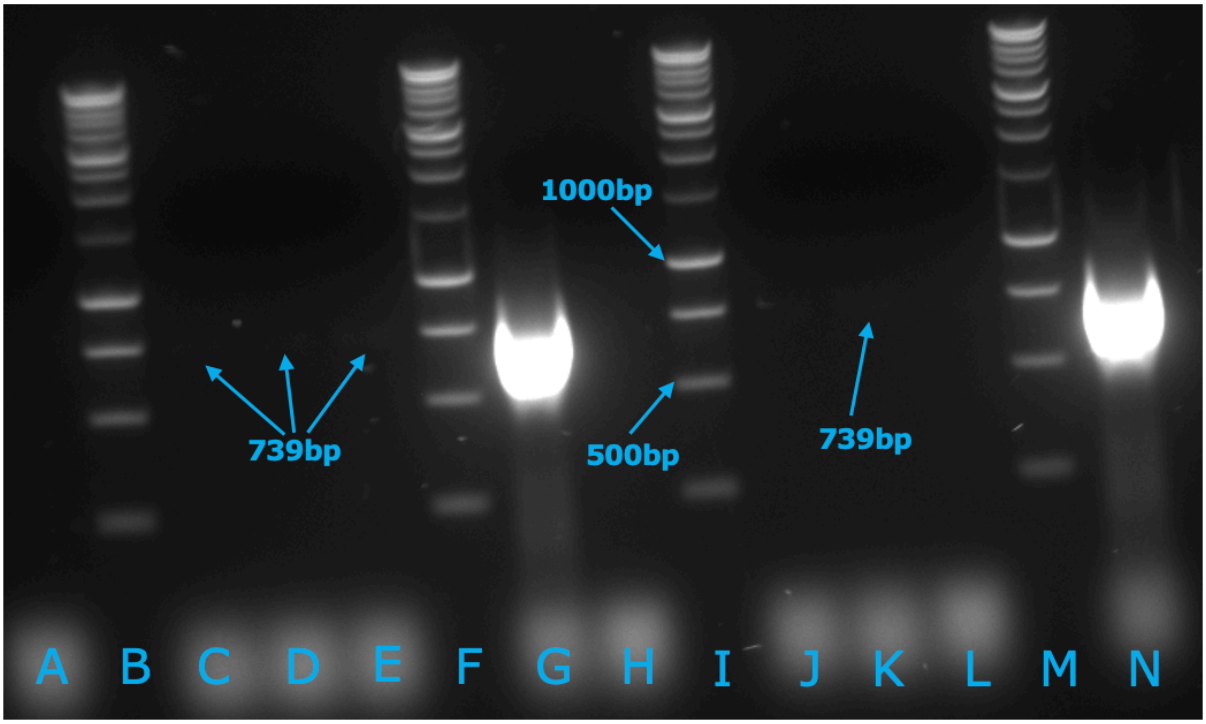

Figure 3.37 Positive V_3V_6 PCR of tilapia muscle Ta48 DNA 1 and 2 (2nd batch). This image shows two PCRs – Ta48 DNA 1 *(left)* and Ta48 DNA 2 *(right)*. There are positive results with the expected band size of 739bp for bacterial DNA presence in lanes C, D and E of Ta7 DNA 1 *(left)* and lane K of Ta48 DNA 2 *(right)*. V_3V_6 primers (Chakravorty et al., 2007) were used, at an annealing temperature of 58°C. Lanes A and H are negative controls and lanes G and N are positive controls using *Streptococcus uberis* DNA. Lanes B, F, I and M are 1kb ladder (Promega)

3.11.2 Streptococcus uberis

Primers to *sub0888* (Leigh et al., 2010) were used to determine if S*treptococcus uberis* was one of the species of bacteria present in the plastisphere that were isolated from the micro- and macroplastics. None of the samples were positive.

3.11.3 Klebsiella pneumoniae

Primers to *tyrB* (Heilbronn et al., 1999) were used to determine if *Klebsiella pneumoniae* was one of the species of bacteria present, however none of the samples were positive.

3.11.4 Escherichia coli

Primers to *uspA* (Chen and Griffiths, 1998) and *uidA* (Heijnen and Medema, 2006) were used to determine if *Escherichia coli* was one of the species of bacteria present; none of the samples were positive.

3.11.5 Campylobacter coli and Campylobacter jejuni

Primers to *porA*, an outer membrane protein (Fontanot et al., 2014), and *jej*, which targets the 16S rRNA (Linton et al., 1997), were used to determine if *Campylobacter coli* or *C. jejuni* were one of the species of bacteria present; none of the samples were positive.

3.11.6 Lactobacillus

Primers to *lact* (Dubernet et al., 2002) were used to determine if *Lactobacillus* was one of the species of bacteria present, however none of the samples were positive.

3.11.7 Summary of PCR results

An overview of all the PCR results collected is shown in Tables 3.38 and 3.39. Tilapia muscle (Ta), gastrointestinal tract contents (GI) and intact gastrointestinal tracts (GIT) (Table 3.38), as well as macroplastic litter results are shown (Table 3.39).

	Ta7	Ta18	Ta20	Ta33	Ta44	Ta48	Ta61	Ta66	Ta69	Ta72
V_3V_6	+	-	+	-	-	+	-	-	-	-
Streptococcus uberis	N.T	N.T	N.T	N.T	N.T	N.T	N.T	N.T	N.T	N.T
Klebsiella pnuemoniae	N.T	N.T	N.T	N.T	N.T	N.T	N.T	N.T	N.T	N.T
Escherichia coli (uspA)	N.T	N.T	N.T	N.T	N.T	N.T	N.T	N.T	N.T	N.T
Escherichia coli (uidA)	N.T	N.T	N.T	N.T	N.T	N.T	N.T	N.T	N.T	N.T
Campylobacter coli (porA)	-	N.T	N.T	N.T	N.T	-	N.T	N.T	N.T	N.T
Campylobacter jejuni (porA)	-	N.T	N.T	N.T	N.T	-	N.T	N.T	N.T	N.T
Campylobacter coli (jej)	-	N.T	N.T	N.T	N.T	-	N.T	N.T	N.T	N.T
Campylobacter jejuni (jej)	-	N.T	N.T	N.T	N.T	-	N.T	N.T	N.T	N.T
Lactobacillus	-	N.T	N.T	N.T	N.T	-	N.T	N.T	N.T	N.T

Table 3.38 Overview of PCR results from tilapia samples. This table shows the PCR results collected for the 10 tilapia muscle samples (Ta7, Ta18, Ta20, Ta33, Ta44, Ta48, Ta61, Ta66, Ta69 and Ta72), screened with primers for *V_3V_6, sub0888, tyrB, uspA, uidA, 'porA', 'jej',* and *'lact'* primers. Positive PCR results are shown with a (+) and negative PCR results are shown with a (-). Not tested samples (N.T) was when primers were not tested on this sample.

	Blue net	Yellow net	Green net	Sandwich bag
V3V6	+	+	+	+
Streptococcus uberis	-	-	-	-
Klebsiella pnuemoniae	-	N.T	N.T	-
Escherichia coli (uspA)	-	-	-	-
Escherichia coli (uidA)	-	-	-	-
Campylobacter coli (porA)	N.T	-	N.T	-
Campylobacter jejuni (porA)	N.T	-	N.T	-
Campylobacter coli (jej)	N.T	-	N.T	-
Campylobacter jejuni (jej)	N.T	-	N.T	-
Lactobacillus	N.T	-	N.T	-

Table 3.39 Overview of PCR results from macroplastic litter. This table shows the PCR results collected for the macroplastic litter and nets collected from Lake Victoria (blue net, yellow net, green net and sandwich bag), screened with primers for *V_3V_6, sub0888, tyrB, uspA, uidA, 'porA', 'jej'* and *'lact'* primers. Positive PCR results are shown with a (+) and negative PCR results are shown with a (-). Not tested samples (N.T) was when primers were not tested on this sample.

3.12 Cloning

The PCR products of V_3V_6 PCR were cloned for downstream sequencing with the aim of identifying the species of bacteria present. A TOPO TA cloning kit was used and white colonies were picked for further analysis (Figure 3.40).

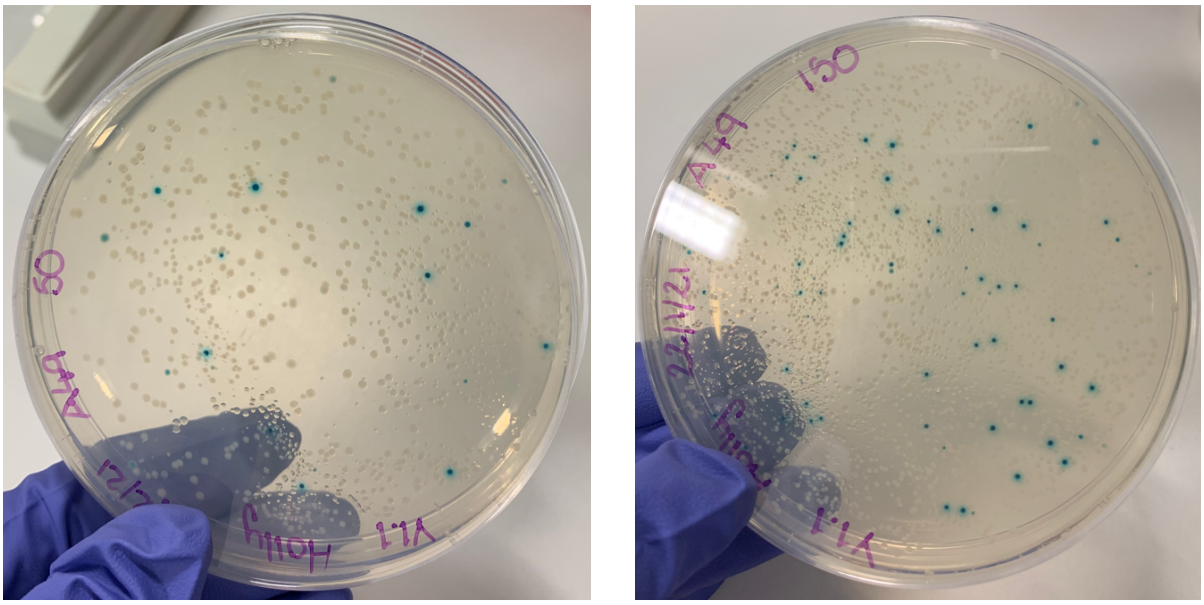

Figure 3.40 Cloned colonies from yellow net DNA 1. This image shows the white colonies that were obtained from a ligation of yellow net DNA 1 into the TA cloning vector pCR™2.1-TOPO® (Invitrogen). Only white colonies were circled, numbered on the plate and picked with a pipette tip and put into nutrient broth containing either ampicillin or kanamycin.

3.12.1 Screening of colonies isolated

White colonies were screened for presence of the inserted V3V6 product using M13 reverse and T7 primers, which anneal to the multiple cloning site of the pCR™2.1-TOPO® vector. Only 2 colonies (colony 9 and 11) from the yellow net sample DNA 1 produced bands of the expected size (Figure 3.41)

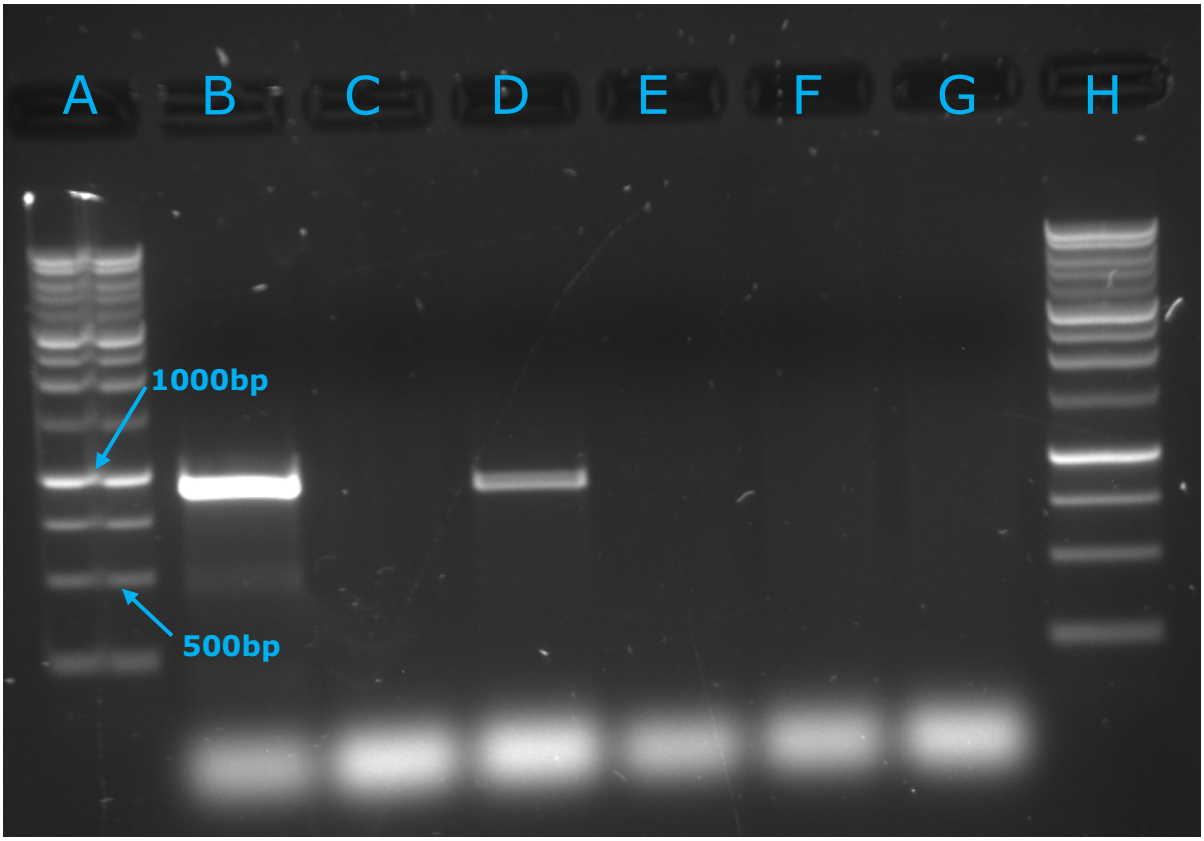

Figure 3.41 PCR from colony from ligation with yellow net DNA 1 sample. This image shows the positive PCR using M13 reverse and T7 primers, which anneal to the multiple cloning site of the pCR™2.1-TOPO® vector. Lanes B and D show positive results with the expected band size. PCR was conducted at an annealing temperature of 58°C. Lanes A and H are 1kb ladder (Promega).

3.13 ESEM/EDX screening

ESEM was used to provide high resolution images which facilitated the visualisation and characterisation of surfaces within the samples, as well as elemental compositions. This was used to screen for microplastics and biofilm presence and rule out any non-plastic artefacts.

3.13.1 Screening of control samples

In order to visualise and characterise what the introduced surfaces (e.g. the filter paper) and methodology used to prepare the samples (e.g. the KOH) were having on the potential ESEM results, several controls were incorporated into the screening.

3.13.1.1 Filter paper with no reagents

A section of plain Whatman microfibre filter paper, with no reagents, was analysed by ESEM/EDX screening as a control, highlighting any interference coming directly from the filter paper. The filter paper had a fibrous appearance (Figure 3.42A), that could have been misinterpreted as microfibres. EDX analysis of the filter paper (spectrum 124) detected low carbon (C) levels demonstrating that the material was non-organic (Figure 3.42D), there were also medium levels of silicon (Si) and oxygen (O) and trace levels barium (Ba) associated with the structure. Small spherical bead structures were also identified (spectrum 122 and 123), with EDX analyses highlighting medium levels of O and Si, and low levels of chlorine (Cl) and Ba associated with the structure in spectrum 122 (figure 3.42B), and similarly highlighting medium levels of O and Si, and low levels of Cl and Ba associated with the structure in spectrum 123 (Figure 3.42C).

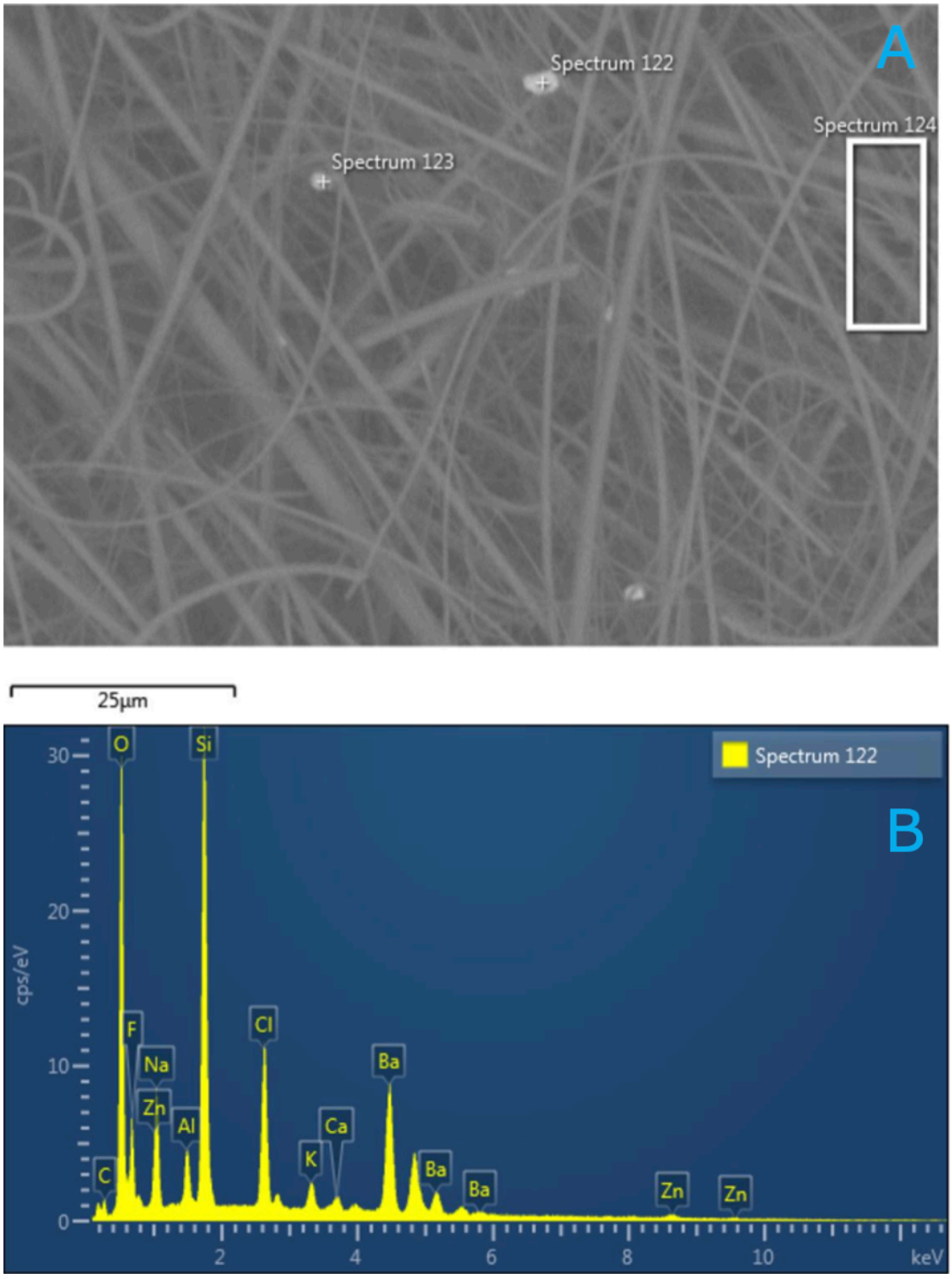

Figure 3.42 ESEM with EDX spectra of Whatman glass microfiber filters. *(A)* ESEM greyscale image taken of a Whatman glass microfiber filter (Sigma-Aldrich) used in this study. A scale was developed to group detected elements by their concentrations measured in cps/ev; >100 cps/ev is very high, 60-99 cps/ev is high, 20-59 cps/ev is medium, 10-19 cps/ev is low and <10 cps/ev is trace. *(B)* EDX spectra of spectrum 122 showing medium levels of oxygen (O) and silicon (Si) and low levels of chlorine (Cl) and barium (Ba) associated with the structure within the image.

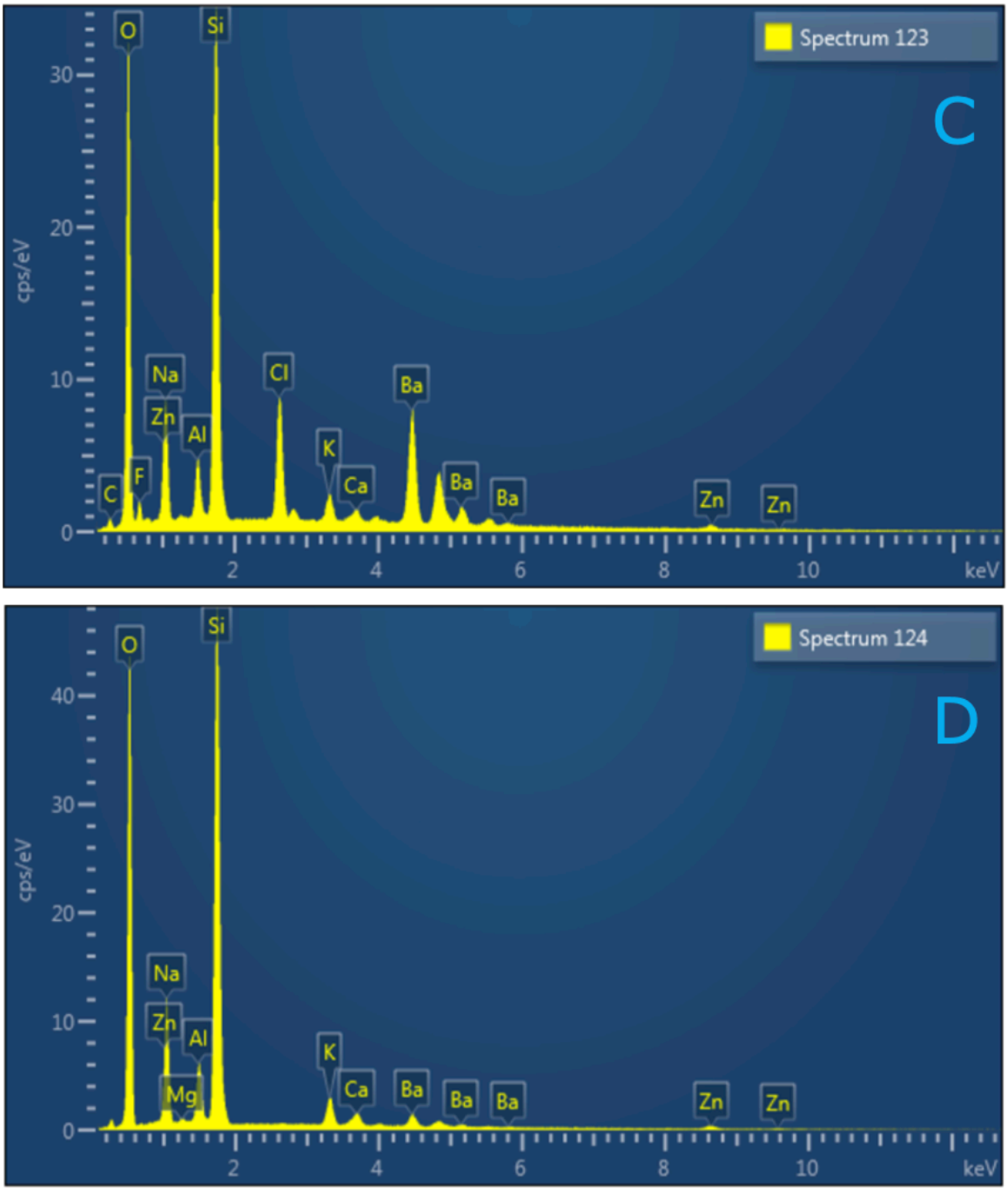

Figure 3.42 (continued) ESEM with EDX spectra of Whatman glass microfiber filters. *(C)* EDX spectra of spectrum 123 showing medium levels of oxygen (O) and silicon (Si) and low levels of chlorine (Cl) and barium (Ba) associated with the structure. *(D)* EDX spectra of spectrum 124 showing medium levels of O and Si and trace levels Ba associated with the structure.

3.13.1.2 Filter paper with KOH

Filter paper with KOH (10% solution) was also analysed by ESEM/EDX screening as a control. The fibrous appearance of the filter paper was seen again on the greyscale EDX image (Figure 3.43A), however there were also clusters of lighter grey areas (spectrum 152). EDX analysis showed these having medium levels of potassium (K) (Figure 3.43C), Si levels were also lower here than observed on the filter paper alone. Spherical bead structures were identified (spectrum 151), with EDX analyses highlighting medium O, Si and K levels, and a K level was lower than that of filter paper alone (Figure 3.43B). There was also a low level of Ba and a trace level of C associated with the structure.

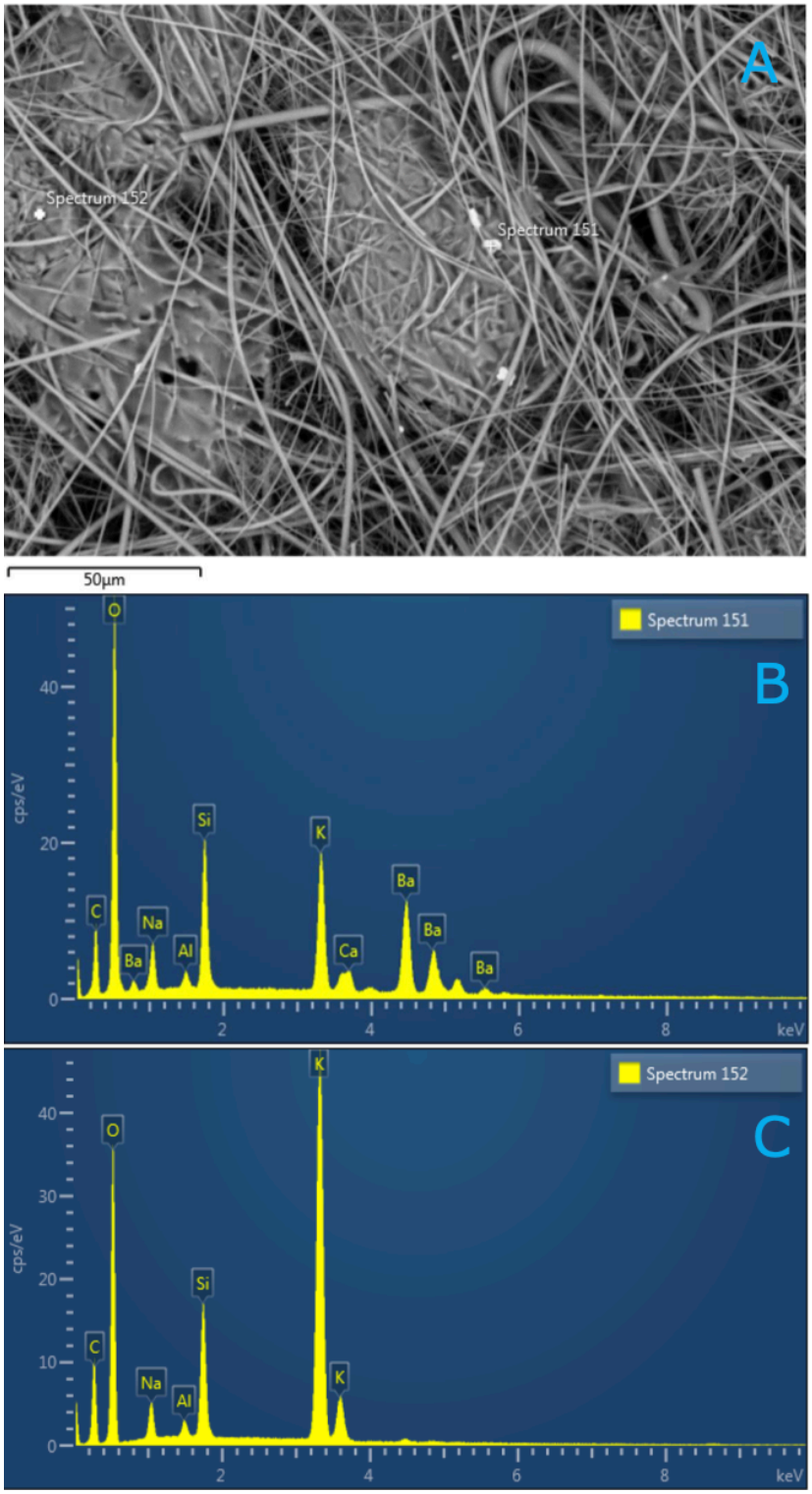

Figure 3.43 ESEM with EDX spectra of Whatman glass microfiber filters with potassium hydroxide. *(A)* ESEM greyscale image taken of a Whatman glass microfiber filter (Sigma-Aldrich) with potassium hydroxide (KOH) (10% solution) on its surface. *(B)* EDX spectra of spectrum 151 showing medium levels of oxygen (O), silicon (Si) and potassium (K), a low level of barium (Ba), and a trace level of carbon (C) associated with the structure in the image. *(C)* EDX spectra of spectrum 152 showing medium levels O, Si and K, and a trace level of C associated with the structure in the image.

3.13.1.3 Filter paper with Nile Red and DAPI stains

Filter paper that had been stained with Nile Red and DAPI was analysed by ESEM/EDX screening as a third control. The fibrous filter paper appearance was seen again on the greyscale EDX image, along with sphere shaped deposits across its surface (Figure 3.44A). These were focussed on for EDX analyses (spectrum 128) and found medium levels of O, Si, Cl and sodium (Na) (Figure 3.44B) and trace levels of Ba, zinc (Zn) and aluminium (Al). Analysis of a second sphere (spectrum 129) was similar highlighting medium levels of O, Si, Cl and Na (Figure 3.44C), however there were lower levels of O and Si and higher levels of Na and Cl than the structure in spectrum 128. It also had trace levels of Ba, Zn and Al.

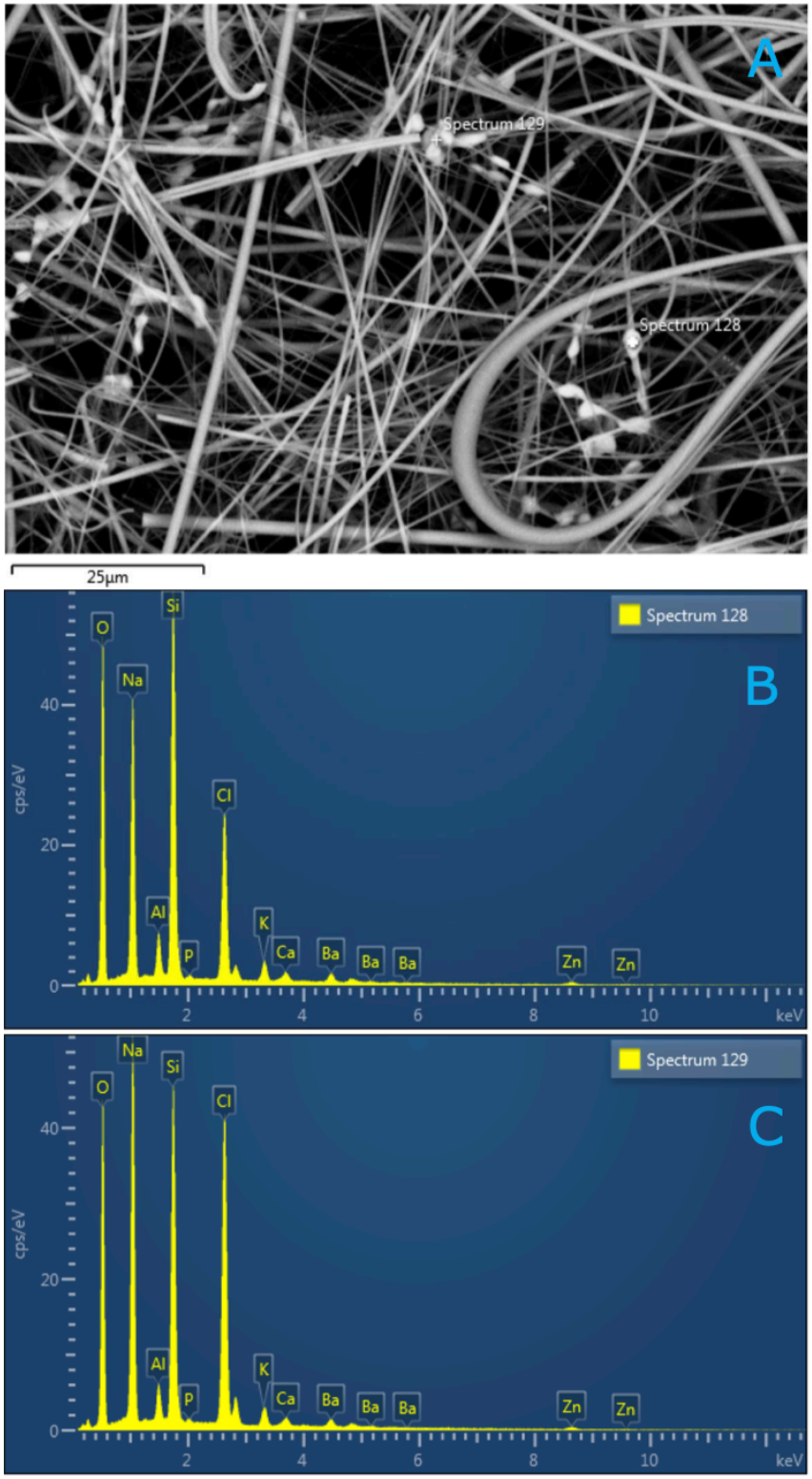

Figure 3.44 ESEM with EDX spectra of Whatman glass microfiber filters with Nile Red and DAPI stains. *(A)* ESEM greyscale image taken of a Whatman glass microfiber filter (Sigma-Aldrich) with Nile Red and DAPI stains on its surface. *(B)* EDX spectra of spectrum 128 showing medium levels of oxygen (O), silicon (Si), chlorine (Cl) and sodium (Na), and trace levels barium (Ba), zinc (Zn) and aluminium (Al) associated with the structure in the image. *(C)* EDX spectra of spectrum 129 showing medium levels O, Si, Cl and Na, and trace levels of Ba, Zn and Al associated with the structure.

3.13.1.4 Macroplastic litter and microbeads

A selection of macroplastic litter and netting collected from Lake Victoria, plus extracted microbeads from the Clean & Clear facewash, were also analysed. These had been treated with KOH, Nile Red and DAPI stains. Their structure and elemental composition were recorded. ESEM grey scale and single-elemental-coloured images were taken of these samples, however no EDX spectras were taken.

ESEM screening of a mixture of microbeads and netting showed uniformly spherical structures and clusters of lighter grey areas, on the surface of a fibrous background material (Figure 3.45A). Single-elemental-coloured images taken of the same area, showed the strong association of Ba with the sphere structures (Figure 3.45G), with K (Figure 3.45D) and C (figure 3.45E) associated with the lighter grey areas. Si (Figure 3.45B), O (Figure 3.45C) and Na (Figure 3.45F) were also associated with the fibrous background structures.

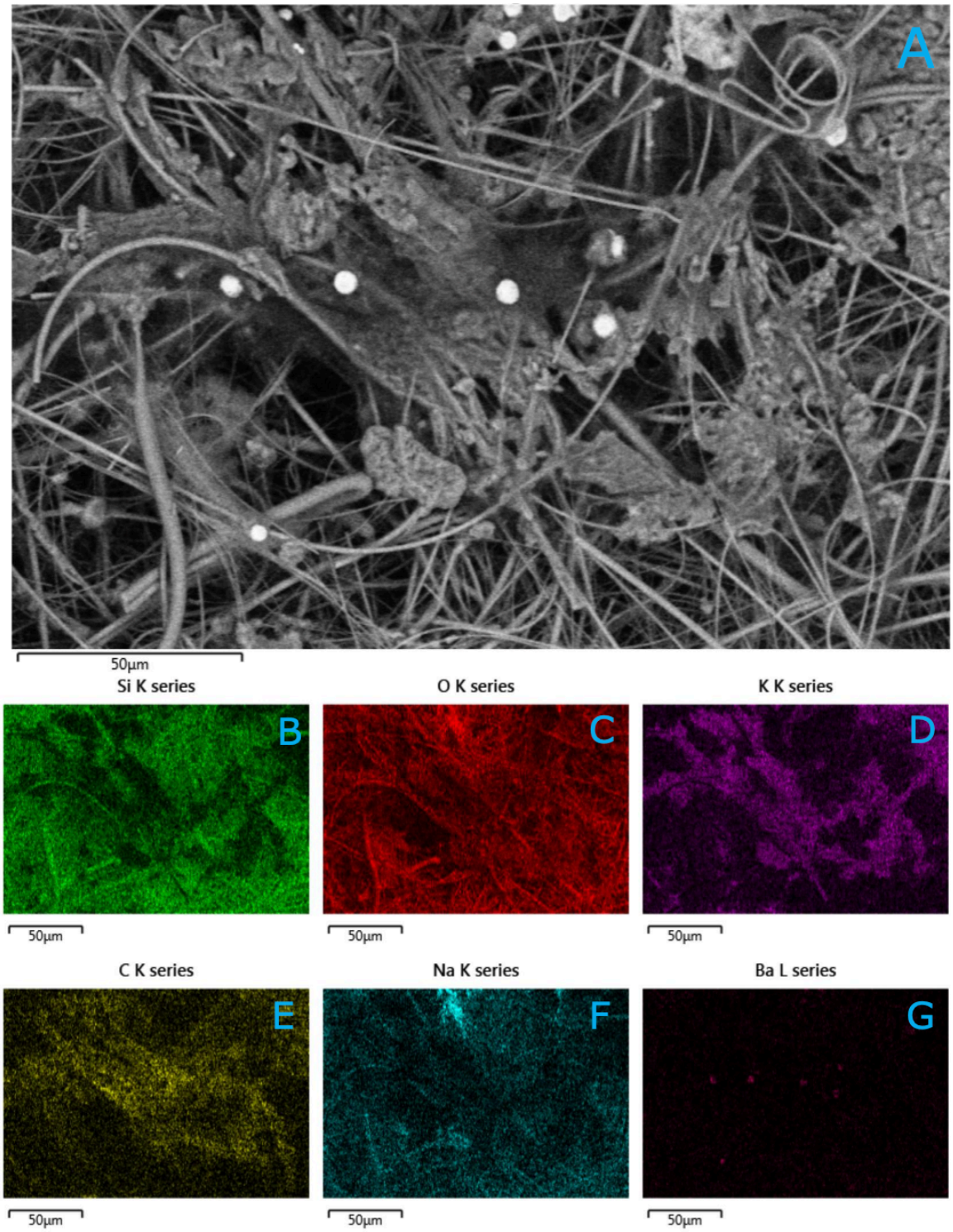

Figure 3.45 ESEM greyscale with single-elemental-coloured images of macroplastic litter and microbeads. *(A)* ESEM greyscale image taken of a mixture of microbeads (extracted from 2017 Clean & Clear facewash) and netting collected from Lake Victoria. Single-elemental-coloured (SEC) images showing the presence of; *(B)* silicon (Si) associated with the structure within the image, *(C)* oxygen (O) associated with the structure, *(D)* potassium (K) associated with the structure, *(E)* carbon (C) associated with the structure, *(F)* sodium (Na) associated with the structure, *(G)* barium (Ba) associated with the structure.

3.13.1.5 Macroplastic litter without reagents

Untreated macroplastic litter collected from Lake Victoria, with no reagents or filter paper present, was screened by ESEM and single-elemental-coloured images were taken, however no EDX spectras were taken. ESEM screening on one chosen area of this material showed numerous cube-shaped structures (Figure 3.46A), on the surface of a rougher material containing many grooves and pits. Single-elemental-coloured images taken of the same area, showed O and calcium (Ca) were associated with the cube structures (Figure 3.46C and F). The presence of C (Figure 3.46B), O (Figure 3.46C) and Si (Figure 3.46D) were associated with the unsmooth background material. There were also lower levels of sulphur (S) (Figure 3.46E) and iron (Fe) (Figure 3.46G) associated with this structure within the image.

ESEM screening on another chosen area on this material showed a larger (~900µm in length) elliptical shaped structure on a smoother material that was not uniform in appearance (Figure 3.47A). Single-elemental-coloured images taken of this same area, showed the structure to have a high content of O (Figure 3.47C), Ca (Figure 3.47D), phosphorus (P) (Figure 3.47F), with Ca and P specifically associated with this elliptical structure. Oxygen was also associated with the background material, as well as C (Figure 3.47B) with the latter not associated with the elliptical structure. There were also low levels of Si (Figure 3.47E) and Fe (Figure 3.47G) associated with the background structure within the image.

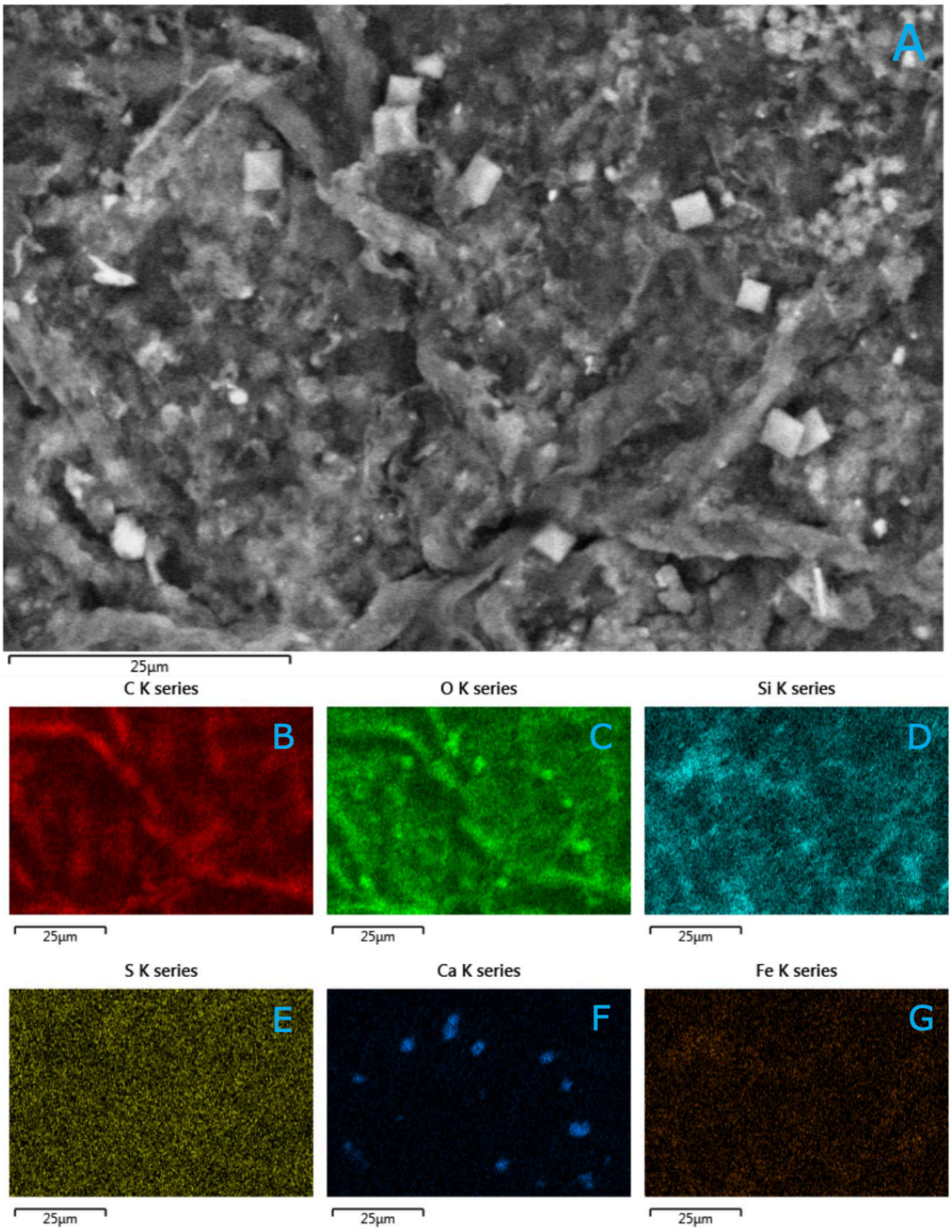

Figure 3.46 ESEM greyscale with single-elemental-coloured images of untreated macroplastic litter. *(A)* ESEM greyscale image taken of a section of macroplastic litter collected from Lake Victoria. Single-elemental-coloured (SEC) images showing the presence of; *(B)* carbon (C) associated with the structure within the image, *(C)* oxygen (O) associated with the structure, *(D)* silicon (Si) associated with the structure, *(E)* sulphur (S) associated with the structure, *(F)* calcium (Ca) associated with the structure and *(G)* iron (Fe) associated with the structure.

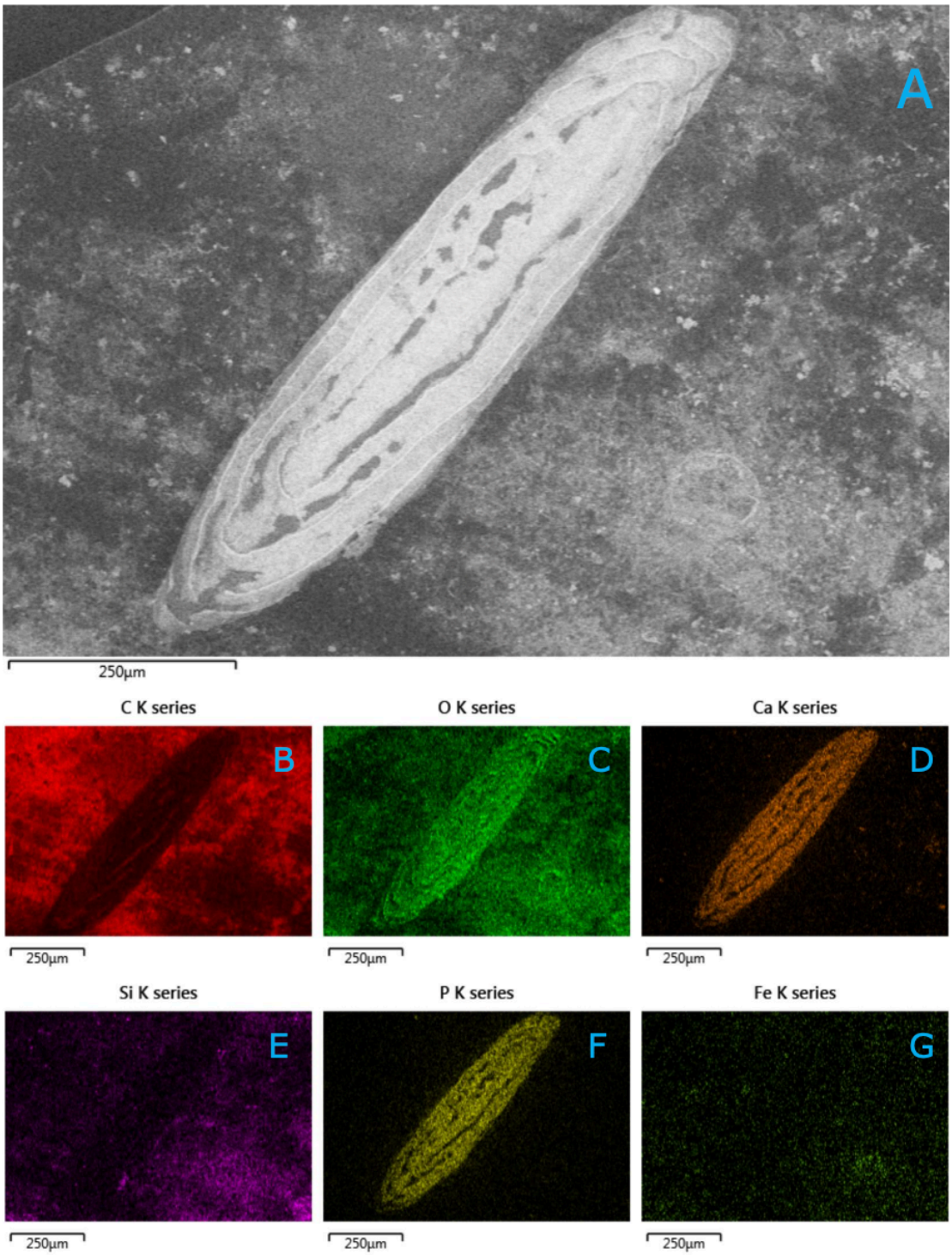

Figure 3.47 ESEM greyscale with single-elemental-coloured images of untreated macroplastic litter. *(A)* ESEM greyscale image taken of a different section of macroplastic litter collected from Lake Victoria. Single-elemental-coloured (SEC) images showing the presence of; *(B)* carbon (C) associated with the structure within the image, *(C)* of oxygen (O) associated with the structure, *(D)* calcium (Ca) associated with the structure, *(E)* silicon (Si) associated with the structure, *(F)* phosphorus (P) associated with the structure and *(G)* iron (Fe) associated with the structure.

3.13.2 Screening of the macroplastic

Untreated macroplastic litter collected from Lake Victoria was screened for potential biofilm and bacterial presence.

3.13.2.1 Presence of diatoms on plastic litter

Numerous different shaped diatoms (Figure 3.48) were identified. These included circular flukes, longer rods and 3D diatoms. The long thin shaped diatom in Figure 3.48A was potentially identified as the genus *Fragilaria*. Circular diatoms (Figures 3.48B, C and D) were tentatively identified as the genus *Cocconeis.* The cylindrical shaped diatom in Figure 3.48C was potentially identified as the genus *Aulacoseira*. The ellipsoid shaped diatom in Figure 3.48D was potentially identified as the genus *Achnanthes* and the rectangular diatom in Figure 3.48D was potentially identified as the genus *Tabellaria*.

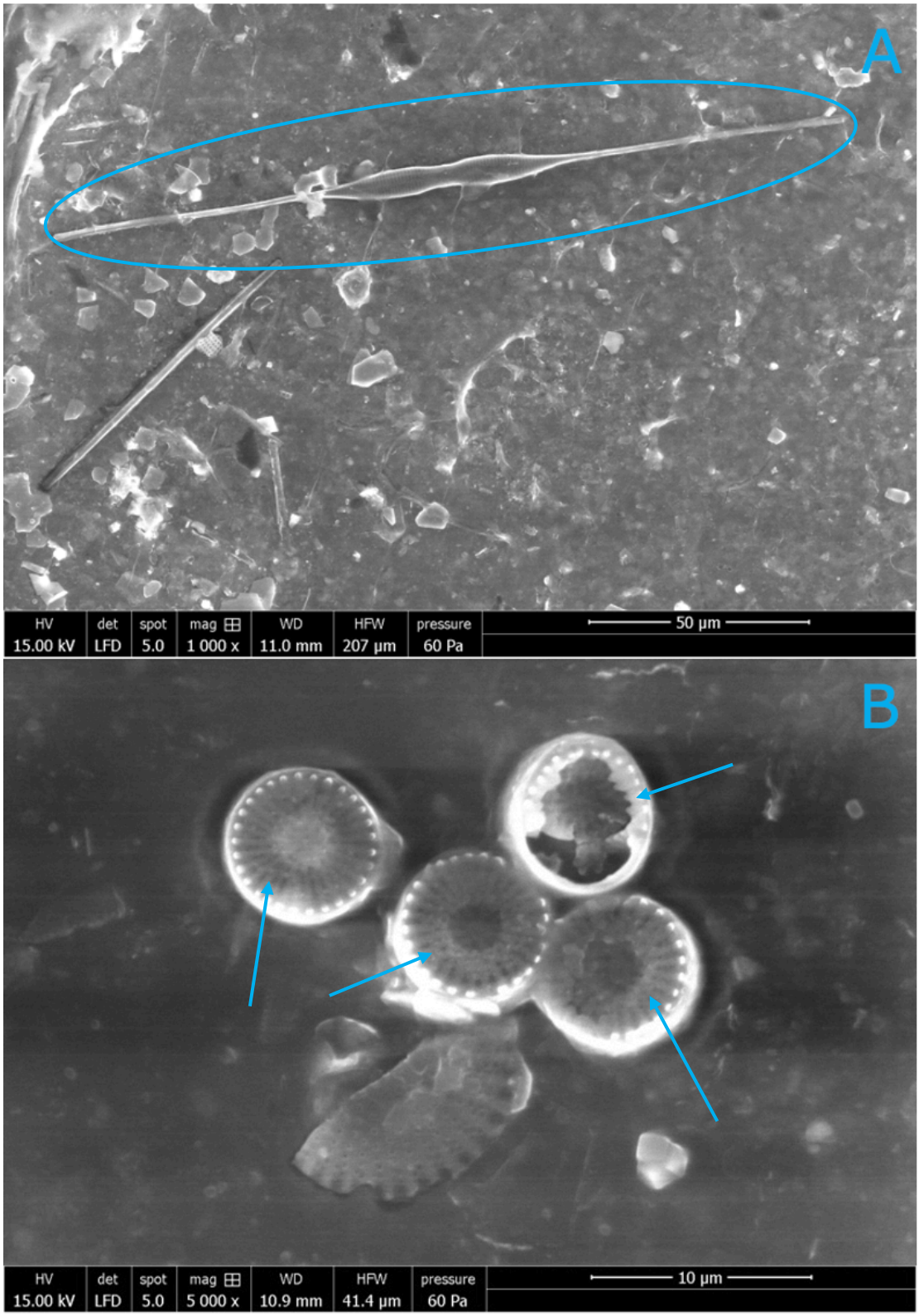

Figure 3.48 ESEM greyscale images of diatoms found on plastic litter from Lake Victoria. These greyscale images taken on the ESEM show different shapes of diatoms identified (shown by blue ring and arrows) on the biofilm of a section of macroplastic litter collected from Lake Victoria. *(A)* shows a long rod-shaped diatom, potentially identified as from the diatom genus *Fragilaria*. *(B)* shows a collection of circular fluke shaped diatoms, which were tentatively identified from the diatom genus *Cocconeis.*

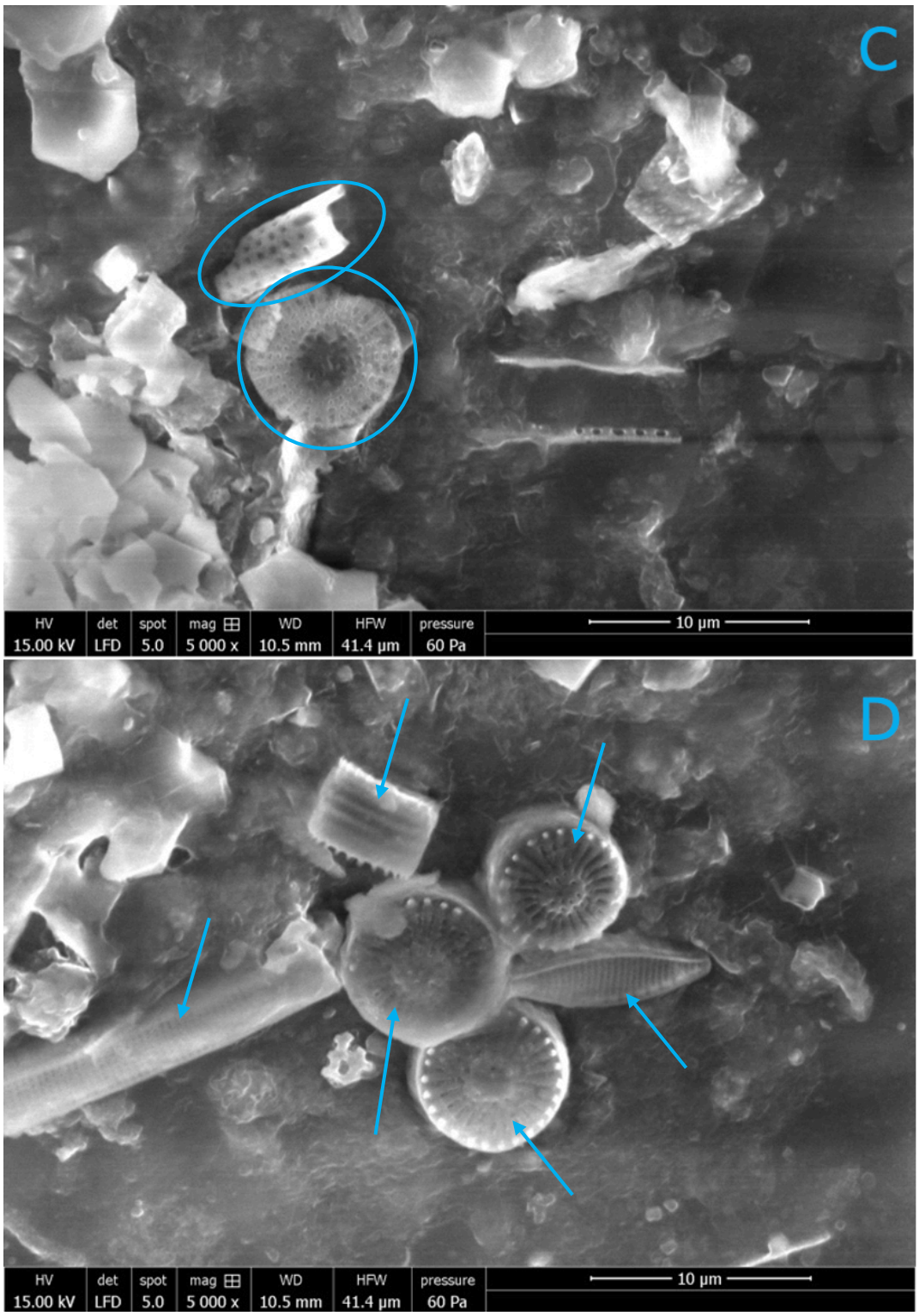

Figure 3.48 (continued) ESEM greyscale images of diatoms found on plastic litter from Lake Victoria. These greyscale images taken on the ESEM show different shapes of diatoms identified (shown by blue rings and arrows) on the biofilm of a section of macroplastic litter collected from Lake Victoria. *C)* shows a circular diatom potentially identified as from the diatom genus *Cocconeis* and a cylindrical diatom potentially identified as from the genus *Aulacoseira. (D)* shows a group of different shaped 3D diatoms, which were tentatively identified as from the diatom genera *Cocconeis*, *Achnanthes*, and *Tabellaria*.

3.13.3 Screening of the filtered muscle

The same filter paper samples used for fluorescent microscopy were sent for SEM analysis. These samples included 4 tilapia muscle samples (Ta18, Ta33, Ta44 and Ta48). ESEM screening included greyscale imaging, single-elemental-coloured imaging and EDX analysis.

3.13.3.1 Filtered muscle - Ta18

ESEM screening of the filtered muscle from sample Ta18 (CT, site 9B) identified a fibrous structure (Figure 3.49A), larger (>50µm in length) in size than the typical filter paper fibres observed (Figure 3.42A), with deposits on its outside structure; these were focussed on for EDX analyses. EDX analysis of these deposits (spectrum 44) showed high C and O levels (Figure 3.49B) and medium levels of Na, Si, K and Ba associated with them. EDX analysis of the larger fibrous structure (spectrum 45) had high levels of C, O and K (Figure 3.49C), with C and K levels higher and O level lower than the external deposits observed (spectrum 44). It also had trace levels of Ba, which were lower than observed in the external deposits (spectrum 44).

Single-elemental-coloured (SEC) images were taken of the same area. These showed the presence of C (Figure 3.50D), Cl (Figure 3.50H) and S (Figure 3.50K), associated with the large fibrous structure.

The presence of K (Figure 3.50A) and P (Figure 3.50G) were associated with both the fibrous structure and the background material. Presence of O (Figure 3.50B) and Na (Figure 3.50E) were associated with part of the large fibrous structure and the background material to the right of it.

The presence of Si (Figure 3.50C) and Ca (Figure 3.50I) were associated with only the background material. The presence of Ba (Figure 3.50F) was associated with

the deposits on the outside of the fibrous structure, and the presence of magnesium (Mg) (Figure 3.50J) was associated with part of the background material to the right of the fibrous structure.

A small elliptical structure (~7μm in length), shown by the blue arrow (Figure 3.49A) was identified through SEC imaging, these highlighted the highest levels of K (Figure 3.50A), Cl (Figure 3.50H), Ca (Figure 3.50I) detected out of all the structures in view, associated with this elliptical structure.

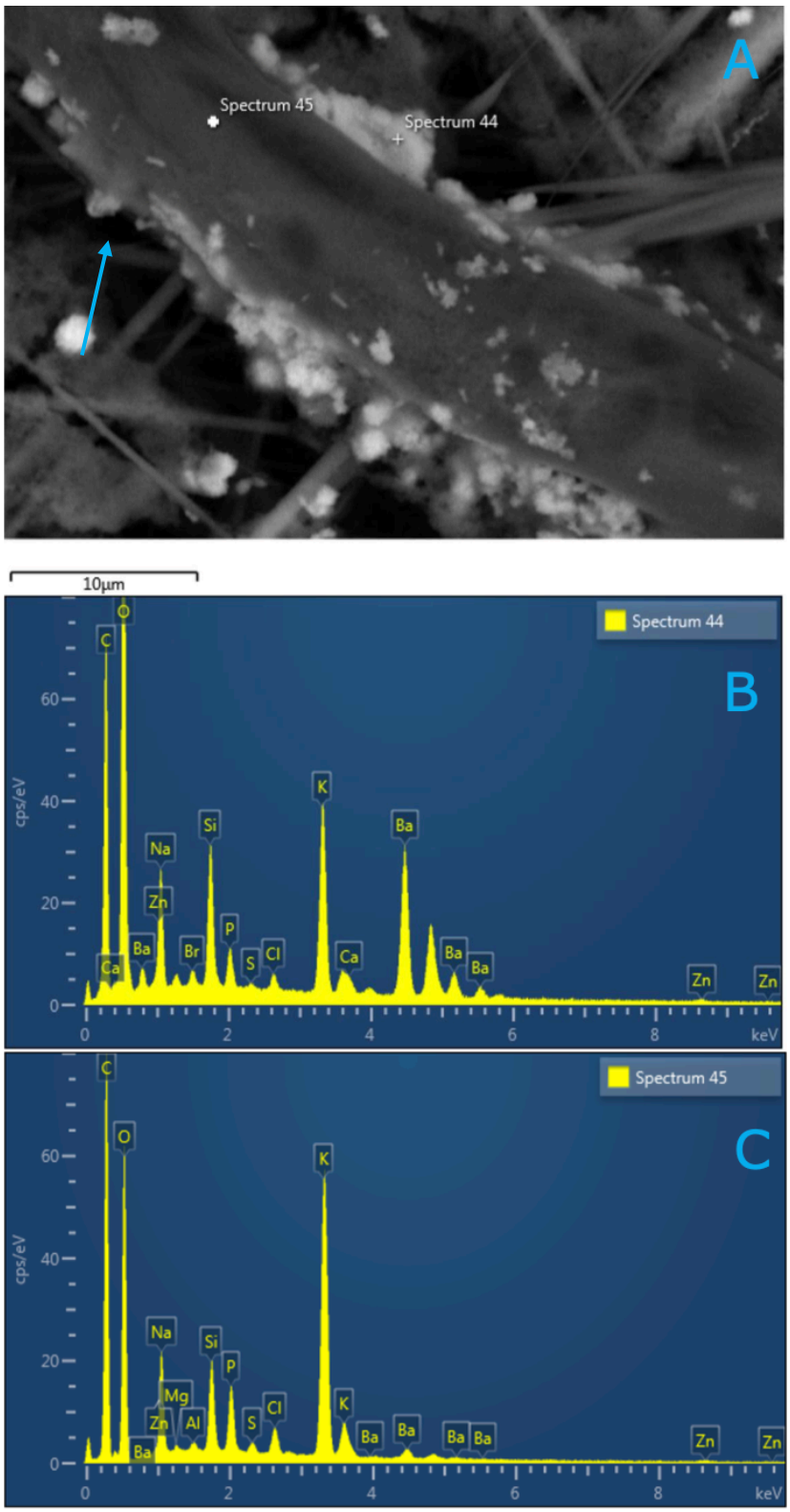

Figure 3.49 ESEM with EDX spectra of filtered muscle. *(A)* ESEM greyscale image taken of a filtered muscle sample (Ta18, caged tilapia, site 9B), containing potassium hydroxide (10% solution), Nile Red and DAPI stains. *(B)* EDX spectra of spectrum 44 showing high levels of carbon(C) and oxygen (O), and medium levels of sodium (Na), silicon (Si), potassium (K) and barium (Ba). *(C)* EDX spectra of spectrum 45 showing high levels of C, O and K and a trace level of Ba.

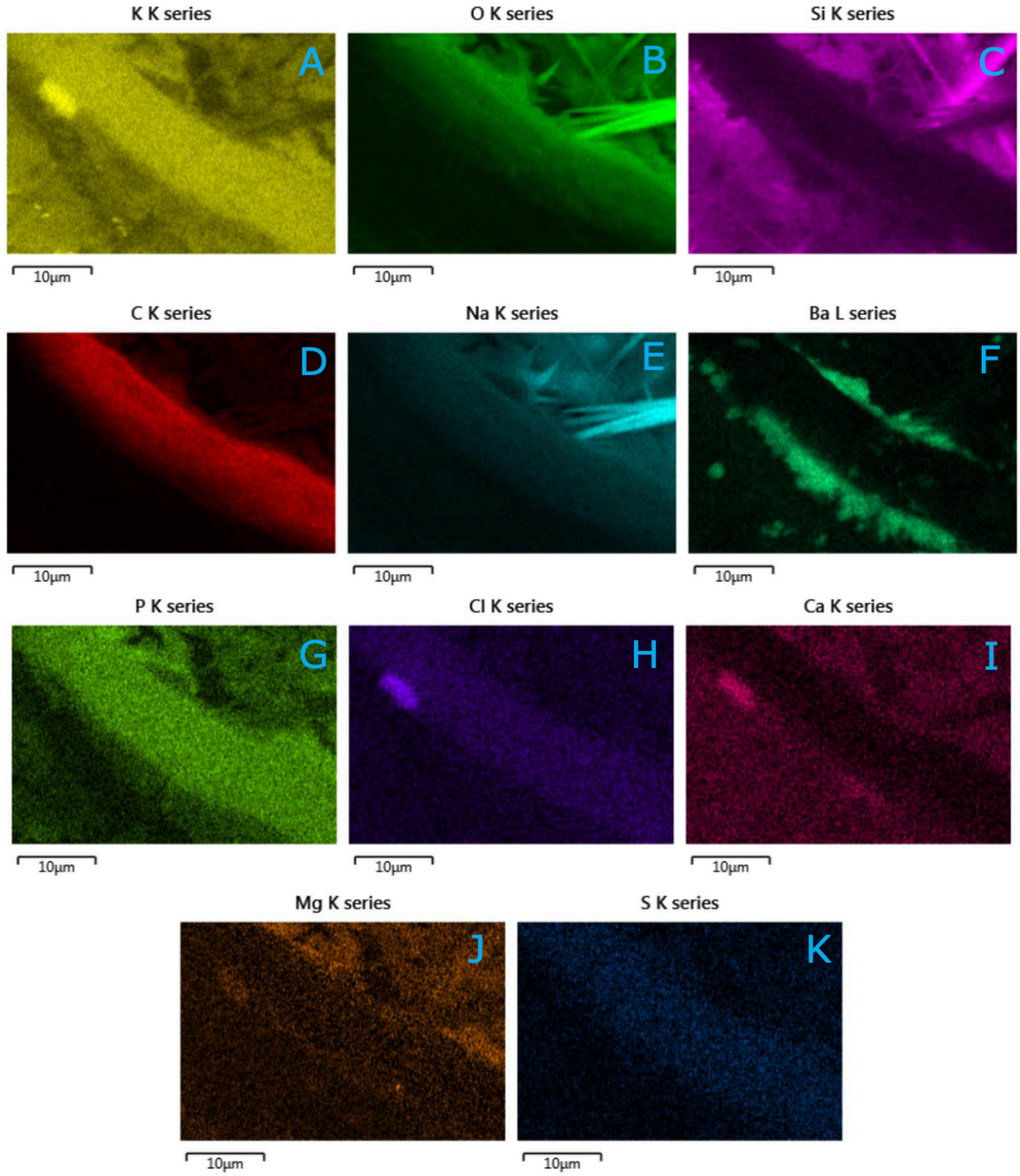

Figure 3.50 ESEM single-elemental-coloured images of filtered muscle. ESEM single-elemental-coloured (SEC) images taken of filtered muscle Ta18 (caged tilapia, site 9B). SEC images showing the presence of; *(A)* potassium (K) associated with the structure within the image, *(B)* (O) associated with the structure within the image, *(C)* silicon (Si) associated with the structure, *(D)* carbon (C) associated with the structure, *(E)* sodium (Na) associated with the structure, *(F)* barium (Ba) associated with the structure, *(G)* phosphorus (P) associated with the structure, *(H)* chlorine (Cl) associated with the structure, *(I)* calcium (Ca) associated with the structure, *(J)* magnesium (Mg) associated with the structure and *(K)* sulphur (S) associated with the structure.

3.13.3.2 Filtered muscle – Ta33

ESEM screening of the filtered muscle from sample Ta33 (wild tilapia, site 4D) identified another larger (>30µm in length) fibrous structure (Figure 3.51A) running down the centre of the image shown and larger in size than the filter paper fibres (Figure 3.42A), with deposits on its outside surface. Single-elemental-coloured images were taken of this same area and showed the presence of C associated only with the large fibrous structure (Figure 3.51E). The presence of Si (Figure 3.51B) was exclusively associated with the background material. The presence of K (Figure 3.51D) was associated with all structures in the image, with lower levels of O (Figure 3.51C) and Na (Figure 3.51F) also associated with all structures. The presence of Ba was only associated with the outside deposits on the larger fibrous structure, and deposit clusters on the background material (Figure 3.51G).

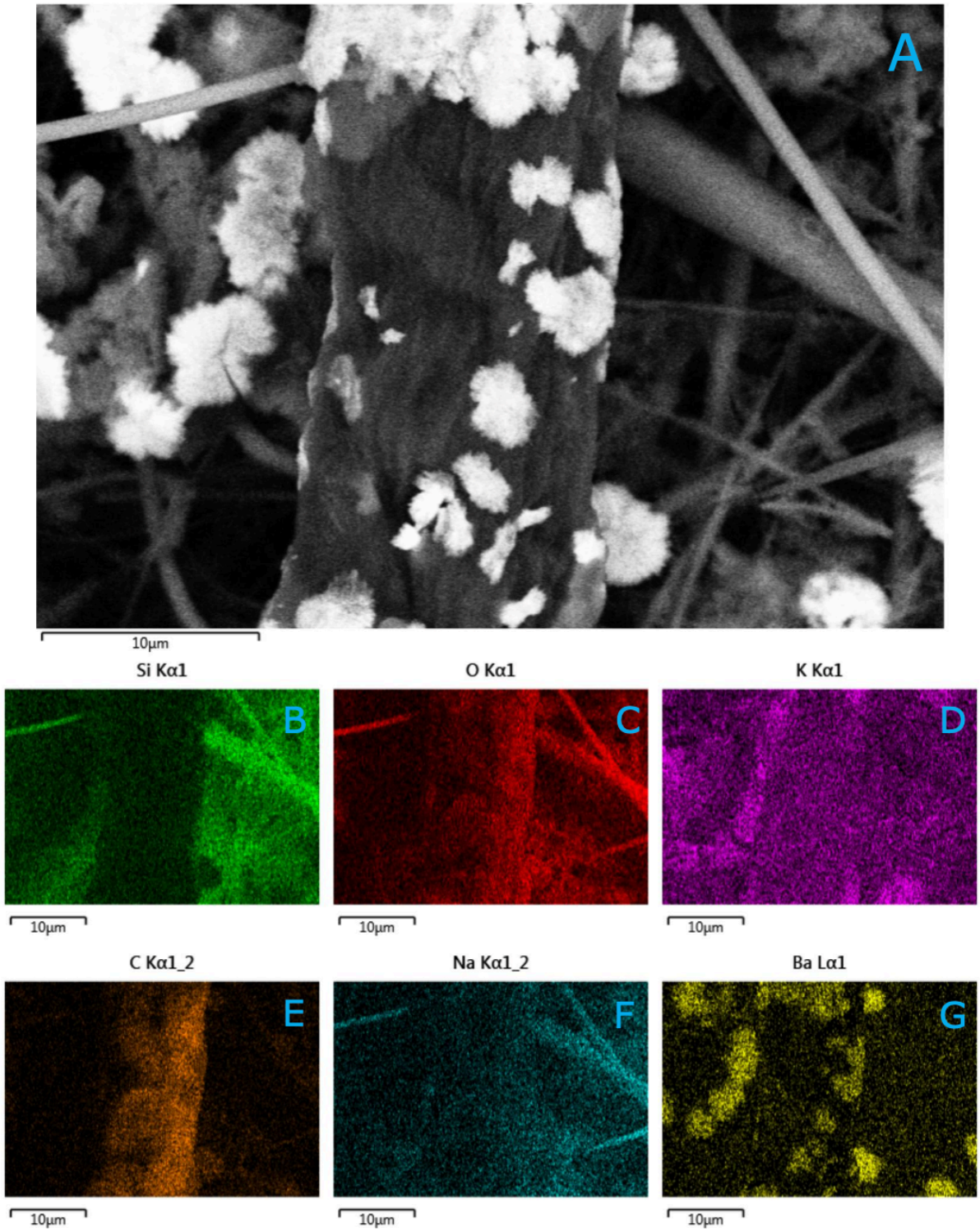

Figure 3.51 ESEM greyscale with single-elemental-coloured images of filtered muscle. *(A)* ESEM greyscale image taken of a section of filtered muscle sample Ta33 (wild tilapia, site 4D). Single-elemental-coloured (SEC) images showing the presence of; *(B)* silicon (Si) associated with the structure within the image, *(C)* oxygen (O) associated with the structure, *(D)* potassium (K) associated with the structure*, (E)* calcium (C) associated with the structure, *(F)* sodium (Na) associated with the structure and *(G)* barium (Ba) associated with the structure.

3.13.3.3 Filtered muscle – Ta44

ESEM greyscale screening of the filtered muscle from sample Ta44 (wild tilapia, site 7D) identified a larger (>75µm in length) darker grey structure on top of the fibrous background material (Figure 3.52A). The fibrous background had two small deposits similar to those observed in the other muscle samples. Single-elemental-coloured images were taken of this same area and showed the presence of C (Figure 3.52C) associated with only the darker grey structure. The presence of Si (Figure 3.52B), O (Figure 3.52D) and Na (Figure 3.52E) were only associated with the fibrous background material. The presence of Ba (Figure 3.52F) and Ca (Figure 3.52G) were associated exclusively with the two deposits on the background material, with Ca at a lower level.

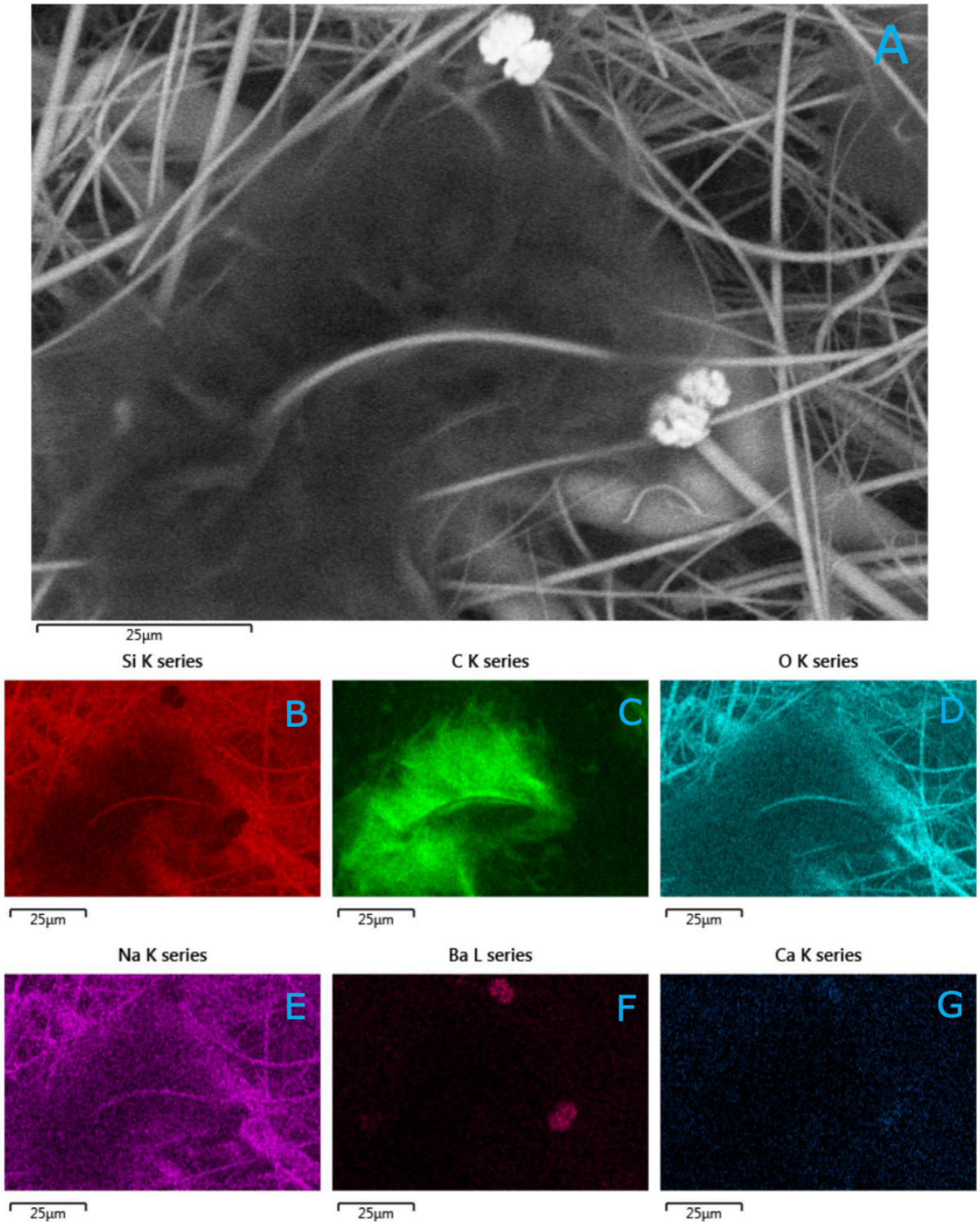

Figure 3.52 ESEM greyscale with single-elemental-coloured images of filtered muscle. *(A)* ESEM greyscale image taken of a section of filtered muscle sample Ta44 (wild tilapia, site 7D). Single-elemental-coloured (SEC) image showing the presence of; *(B)* silicon (Si) associated with the structure within the image, *(C)* carbon (C) associated with the structure, *(D)* oxygen (O) associated with the structure, *(E)* sodium (Na) associated with the structure, *(F)* barium (Ba) associated with the structure and *(G)* calcium (Ca) associated with the structure.

3.13.3.4 Filtered muscle – Ta48

ESEM greyscale screening of the filtered muscle from sample Ta44 (wild tilapia, site 15D) identified an artefact (>75µm in length), with a rough structural appearance (Figures 3.53A and 3.54A), which was on top of the fibrous background material. Single-elemental-coloured images were taken of this same area and showed the presence Ca (Figure 3.53F) and P (Figure 3.53G) exclusively associated with this artefact. Higher levels of C (Figure 3.54H) and Mg (Figure 3.54I) were observed in this artefact when compared to the background structure. K (Figure 3.53D) was also associated with this artefact, but its presence was not uniform across the structure. The presence of O (Figure 3.53B) and Na (Figure 3.53E) were similarly associated with the fibrous background material and a smaller area potentially on the surface of this artefact. There were also small areas of Ba (Figure 3.54J) and Cl (Figure 3.54K) associated with the artefact. The presence of Si (Figure 3.53C) was higher in the fibrous background material than in the artefact.

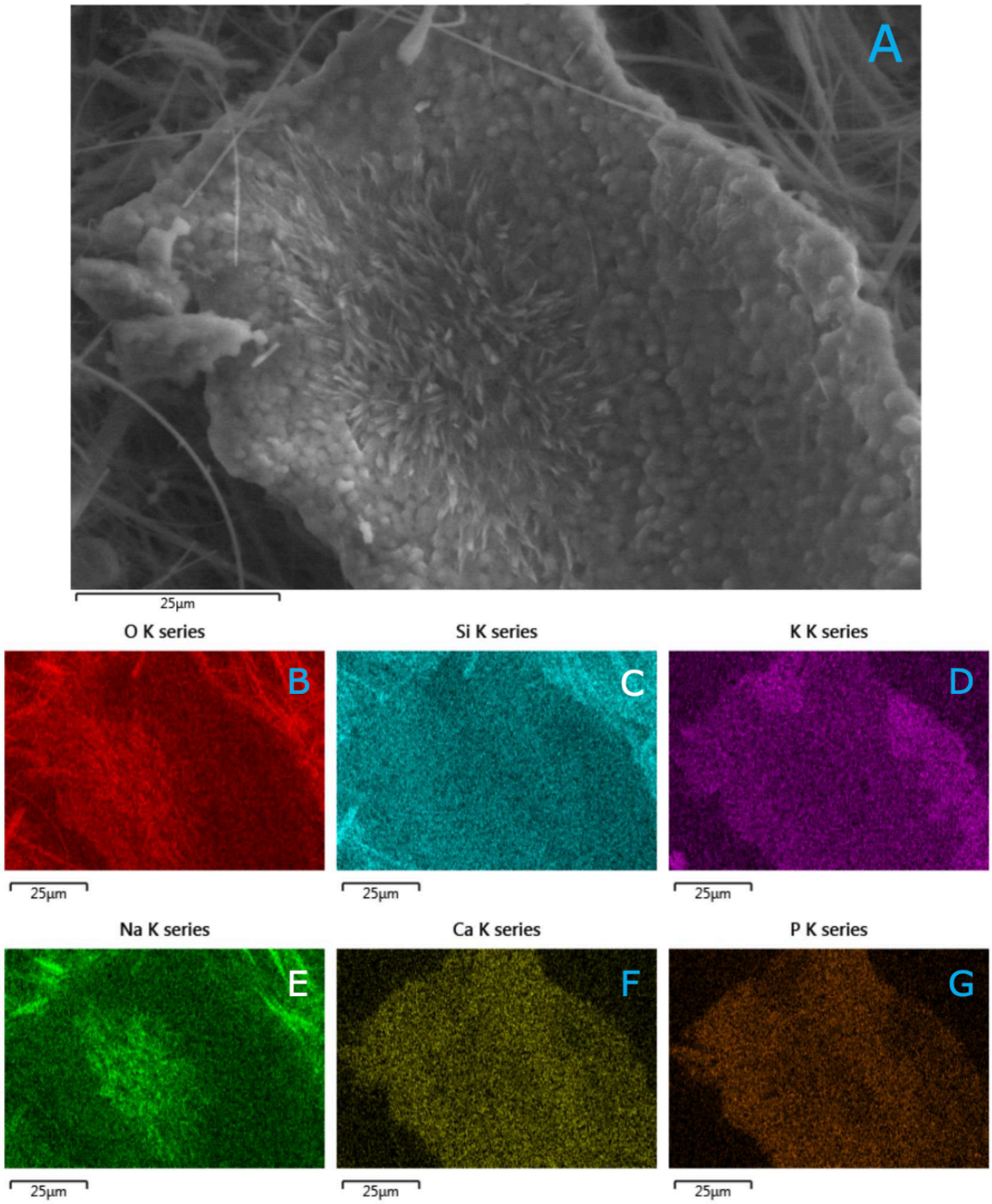

Figure 3.53 ESEM greyscale with single-elemental-coloured images of filtered muscle. *(A)* ESEM greyscale image taken of a section of filtered muscle sample Ta48 (wild tilapia, site 15D). Single-elemental-coloured (SEC) image showing the presence of; *(B)* oxygen (O) associated with the structure within the image, *(C)* silicon (Si) associated with the structure, *(D)* potassium (K) associated with the structure, *(E)* sodium (Na) associated with the structure, *(F)* calcium (Ca) associated with the structure and *(G)* phosphorus (P) associated with the structure.

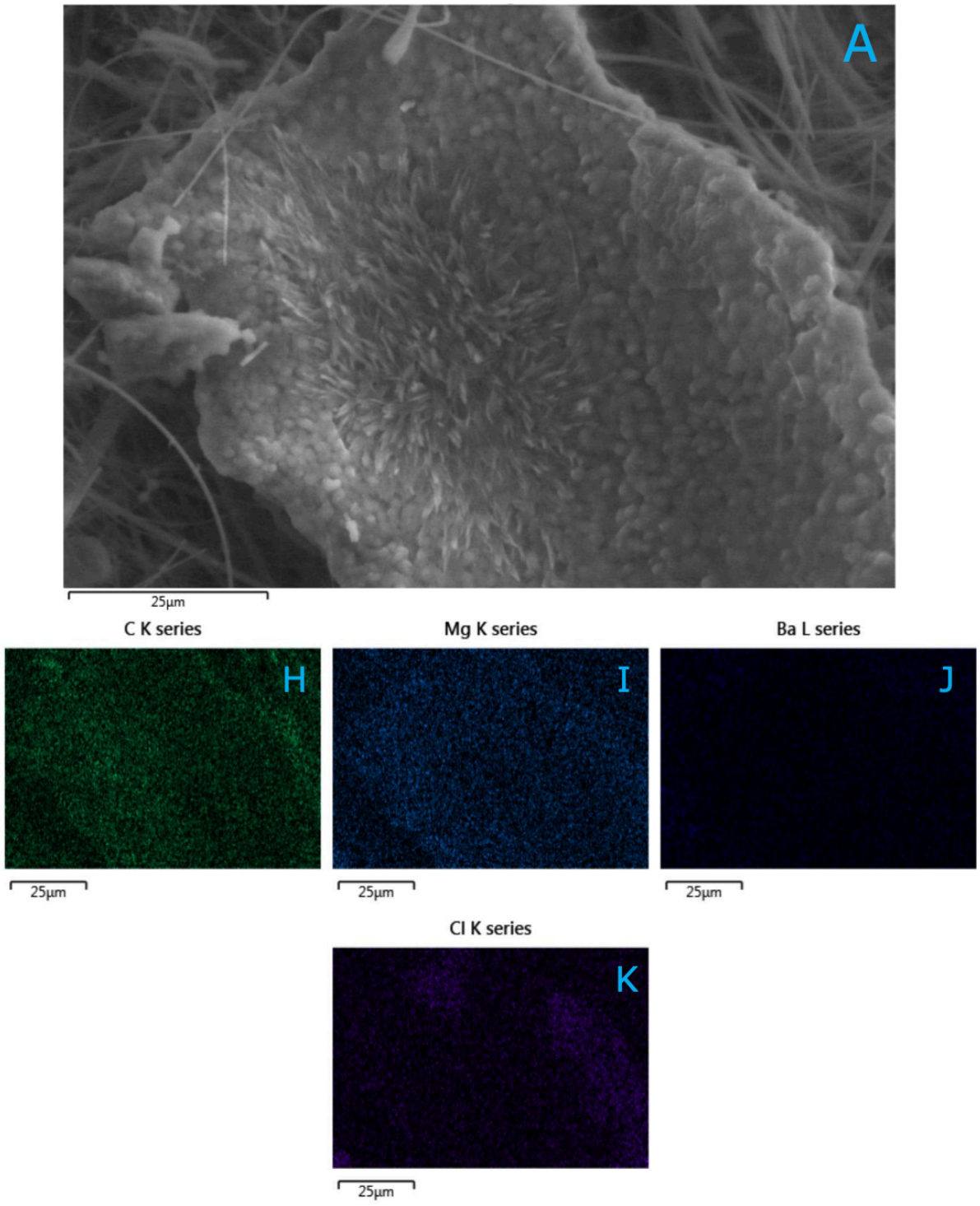

Figure 3.54 ESEM greyscale with single-elemental-coloured images of filtered muscle. *(A)* ESEM greyscale image taken of a section of filtered muscle sample Ta48 (wild tilapia, site 15D). Single-elemental-coloured (SEC) image showing the presence of; *(H)* carbon (C) associated with the structure within the image, *(I)* magnesium (Mg) associated with the structure, *(J)* barium (Ba) associated with the structure and *(K)* chlorine (Cl) associated with the structure.

3.13.4 Screening of the filtered gastrointestinal tract contents

The same filter paper sample used for fluorescent microscopy was sent for SEM analysis. One filtered GIT contents sample was sent for ESEM screening (GI5). ESEM screening included greyscale imaging, single-elemental-coloured imaging and EDX analysis.

3.13.4.1 Filtered gastrointestinal tract contents – GI5

ESEM greyscale screening of the filtered GIT contents from sample GI5 (wild tilapia, site 9E) identified an artefact (>75µm in length), with a mesh structural appearance (Figures 3.55A), with paler grey deposits on its surface. This artefact was on top of the fibrous background material. Single-elemental-coloured images were taken of this same area and showed high levels of C (Figure 3.55D) only associated with this mesh artefact.

Higher levels of O (Figure 3.55B) were associated with the mesh artefact compared to the fibrous background material and the pale grey deposits observed on the mesh structure. The presence of Si (Figure 3.55E) was only associated with the fibrous background material. The presence of K (Figure 3.55C) was associated with the deposits on top of the mesh artefact, with no C present in areas where K was present on the mesh artefact. The presence of an area rich in Cl (Figure 3.55F) was also associated with some of the deposits seen in the greyscale image, and there was also no C present where the Cl deposits were. The deposits observed seem to be of two different components.

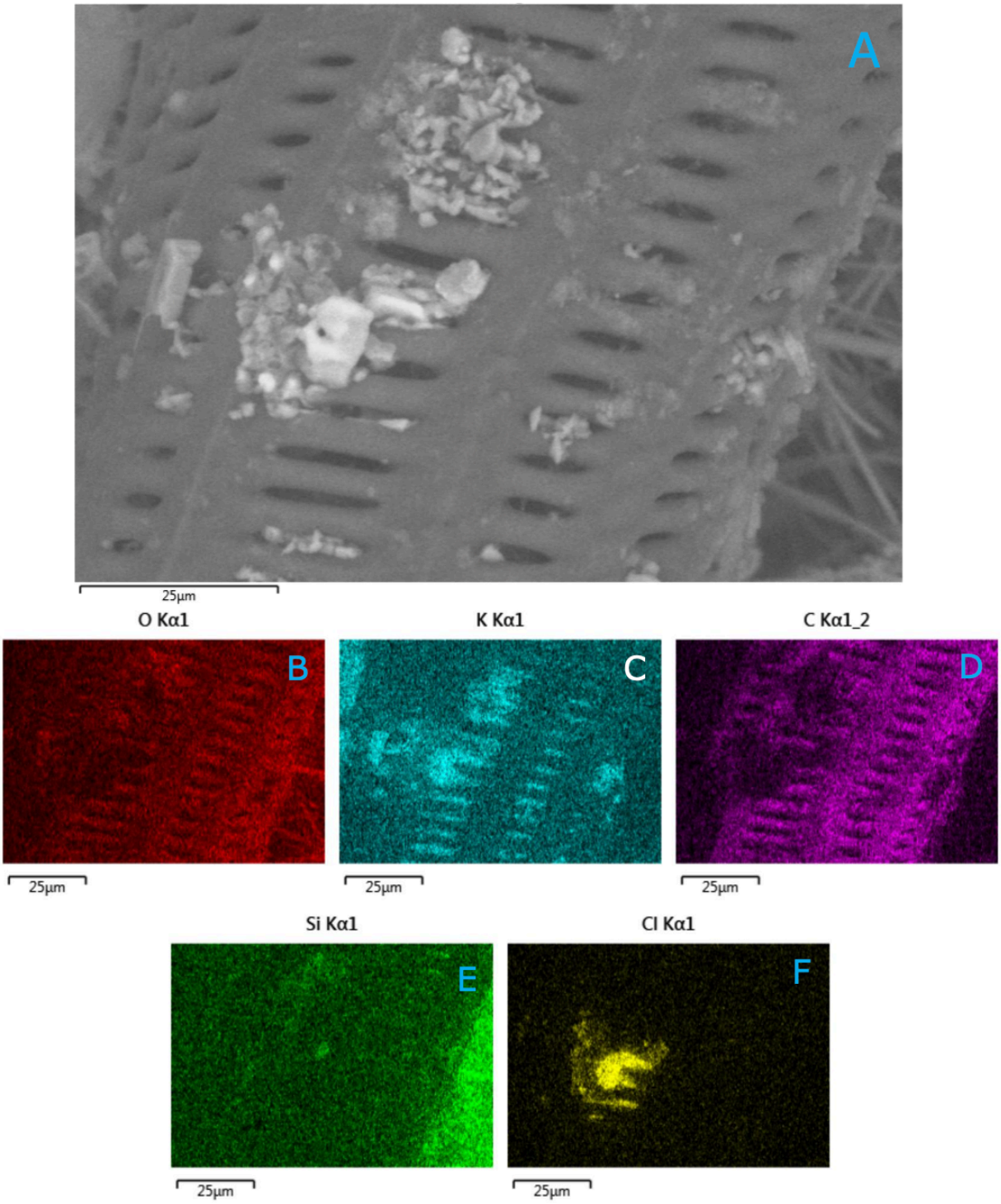

Figure 3.55 ESEM greyscale with single-elemental-coloured images of filtered gastrointestinal tract contents. *(A)* ESEM greyscale image taken of a section of filtered gastrointestinal tract contents sample GI5 (wild tilapia, site 9E). Single-elemental-coloured (SEC) image showing the presence of; *(B)* oxygen (O) associated with the structure within the image, *(C)* potassium (K) associated with the structure, *(D)* carbon (C) associated with the structure, *(E)* silicon (Si) associated with the structure and *(F)* chlorine (Cl) associated with the structure.

3.13.5 Screening of the unfiltered muscle

Four untreated muscle samples (Ta20, Ta66, Ta69 and Ta72) were also sent for ESEM screening. ESEM screening included greyscale imaging, single-elemental-coloured imaging and EDX analysis.

3.13.5.1 Unfiltered muscle – Ta20

3.13.5.1.1 Spectrum 18 and 19

Analysis of the unfiltered muscle from sample Ta20 (caged tilapia, site 13B) identified a group of fibrous rectangular structures, similar to that of microfibres, ranging from ~10 to 30µm in length (Figure 3.56A). Two of these fibre-like structures were focussed on for EDX analyses, see spectrum 18 (Figure 3.56B) and spectrum 19 (Figure 3.56C). EDX analysis of the structure analysed in spectrum 18 found it to have a high C level (Figure 3.56B), medium levels of O and Si, and a trace amount of Na associated with it. EDX analysis on another of these fibrous structures (spectrum 19) was similar, with a high C level (Figure 3.56C) and a medium level of O associated with it. However, its Si and Na levels were both lower than that found in the first structure analysed (spectrum 18). In both structures, trace levels of Al, Mg, P, S, Ca, Ba, Zn and titanium (Ti) were also detected.

Single-elemental-coloured images were also taken of this same area. A high level of Si (Figure 3.57G) was associated exclusively with the fibrous rectangular structures. The presence of O (Figure 3.57B) was also associated with these fibrous structures and the background material. The presence of C (Figure 3.57A), P (Figure 3.57C), K (Figure 3.57D) and S (Figure 3.57E) were all associated exclusively with the background material. There were also high levels of Ti (Figure 3.57F) associated with two smaller areas on top of the background material.

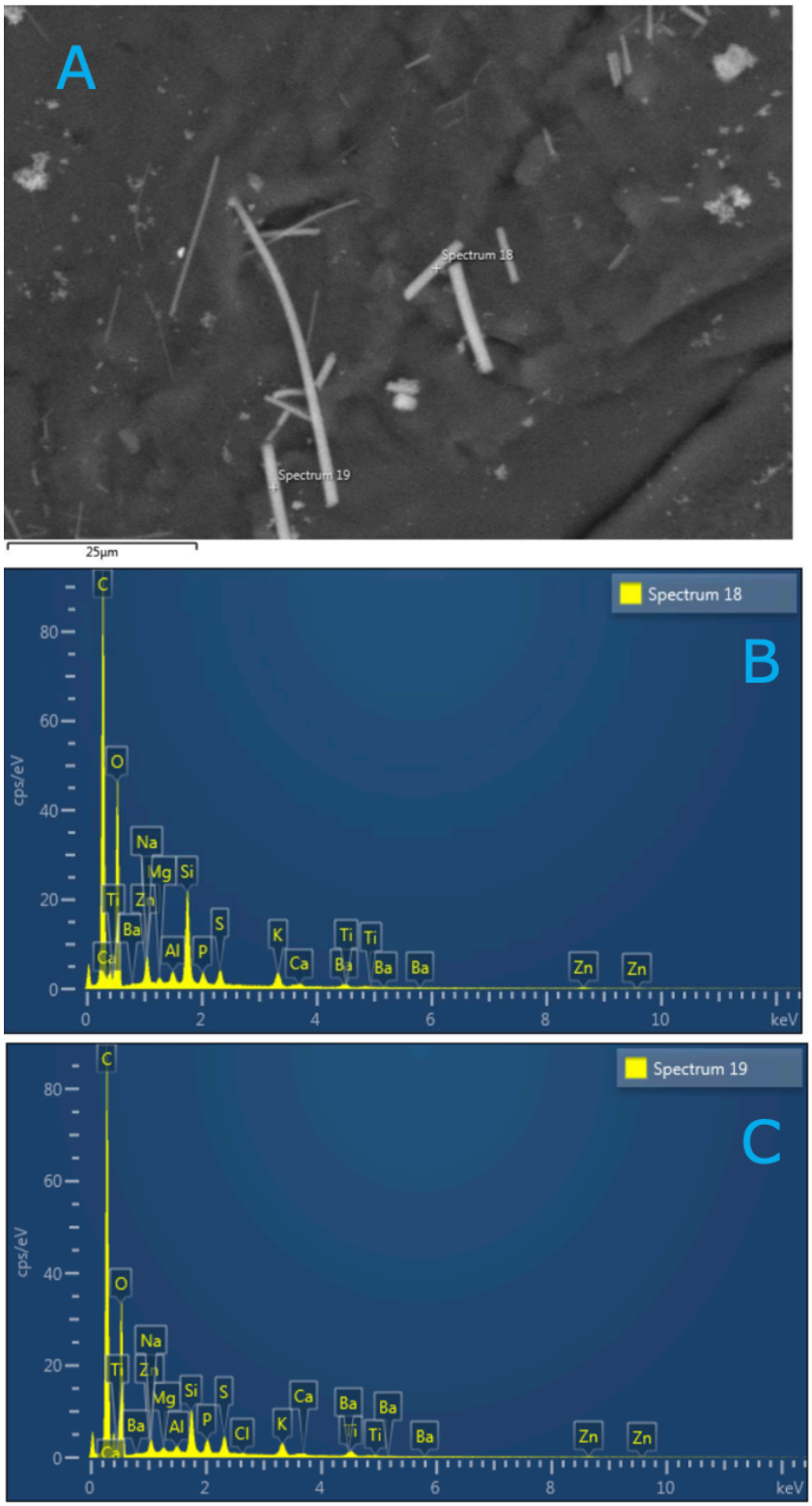

Figure 3.56 ESEM with EDX spectra of unfiltered muscle. *(A)* ESEM greyscale image taken of a section of unfiltered muscle sample (Ta20, caged tilapia, site 13B), showing group of fibrous rectangular structures. *(B)* EDX spectra of spectrum 18 showing a high level of carbon (C), medium levels of oxygen (O) and silicon (Si), and a trace amount of sodium (Na) associated with the structure. *(C)* EDX spectra of spectrum 19 showing a high level of C, a medium level of O, a low level of Si and a trace amount of Na associated with the structure.

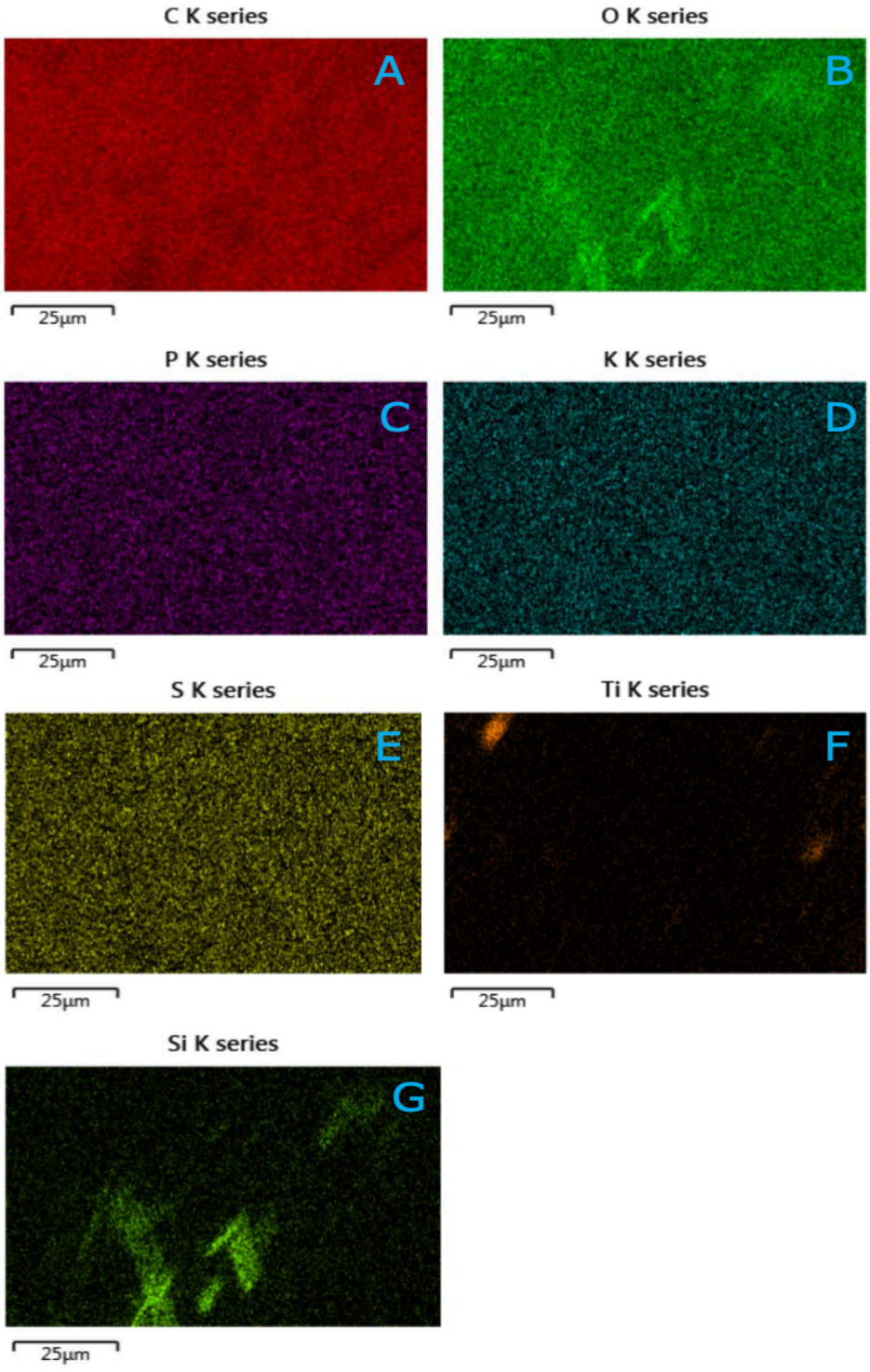

Figure 3.57 ESEM single-elemental-coloured images of unfiltered muscle. ESEM single-elemental-coloured (SEC) images taken of a section of unfiltered muscle sample Ta20 (caged tilapia, site 13B). SEC image showing the presence of; *(A)* carbon (C) associated with the structure within the image, *(B)* oxygen (O) associated with the structure, *(C)* phosphorus (P) associated with the structure, *(D)* potassium (K) associated with the structure, *(E)* sulphur (S) associated with the structure, *(F)* titanium (Ti) associated with the structure, and *(G)* silicon (Si) associated with the structure.

3.13.5.1.2 Spectrum 20 and 21

The two areas identified in sample Ta20 as having a high Ti content (Figure 3.57F), were screened further. Analysis identified an artefact (~7µm in length) with a different appearance to the background structure (Figure 3.58A). This artefact and the background structure were focussed on for EDX analyses, see spectrum 20 (Figure 3.58B) and spectrum 21 (Figure 3.58C). EDX analysis of the artefact analysed in spectrum 20 found it to have a high C level (Figure 3.58B) and medium levels of O and Ti associated with it. EDX analysis of the background structure analyses in spectrum 21 found it to have a very high C level (Figure 3.58C) and medium level of O associated with it. There were only trace levels of Ti detected in the background material (spectrum 21).

Single-elemental-coloured images were also taken of this same area. High levels of Ti (Figure 3.59F) were associated exclusively with the artefact marked by spectrum 20. The presence of C (Figure 3.59A) and S (Figure 3.59E) were associated only with the background structure. Higher levels of O (Figure 3.59B) were observed in the artefact when compared to the background structure, while P (Figure 3.59C) and K (Figure 3.59D) were associated with both the artefact and the background material. The artefact and background structure when compared had different compositions.

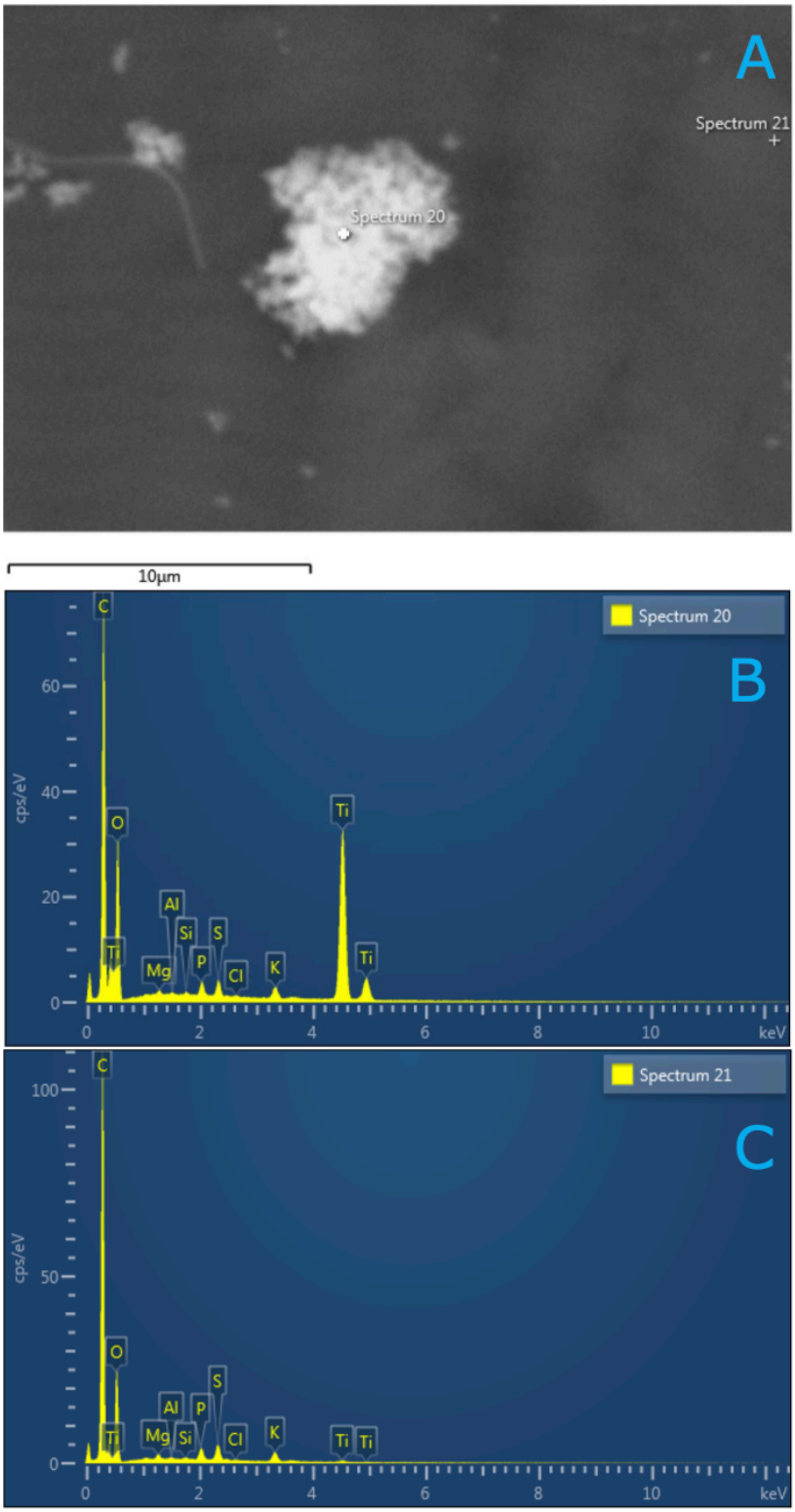

Figure 3.58 ESEM with EDX spectra of unfiltered muscle. *(A)* ESEM greyscale image taken of a different section of unfiltered muscle sample (Ta20, caged tilapia, site 13B), showing an artefact. *(B)* EDX spectra of spectrum 20 showing a high level of carbon (C), and medium levels of oxygen (O) and titanium (Ti) associated with the structure. *(C)* EDX spectra of spectrum 21 showing a very high level of C, a medium level of O, and a trace level of Ti.

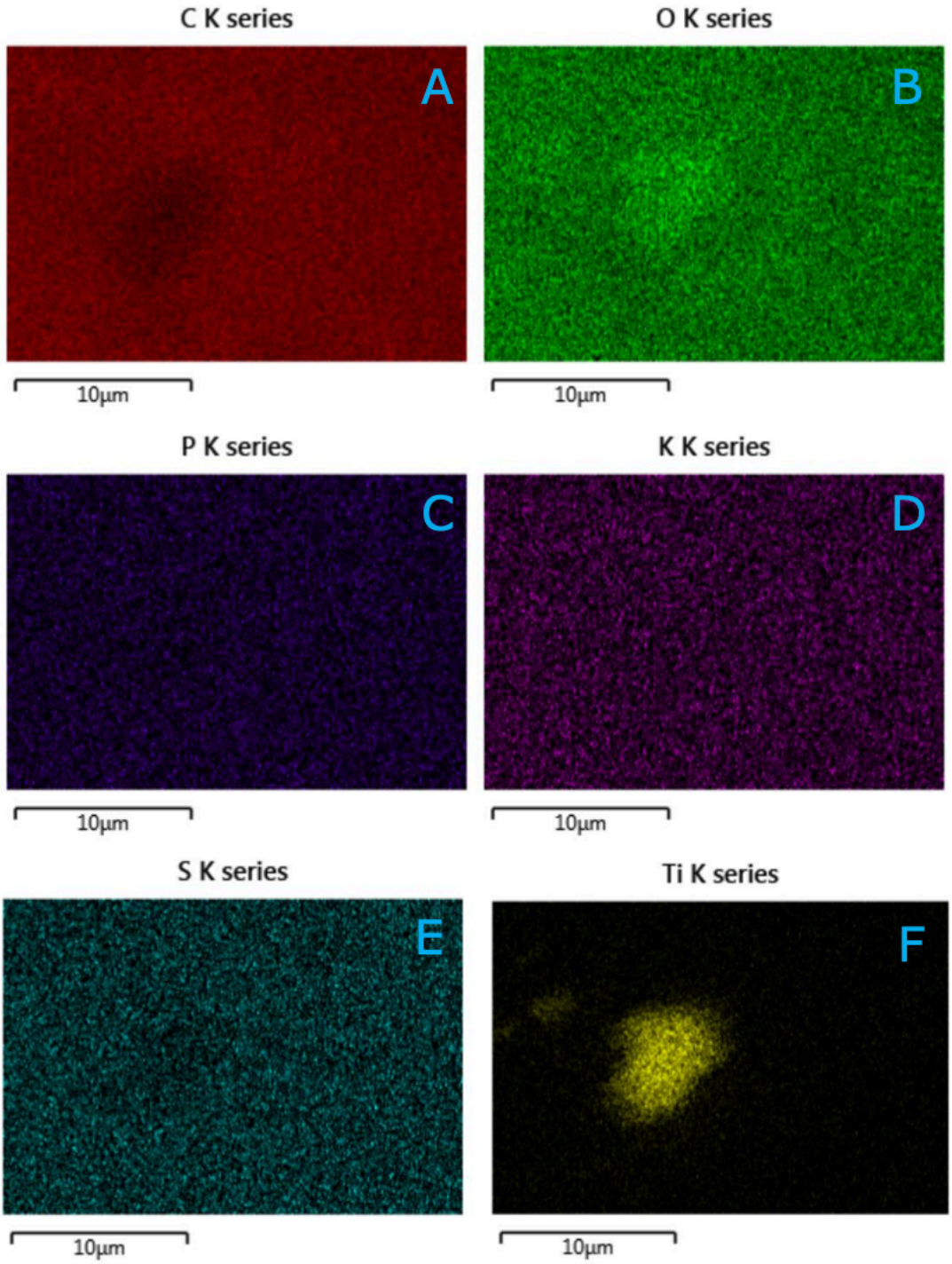

Figure 3.59 ESEM single-elemental-coloured images of unfiltered muscle. ESEM single-elemental-coloured (SEC) images taken of a different section of unfiltered muscle sample Ta20 (caged tilapia, site 13B). SEC image showing the presence of*; (A)* carbon (C) associated with the structure within the image, *(B)* oxygen (O) associated with the structure, *(C)* phosphorus (P) associated with the structure*, (D)* potassium (K) associated with the structure, *(E)* sulphur (S) associated with the structure*,* and *(F)* titanium (Ti) associated with the structure.

3.13.5.1.3 Spectrum 26, 27 and 28

Analysis of a different section of the unfiltered muscle from sample Ta20 identified another larger artefact with a similar structure to that seen in Figure 3.58A. ESEM greyscale screening identified an artefact with a rough surface (~50µm in length), which had a different appearance to the background structure (Figure 3.60A). This artefact and two different locations on the background structure were focussed on for EDX analyses, see spectrum 26 (Figure 3.60B), spectrum 27 (Figure 3.60C) and spectrum 28 (Figure 3.60D).

EDX analysis of the structure analysed in spectrum 26 found it to have a very high C level (Figure 3.60B), a high level of Ti and a medium level of O associated with it. EDX analysis of the background material analysed in spectrum 27 found it to have a high C level (Figure 3.60C), with C level higher than in the artefact observed (spectrum 26). It also had a medium level of O, and a trace amount of Ti associated with it. EDX analysis of a different section of the background structure (spectrum 28) was similar and showed a very high C level (Figure 3.60D), with C level lower than that of the other background structure analysed (spectrum 27). It also had a medium level of O and a trace amount of Ti associated with it. The two sections of the background structure analysed had similar compositions, while the identified artefact's composition was different to them.

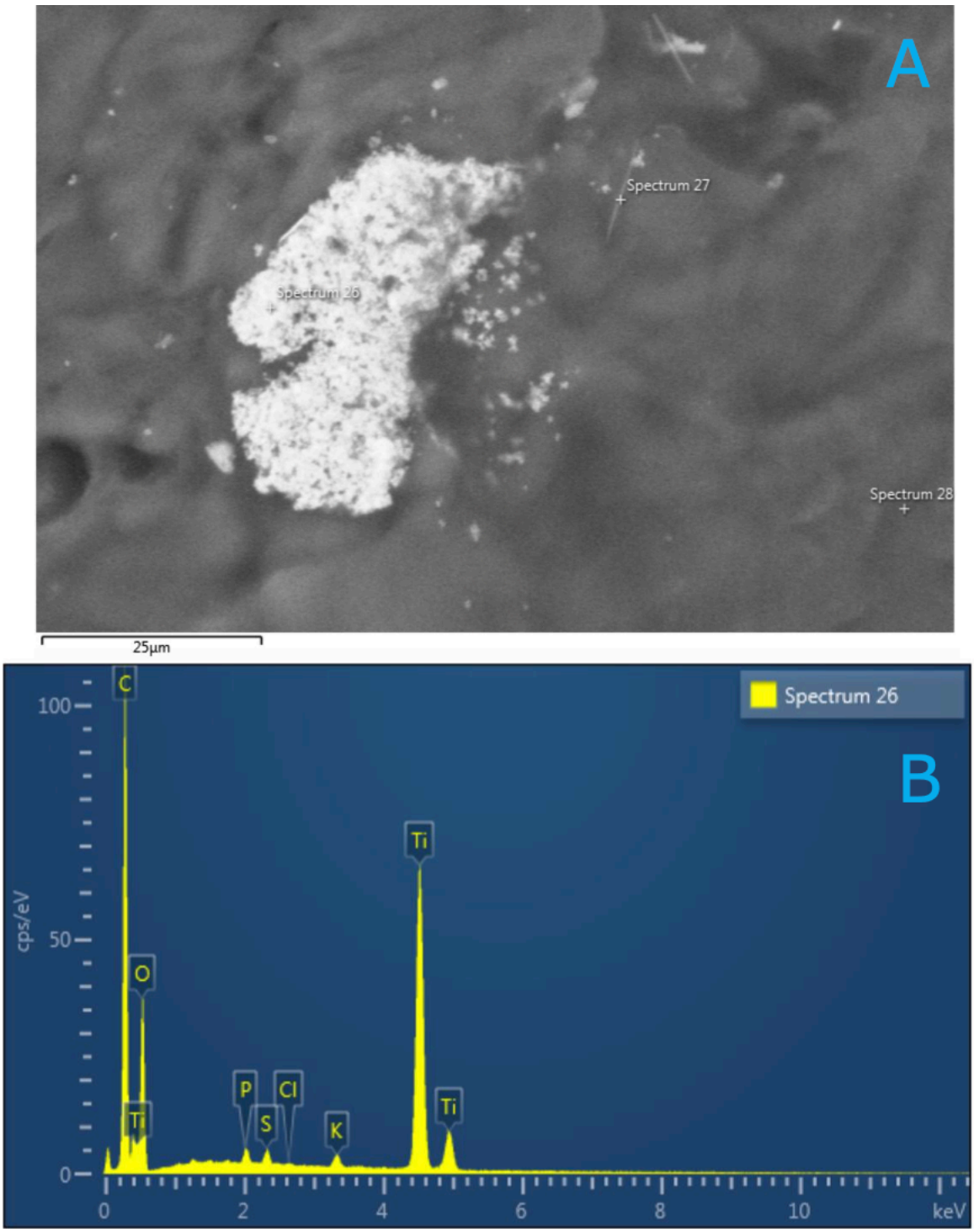

Figure 3.60 ESEM with EDX spectra of unfiltered muscle. *(A)* ESEM greyscale image taken of a different section of unfiltered muscle sample (Ta20, caged tilapia, site 13B), showing an artefact. *(B)* EDX spectra of spectrum 26 showing a very high level of carbon (C), a high level of titanium (Ti) and a medium level of oxygen (O) associated with the structure.

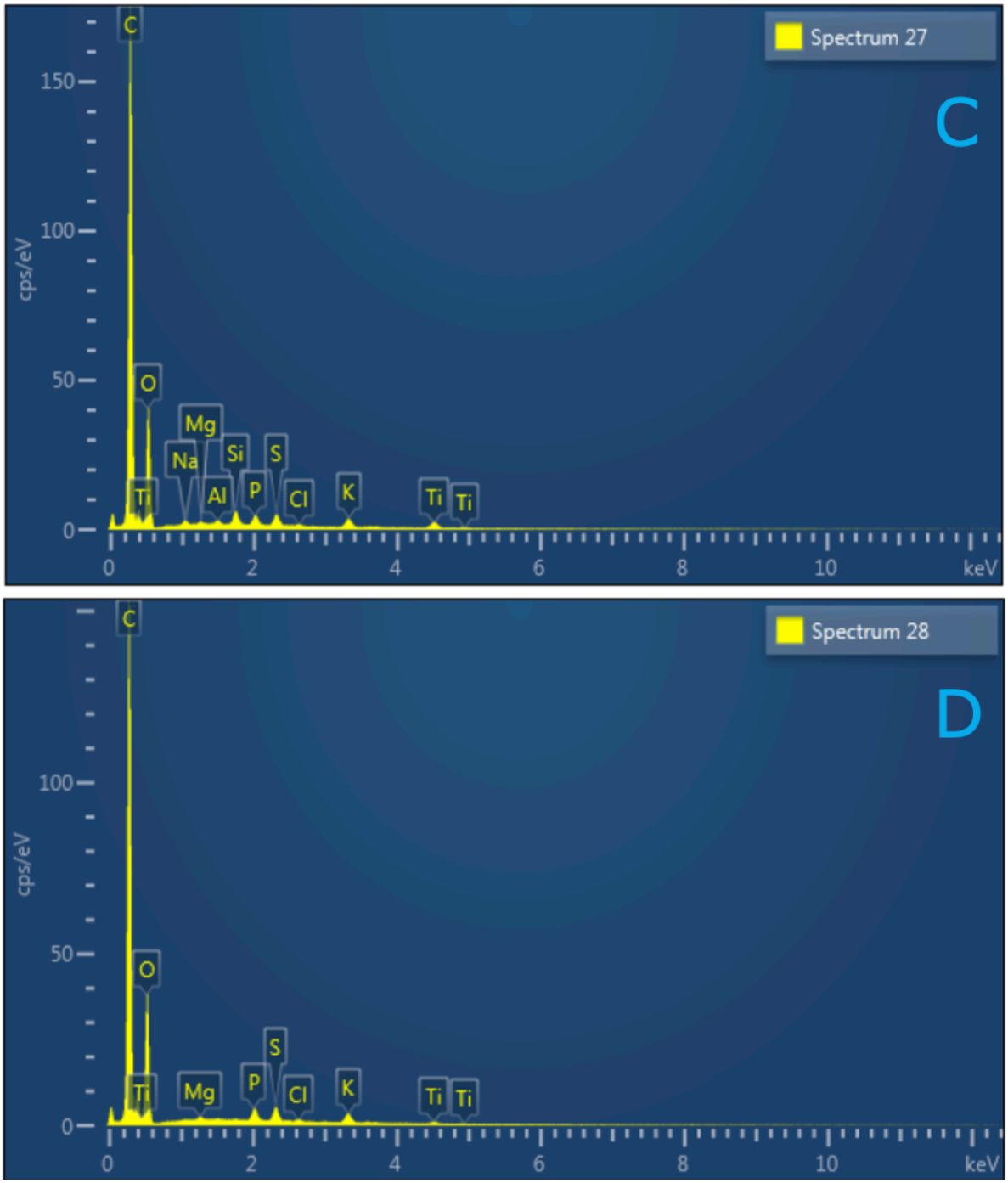

Figure 3.60 (continued) ESEM with EDX spectra of unfiltered muscle. *(C)* EDX spectra of spectrum 27 showing a very high level of carbon (C), a medium level of oxygen (O) and a trace level of titanium (Ti) associated with the structure. *(D)* EDX spectra of spectrum 28 showing a very high level of carbon (C), a medium level of oxygen (O) and a trace level of titanium (Ti) associated with the structure.

3.13.5.1.4 Spectrum 35

Analysis of another different section of the unfiltered muscle from sample Ta20, by ESEM greyscale imaging, identified a fibre-like artefact (~25µm in length), lodged into the background structure (Figure 3.61A). Only this fibre-like artefact was focussed on for EDX analysis, see spectrum 35 (Figure 3.61B). EDX analysis of the fibre-like artefact observed (spectrum 35) found it to have a high level of C (Figure 3.61B) and medium levels of O and Fe associated with it. However no EDX analysis of the background structure was performed.

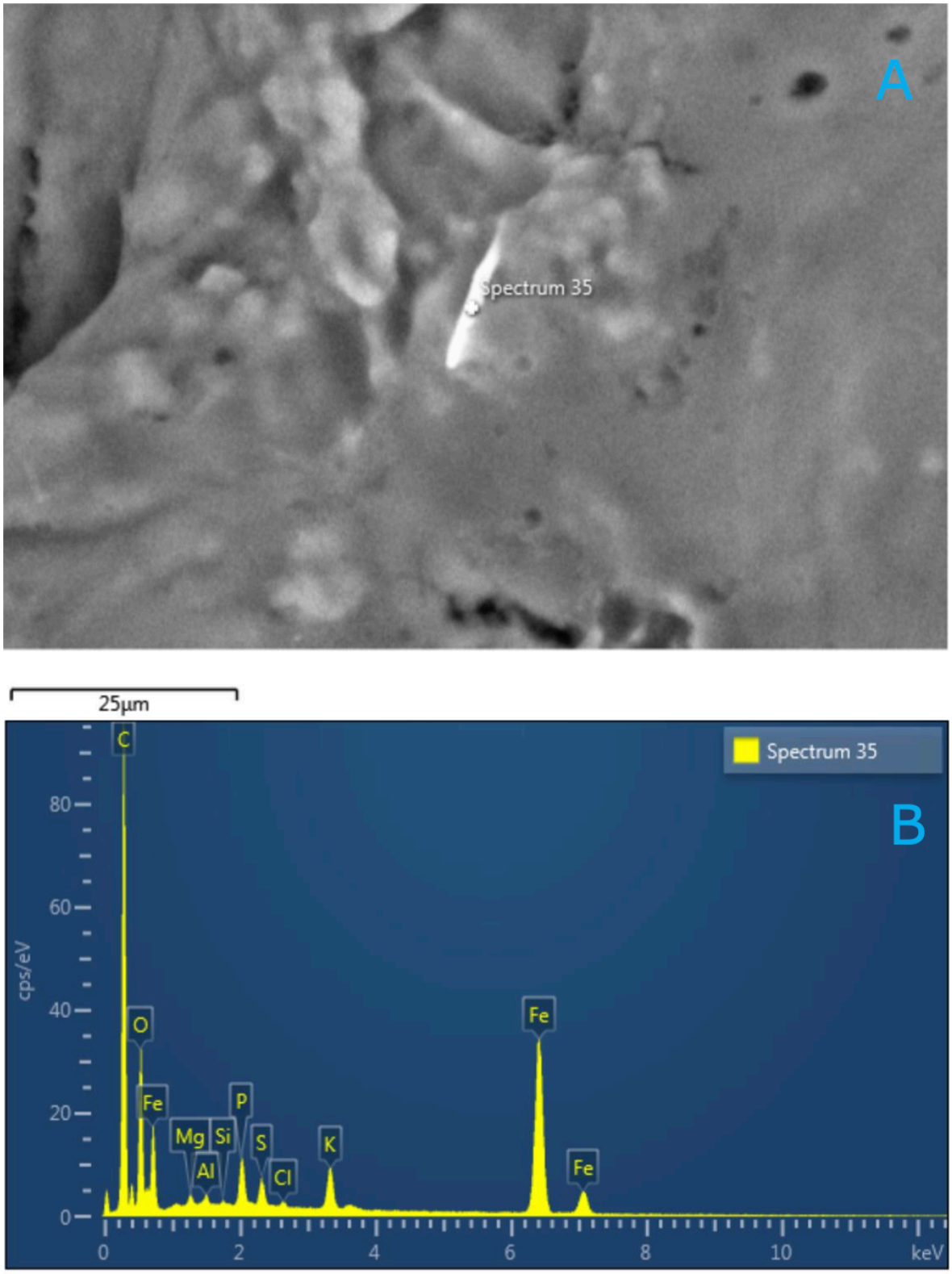

Figure 3.61 ESEM with EDX spectra of unfiltered muscle. *A)* ESEM greyscale image taken of a different section of unfiltered muscle sample (Ta20, caged tilapia, site 13B), showing a fibre-like artefact. *(B)* EDX spectra of spectrum 35 showing a high level of carbon (C), and medium level of oxygen (O) and iron (Fe) associated with the structure.

3.13.5.2 Unfiltered muscle – Ta66

3.13.5.2.1 Spectrum 107 and 108

Analysis of the unfiltered muscle from sample Ta66 (caged tilapia, site 1B) identified a spherical bead shaped artefact (~20µm in length), which had a rough surface (Figure 3.62A). This bead and the background structure were focussed on for EDX analyses, see spectrum 107 (Figure 3.62B) and spectrum 108 (Figure 3.62C). EDX analysis of the bead analysed in spectrum 107 found it to have very high levels of C and O (Figure 3.62B), and medium levels of Cu, Zn, Al and Si associated with it. EDX analysis of the background structure analysed in spectrum 108 showed it to have a very high C level and a high O level (Figure 3.62C). Higher levels of C, but lower levels of O were observed in the background structure when compared to the bead. It also had trace amounts of P, S and K.

Single-elemental-coloured images were also taken of this same area. High levels of Zn (Figure 3.63F) and Cl (Figure 3.63G) were associated exclusively with the bead-shaped artefact. The presence of O (Figure 3.63B) was associated with both the artefact and the background material. A higher level of O was observed in the bead when compared to the background structure. The presence of C (Figure 3.63A) was associated with the background material and potentially part of the bead, however this was a very small area of C on the bead, with C presence higher in the background structure. The presence of K (Figure 3.63C), P (Figure 3.63D) and S (Figure 3.63E) were associated with the background material and bead artefact. The bead identified had a different composition compared to the background structure.

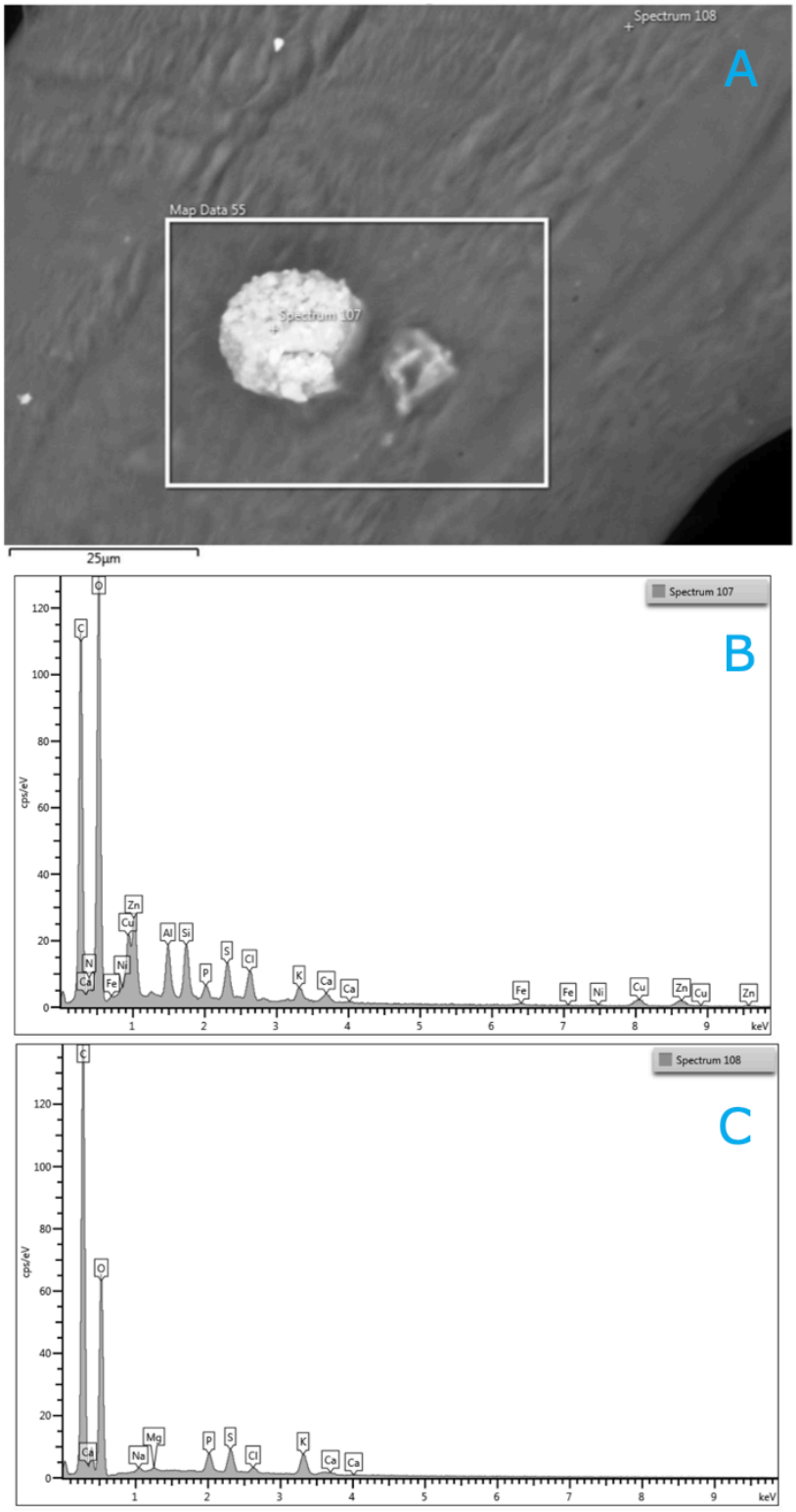

Figure 3.62 ESEM with EDX spectra of unfiltered muscle. *A)* ESEM greyscale image taken of a section of unfiltered muscle sample (Ta66, caged tilapia, site 1B), showing a bead-like artefact. *(B)* EDX spectra of spectrum 107 showing very high levels of carbon (C) and oxygen (O), and medium levels of copper (Cu), zinc (Zn), aluminium (Al) and silicon (Si) associated with the structure. *(C)* EDX spectra of spectrum 108 showing a very high level of C and a high level of O, and trace amounts of phosphorus (P), sulphur (S) and potassium (K) associated with the structure.

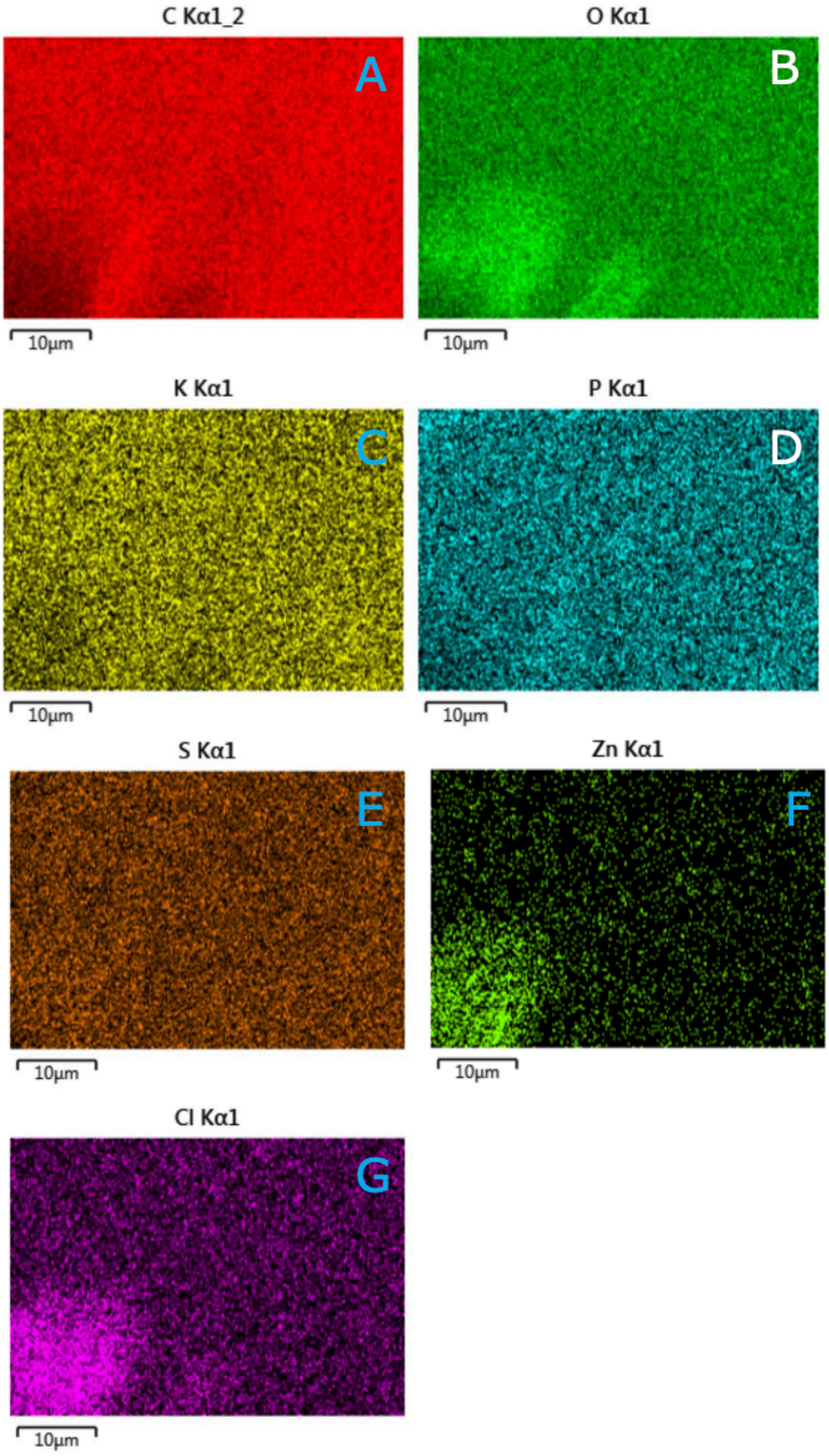

Figure 3.63 ESEM single-elemental-coloured images of unfiltered muscle. ESEM single-elemental-coloured (SEC) images taken of a section of unfiltered muscle sample Ta66 (caged tilapia, site 1B). SEC image showing the presence of; *(A)* carbon (C) associated with the structure within the image, *(B)* oxygen (O) associated with the structure, *(C)* potassium (K) associated with the structure, *(D)* phosphorus (P) associated with the structure, *(E)* sulphur (S) associated with the structure, *(F)* zinc (Zn) associated with the structure, and *(G)* chlorine (Cl) associated with the structure.

3.13.5.2.2 Spectrum 118

ESEM greyscale screening of a different section analysed from the unfiltered muscle sample from Ta66 identified a triangular-like fragment (~30µm in length) (Figure 3.64A), lodged into the background structure. This fragment observed was focussed on only for EDX analysis, see spectrum 118 (Figure 3.64B). EDX analysis of the structure analysed in spectrum 118 found it to have high level of C and O (Figure 3.64B), and low levels of nickel (Ni), Cu, Cl and Zn associated with it. However no EDX analysis of the background structure was performed here.

Single-elemental-coloured images were taken of this same area. There were high levels of Cl (Figure 3.65F), Na (Figure 3.65G) and Ni (Figure 3.65I) associated exclusively with the triangular-like fragment observed. The presence of C (Figure 3.65A) and P (Figure 3.65E) were associated only with the background material. The presence of O (Figure 3.65B), S (Figure 3.65C), K (Figure 3.65D) and Ca (Figure 3.65H) were all associated with both the fragment and background material, with K and Ca levels across both structures being lower than that of O and S levels. The triangular-like fragment identified had a different composition compared to the background structure.

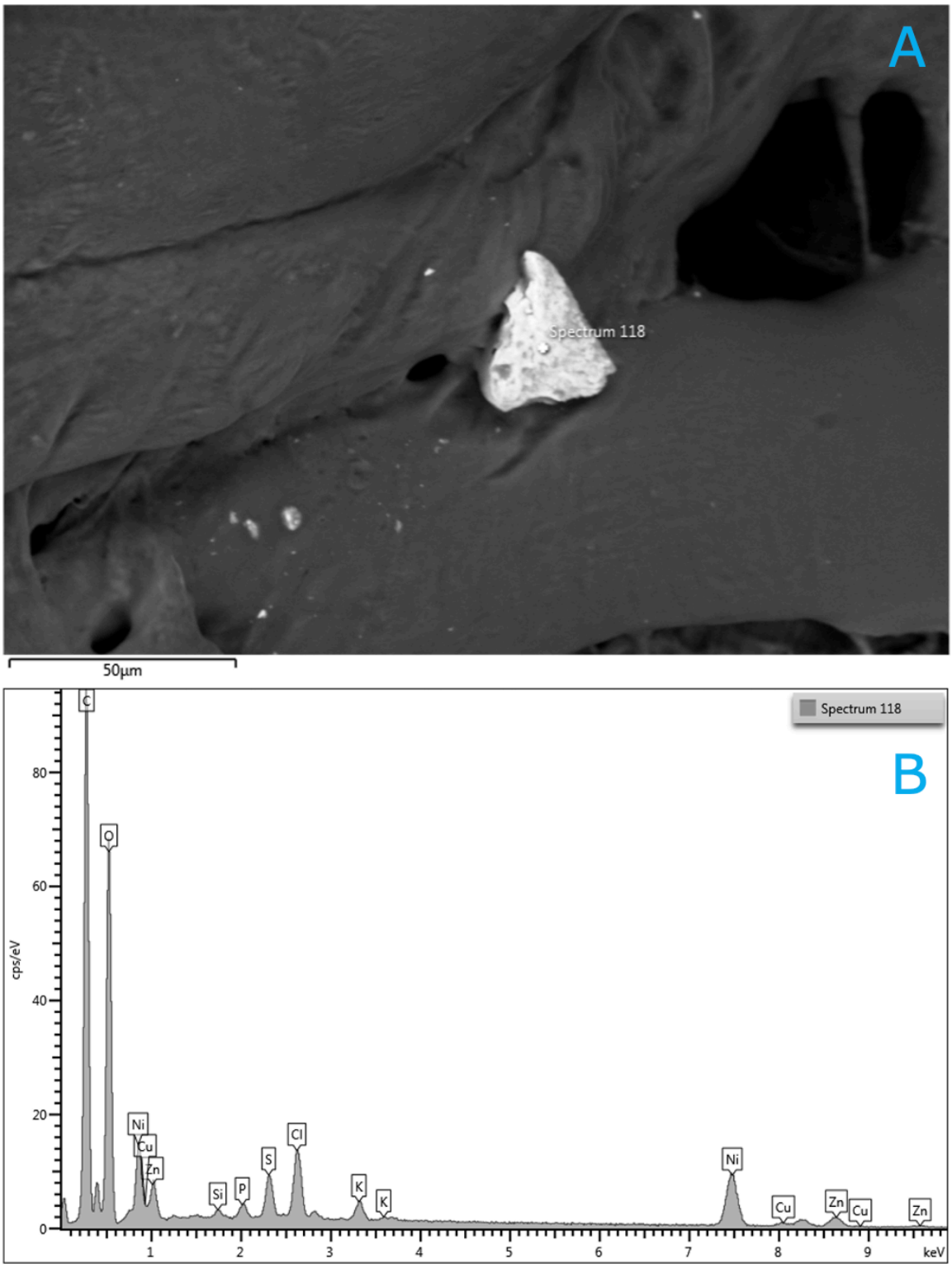

Figure 3.64 ESEM with EDX spectra of unfiltered muscle. *A)* ESEM greyscale image taken of a different section of unfiltered muscle sample (Ta66, caged tilapia, site 1B), showing a fragment-like artefact. *(B)* EDX spectra of spectrum 118 showing high levels of carbon (C) and oxygen (O), and low levels of nickel (Ni), cupper (Cu), zinc (Zn) and chlorine (Cl) associated with the structure.

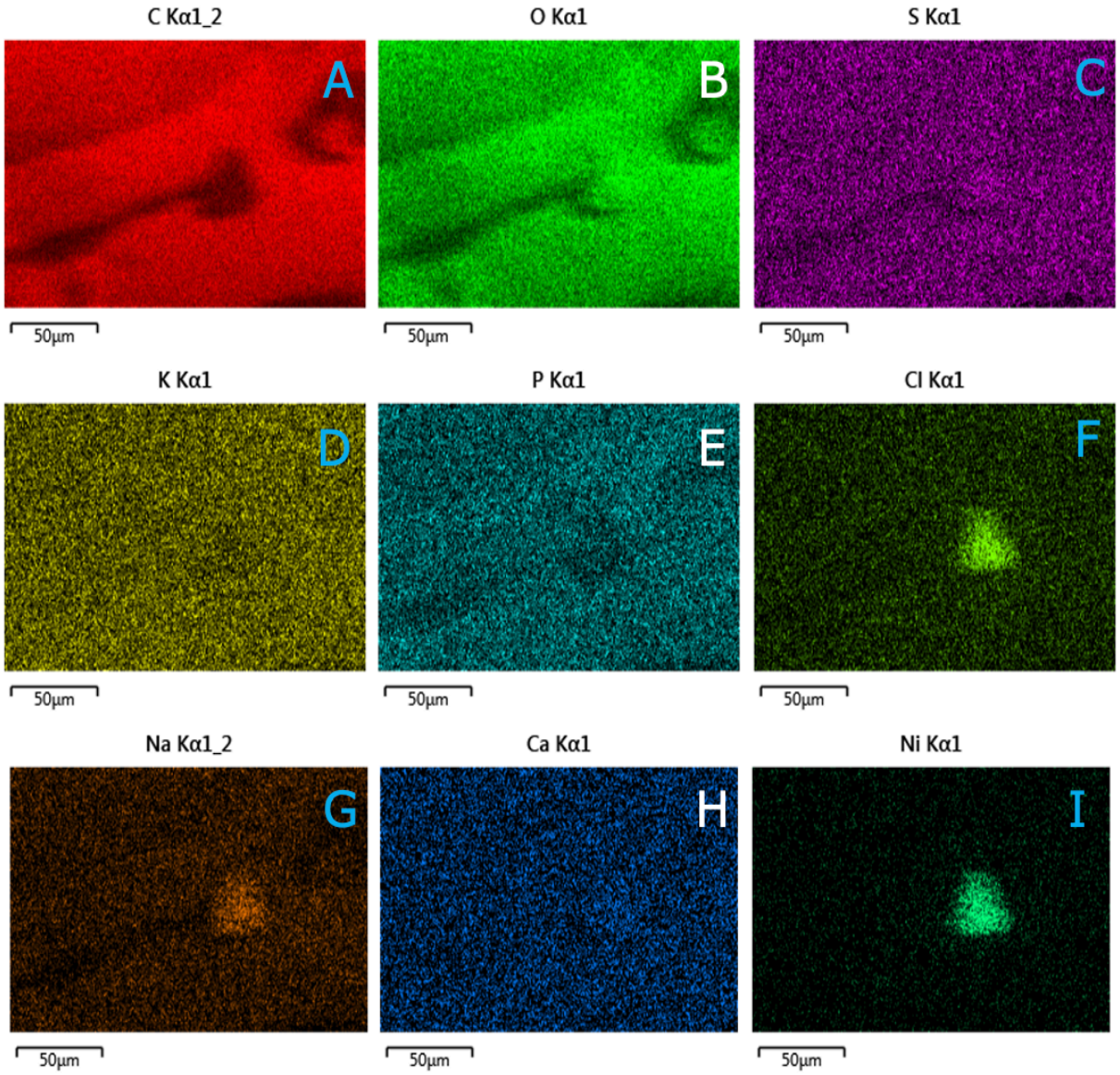

Figure 3.65 ESEM single-elemental-coloured images of unfiltered muscle. ESEM single-elemental-coloured (SEC) images taken of a different section of unfiltered muscle sample Ta66 (caged tilapia, site 1B). SEC image showing the presence of; *(A)* carbon (C) associated with the structure within the image, *(B)* oxygen (O) associated with the structure, *(C)* sulphur (S) associated with the structure, *(D)* potassium (K) associated with the structure, *(E)* phosphorus (P) associated with the structure, *(F)* chlorine (Cl) associated with the structure, *(G)* sodium (Na) associated with the structure, *(H)* calcium (Ca) associated with the structure and *(I)* nickel (Ni) associated with the structure.

3.13.5.3 Unfiltered muscle – Ta69

Analysis of the unfiltered muscle sample from Ta69 (caged tilapia, site 4) as shown by ESEM greyscale imaging, identified a sphere-shaped artefact (~20µm in length) (Figure 3.66A). Only this sphere-shaped artefact was focussed on only for EDX analysis, see spectrum 69 (Figure 3.66B). EDX analysis of the sphere-shaped artefact analysed in spectrum 69 found it to have a medium level of C (Figure 3.66B) and low levels of O, P and K associated with it. However no EDX analysis of the background structure was performed here.

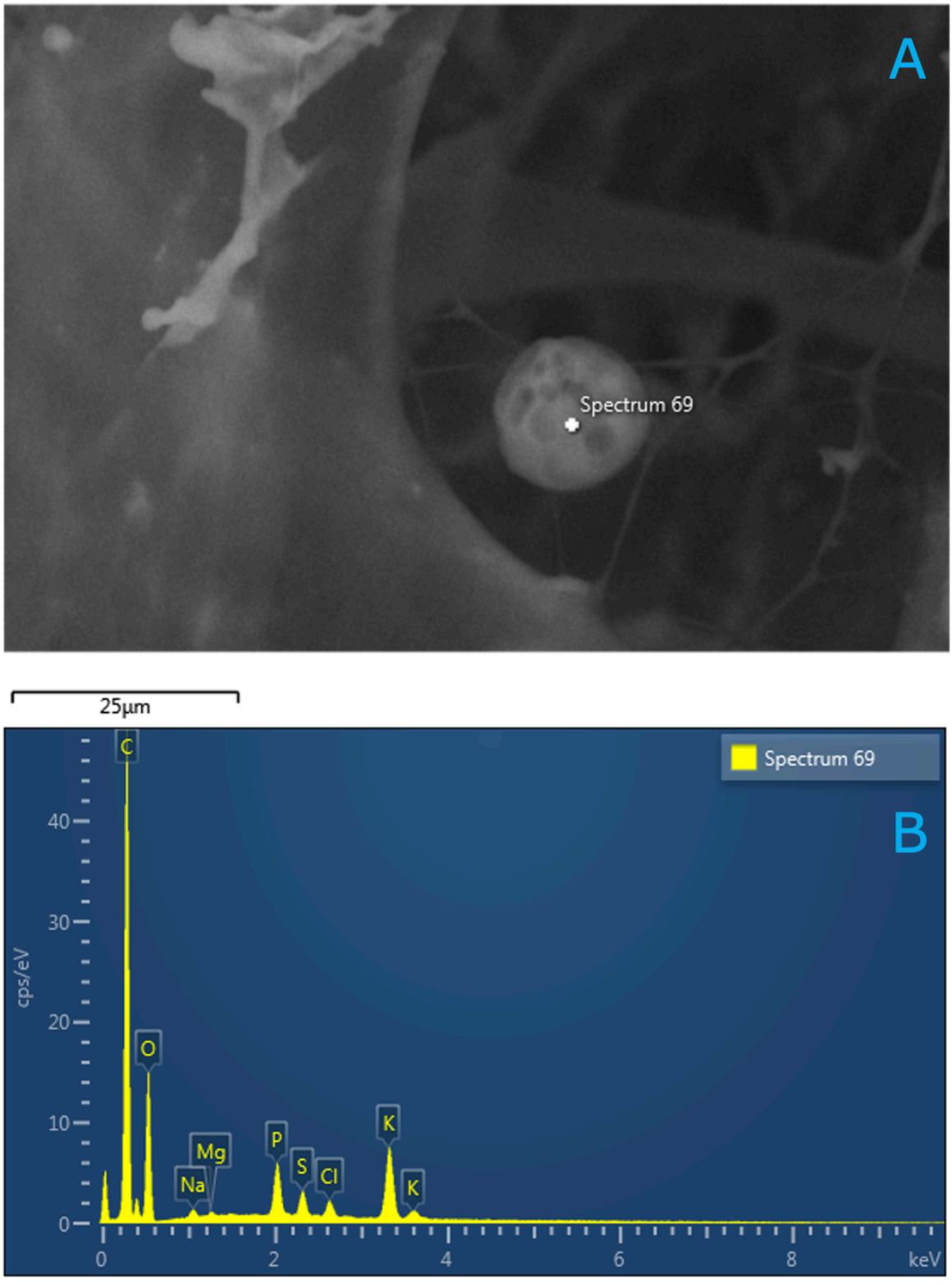

Figure 3.66 ESEM with EDX spectra of unfiltered muscle. *A)* ESEM greyscale image taken of a different section of unfiltered muscle sample (Ta69, caged tilapia, site 4), showing a bead-like artefact. *(B)* EDX spectra of spectrum 69 showing a medium level of carbon (C) and low levels of oxygen (O), phosphorus (P) and potassium (K) associated with the structure.

3.13.5.4 Unfiltered muscle – Ta72

3.13.5.4.1 Spectrum 100

Analysis of the unfiltered muscle from sample Ta72 (wild tilapia, site 4) identified a group of elliptical shaped rods, which ranged in length from ~5-10µm (Figure 3.67A). Only one of these rods was focussed on for EDX analysis, see spectrum 100 (Figure 3.67B). EDX analysis of the rod structure analysed in spectrum 100 found it to have very high levels of C and O (Figure 2.67B), and a medium level of P associated with it. There were also low levels of Mg and Ca associated it. However no EDX analysis of the background structure was performed here.

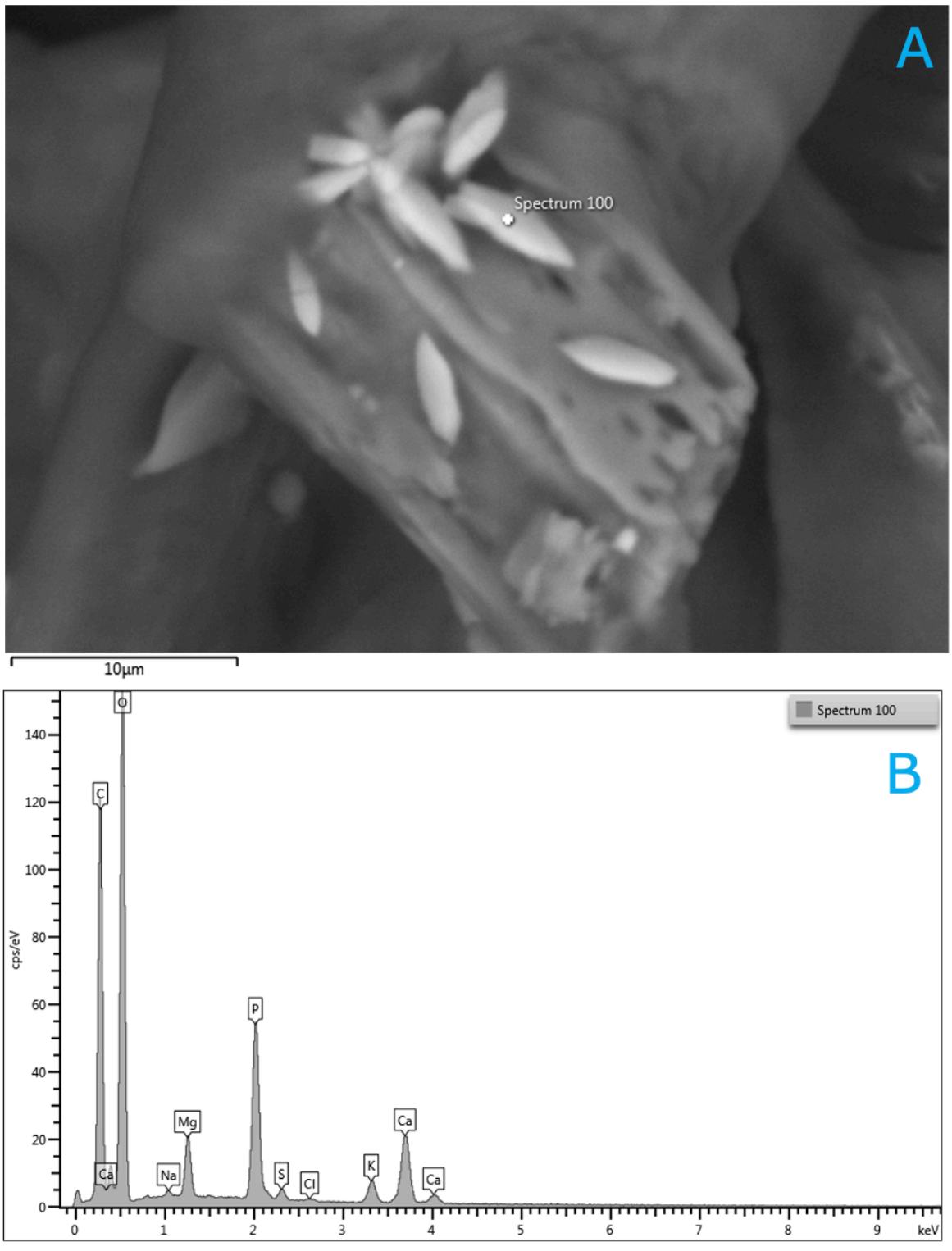

Figure 3.67 ESEM with EDX spectra of unfiltered muscle. *A)* ESEM greyscale image taken of a section of unfiltered muscle sample (Ta72, wild tilapia, site 4), showing a group of elliptical shaped rods. *(B)* EDX spectra of spectrum 100 showing very high levels of carbon (C) and oxygen (O), a medium level of phosphorus (P) and low levels of magnesium (Mg) and calcium (Ca) associated with the structure.

3.13.5.4.2 Spectrum 103 and 104

ESEM greyscale screening of a different section of the unfiltered muscle from sample Ta72 identified two artefacts with different structural appearances to the background structure (Figure 3.68A). These two artefacts were focussed on for EDX analyses, see spectrum 103 (Figure 3.68B) and spectrum 104 (Figure 3.68B). EDX analysis of the larger artefact (~50µm in length) analysed in spectrum 103 found it to have very high levels of C and O (Figure 3.68B), and a high level of Ca associated it. EDX analysis of the other smaller artefact (~20µm in length) in spectrum 104 found it to have a high level of C (Figure 3.68C), and medium levels of O, P and Ca associated with it. These two artefacts identified had similar elemental compositions, however the larger structure observed in spectrum 103 had a higher content of C, O and Ca, compared to the smaller structure observed in spectrum 104, which had an additional presence of P.

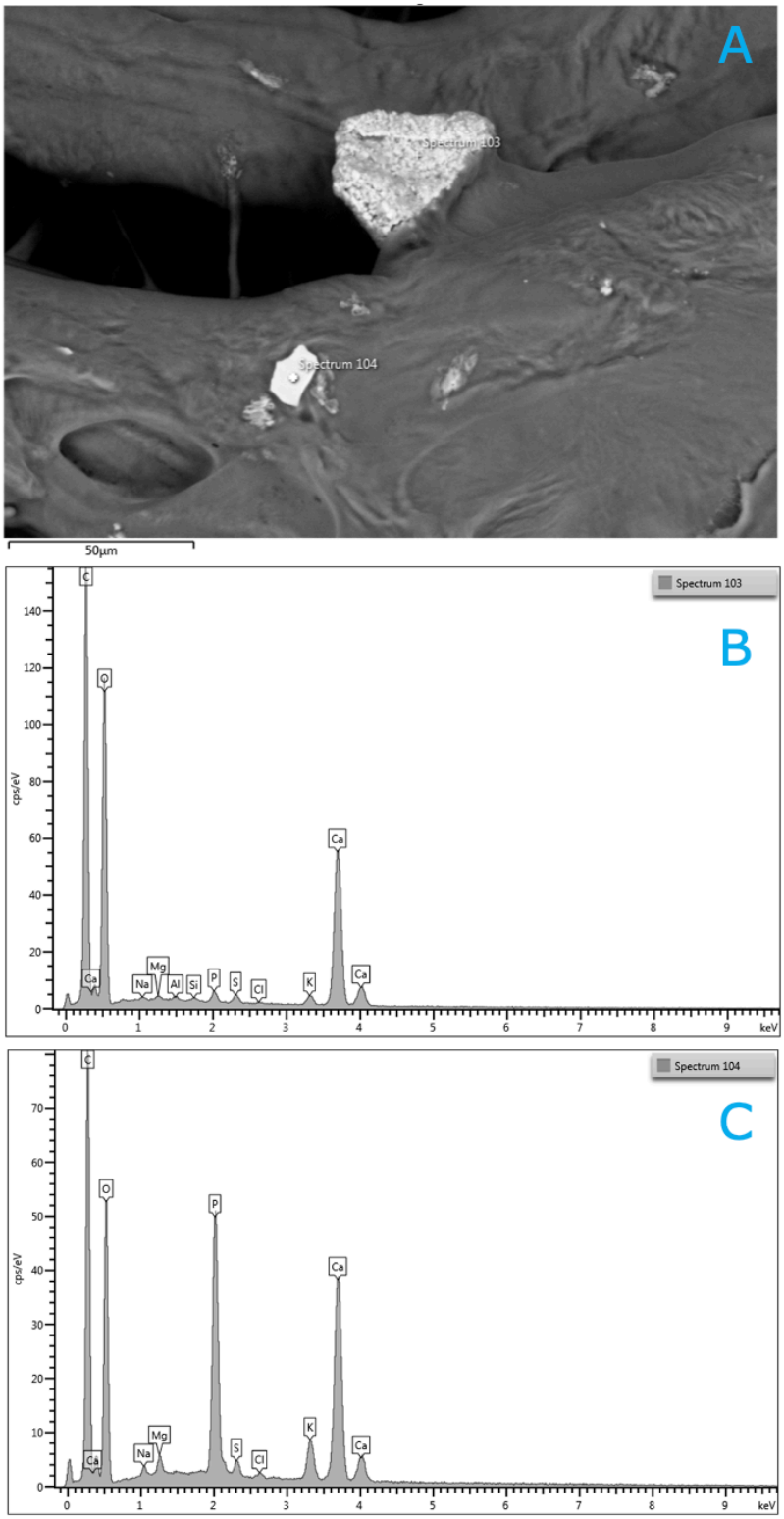

Figure 3.68 ESEM with EDX spectra of unfiltered muscle. *A)* ESEM greyscale image taken of a different section of unfiltered muscle sample (Ta72, wild tilapia, site 4), showing two artefacts. *(B)* EDX spectra of spectrum 103 showing very high levels of carbon (C) and oxygen (O), and a high level of calcium (Ca) associated with the structure. *(C)* EDX spectra of spectrum 104 showing a high level of C, and medium levels of O, P and Ca associated with the structure.

3.13.5.4.3 Spectrum 105 and 106

ESEM greyscale screening of a different section of the unfiltered muscle from sample Ta72 identified two fibre-like structures with a fragment structure located between them (Figure 3.69A). One of the fibres and the fragment were focussed on for EDX analyses, see spectrum 105 (Figure 3.69B) and spectrum 106 (Figure 3.69C). EDX analysis of the fibre-like structure analysed in spectrum 105 found it to have very high levels of C and Si (Figure 3.69B), and a medium level of O associated with it. EDX analysis of the fragment structure analysed in spectrum 106 found it to have high levels of C, Zn and Na (Figure 3.69C), medium levels of O and Si and a trace amount of chromium (Cr) associated with it.

Single-elemental-coloured images were also taken of this same area. A high presence of Si (Figure 3.70B) was associated exclusively with the two fibre-like structures. There was a high presence of Cl (Figure 3.70G) and Zn (Figure 3.70I) associated only with the fragment between the fibres, and an additional small area of Cl located below the fragment. The presence of O (Figure 3.70C) and P (figure 3.70F) were associated with the background structure and the two fibre-like structures observed. Higher levels of O were also observed in the fragment when compared to the two fibres or the background structure. The presence of C (Figure 3.70A) and K (Figure 3.70D) were associated exclusively with the background structure. The presence of S (Figure 3.70E) was associated with the fragment identified and the background structure, with a higher level of S observed in the fragment when compared to the background structure. The fibre-like structure observed in spectrum 105, had a different elemental composition to the fragment observed in spectrum 106, and both were different to the background structure.

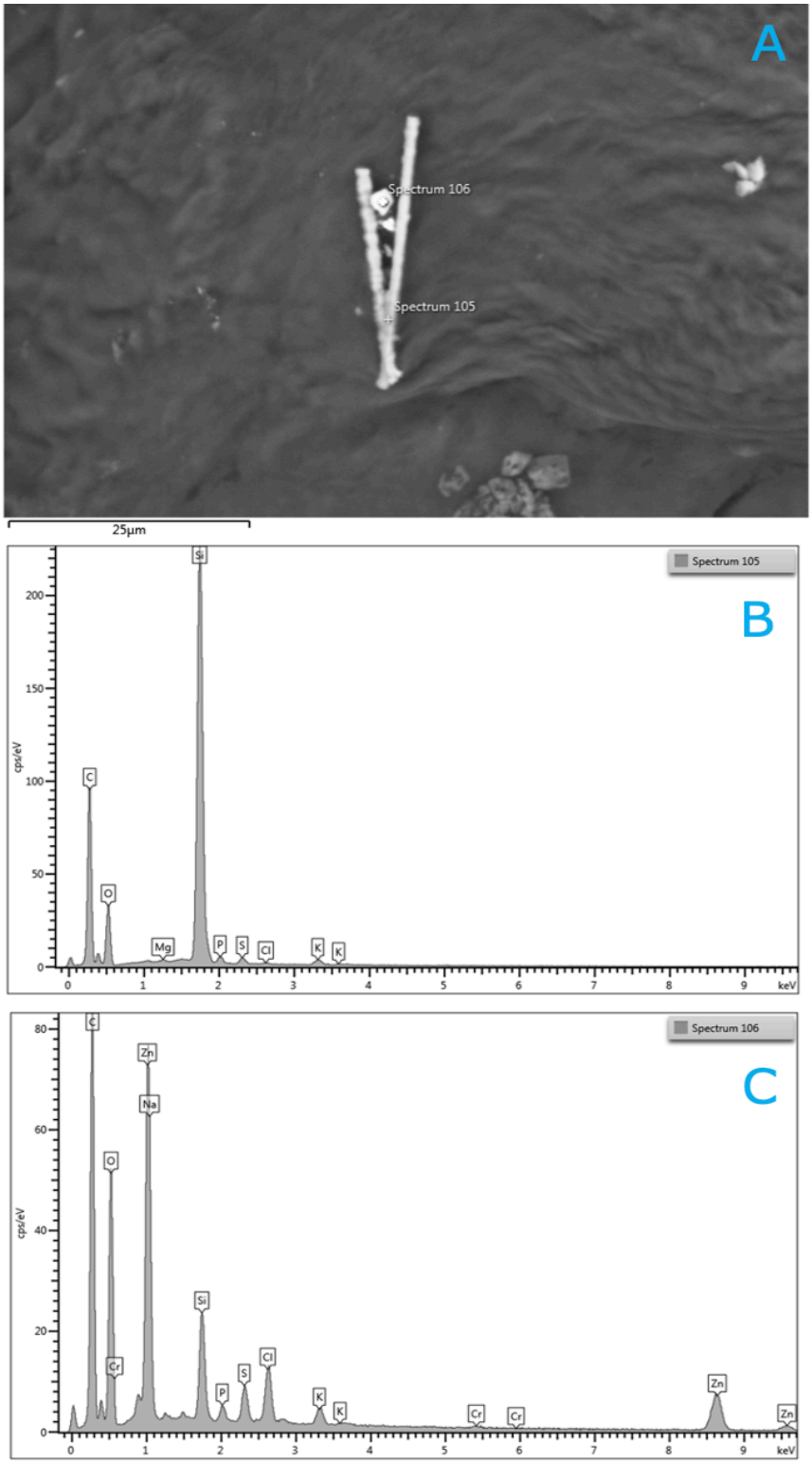

Figure 3.69 ESEM with EDX spectra of unfiltered muscle. *A)* ESEM greyscale image taken of a different section of unfiltered muscle sample (Ta72, wild tilapia, site 4), showing two fibre-like structures and a fragment. *(B)* EDX spectra of spectrum 105 showing very high levels of carbon (C) and silicon (Si), and a medium level of oxygen (O) associated with the structure. *(C)* EDX spectra of spectrum 106 showing a high level of C, Zn and Na, and medium levels of O and Si, and a trace level of chromium (Cr) associated with the structure.

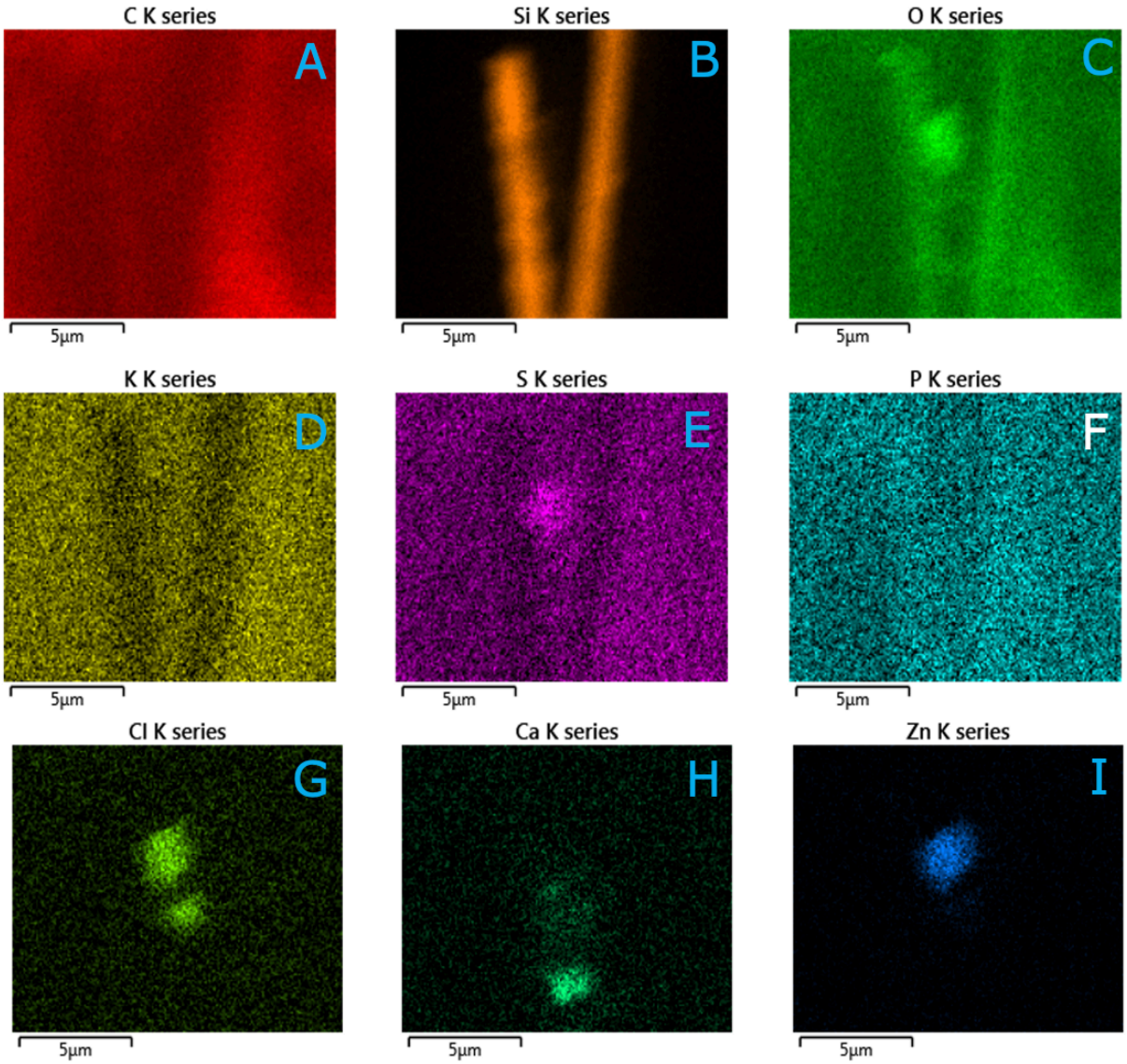

Figure 3.70 ESEM single-elemental-coloured images of unfiltered muscle. ESEM single-elemental-coloured (SEC) images taken of a section of unfiltered muscle sample Ta72 (wild tilapia, site 4). SEC image showing the presence of; *(A)* carbon (C) associated with the structure within the image, *(B)* silicon (Si) associated with the structure, *(C)* oxygen (O) associated with the structure, *(D)* potassium (K) associated with the structure, *(E)* sulphur (S) associated with the structure, *(F)* phosphorus (P) associated with the structure, *(G)* chlorine (Cl) associated with the structure, *(H)* calcium (Ca) associated with the structure and *(I)* zinc (Zn) associated with the structure.

3.13.5.5 Diatom in unfiltered muscle

ESEM greyscale screening of a different section of the unfiltered muscle from sample Ta72 identified a structure (Figure 3.71) potentially similar to that of the diatoms identified on the macroplastic litter from Lake Victoria (Figure 3.48). This structure (shown by a blue ring in Figure 3.71) was cylindrical shaped (~20µm in length), and had a mesh-like structure. This structure was potentially similar to diatom from the genus *Aulacoseira.*

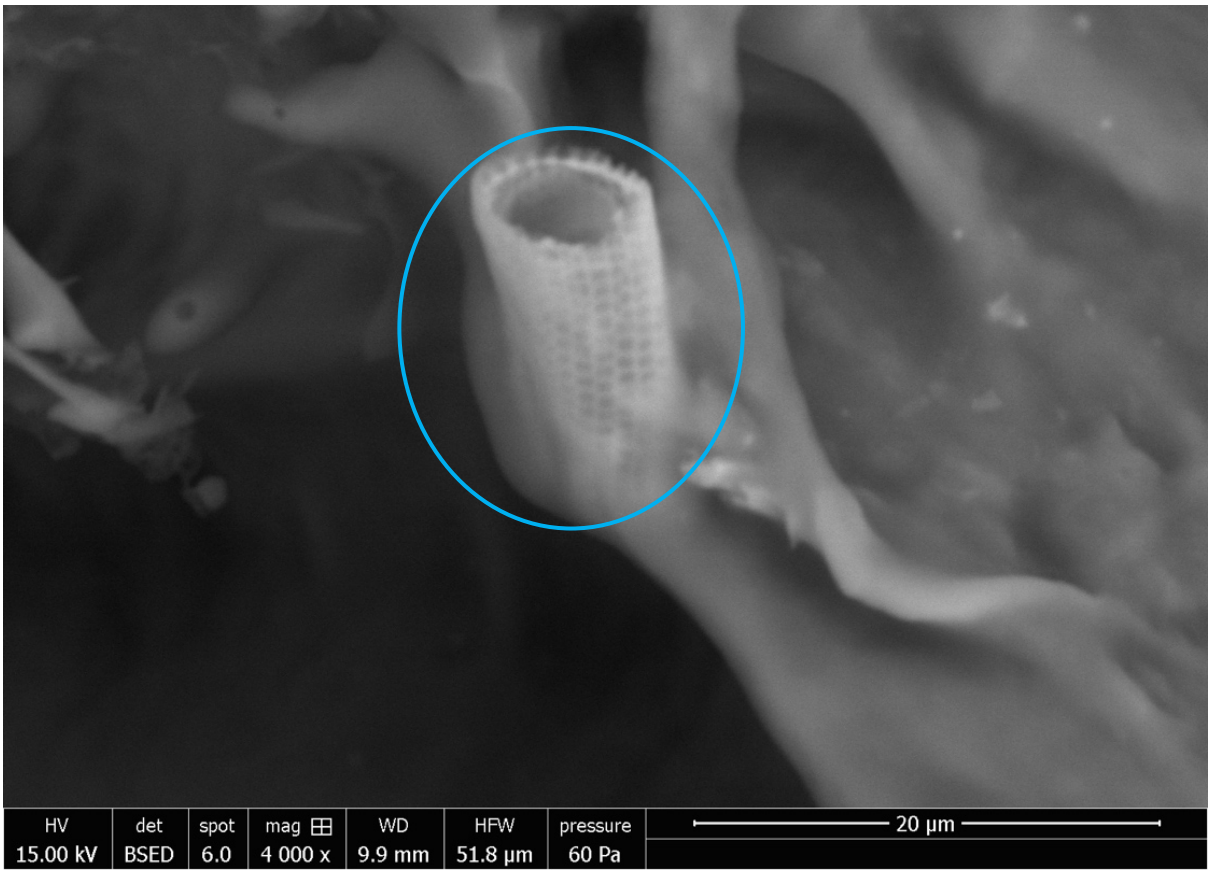

Figure 3.71 ESEM greyscale image of potential diatom found on unfiltered muscle. This greyscale image taken on the ESEM shows a cylindrical shaped artefact identified (shown by blue ring), with a mesh-like structure, potentially similar to the diatom from the genus *Aulacoseira*.

3.13.6 Screening of the unfiltered intact gastrointestinal tract

One untreated intact GIT sample was sent for ESEM screening (GIT20). ESEM screening included greyscale imaging, single-elemental-coloured imaging and EDX analysis.

3.13.6.1 Unfiltered intact gastrointestinal tract – GIT20

Analysis of the unfiltered GIT from sample GIT20 (wild tilapia, site 1B) identified two fragment-like structures lodged into the background structure (Figure 3.72A). These two fragments were focussed on for EDX analyses, see spectrum 84 (Figure 3.72B) and spectrum 85 (Figure 3.72C). EDX analysis of the fragment-like structure (~8µm in length) analysed in spectrum 84 found it to have a high level of C, O and Si (Figure 3.72B) associated with it. With the structure having a higher Si level, than C and O associated with it. EDX analysis of the other fragment-like structure (~5µm in length) analysed in spectrum 85 found it to have a high level of C (Figure 3.72C), a medium level of O and low levels of Al, Si and Fe associated with it. The level of C was similar between the two structures, however the structure observed in spectrum 84 had a greater content of Si than the other structure observed in spectrum 85. However the structure observed in spectrum 85 had a greater presence of different inorganic elements, such as Al and Fe.

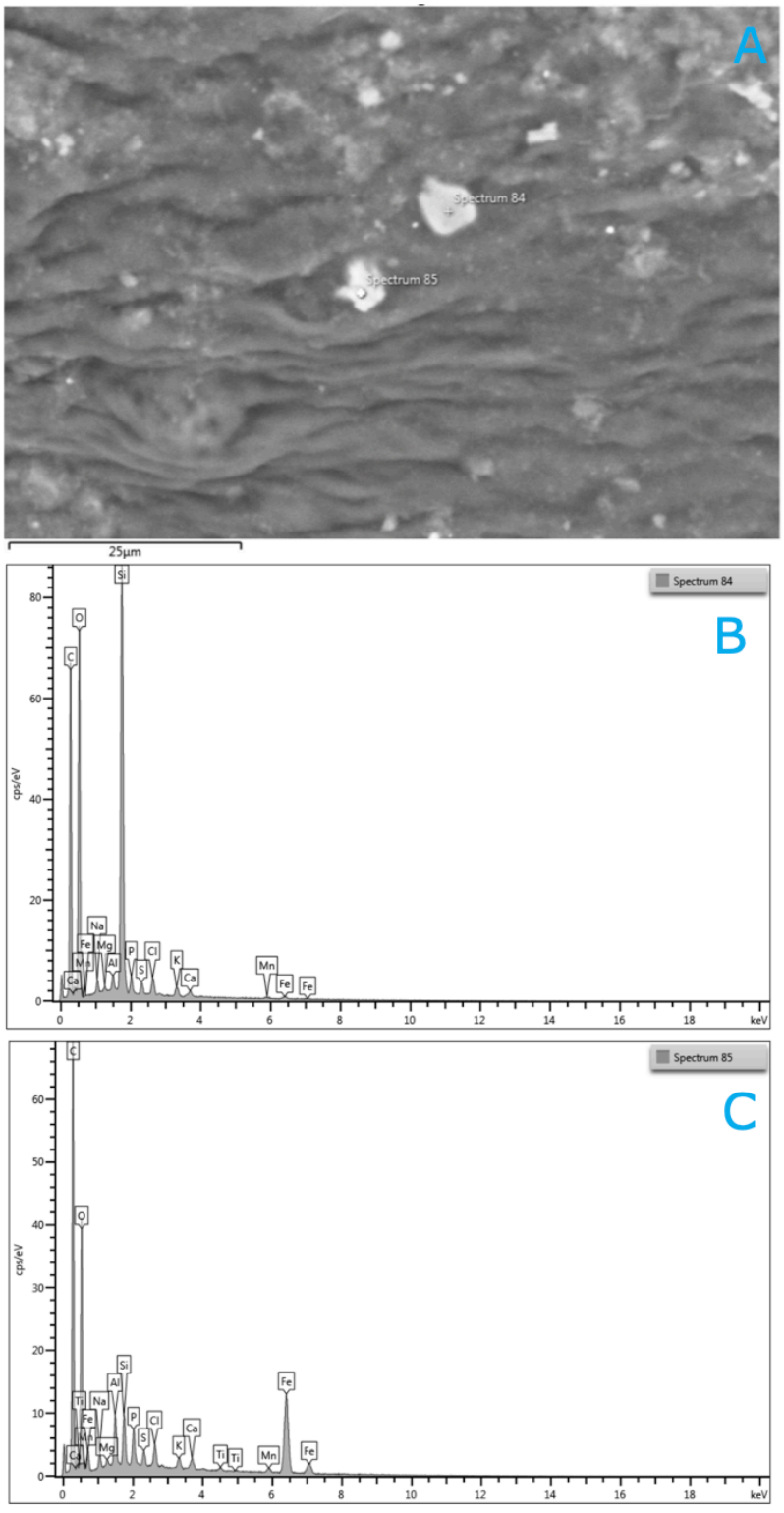

Figure 3.72 ESEM with EDX spectra of unfiltered intact gastrointestinal tract. *A)* ESEM greyscale image taken of a section of unfiltered intact gastrointestinal tract (GIT20, wild tilapia, site 1B), showing two fragment-like structures lodged into the background structure. *(B)* EDX spectra of spectrum 84 showing high levels of carbon (C), silicon (Si) and oxygen (O) associated with the structure. *(B)* EDX spectra of spectrum 85 showing a high level of C, a medium level of O, and low levels of Al, Si and Fe associated with the structure.

3.13.6.2 Diatoms in the unfiltered intact gastrointestinal tract

ESEM greyscale screening of a different section of the unfiltered GIT from sample GIT20 identified two structures (Figure 3.73) similar to that of the diatoms identified on the macroplastic litter from Lake Victoria. The structure shown by the green ring in Figure 3.73 was cup shaped (~20µm in length) and had valves and pores on its surface, and was potentially similar to the diatom from the genus *Aulacoseira*. The structure shown by the blue ring in Figure 3.73 was longer and thinner (~25µm in length) and had valves as well, and was potentially similar to the diatom from the genus *Nitzschia*.

Figure 3.73 ESEM greyscale image of two potential diatoms found on unfiltered intact gastrointestinal tract. This greyscale image taken on the ESEM shows two structures similar that of diatoms. The structure in the green ring is potentially similar to the diatom from the genus *Aulacoseira* and the structure in the blue ring is potentially similar to the diatom from the genus *Nitzschi.*

Both potential diatoms seemed adhered to a larger spherical artefact shown in Figure 3.73. Single-elemental-coloured images were taken of this same area to investigate this artefact. The presence of two areas rich in Si (Figure 3.74C) were associated exclusively with the two potential diatom structures. The presence of O (Figure 3.74B) was associated with both diatom structures, the artefact and background structure. Higher levels of O were also associated with the two diatom structures compared to the artefact and the background structure. The presence of C (Figure 3.74A) was associated with the artefact and the background material. However there was a similar area on the artefact where there was no presence of O or C. A lower presence of Cl (Figure 3.74D) and Na (Figure 3.74G) were associated exclusively with the background structure. Low levels of P (Figure 3.74E), S (Figure 3.74F), K (Figure 3.74H), Ca (Figure 3.74I), Fe (Figure 3.74J) and Mg (Figure 3.74K) were found across all structures within the image.

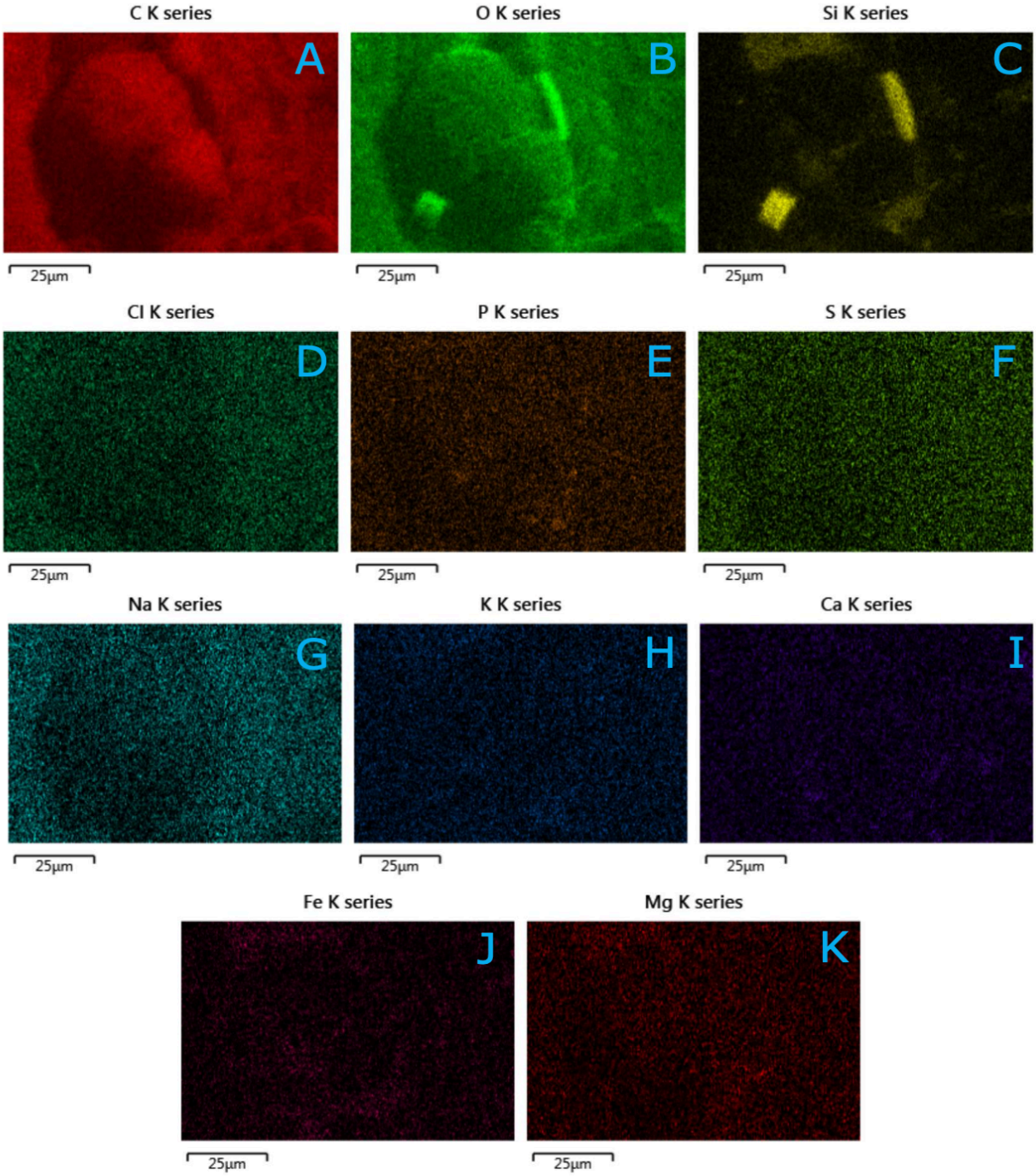

Figure 3.74 ESEM single-elemental-coloured images of unfiltered muscle. ESEM single-elemental-coloured (SEC) images taken of a section of unfiltered muscle sample Ta72 (wild tilapia, site 4). SEC image showing the presence of; *(A)* carbon (C) associated with the structure within the image, *(B)* oxygen (O) associated with the structure, *(C)* silicon (Si) associated with the structure, *(D)* chlorine (Cl) associated with the structure, *(E)* phosphorus (P) associated with the structure, *(F)* sulphur (S) associated with the structure, *(G)* sodium (Na) associated with the structure, *(H)* potassium (K) associated with the structure, *(I)* calcium (Ca) associated with the structure, *(J)* iron (Fe) associated with the structure and *(K)* magnesium (Mg) associated with the structure.

4.0 Discussion

Fish are an essential component of freshwater ecosystems, providing significant nutritional and economical value worldwide. Developing countries account for 94% of all freshwater fisheries (FAO, 2020b), granting food and livelihoods to millions of people, and bringing economic wellbeing through tourism, exportation and restoration.

The increasing concentration of people and growth of towns and cities around freshwater ecosystems, together with increasing human demands for water, have resulted in growing levels of degradation, pollution and threats to biodiversity within these ecosystems (Arthington et al., 2016). Organic substances constitute one of the main freshwater pollutants, coming from domestic sewage discharges (even after treatment) and from industries such as food processing. Other anthropogenic activities, such as agricultural, industrial and mining industries, all contribute to the contamination of aquatic ecosystems (Bashir et al., 2020), However, plastics are now considered the dominant pollutant in freshwater ecosystems (Azevedo-Santos et al., 2021)

Annual global plastic production has increased from 1.5 million tonnes in the 1950s to over 381 million tonnes today, and is set to double by 2034 (Condor Ferries Ltd., 2020). Plastic production continues to increase in developing countries, as they adopt the use-and-dispose culture (Pinheiro, 2017). This high production, along with plastic's high durability and inappropriate waste management, has led to the extensive accumulation of aquatic plastic debris in freshwater habitats. Of particular concern are microplastics, with their ability to adsorb persistent organic pollutants, transfer them around the environment and into the food webs of organisms at all trophic levels of the aquatic system (Andrady, 2011) (Gallo et al.,

2018), polluting the environment and threatening aquatic life and consumers of fish and their products.

This study investigated the presence of microplastics in tilapia, both farmed and wild, harvested from Lake Victoria in Kenya, who are a growing aquaculture producer. This study analysed microplastic presence in samples of tilapia GIT contents and intact GITs, and compared these with the microplastic prevalence in tilapia muscle, the part of the fish consumers would eat. The surfaces of microplastics were also analysed for the potential presence of biofilms.

With a growing global population and an ever-increasing need for a cheap and sustainable food source, the demand for fish as a key source of protein that is free of pollutants, such as microplastics, is critical for the future of human health.

4.1 The importance of tilapia

Besides livestock, fish is the major source of animal protein supply, however depleting wild stocks is an increasing concern for fishermen, environmental organisations and policymakers. Sustainable aquaculture is playing an important role in the transition to a more environmentally and economically viable fish production, with selection of fish species key to this burgeoning industry (Yue et al., 2016)

Tilapia are the third most produced aquatic species globally (Elizabeth Cruz-Suarez et al., 2006). They are a hardy, prolific and fast-growing fish, with an adaptable and herbivorous diet (Yue et al., 2016). With their production performances improved through breeding, farmed tilapias reach market size (i.e. 600-900g) in 6-9 months of culture (Ahmed, 2009). Farmed in over 120 countries, including Kenya, they were a plausible choice for monitoring microplastic

contamination in Lake Victoria, due to their recognition as a dominant ecological and commercial species.

4.1.1 Choice of tissues used for analyses

This study looked at fish tissue, consisting of skin and muscle, this was used as a representative biological model, as it is the key part of the fish entering the human food chain. Biological samples are important in representing the fate and sources of plastic pollution, if we are to consider the potential effects on human health, and therefore applicable for the quantification of microplastic load. Fish are bioindicators of the contaminants which directly reflect the condition of the environment. The skin is one of the largest organs in the fish body and is one of the first barriers pollutants encounter.

The entire tilapia GIT as well as the contents of the GIT were also analysed. Over 220 different fish species have been found to consume microplastics in the natural environment (Lusher, Welden, et al., 2017). When ingested, microplastics are thought to be concentrated in the GIT of the fish (Foekema et al., 2013) (Khan et al., 2020), causing physical harm, such as the internal abrasion or blockage, and they can also promote a deceptive sense of satiation, leading to a decrease in consumption of their true food. An additional and harmful aspect of plastic ingestion is the potential hazardous chemicals that could leach out from the plastic and into other essential organs of the fish (Baalkhuyur et al., 2018).

4.1.2 A reproducible and cost-effective method to investigate microplastic presence

Microplastic presence is typically assessed by digestion of an organism's biological tissues and consequent analysis of the filtrates. Numerous methods have been

established, however most are not suitable as they are too expensive or time consuming to be reproduced on a large scale particularly in LMICs. Zinc chloride was considered a fairly inexpensive and effective flotation media, although there were reports of the degradation of the plastic polymer polyamide and its inability to fully digest GI contents (Coppock et al., 2017). Sodium chloride is a cheap and inert option for microplastic recovery, but studies have shown that its use could result in an underestimate of microplastic abundance, especially with high density plastics (Grbic et al., 2019).

Strong alkaline bases, such as KOH, hydrolyse chemical bonds and denature proteins, allowing biological material to be removed. However, this is less applicable for fish digestive tracts, due to the higher presence of inorganic material. Following a 2-3 week incubation of KOH at 10%, excised stomach and intestines from fish have shown successful digestion of organic material (Foekema et al., 2013). This protocol was developed to allow the dissolution of whole GIT in fish and their muscle tissue at higher temperatures and shorter durations, without polymer degradation. Plastic polymers have shown resistance to KOH (Foekema et al., 2013), with no impact on polymer form or mass, except for polycarbonate (PC) and PET which have shown minor degradation (Lusher, Welden, et al., 2017) (Alexandre et al., 2016).

4.1.2.1 Visualising microplastics

The use of the dye Nile Red to visualise and quantify microplastics is increasingly common (Joon Shim et al., 2016). It absorbs on the surface of plastic, and is recommended at 10µg/ml with an incubation for 30-60min (Maes et al., 2017). The use of higher concentrations has resulted in an increase in the fluorescence intensity, but also an increase in unwanted background signal from the filter paper

(Maes et al., 2017). Incubation was tested for 60min but found no difference in fluorescence between those that were incubated at 30min compared to those incubated for 60min, therefore 30min was chosen for the subsequent analysis of the remaining samples.

False positives have been found to arise with Nile Red, where an artefact will fluoresce, but might not be a microplastic (Stanton et al., 2019). The additional use of DAPI, following staining with Nile Red, allows any biological material that could have been wrongly identified as microplastics, to be correctly classified.

4.2 The importance of having controls

Controls were essential in ensuring confidence in any microplastics detected in the tilapia samples being correctly identified. The structure, size and elemental composition of microbeads from a facewash and macroplastic litter collected from Lake Victoria were analysed and the results were used to help the interpretation of results from the fish muscles, GIT and GIT contents.

4.2.1 Microbeads from facewash

The extracted blue and white microbeads from a facewash were easily visible to the naked eye at ~5mm in diameter. In a single shower, it is estimated that 100,000 microbeads are washed down our drains, potentially ending up in our global water bodies (McGrath, 2018). Their small size results in them not being filtered out by most wastewater treatments, and entering the aquatic environment. The main concern is their ability to function like tiny sponges, adsorbing toxic chemicals from the surrounding waters (Nerín et al., 1996) and acting as a host for the development of biofilms (Harrison et al., 2018a). However, this can make them smell and taste similar to the normal diet of aquatic life, such

as fish, resulting in their ingestion across numerous aquatic species. Microbeads have been reported to be a million times more toxic than their surrounding waters (Animals Australia, 2019). The UK cosmetic industry recognised their pollution implications and placed a ban on their use in cosmetic products in 2018 (Pro, 2017), replacing them with biodegradable alternatives such a jojoba beads.

The extracted beads were used to spike fish samples as a control to endorse the reliability of both Nile Red and DAPI stain protocols following digestion. Alkaline digestion with KOH allowed the microbeads to collect at the top of the solution, from flotation based on their density, and they were seen collecting at the top edges of the filter paper. This area was focussed on when searching for microplastic presence in the tilapia samples. This also helped in method optimisation, as the KOH used demonstrated successful digestion of organic material present in the samples.

Interestingly, when analysed by light microscopy the larger blue spiked microbeads used appeared as dark circles and did not fluoresce. Whilst an issue with the methodology was originally suspected, a previous study has showed that Nile Red struggles to adhere to larger microbeads (Hantoro et al., 2019). It is also possible that the staining incubation time with Nile Red was not sufficient for staining the larger beads (Maes et al., 2017). In addition, white polymers have been found to stain with Nile Red, while blue polymers, similar to these from the face wash, have been shown to be less absorbent (Mayes, 2018).

4.2.2 Macroplastic litter from Lake Victoria

Light microscopy of strands of the macroplastic netting collected from Lake Victoria revealed strong fluorescing fibre structures after staining with Nile Red,

for all the different coloured net pieces investigated. None of the net pieces fluoresced with DAPI confirming its reliability as a second stain.

The macroplastic litter was also used in the screening for bacterial DNA and therefore biofilm presence. All the different coloured net pieces analysed were positive for bacterial DNA, highlighting the potential presence of a biofilm on the surface of the macroplastic.

4.2.2.1 Diatoms found on macroplastic litter

Studies have found diatoms and bacteria as the most common biota to exist on the microplastic's biofilm (Reisser et al., 2014) (De Tender et al., 2017) (Schlundt et al., 2019). Macroplastic litter collected from Lake Victoria's waters was screened by ESEM imaging for potential biofilm presence. Numerous different shaped diatoms (Figure 3.48) were potentially identified, including circular flukes, longer rods and 3D diatoms. These were tentatively identified as the diatom genera *Fragilaria*, *Cocconeis*, *Aulacoseira*, *Achnanthes* and *Tabellaria* which are all freshwater diatoms (Poulíčková and Manoylov, 2019) (Forrest et al., 2020) (Amoatey and Baawain, 2019).

Studies based on Lake Victoria's waters have shown diatoms from the genera *Navicula*, *Aulacoseira*, *Nitzschia and Pinnularia* are abundant in the lake (Triest et al., 2012) (Stager et al., 2009). The diatom genus *Aulacoseira* has been shown to be abundant in the lake in the wet season (January to May), while the genus *Nitzschia* is abundant in the dry season (June to July) (Sitoki et al., 2012). In the Nyando river, feeding into the Winam gulf, the genus *Cocconeis* was found to exist in high abundance (Triest et al., 2012). Specifically in the Winam Gulf, the diatom genera *Aulacoseira* and *Nitzschia* have been the dominant types occupying the lake (Kundu et al., 2017). This supported the possibility of the structures identified

on the macroplastic litter being diatoms, as a cylindrical shaped structure similar to that from the diatom genus *Aulacoseira* was identified, and there was also a number of potential circular structures similar to that of the genus *Cocconeis* identified. These two freshwater diatom species have been identified in Lake Victoria and the rivers feeding into the lake.

4.3 Is microplastic prevalence greater in wild or farmed fish?

While analysing muscle, GIT and GIT contents, we were able to compare microplastic prevalence in these different tissues between the wild and the farmed tilapia.

4.3.1 Fish muscle from wild fish contains greater numbers of microplastics

The muscle of the wild tilapia had a greater prevalence of microplastics, with 46 identified in 19 (50%) of the fish. In comparison, only 35 microplastics were found, present in 19 (45%) of the farmed/caged fish. This was in line with findings from a study on salmon, where wild caught salmon contained greater microplastic amounts than farmed (Moore, 2019). This result was thought to be the consequence of diet. Wild fish are allowed to travel freely and therefore have the potential to be exposed to more plastic pollution. Wild fish are also more likely to feed on smaller marine life, such as zooplankton, where studies have found high levels of microplastics ingested by 39 species of zooplankton (Botterell et al., 2019).

Feeding behaviour can also play a part in the uptake of microplastics, where the number of microplastics ingested was high when there was no or limited food available. This increase is because these fish are actively foraging on microplastics

when no food is available (Roch et al., 2020). This will occur more in the wild fish, as farmed fish are typically fed a minimum of twice a day (Njiru et al., 2004b). Wild fish can also vary in age, with older fish being potentially exposed to more plastic pollution, whereas farmed fish are usually harvested in Lake Victoria after only 6 months. With wild fish caught at an older age, this could allow more time for microplastics to translocate across the GIT epithelium into the muscle, and therefore result in the increase in the wild muscle (Abbasi et al., 2018) (Jovanović et al., 2018). The effects of accumulation in the muscle may be significant, especially with implications for food web transfer and fish as a food source (Roch et al., 2020).

4.3.2 Is microplastic prevalence greater in the GIT from farmed tilapia?

The farmed tilapia GIT contents analysed in this study had a higher microplastic content (3 pieces) than the wild GIT contents samples (2 pieces), however only small numbers of fish were analysed in this part of the study, 4 farmed and 1 wild tilapia. Interestingly when the intact GIT was analysed, farmed tilapia were found to again have a high microplastic content (19 pieces) compared to the wild fish (9 pieces), with equal numbers of fish investigated (n=3).

Taken together, these results suggest that the farmed tilapia have a greater prevalence of microplastics within their GIT than the wild fish. Aquaculture extensively uses plastic for both equipment and packaging, everything from polystyrene foam-filled fish cage collars, to plastic feed sacks and harvest bins (Holmyard, 2019). Farmed fish are fed commercial pellets and are enclosed in a netted environment, usually made of PE and PP plastics (Njiru et al., 2018). Damage to these cages by UV radiation, weathering and ageing could cause microplastics to be broken off and contribute, through ingestion, to the greater

prevalence of microplastics seen in the GIT from farmed fish. In addition, farmed fish can exhibit inquisitive behaviour towards parts of their cages, providing further potential to ingest harmful plastics through this behaviour (Roch et al., 2020). Ghost gear when old and broken can get dropped by fishermen, with 640,000 tonnes abandoned in global waters annually (World Animal Protection, 2018). This often occurs in the vicinity of the bays where the fishermen are from, with these inshore regions the preferred location of fish farms (Xue et al., 2020). This can contribute to a high density of microplastics in these caged areas (Nelms et al., 2021).

A study on the composition of a commercial fishmeal product used in the feeding of farmed fish was carried out to detect microplastic content (Gündoğdu et al., 2021). Fishmeal is a dry, high-protein feed component primarily used in the aquaculture sector. The study tested 26 fishmeal products and found plastic content between 0-526.7 n kg^{-1} (Gündoğdu et al., 2021). Farmers using fishmeal or other commercial feed product could be adding another pathway for plastics to enter the food chain of farmed fish.

The higher prevalence of microplastics found in the intact GIT compared to the GIT contents suggests that microplastics have the potential to become closely associated with the GIT structure, and therefore not easily removed when extracting the GIT contents. This is supported by studies which show the potential for accumulation in the GIT of marine and freshwater species across the world (De Sales-Ribeiro et al., 2020) (Neves et al., 2015) (Ding et al., 2018), and specifically in fish sourced from Lake Victoria, where 20% of caught Nile perch and Nile tilapia were found to contain plastics within their GITs (Biginagwa et al., 2016).

However with such low numbers of microplastics and a greater number of farmed fish (n=4) analysed compared to wild (n=1), further work is needed to determine

whether caged fish are more likely to encounter and ingest microplastic than wild fish, and also to investigate the sources of these microplastics.

4.4 Microplastics prevalence varies with geographical location

Cities, towns, rivers, urbanisation and industrial activities all contribute to the plastic pollution of an aquatic environment. Lake Victoria is the central receiver of industrial and domestic waste from towns and cities around its basin and from industrial and agricultural waste from regions rich in mining activities and agriculture (Ngure et al., 2014). This is exacerbated by the numerous rivers which feed into the lake, carrying pollution from further afield (Oguttu et al., 2008).

4.4.1 Kisumu

Site 1A and 1B (Dunga), located on the Eastern shore of the Winam Gulf, in close proximity to the city of Kisumu, had the greatest number of fish analysed (n=20) and a high content of microplastics identified. Of the muscle samples analysed (n=18) at this site 50% were found to contain microplastics (Ta12, Ta55, Ta61, Ta62, Ta63, Ta65, Ta66, Ta67 and Ta68), with 13 microplastics identified in all the muscles. Two GITs (GIT15 and GIT19) were also analysed from this site and were found to contain 9 microplastic pieces between them. Kisumu, Kenya's third largest city and the second largest city on the Lake Victoria basin (after Kampala, Uganda), sits on the Eastern edge of the Winam Gulf. Kisumu is the immediate former capital of Nyanza Province, and is an important link in the trade route between Lake Victoria and Mombasa because of its water and rail connections. It is also the chief terminus for the agricultural produce of Nyanza and Western provinces. Kisumu has a population of 721,082, with a rural population within Kisumu Country of 714,688 (KNBS, 2019). Like many growing urban areas of

developing countries, solid waste management is a major environmental and public health concern. Kisumu is facing increasing waste generation, an overflowing dumpsite and pollution from uncontrolled discarding of waste. Despite having an environmental department to manage solid waste services, the department lacks financial resources and the adequate technical capacity to effectively manage the waste generated (Sibanda et al., 2017).

4.4.2 Northern Winam Gulf

Site 15B (Port Buyala), located on the North-West shore of the Winam Gulf, had a high prevalence of microplastics identified (n=9) in all of the three fish analysed from the site (Ta39, Ta40 and Ta48). Fish also sourced from the nearby site 16B (Mageta Island), located on the North shore of the Winam Gulf, had the greatest amount of microplastics identified (n=14) when comparing all the fish from all the sites. Three fish were analysed (Ta35, Ta36 and Ta38) and all the samples contained microplastics, however the majority were found in one fish (Ta38), where 11 fibres were identified. Research has found Lake Victoria's waters to exhibit an anti-clockwise flow (Nyamweya et al., 2016a). As there is a constant high volume of municipal pollution coming from Kisumu on the Eastern shore of the lake, this anti-clockwise current could be bringing an array of pollution from the city to the Northern shores of the Winam Gulf and polluting the aquatic environment and thereby the fish at sites 15B (Port Bunyala) and 16B (Mageta Island). Furthermore, poor education, typical of many smaller urbanisations in developing countries, has led to inhabitants directing the majority of their wastewater into the lake. A high amount of microfibres (n=13) were detected in the fish from site 16B. Washing machine and manual clothes washing runoff can deposit large amount of microfibres into the lake (GESAMP, 2016).

Sites 15B and 16B are also located near to areas of high mining and agricultural activities. Agricultural wastewater can run off into surrounding rivers and the lake, carrying pollution with them. Wastewater treatment sludge by-products are applied to agricultural lands and have been found to contain synthetic clothing microfibres (Bashir et al., 2020). These can persist in the soil or sludge for up to 5 years post application, with some detecting them in field sites up to 15 years after application (Zubris and Richards, 2005). Here microplastics are retained in sludge, which is then applied as fertiliser, releasing the microplastics as a persistent terrestrial contaminant. This is escalated by the degradation of PE agricultural mulch films, which are used to modify soil moisture and temperature (Qi et al., 2020). As soil-contaminated films are non-recyclable and are often so thin, their extraction from the soil is difficult and they are left to contaminate the soil.

In Kenya, mining is known to provide great socio-economic benefits, however it is also considered to be the largest pollution source, after the agricultural industry (Mitchell et al., 2020). Gold mining generates large amounts of mine waste and effluents, with considerable amounts of persistent harmful elements, that cause great environmental and human health concerns (Ogola et al., 2002). These harmful elements can be released into the lake and be picked up by microplastics, which could be acting as transport vectors into the fish and threatening their health. Fish from Lake Victoria have been found to contain concentrations of cadmium (Cd), lead (Pb), arsenic (As) and mercury (Hg) that were above the WHO and FAO maximum allowable concentration (Ngure et al., 2014).

4.4.3 Rivers

Rivers play an important role in the transport of plastics into the lake. They can bring pollution from tourism, on-water activities and improper dumping of terrestrial waste. Furthermore storm and rainwater drainage, flooding and wind can transport plastic litter into freshwater ecosystems (Bellasi et al., 2020). Moreover, rivers and lakes operate as secondary microplastic producers, fragmenting the pollution by weathering and water currents. Sites 4 and 4D (Uyoma Point) are located at the mouth of the River Awach. A study tested water from the Awach mouth and found the water unsuitable for direct drinking water supply (Lalah et al., 2008). The close proximity to the market towns here was thought responsible for the high pollution levels. Microplastics were found in abundance (n=9) in the two intact GIT samples analysed from site 4 and in the wild muscle samples analysed from site 4D, with all three fish analysed containing a total of 5 microplastics.

4.4.4 Entrance to the main lake body

Sites 7B and 7D (Mbeo cages) and sites 13B and 13D (University of Eldoret pond) are located in the entrance to the Winam Gulf from the main lake body. This is the only entrance/exit that fishermen can use to access the main body of the lake. As they use this channel, they will often be pulling trawl nets, which are made from plastics, including PP, PE, PA, PS and PVC. These nets are often abandoned, lost, or discarded in this area, especially if breakage occurs from the net getting trapped on obstacles in the water (Nelms et al., 2021). Proper disposal of discarded fishing nets is costly, and some fisheries will often dump their nets into the water if they cannot afford the fee (Bracenet, 2020). Ghost gear is estimated to make up 30-50% of the total plastic pollution found in our waters (The

Guardian, 2019). It causes harm to aquatic life by entanglement, and the persistence of microfibres in the water, which the net releases through ageing in the water, these can then be ingested by fish and other aquatic organisms. Microfibres were one of the most commonly identified microplastic type in the muscle samples, with 35 microfibres identified in all the muscle samples, and were identified in fish analysed from sites 7B and 7D and sites 13B and 13D.

There is little exchange between the Winam Gulf with the open lake (Nyamweya et al., 2016b), resulting in different water quality and often higher levels of pollution build up reported at those sites. Fish from those sites located in the Winam Gulf; sites 1A and 1B (Dunga), sites 4 and 4D (Uyoma Point), site 6B (Off Ngodhe), sites 7A and 7B (Mbeo cages), sites 13B and 13D (University of Eldoret pond), site 15B (Port Bunyala) and site 16B (Mageta Island), were all found to contain microplastics. As the Winam Gulf has many rivers feeding into it, and a high amount of agricultural, industrial, mining and domestic activity around its shores, it is perhaps no surprise that pollution amounts are markedly greater than in the main body of the lake (Kundu et al., 2017).

There is a spatial association between human activities and microplastic prevalence. Microplastic pollution sources in Lake Victoria are from numerous industries, such as mining, shipping, agro-processing factories, pharmaceutical industries and fisheries themselves. Levels at any one site across the lake can be affected by proximity to river mouths, industry and human activity.

4.5 Are the bacteria detected from the plastisphere?

Bacterial DNA was detected in some of the samples, despite the isolation of genomic DNA in low quantities. However, we cannot be sure that the bacteria from

which the DNA originated were part of the microplastic's plastisphere. The bacteria could have been attached to other materials present in the samples.

The microfibre filters used had 1.6µm pores (Sigma-Aldrich, 2020), which should have allowed any bacteria not attached to microplastics to pass through. However, bacteria could have been attached to plant material particularly in the GIT samples. Attempts to identify some of the bacteria were not fruitful.

ESEM analysis of the unfiltered muscle from sample Ta72 identified a group of elliptical shaped rods (Figure 3.67A), which ranged in length from 5-10µm. Most bacteria are said to be 1-2µm in diameter and 5-10µm in length (Levin and Angert, 2015), which supported the possibility of this group of structures potentially being bacteria. Furthermore, EDX analysis of one of these rods (Figure 3.67B) found it to have a very high C and O content, as well as a medium level of P and low levels of Mg and Ca associated with it. Aquatic bacteria have been found to require C, O and P for their growth and success (Vrede et al., 2002). Bacterial cell walls have also been found to show favourable conditions for calcium carbonate precipitation provided by the cell wall and the extracellular polymeric substance (Enyedi et al., 2020), so that calcium and magnesium ions can then bind on the bacteria's surface. This research supported the elemental composition of one of the rods identified, however it was felt that there was not enough evidence to fully support these rod structures as being bacteria. Further work using SEM imaging incorporating staining for bacteria and species could be used to clarify whether there was a plastisphere present and potentially identify some of its components.

4.6 Can the plastisphere be visualised?

Plastic debris acts as an appealing substrate for microorganisms to adhere to as it will persist longer than other natural floating substrates, and has been shown

to act as a transport vector for POPs (Zettler et al., 2013). Previous studies have used SEM imaging to visualise this plastisphere and to categorise any microbial communities living on the surface (Zettler et al., 2013) (Oberbeckmann et al., 2014) (De Tender et al., 2017) (Kirstein et al., 2019). In this study ESEM and EDX analysis was used to screen samples for microplastic presence, based on their surface characteristics and elemental composition. It was also used in determining the microplastic content, and visualisation of the plastisphere.

Biofilms formation typically constitutes a change in the lifestyle of the microorganism, whereby the genes involved in adhesion, chemotaxis and substrate transport are expressed to enable cells to from a matrix, and fluid channels to distribute nutrients between cells (Amaral-Zettler et al., 2020). SEM imaging from the samples analysed in this study has shown the plastisphere as a diverse microbial ecosystem, with members including cyanobacteria and diatoms. Diatom-like structures were identified on the macroplastic litter from Lake Victoria, and tentatively identified as the diatom genera *Fragilaria*, *Cocconeis*, *Aulacoseira*, *Achnanthes* and *Tabellaria*. ESEM screening of the unfiltered muscle from sample Ta72 identified a cylindrical shaped artefact, with a mesh-like structure, similar to that of the diatom genus *Aulacoseira*. The structure identified was ~20µm in length and had a unique mesh-like appearance similar to that of a diatom. The size of diatoms is said to range from 2-200µm in length, with the genus *Aulacoseria* being between 5-20µm in length (Genkal and Popovskaya, 1991).

Another structure similar to that from the diatom genus *Aulacoseria* was identified in the ESEM screening of an unfiltered GIT. This structure was cup shaped and 20µm in length, with valves and pores on its surface, similar to the diatom from the *Aulacoseria* genus.

Another longer and thinner structure with valves on its surface was also identified in sample GIT20. This structure was ~25µm in length, and resembled the diatom from the genus *Nitzschia.* Diatoms from the genus *Nitzschia* are between 8-30µm in length (Kelly et al., 2015) and are commonly found in freshwater environments. Studies based on Lake Victoria's waters have shown diatoms from the genera *Navicula*, *Aulacoseira*, *Nitzschia and Pinnularia* are abundant in the lake (Triest et al., 2012) (Stager et al., 2009).

A previous study attempting to visualise the plastisphere using SEM imaging, identified diatoms from the bacillariophyte genera including *Navicula*, *Nitzschia* and *Sellaphora* (Zettler et al., 2013), which are known biofilm formers in the aquatic environment (Congestri and Albertano, 2011). Another study found frequent diatoms from the genera *Nitzschia*, *Cocconeis*, *Achnanthes* and *Amphora*, when screening aquatic plastic debris by SEM imaging, with the genus *Nitzschia* as the most frequent diatom identified (Reisser et al., 2014). The diatom genera findings in this study were in line with common diatoms found on aquatic plastic debris in previous studies, as well as with common diatoms found in the waters of Lake Victoria. Furthermore, diatoms are not usually found in the muscle of fish and would not be present unless they had adhered to a substrate such as a microplastic. However they could have resulted from cross-contamination of the GIT during the processing of the fish, although this was felt unlikely as the sample preparation was performed in such a way to ensure no contamination between different samples of the fish would occur.

Both of these potential diatoms were seen adhered to a larger spherical artefact (Figure 3.73), which when screened by EDX analysis was found to have a high carbon content associated with it. Plastics are commonly carbon based and due to its spherical shape, this structure was suspected as a microbead with the two

diatoms colonised on its plastisphere. Microorganisms have been found to colonise plastic substrates within hours of entering the aquatic environment (Harrison et al., 2018a). SEM images have shown various pennate diatoms colonising a PE biofilm after 1 week, but after 2 weeks many diatoms are pushed off from the surface as other microorganisms such as cyanobacteria attach to the biofilm community (Amaral-Zettler et al., 2020).

A strong Si content can be indicative of diatoms (Wang et al., 2017a). Using ESEM alone, this could lead to diatoms being mistaken for microplastics as their structure is alike. ESEM screening of the filtered GIT contents from sample GI5 demonstrated this, as an artefact was identified with a similar structure of a diatom. This however was ruled out, as the presence of Si was only associated with the fibrous background material. Instead, the meshed artefact had a high C content, with an area on its surface that was rich in Cl. This Cl-rich area could have indicated the unique property and presence of the plastic polymer PVC, however as the Cl area did not cover the whole of the mesh-like structure further work would be needed to confirm if this was a PVC plastic particle.

4.7 Can SEM be used to screen for microplastic presence?

Plastics are carbon based, so strong carbon peaks exhibited by EDX analyses of the fish samples were thought to be indicative of potential microplastic presence, as other materials present were expected to be non-organic.

4.7.1 Microplastic misidentification

A possible source of microplastic misidentification has been found to be from fractured fish bones (Wang et al., 2017a), which is characterised by an EDX spectra exhibiting high levels of calcium and phosphorus, this is usually common

in the screening of fish GIT contents but was found in this study in fish muscle. Screening of the filtered muscle from sample Ta48, highlighted an artefact (>75µm in length) with a similar structure to a microplastic fragment. Using SEM imaging, this structure was found to contain high amounts of Ca and P, with lower amounts of C and Mg. As this was found in the fish muscle, this artefact is potentially a fish scale. Its fragment-like structure could have led to this being mistaken for a microplastic, but this was ruled out by the high Ca/P content identified through SEM screening.

A similar result was found in the screening of the unfiltered muscle from sample Ta72, where two fragment-like artefacts were identified which had a different appearance to the background structure. EDX analysis highlighted the larger of the artefacts (50µm in length) had a high Ca content, as well as very high levels of C and O associated with it. EDX analysis of the smaller artefact (20µm in length) found a high C level and medium levels of O, P and Ca associated with it. A study that analysed Atlantic fish using SEM/EDX imaging for microplastic prevalence found that shells and their fragments in the fish samples exhibited a strong Ca peak on EDX analysis (Wagner et al., 2017). Despite the high C content of these two artefacts, it was decided that the high presence of Ca and P suggest they were not plastic in origin but potentially fragments from shells, scales or bones.

4.7.2 Determination of microfibre

The screening of the unfiltered muscle from sample Ta20 identified a group of rectangular structures similar to that of microfibres, which ranged in length from 10-30µm. When two of these fibre-like structures were focussed on by EDX analyses, they were both found to have high C levels, which supported their possibility of being microfibres. They were also found to both contain medium

levels of O, which correlates with a previous study which found that microfibres can exhibit a smaller O peak when examined with SEM/EDX (Blair et al., 2019). Single-elemental-coloured images were also taken of this same area and found these two fibres to contain high amounts of Si which was not indicated on the EDX analyses. Si is often added to plastic to form silicones which produce malleable rubber items, hand-resins and spreadable fluids (LifeWithoutPlastic, 2020). Silicones do not biodegrade, are completely inert and have been found to leach certain synthetic toxic chemicals at low levels (Jenke et al., 2006), with the chance of leaching increased in fatty substances, such as the muscle of the fish. While full confidence cannot be placed in the identification of these fibre-like structures in this sample being silicone plastic microfibres, organic structures with high Si contents should still not be found in the muscle of the fish, and it does raise concern for the possible leaching of toxic chemicals that could be occuring in the fish muscle.

4.7.3 Determination of microbead

A bead shaped artefact was identified, in the unfiltered muscle from sample Ta66, ~20µm in length, with a sphere shape and a rough surface, which could have come from weathering and polymer degradation in the aquatic environment. EDX analysis of this bead found it to have a very high C level, which supported a plastic origin. Many inorganic elements were also detected, with medium levels of Cu, Zn, Al, and Si. EDX analysis allowed us to compare the background structure (muscle), which contain no Cu or Zn. Cu and Zn are both used as coatings on plastic, to reduce diffusion of O and protect the plastic (Bilek et al., 1966). These elements are often found together in PEN plastic and sometimes PVC (Papagiannis et al., 2004). However, they both raise concerns as they can accumulate in high

concentrations in the fish's liver, causing toxicity to fish and a threat to human health if they translocate into the fish muscle, which was seen in this sample (Papagiannis et al., 2004). The adsorption of Cu and Zn from aquatic environments has been found to be higher from aged (sun-exposed) PVC and PS microbeads than for their virgin counterparts (Brennecke et al., 2016). As the bead shaped artefact in this sample had a very high C content and seemed to appear aged from its rough surface, it seemed probable that this could be a PVC or PS microbead. Furthermore the inorganic levels of Cu and Zn, that can appear at high levels in freshwater lakes (Papagiannis et al., 2004), supported the conclusion that this microbead could have adsorbed these from the aquatic environment and transported them into the fish.

Another bead-like artefact (~20µm in length) was identified in the unfiltered muscle from sample Ta69, and found to have a high C peak, however this C level was not as high as those identified in the potential microplastics found in the other fish samples. The structure also had a low level of O, P and K associated with it. However, despite the distinctive sphere appearance of this artefact, there was no EDX analysis taken of the background structure (muscle) to compare the compositions, and therefore insufficient details to confirm that this artefact was a microbead.

4.7.4 Determination of fragment

Screening of a different section of the unfiltered muscle from sample Ta66 identified a triangular-like fragment, ~30µm in length, lodged into the background structure (muscle) of the sample. When analysed it was found to have a high C content, and also medium peaks of Ni and Cl. SEC images were also taken of this same area and found the fragment structure to exclusively contain high amounts

of Cl, Na and Ni, but no C. Ni plating is used on plastics in the finishing industry, to prevent corrosion of the material (Naqash et al., 2020). If ingested, it can be toxic at high levels, and has been found to cause impairment of gas exchange (Blewett and Leonard, 2017), inhibit ion regulation and promote oxidative stress (Naqash et al., 2020) in fish. PVC plastic can be detected through SEM/EDX analysis from its unique elemental signature of containing Cl (Wang et al., 2017b), however as this fragment was shown to contained no C, it was felt unlikely that this was a microplastic fragment.

4.8 Can microplastics act as a transport vector for harmful chemicals?

4.8.1 Barium presence

SEM screening detected low levels of Ba in all the filtered fish samples. This originally raised concern as Ba compounds are amongst the densest used as heat stabilisers (McKeen, 2019), especially in PVC (Turner and Filella, 2020a), and once ingested in fish have been shown to cause metabolic, neurological and kidney diseases (Turner and Filella, 2020a). There are even reports of breast cancer that have resulted from exposure to Ba in humans (Campanale et al., 2020). Screening of a plain section of the microfibre filter paper as a control, highlighted small bead structures on top of the fibrous filter paper material. When one of these bead structures was focussed on by EDX analysis it was found to have a low Ba content. As the filter paper had been screened without the addition, it suggested that the Ba must have been part of the composition of the filter paper.

When screening one of the filtered muscles (sample Ta44), where a larger (>75µm in length) darker grey structure was identified on top of the fibrous background material. Single-elemental-coloured imaging revealed some deposits surrounding this structure, which were exclusively associated with high levels of Ba (Figure

3.52F). These structures were similar in shape to that of microbeads, however with Ba deposits detected in the composition of the filter paper, the potential for these to be microbeads was ruled out.

4.8.2 Titanium presence

To avoid unwanted interference from elements in the filter paper or reagents used in the filtering process, untreated sections of muscle and the GIT were also screened.

The screening of the unfiltered muscle from sample Ta20 highlighted an artefact (~7µm in length) with a different appearance to the background structure. It was found to be rich in C with medium levels of Ti. Analysis of the background structure found it to also contain a very high level of C, but with no Ti. Single-elemental-coloured images were also taken of this same area and confirmed that Ti was exclusively associated with the artefact identified. The results suggested that this artefact was potentially plastic in origin with possible titanium dioxide (TiO_2) nanoparticles absorbed to it. TiO_2, a common additive used in plastic manufacturing, acts as a UV blockers, preventing the polymer's degradation (Cho and Choi, 2001). Studies however have shown that this TiO_2 may be toxic to algae, bacteria and fish (Handy et al., 2008), by inducing oxidative DNA damage, lipid peroxidation and even cause an increase in nitric acid or hydrogen peroxide production in human bronchial epithelial cells if ingested by humans (Shah et al., 2017).

4.8.3 Iron presence

Screening of a different section of the unfiltered muscle from sample Ta20 identified a fibre-like structure (~25µm in length) lodged into the background

structure of the sample. Further analysis of this fibre-like structure found a high level of C, and medium levels of O and Fe. Although no EDX analysis of the background structure was performed, the presence of a fibre-like structure containing Fe in the fish muscle was unexpected. Iron oxide (Fe_3O_4) is a heavily used heat stabiliser additive in plastics, and also commonly used to achieve metallic finishes for aesthetic satisfaction (Sastri, 2014). High levels of Fe in fish have been found to damage fish gills (Hahladakis et al., 2018). We cannot be confident that this fibre was of microplastic origin. Future investigation to determine the source of origin is needed, as iron does not naturally occur in aquatic environments. Metallic pellets found, such as observed here, could indicate contaminants relating to mining and industrial activities (CIRDI, 2018).

4.8.4 Magnesium presence

Low levels of Mg were detected in many of the screened samples, including muscle and the GIT. Screening of the filtered muscle from sample Ta18 identified a large fibrous structure (>50µm in length), larger than the fibres observed in the filter paper. This large fibrous structure had external surface deposits rich in Ba (Figure 3.50F). However given the Ba content of the filter paper, it was inconclusive as to whether this Ba originated from the filter paper or through plastic adhesion. The large fibrous structure contained high levels of C, Cl and S, which supported the possibility of it being a plastic microfibre. A smaller elliptical structure, on the outside structure of the larger fibrous artefact, was also identified that was not seen on the ESEM greyscale image. It was characterised by the highest levels of K, Cl, Ca and Mg detected from all the structures screened. SEM screening can sometimes result in Al interference detected in samples, as this can come from the gas chamber used (Abbasi et al., 2018), and it can therefore be difficult to

decide the origin of Al. The presence of Mg may result from the use of active magnesium oxide which is a plastic reinforcer added to rubber compounds, with its main function being the neutralisation of HCl that can be released during processing and degrade the plastic material (NikoMag, 2021). Mg is an important mineral for muscle and nerve function but can be toxic when greater than natural environmental levels. Magnesium sulphate, dependent on Ca concentrations present, has been found to be toxic to aquatic environments (Luo et al., 2016). While the presence of Mg detected on artefacts in the fish was unexpected and could be of health concern, it still could not be concluded whether this chemical contamination has entered the fish muscle by microplastics as a transport vector or through another route.

While the presence of many of these detected elements (Cl, Cu, Zn, Ni, Ti, Fe, Mg) is not expected in the muscle and GIT of fish, it could not be conclusively determined if they had originated either from microplastics leaching common plastic additives, or from microplastics acting as a transport vector carrying chemicals into the fish body. Regardless, their presence provides evidence of the chemical risk posed by aquatic plastic debris, as some of these elements detected at high quantities can be toxic and/or have endocrine disrupting properties (Mato et al., 2001) (Koelmans et al., 2016b) (Turner and Filella, 2020b).

4.8.5 Essential elements in tilapia

Tilapia muscle for human consumption is known to provide several key essential elements, these include selenium (Se), Ca, Fe, Mg, K and Zn (Outa, Kowenje, et al., 2020). The results obtained in this study where higher levels of these elements were observed, may merely reflect what is already present in the fish muscle, and not be from microplastic contamination. However this would also have to be true

in the GIT samples, and as there were other elements identified such as Ti and Cr, it suggests that these elements were not from fish origin.

4.9 Microplastics toxicity risk to fish

The toxicity of microplastics in freshwater systems is not well studied. It is estimated that between 32% and 100% of freshwater invertebrates ingest microplastics (Watts et al., 2016). Ingestion depends on their abundance, shape, colour, smell and taste, which will be influenced by the microbial biofilm on the surface (GESAMP, 2016). Microplastics have been found in the GIT of commercially important fish for human consumption (Neto et al., 2020). Research on the interaction between the Nile tilapia and microplastics is still limited. One study confirmed microplastic presence in the GIT of Nile tilapia and Nile perch from the Tanzanian side of Lake Victoria (Biginagwa et al., 2016), but the presence of microplastics in the GIT of fish, does not provide direct evidence for human exposure risks, as this organ is not usually consumed. There is a concern however for the potential of translocation across the epithelium of the fish GIT into other organs or tissue parts consumed, as evidenced from the results of this study.

Laboratory studies have demonstrated plastic particle translocation in fish. Translocation of PS nanoparticles has been observed in the brain of Crucian carp, penetrating the blood brain barrier, causing behavioural disorders, effecting their hunting and eating behaviour (Mattsson et al., 2017), and in the liver of the commercial species of European anchovies (Collard et al., 2018). Within the limited research on freshwater fish, Japanese medaka *(Oryzias latipes)* exposed to PE microplastics were found to have induced hepatic stress, resulting in glycogen depletion and cell necrosis in the fish (Rochman et al., 2013). It has been argued that the likelihood of translocation in fish to be small, however

previously it was felt that there was a lack of analytical methods capable of characterising and quantifying the small-sized plastic particles (Wagner et al., 2017).

It is still not clear whether the harmful effects observed in fish from microplastic ingestion are the result of additives and contaminants that leach from the plastic particles into the fish, or from the physical impact of the plastic itself. Effects such as oxidative stress, inflammation and immunological responses have been observed after exposure to microplastics and attributed to their physical impact (GESAMP, 2016).

4.10 Microplastics toxicity risk to humans

Since fish and their products constitute an important food source, especially in developing countries, there is an urgent need to assess the potential risks to humans involved. Although microplastics and human health is an emerging field, existing fields indicate potential particle, microbial and chemical hazards. Ingested microplastics can accumulate and employ a localised toxicity by inducing an immune response (Wright and Kelly, 2017). Chemical toxicity could occur from the leaching of additives or contaminants absorbed from the surrounding polluted aquatic environment (Wright and Kelly, 2017).

With regards to existing research on the impacts of microplastics in humans, release of microplastics from the wear of prosthetic plastic implants has shown to have diverse internal effects, from DNA damage, necrosis, apoptosis, oxidative stress, inflammation and bone osteolysis (Lusher, Hollman, et al., 2017). Although there are no current studies related directly to the consumption of fish contaminated with microplastics or their contaminants, this is not surprising giving the complexity of this issue (Gallo et al., 2018). The FAO has reported that there

is a lack of basic toxicological data on the consumption of microplastics and also nanoplastics in humans as a food safety risk (Lusher, Hollman, et al., 2017). There is no data on the impact that the cooking and processing of fish and their products at high temperatures may have on the toxicity of microplastics. The European Food Safety Authority (EFSA) has estimated human exposure to microplastics following consumption of a portion of mussels (225g) to be 7µg of plastics (EFSA, 2016). On average 4% of the weight of microplastics are additives (Bouwmeester et al., 2015), suggesting that the mussels could contain about 0.28µg of additives (4% of 7µg of plastic). There is some concern on endocrine function disruption from the ingestion of additives such as phthalates and bisphenol A (Bouwmeester et al., 2015), however it has been concluded that this amount of ingestion of additives would be small and not cause harm in humans (Gallo et al., 2018).

Translocation across the human GIT epithelium is of concern, as this would imply internal organs and tissues were being exposed to these particles. Translocation in humans from the GIT into the lymphatic system of various types and sizes of microplastics has been found (Hussain et al., 2001). Major sites of entry were found to be M-cell rich Peyer's patch in the intestines and the portal vein, thus resulting in microplastics reaching the liver (Volkheimer, 1975). Phagocytosis and endocytosis of the microplastic particles in the intestinal epithelium has also been reported to occur (Yoo et al., 2011). There are no studies on the harmful effects of microplastics in humans. Of the small fraction that may enter the lymphatic system, most will probably be eliminated via the spleen. However, localised effects in the GIT might be possible, as the presence of microplastics' large surface area in the GIT lumen could interact with the GIT fluid present and result in large proteins adsorbing to the surface of the microplastics, this could cause local inflammation (Powell et al., 2007).

As the health concern from the leaching of chemicals adsorbed to the microplastics is of greater concern than the physical impact of the plastic particle in the human body, further research into leaching data and investigation into factors affecting the release of these compounds is needed.

4.11 Disease level of fish in Lake Victoria

In Kenya, there is a significant health risk to the people who are handling the fish. Men do the fishing, while the women will process and sell the fish, meaning they are at a higher risk of contamination. Fish are typically gutted on the floor of the beaches and surrounding shores of the lake, and then either cooked or directly sold by the women, usually on large tarpaulin sheets in the open sun (Wright and Kelly, 2017). Birds and stray animals, including dogs, can access the fish and potentially defecate and contaminate the product. The women have been encouraged to sell their fish off the ground in covered stalls, however the expense of building these stalls is often unaffordable and the advice is predominantly ignored.

In this study, there was a correlation between high levels of microplastics and key sites, suggesting that these are less preferable sites to farm fish in Lake Victoria. These included sites located next to Kisumu city, the mouth of the river Awach, in the main entrance/exit way to the main body of the lake and near high industrial and agricultural activities. When selecting a site for a fish farm, proximity to cities, industrial, agricultural and mining activities and away from rivers and their mouths should always be considered, given the potential for higher levels of pollutants, as described here form microplastics.

4.12 Importance of microplastic monitoring in aquatic systems

The staining methods used in this study were simple, cheap and easy to follow and could easily be reproduced in LMICs, such as Kenya, as a method of monitoring microplastic presence in their aquatic systems. A microscope is the only equipment needed for the screening, and the KMFRI at Lake Victoria have access to this equipment within their laboratories. Light microscopy enabled classification of the five microplastic types (fragment, foam, film, fibre and bead) and quantification of the particle sizes, which would facilitate regular screening for microplastic types in the waters and potentially determine microplastic pollution origins. For example, if there is a high amount of microfibres detected, this could be indicative of synthetic textile fibres entering the lake from washing machine runoff. By identifying the main types of microplastic pollutants, there is the potential to identify sources and consider mitigation strategies to reduce any further risk to both fish and human health.

As we found that microplastic prevalence was greater in the muscle of wild fish, than in the muscle from farmed fish, this could potentially mean that eating farmed fish, that are grown only for 4-5 months could result in less microplastics potentially being ingested by humans. It therefore could be safer for humans to consume younger farmed fish, and with the aquaculture sector in Kenya set to grow in forthcoming years, this finding favours this growth more.

Microplastic monitoring could also help fish farmers decide on sites to farm their fish. Areas could be assessed prior to aquaculture setup for pollution and microplastic levels, with those with the lowest pollution levels being the best location sites for the fish farms. For already established fish farm sites, microplastic pollution levels could still be monitored, as the fish farmers could rotate their caged areas within the site regularly, to ensure they are not farming

in the same location always, as over time this would result in a great increase of pollution build up. Given the potential for the actual fish cages to be a source of microplastic pollution, further work into the plastic used to make the cages may identify one more resistant to degradation.

4.13 Limitations

While over 80 tilapia were sampled for analysis in this study, they were predominantly from 2019, it would be interesting to analyse more recent samples from the same sites to determine if pollution levels have amplified, particularly given the increase in plastic waste from the COVID-19 pandemic. We were planning to return to Kenya to collect further samples as part of this study, however this was not possible as a result of the pandemic.

With only five GIT contents analysed in this study, and only one from a wild fish, this restricted comparisons between the two sample types. Furthermore, the GIT contents were prepared by squeezing them into separate bags. As microplastics are small, it is inevitable that some remained caught between the microvilli folds of the intestines and were therefore not extracted; these microplastics could potentially be causing more harm. It would be good to have done histopathological investigations of the GIT looking for the location of microplastics.

Some of the samples could not be analysed as there was too much undigested debris present, making the sample unreadable under the microscope. Shell pieces from bivalves are commonly found in the GIT of fish and these were found to be resistant to the digestion method used. Additionally scales and other strong structures such as bones may not be removed after acid digestion (Pearson et al., 2013). Further optimisation of the methodology is needed to ensure it can be successful for all samples. An extra step to separate such high density materials

from whole fish digestates could be incorporated before microscopic analysis. (Karami et al., 2017).

Diatoms were found on the macroplastic litter and fishing nets from Lake Victoria's waters and in some samples. It cannot be guaranteed that these diatoms were part of the plastisphere in these samples, particularly in the GITs where diatoms can be frequently found (Kamanyi, 1997). Potential contamination could have occurred during the processing of the fish samples whereby diatoms from the GIT samples could have contaminated the muscle samples.

Furthermore while we detected bacterial DNA from the macroplastic litter, net strands and in the tilapia samples, we cannot conclusively say whether the bacterial DNA originated from the plastisphere of the microplastic.

4.14 Future work

An extra step in the dissolving of the thicker and more debris filled GIT samples prior to filtration would prevent sample loss. Additionally, an extra step of flushing out the GIT during the sample preparation may ensure that the majority of the microplastics present in the GIT are recovered. However, the opening of the GIT may also allow the use of techniques such as histopathology to both visualise the location of the microplastics and determine if they cause changes in the GIT microstructure.

As only a small number of fish GIT contents samples were analysed for microplastic prevalence in this study, further work is needed to determine whether farmed fish may be better for human consumption than wild fish, and also consider which is best for the health of the fish.

Despite screening for numerous bacteria in the genomic DNA isolated, none that were looked for were detected. There are many common freshwater fish bacterial

species that were not tested for, such as *Vibrio*, *Salmonella* and *Shigella* (Schneeberger et al., 2019) (Onjong et al., 2018) (Journal and Hydrobiology, 2018), and these could be screened for in any future work. Equally with such low levels of DNA isolated, we could include an enrichment step by first incubating the microplastic in bacterial growth media, prior to DNA extraction.

Previous studies have used stains to highlight bacterial specific species during SEM screening (Priester et al., 2007) (Golding et al., 2016) (Bryant et al., 2016), and this is an approach which could be used in follow up work for this project. Metagenomic sequencing has also been used as a fast method to identify the range of species of bacteria present (Wright et al., 2020) (Yang et al., 2019) (Harrison et al., 2018b). Most studies focus on marine ecosystems, and there is a distinct lack of information concerning plastispheres assemblages within freshwater. By demonstrating an understanding of the repercussions associated with the microorganism-microplastic bond and carrying out more research into the ecological risks from antibiotic resistance genes in microbial communities on the aquatic plastisphere, this should highlight any critical threats for the future of aquatic ecosystems and also human health.

Finally further research into the possible effect that leaching of chemicals, that may be being transported by microplastics into organisms, could be having on the health of fish and also humans is critical, as these chemicals are of the most concern due to potential endocrine disruption that they may cause.

4.15 Conclusion

This study highlights the importance of monitoring microplastic prevalence in fish farmed or caught for human consumption and the monitoring of microplastic pollution in the aquatic environment. It specifically highlights the importance of

the monitoring of microplastics in Kenya, and other developing countries, to ensure a sustainable and safe food source of fish is available for future populations.

The FAO and WHO highlight that fish provides a cheap and easy source of protein and essential nutrients (FAO, 2020b) (WHO, 215AD), especially to those in LMICs, like Kenya. In many countries, there is no other affordable substitute for this high value food source, but its benefits could be negatively affected by the pollution from microplastics.

This study found 48% of the tilapia muscle samples and 100% of the GIT samples analysed to be contaminated with microplastics. The most identified microplastic type in the muscle samples was fibres, with the muscle of wild fish having a greater prevalence than farmed fish. The most identified type in the GIT samples was beads, with the GIT of farmed fish having a greater prevalence than wild fish. Fish sourced key sites were found to be the most contaminated with microplastics. With pollution levels at any one site across the lake being affected by proximity to river mouths, cities, industry and human activity, the consideration of pollutant levels into the choice of sites for new fish farms should be a key factor.

Potentially harmful elements were identified on the microplastics found in these fish, and there was an attempt to visualise the plastisphere, with future work needing to screen the specific species of bacteria on this plastisphere and the potential harm these could cause to fish and humans.

There is a spatial association between human activities and microplastic prevalence. To ensure a future for fish as a safe food source and valued commodity, it is essential that all countries monitor their levels of microplastic pollution in the environment and in the fish they catch or harvest. With the

growing global resilience of fish as a source of protein and with the ever-increasing mass of plastic pollution, research such as this could not be more timely.

5.0 References

Abbasi, S., Soltani, N., Keshavarzi, B., Moore, F., Turner, A. and Hassanaghaei, M. (2018), "Microplastics in different tissues of fish and prawn from the Musa Estuary, Persian Gulf", *Chemosphere*, Elsevier Ltd, Vol. 205, pp. 80–87.

AFP. (2020), "Kenya bans single-use plastics in protected areas", *Physorg*, available at: https://phys.org/news/2020-06-kenya-single-use-plastics-areas.html (accessed 19 March 2021).

Africa Population. (2021), "Africa Population 2021 (Demographics, Maps, Graphs)", *World Population Review*, available at: https://worldpopulationreview.com/continents/africa-population (accessed 22 February 2021).

AGMRC. (2018), "Aquaculture Fin Fish Species | Agricultural Marketing Resource Center", *Agricultural Marketing Resource Center*, available at: https://www.agmrc.org/commodities-products/aquaculture/aquaculture-fin-fish-species#Tilapia (accessed 11 February 2021).

Ahmed, N. (2009), *Development of Tilapia Marketing Systems in Bangladesh: Potential for Food Supply Final Report CF # 8/07 This Study Was Carried out with the Support of the National Food Policy Capacity Strengthening Programme*.

Alexandre, D., Anne-Laure, C., Laura, F., Ludovic, H., Charlotte, H., Emmanuel, R., Gilles, R., et al. (2016), "Microplastics in seafood: Benchmark protocol for their extraction and characterization", Vol. 215, pp. 223–233.

Amaral-Zettler, L.A., Zettler, E.R. and Mincer, T.J. (2020), "Ecology of the plastisphere", *Nature Reviews Microbiology*, Nature Research, 1 March.

Amoatey, P. and Baawain, M.S. (2019), "Effects of pollution on freshwater aquatic organisms", *Water Environment Research*, John Wiley and Sons Inc., Vol. 91 No. 10, pp. 1272–1287.

Andrady, A.L. (2011), "Microplastics in the marine environment", *Marine Pollution Bulletin*, August.

Animals Australia. (2019), "Plastic (not) fantastic: microbeads are poisoning our oceans | Animals Australia", *Australia, Animals*, available at: https://animalsaustralia.org/features/plastic-microbeads-poisoning-marine-life.php (accessed 19 November 2019).

Ardjosoediro, I. and Neven, D. (2008), "The Kenya Capture Fisheries Value Chain : an AMAP-FSKG Value Chain Finance Case", No. October, pp. 1–50.

Arthington, A.H., Dulvy, N.K., Gladstone, W. and Winfield, I.J. (2016), "Fish conservation in freshwater and marine realms: status, threats and management", *Aquatic Conservation: Marine and Freshwater Ecosystems*, John Wiley and Sons Ltd, Vol. 26 No. 5, pp. 838–857.

ASC. (2018), "ASC leads fight against plastic waste from aquaculture with planned requirements on proper disposal - Aquaculture Stewardship Council", available at: https://www.asc-aqua.org/news/latest-news/asc-leads-fight-against-plastic-waste-from-aquaculture-with-planned-requirements-on-proper-disposal/ (accessed 6 November 2019).

Azevedo-Santos, V.M., Brito, M.F.G., Manoel, P.S., Perroca, J.F., Rodrigues-Filho, J.L., Paschoal, L.R.P., Gonçalves, G.R.L., et al. (2021), "Plastic pollution: A focus on freshwater biodiversity", *Ambio*, Springer Science and Business Media B.V., available at:https://doi.org/10.1007/s13280-020-01496-5.

Baalkhuyur, F.M., Bin Dohaish, E.J.A., Elhalwagy, M.E.A., Alikunhi, N.M., AlSuwailem, A.M., Røstad, A., Coker, D.J., et al. (2018), "Microplastic in the gastrointestinal tract of fishes along the Saudi Arabian Red Sea coast", *Marine Pollution Bulletin*, Elsevier Ltd, Vol. 131, pp. 407–415.
Babayemi, J.O., Nnorom, I.C., Osibanjo, O. and Weber, R. (2019), "Ensuring sustainability in plastics use in Africa: consumption, waste generation, and projections", *Environmental Sciences Europe*, Springer Verlag, Vol. 31 No. 1, p. 60.
Bartley, D.M., De Graaf, G.J., Valbo-Jørgensen, J. and Marmulla, G. (2015), "Inland capture fisheries: status and data issues", *Fisheries Management and Ecology*, Blackwell Publishing Ltd, Vol. 22 No. 1, pp. 71–77.
Bashir, I., Lone, F.A., Bhat, R.A., Mir, S.A., Dar, Z.A. and Dar, S.A. (2020), "Concerns and threats of contamination on aquatic ecosystems", *Bioremediation and Biotechnology: Sustainable Approaches to Pollution Degradation*, Springer International Publishing, pp. 1–26.
Bellasi, A., Binda, G., Pozzi, A., Galafassi, S., Volta, P. and Bettinetti, R. (2020), "Microplastic contamination in freshwater environments: A review, focusing on interactions with sediments and benthic organisms", *Environments - MDPI*, MDPI AG, 1 April.
Bene, C. and Heck, S. (2004), "Fisheries and the Millennium Development Goals: Solutions for Africa".
Bidleman, T.F. (1984), "Estimation of Vapor Pressures for Nonpolar Organic Compounds by Capillary Gas Chromatography", *Analytical Chemistry*, Vol. 56 No. 13, pp. 2490–2496.
Biginagwa, F.J., Mayoma, B.S., Shashoua, Y., Syberg, K. and Khan, F.R. (2016), "First evidence of microplastics in the African Great Lakes: Recovery from Lake Victoria Nile perch and Nile tilapia", *Journal of Great Lakes Research*, International Association of Great Lakes Research, Vol. 42 No. 1, pp. 146–149.
Bilek, J.G., Kollonitsch, V. and Kline, C.H. (1966), "Zinc chemicals in plastics systems", *Industrial and Engineering Chemistry*, Vol. 58 No. 5, pp. 28–36.
Blair, R.M., Waldron, S., Phoenix, V.R. and Gauchotte-Lindsay, C. (2019), "Microscopy and elemental analysis characterisation of microplastics in sediment of a freshwater urban river in Scotland, UK", *Environmental Science and Pollution Research*, Springer Verlag, Vol. 26 No. 12, pp. 12491–12504.
Blewett, T.A. and Leonard, E.M. (2017), "Mechanisms of nickel toxicity to fish and invertebrates in marine and estuarine waters", *Environmental Pollution*, Elsevier Ltd, 1 April.
Botterell, Z.L.R., Beaumont, N., Dorrington, T., Steinke, M., Thompson, R.C. and Lindeque, P.K. (2019), "Bioavailability and effects of microplastics on marine zooplankton: A review", *Environmental Pollution*, Elsevier Ltd, 1 February.
Bouwmeester, H., Hollman, P.C.H. and Peters, R.J.B. (2015), "Potential Health Impact of Environmentally Released Micro- and Nanoplastics in the Human Food Production Chain: Experiences from Nanotoxicology", *Environmental Science and Technology*, American Chemical Society, 4 August.
Bracenet. (2020), "5 Facts you should know about Ghost Nets : Bracenet", *Bracenet*, available at: https://bracenet.net/en/blog/5-facts-you-should-know-about-ghost-nets/ (accessed 7 April 2021).
Bråte, I.L.N., Huwer, B., Thomas, K. V, Eidsvoll, D.P., Halsband, C., Almroth, B.C. and Lusher, A. (2017), *Micro-and Macro-Plastics in Marine Species from Nordic Waters*, *TemaNord*, available at:https://doi.org/10.6027/tn2017-549.

Brennecke, D., Duarte, B., Paiva, F., Caçador, I. and Canning-Clode, J. (2016), "Microplastics as vector for heavy metal contamination from the marine environment", *Estuarine, Coastal and Shelf Science*, Academic Press, Vol. 178, pp. 189–195.
Britannica. (2019a), "Plastic - The polymers | Britannica", available at: https://www.britannica.com/science/plastic/The-polymers#ref82466 (accessed 17 February 2021).
Britannica, T.E. of E. (2019b), "Lake Victoria | Size, Map, Countries, & Facts | Britannica.com", available at: https://www.britannica.com/place/Lake-Victoria (accessed 8 October 2019).
Browne, M.A., Niven, S.J., Galloway, T.S., Rowland, S.J. and Thompson, R.C. (2013), "Microplastic moves pollutants and additives to worms, reducing functions linked to health and biodiversity", *Current Biology*, Vol. 23 No. 23, pp. 2388–2392.
Brummett, R.E., Lazard, J. and Moehl, J. (2008), "African aquaculture: Realizing the potential", *Food Policy*, October.
Bryant, J.A., Clemente, T.M., Viviani, D.A., Fong, A.A., Thomas, K.A., Kemp, P., Karl, D.M., et al. (2016), "Diversity and Activity of Communities Inhabiting Plastic Debris in the North Pacific Gyre", *MSystems*, American Society for Microbiology, Vol. 1 No. 3, available at:https://doi.org/10.1128/msystems.00024-16.
Cai, W. and Arias, C.R. (2017), "Biofilm formation on aquaculture substrates by selected bacterial fish pathogens", *Journal of Aquatic Animal Health*, Taylor and Francis Inc., Vol. 29 No. 2, pp. 95–104.
Calich, H. (2014), "Global population growth, wild fish stocks, and the future of aquaculture – Shark Research & Conservation Program (SRC) | University of Miami", *Shark Research* , available at: https://sharkresearch.rsmas.miami.edu/global-population-growth-wild-fish-stocks-and-the-future-of-aquaculture/ (accessed 1 March 2021).
Campanale, C., Massarelli, C., Savino, I., Locaputo, V. and Uricchio, V.F. (2020), "A detailed review study on potential effects of microplastics and additives of concern on human health", *International Journal of Environmental Research and Public Health*, MDPI AG, 2 February.
Carson, H.S., Nerheim, M.S., Carroll, K.A. and Eriksen, M. (2013), "The plastic-associated microorganisms of the North Pacific Gyre", *Marine Pollution Bulletin*, Vol. 75 No. 1–2, pp. 126–132.
Chae, Y. and An, Y.J. (2018), "Current research trends on plastic pollution and ecological impacts on the soil ecosystem: A review", *Environmental Pollution*, Elsevier Ltd, 1 September.
Chakravorty, S., Helb, D., Burday, M., Connell, N. and Alland, D. (2007), "A detailed analysis of 16S ribosomal RNA gene segments for the diagnosis of pathogenic bacteria", *Journal of Microbiological Methods*, NIH Public Access, Vol. 69 No. 2, pp. 330–339.
Chen, J. and Griffiths, M.W. (1998), "PCR differentiation of Escherichia coli from other Gram-negative bacteria using primers derived from the nucleotide sequences flanking the gene encoding the universal stress protein", *Letters in Applied Microbiology*, Blackwell Publishing Ltd., Vol. 27 No. 6, pp. 369–371.
Cho, S. and Choi, W. (2001), "Solid-phase photocatalytic degradation of PVC-TiO2 polymer composites", *Journal of Photochemistry and Photobiology A: Chemistry*, Elsevier, Vol. 143 No. 2–3, pp. 221–228.
CIRDI. (2018), "Artisanal and Small-Scale Mining in Migori, Kenya | CIRDI -

Canadian International Resource and Development Institute", *CIRDI*, available at: https://cirdi.ca/resource/video-artisanal-and-small-scale-mining-in-migori-kenya/ (accessed 10 March 2021).
Clean&Clear. (2017), "Microbeads Commitment & The Environment | Clean & Clear", *Clean & Clear*, available at: https://www.cleanandclear.co.uk/microbead-commitment (accessed 4 March 2021).
Clear, C.&. (2017), "Microbeads Commitment & The Environment | Clean & Clear", available at: https://www.cleanandclear.co.uk/microbead-commitment (accessed 15 November 2019).
Collard, F., Gasperi, J., Gilbert, B., Eppe, G., Azimi, S., Rocher, V. and Tassin, B. (2018), "Anthropogenic particles in the stomach contents and liver of the freshwater fish Squalius cephalus", *Science of the Total Environment*, Elsevier B.V., Vol. 643, pp. 1257–1264.
Condor Ferries Ltd. (2020), "100+ Plastic in the Ocean Statistics & Facts (2020)", *Condor Ferries*, available at: https://www.condorferries.co.uk/plastic-in-the-ocean-statistics (accessed 5 April 2021).
Congestri, R. and Albertano, P. (2011), "Benthic Diatoms in Biofilm Culture", Springer, Dordrecht, pp. 227–243.
Consultancy.uk. (2019), "Land-origin plastic costs economy $19 billion every year", available at: https://www.consultancy.uk/news/23051/land-origin-plastic-costs-economy-19-billion-every-year (accessed 22 February 2021).
Coppock, R.L., Cole, M., Lindeque, P.K., Queirós, A.M. and Galloway, T.S. (2017), "A small-scale, portable method for extracting microplastics from marine sediments", *Environmental Pollution*, Elsevier Ltd, Vol. 230, pp. 829–837.
CORDIS. (2019), "Making fish farming in eastern Africa's Lake Victoria sustainable", *Phys.Org*, available at: https://phys.org/news/2019-07-fish-farming-eastern-africa-lake.html (accessed 8 October 2019).
Cosier, S. (2018), "Plastic: What Gets Thrown in the Great Lakes, Stays in the Great Lakes | NRDC", *NRDC*, available at: https://www.nrdc.org/stories/plastic-what-gets-thrown-great-lakes-stays-great-lakes (accessed 1 March 2021).
Czigany, T. and Ronkay, F. (2020), "The coronavirus and plastics", *Express Polymer Letters*, Vol. 14 No. 6, pp. 510–511.
David, O.M., Wandili, S., Kakai, R. and Waindi, E.N. (2009), "Isolation of Salmonella and Shigella from fish harvested from the Winam Gulf of Lake Victoria, Kenya", *Journal of Infection in Developing Countries*, Journal of Infection in Developing Countries, Vol. 3 No. 2, pp. 99–104.
Deloitte. (2019), *The Price Tag of Plastic Pollution An Economic Assessment of River Plastic*, *Deloitte*, available at: https://www2.deloitte.com/content/dam/Deloitte/nl/Documents/strategy-analytics-and-ma/deloitte-nl-strategy-analytics-and-ma-the-price-tag-of-plastic-pollution.pdf (accessed 22 February 2021).
Designing Building Wiki. (2020), "Designing Buildings Wiki", *Energy Efficiency of Building*, pp. 8–11.
Ding, J., Zhang, S., Razanajatovo, R.M., Zou, H. and Zhu, W. (2018), "Accumulation, tissue distribution, and biochemical effects of polystyrene microplastics in the freshwater fish red tilapia (Oreochromis niloticus)", *Environmental Pollution*, Elsevier Ltd, Vol. 238, pp. 1–9.
Dubernet, S., Desmasures, N. and GuÃ©guen, M. (2002), "A PCR-based method

for identification of lactobacilli at the genus level", *FEMS Microbiology Letters*, Oxford University Press (OUP), Vol. 214 No. 2, pp. 271–275.
EFSA. (2016), "Presence of microplastics and nanoplastics in food, with particular focus on seafood", *EFSA Journal*, Vol. 14 No. 6, available at:https://doi.org/10.2903/j.efsa.2016.4501.
Elizabeth Cruz-Suarez, L., Guadalupe Nieto-López, M., Alonso Villarreal-Cavazos, D., Garcia, A., Elizabeth Cruz Suárez, L., Ricque Marie, D., Tapia Salazar, M., et al. (2006), *Tilapia Culture in Salt Water: Environmental Requirements, Nutritional Implications and Economic Potentials Production of Cold Tolerant Nile Tilapia View Project AQUACULTURE DEVELOPMENT IN THE NEAR EAST AND NORTH AFRICA View Project Tilapia Culture in Sal*, available at: https://www.researchgate.net/publication/228674236 (accessed 8 November 2019).
Enyedi, N.T., Makk, J., Kótai, L., Berényi, B., Klébert, S., Sebestyén, Z., Molnár, Z., et al. (2020), "Cave bacteria-induced amorphous calcium carbonate formation", *Scientific Reports*, Nature Research, Vol. 10 No. 1, pp. 1–12.
EPA. (2020), "Learn about Polychlorinated Biphenyls (PCBs), United States Environmental Protection Agency".
Ercolini, D., Russo, F., Blaiotta, G., Pepe, O., Mauriello, G. and Villani, F. (2007), "Simultaneous detection of Pseudomonas fragi, P. lundensis, and P. putida from meat by use of a multiplex PCR assay targeting the carA gene", *Applied and Environmental Microbiology*, Appl Environ Microbiol, Vol. 73 No. 7, pp. 2354–2359.
Eriksen, M., Lebreton, L.C.M., Carson, H.S., Thiel, M., Moore, C.J., Borerro, J.C., Galgani, F., et al. (2014), "Plastic Pollution in the World's Oceans: More than 5 Trillion Plastic Pieces Weighing over 250,000 Tons Afloat at Sea", *PLoS ONE*, Public Library of Science, Vol. 9 No. 12, available at:https://doi.org/10.1371/journal.pone.0111913.
Facts, A. (2019), "LAKE VICTORIA - over 15 interesting key facts", *Africa Facts*, available at: https://interesting-africa-facts.com/Africa-Landforms/Lake-Victoria-Facts.html (accessed 8 October 2019).
FAO. (2010), "FAO Fisheries & Aquaculture - Cultured Aquatic Species Information Programme - Oreochromis niloticus (Linnaeus, 1758)", *Http://Www.Fao.Org/Fishery/Culturedspecies/Oreochromis_niloticus/En#tcNA008C*, available at: http://www.fao.org/fishery/culturedspecies/Oreochromis_niloticus/en (accessed 17 February 2021).
FAO. (2015), "FAO Fisheries & Aquaculture - Fishery and Aquaculture Country Profiles - The Republic of Kenya", available at: http://www.fao.org/fishery/facp/KEN/en (accessed 8 November 2019).
FAO. (2018a), *Sustainable Food Systems Concept and Framework WHAT IS A SUSTAINABLE FOOD SYSTEM? WHY TAKE A FOOD SYSTEMS APPROACH? CHANGING FOOD SYSTEMS*, available at: http://www.fao.org/3/ca2079en/CA2079EN.pdf (accessed 8 February 2021).
FAO. (2018b), *WORLD FISHERIES AND AQUACULTURE*, available at: www.fao.org/publications (accessed 25 February 2021).
FAO. (2020a), "Aquaculture | FAO | Food and Agriculture Organization of the United Nations", available at: http://www.fao.org/aquaculture/en/ (accessed 5 November 2019).
FAO. (2020b), *The State of World Fisheries and Aquaculture 2020*, *The State of World Fisheries and Aquaculture 2020*, FAO, available at:https://doi.org/10.4060/ca9229en.

FAO. (2020c), *Aquaculture Growth Potential in Africa: WAPI Factsheet to Facilitate Evidence-Based Policy-Making and Sector Management in Aquaculture*.
FAO. (2021), "AQUACULTURE IN AFRICA", *FAO*, available at: http://www.fao.org/3/x4545e/X4545e38.htm (accessed 13 January 2021).
Fisherproject. (2020), "The Global Fishing Industry", *Fisherproject*, available at: https://fisherproject.org/the-global-fishing-industry (accessed 25 February 2021).
Foekema, E.M., De Gruijter, C., Mergia, M.T., Van Franeker, J.A., Murk, A.J. and Koelmans, A.A. (2013), "Plastic in north sea fish", *Environmental Science and Technology*, Vol. 47 No. 15, pp. 8818–8824.
Fontanot, M., Iacumin, L., Cecchini, F., Comi, G. and Manzano, M. (2014), "PorA specific primers for the identification of Campylobacter species in food and clinical samples", *LWT - Food Science and Technology*, Academic Press, Vol. 58 No. 1, pp. 86–92.
Forrest, S.A., Bourdages, M.P.T. and Vermaire, J.C. (2020), "Microplastics in Freshwater Ecosystems", *Handbook of Microplastics in the Environment*, Springer International Publishing, pp. 1–19.
Gabriel, U.U. and Akinrotimi, O.A. (2007), "Locally produced fish feed: potentials for aquaculture development in subsaharan Africa", *African Journal of Agricultural Research*, Vol. 2 No. 7, pp. 287–295.
Galgani, F., Hanke, G. and Maes, T. (2015), "Global distribution, composition and abundance of marine litter", *Marine Anthropogenic Litter*, Springer International Publishing, pp. 29–56.
Gallo, F., Fossi, C., Weber, R., Santillo, D., Sousa, J., Ingram, I., Nadal, A., et al. (2018), "Marine litter plastics and microplastics and their toxic chemicals components: the need for urgent preventive measures", *Environmental Sciences Europe*, available at:https://doi.org/10.1186/s12302-018-0139-z.
Garcia, S.M. and Rosenberg, A.A. (2010), "Food security and marine capture fisheries: Characteristics, trends, drivers and future perspectives", *Philosophical Transactions of the Royal Society B: Biological Sciences*, Royal Society, 27 September.
Genkal, S.I. and Popovskaya, G.I. (1991), "New data on the frustule morphology of aulacosira islandica (bacillariophyta)", *Diatom Research*, Vol. 6 No. 2, pp. 255–266.
Geographic, N. (2019), "The World's Plastic Pollution Crisis Explained", available at: https://www.nationalgeographic.com/environment/habitats/plastic-pollution/ (accessed 7 October 2019).
GESAMP. (2016), "SOURCES, FATE AND EFFECTS OF MICROPLASTICS IN THE MARINE ENVIRONMENT: PART 2 OF A GLOBAL ASSESSMENT Science for Sustainable Oceans", *GESAMP*, available at: www.imo.org (accessed 21 November 2019).
Godwin, A. (2000), "Plasticizer - an overview | ScienceDirect Topics", *Applied Polymer Science: 21st Centuary*, available at: https://www.sciencedirect.com/topics/chemistry/plasticizer (accessed 18 February 2021).
Golding, C.G., Lamboo, L.L., Beniac, D.R. and Booth, T.F. (2016), "The scanning electron microscope in microbiology and diagnosis of infectious disease", *Scientific Reports*, Nature Publishing Group, Vol. 6 No. 1, pp. 1–8.
Gove, M. (2018), "World leading microbeads ban comes into force - GOV.UK", *GOV.UK*, available at: https://www.gov.uk/government/news/world-leading-microbeads-ban-comes-into-force (accessed 17 February 2021).

Graham Readfearn. (2018), "WHO launches health review after microplastics found in 90% of bottled water", *The Guardian*, pp. 1–4.
Grbic, J., Nguyen, B., Guo, E., You, J.B., Sinton, D. and Rochman, C.M. (2019), "Magnetic Extraction of Microplastics from Environmental Samples", *Environmental Science and Technology Letters*, Vol. 6 No. 2, pp. 68–72.
Gündoğdu, S., Eroldoğan, O.T., Evliyaoğlu, E., Turchini, G.M. and Wu, X.G. (2021), "Fish out, plastic in: Global pattern of plastics in commercial fishmeal", *Aquaculture*, Elsevier B.V., Vol. 534, p. 736316.
Güven, O., Gökdağ, K., Jovanović, B. and Kıdeyş, A.E. (2017), "Microplastic litter composition of the Turkish territorial waters of the Mediterranean Sea, and its occurrence in the gastrointestinal tract of fish", *Environmental Pollution*, Vol. 223, pp. 286–294.
Hahladakis, J.N., Velis, C.A., Weber, R., Iacovidou, E. and Purnell, P. (2018), "An overview of chemical additives present in plastics: Migration, release, fate and environmental impact during their use, disposal and recycling", *Journal of Hazardous Materials*, Elsevier B.V., 15 February.
Haines, B. (2019), "18 Amazing Facts About Lake Victoria, Uganda: Location, Cichlids, Map, Size, Islands | Uganda365", *Uganda365*, available at: https://uganda365.com/facts-about-lake-victoria/ (accessed 8 October 2019).
Handy, R.D., Owen, R. and Valsami-Jones, E. (2008), "The ecotoxicology of nanoparticles and nanomaterials: Current status, knowledge gaps, challenges, and future needs", *Ecotoxicology*, Ecotoxicology, July.
Hantoro, I., Löhr, A.J., Van Belleghem, F.G.A.J., Widianarko, B. and Ragas, A.M.J. (2019), "Microplastics in coastal areas and seafood: implications for food safety", *Food Additives and Contaminants - Part A Chemistry, Analysis, Control, Exposure and Risk Assessment*, Taylor and Francis Ltd., Vol. 36 No. 5, pp. 674–711.
Hardesty, B.D., Good, T.P. and Wilcox, C. (2015), "Novel methods, new results and science-based solutions to tackle marine debris impacts on wildlife", *Ocean and Coastal Management*, Elsevier Ltd, Vol. 115, pp. 4–9.
Harrison, J.P., Hoellein, T.J., Sapp, M., Tagg, A.S., Ju-Nam, Y. and Ojeda, J.J. (2018a), "Microplastic-associated biofilms: A comparison of freshwater and marine environments", *Handbook of Environmental Chemistry*, Vol. 58, Springer Verlag, pp. 181–201.
Harrison, J.P., Hoellein, T.J., Sapp, M., Tagg, A.S., Ju-Nam, Y. and Ojeda, J.J. (2018b), "Microplastic-associated biofilms: A comparison of freshwater and marine environments", *Handbook of Environmental Chemistry*, Vol. 58, Springer Verlag, pp. 181–201.
Heijnen, L. and Medema, G. (2006), "Quantitative detection of E. coli, E. coli O157 and other shiga toxin producing E. coli in water samples using a culture method combined with real-time PCR", *Journal of Water and Health*, IWA Publishing, Vol. 4 No. 4, pp. 487–498.
Heilbronn, J., Wilson, J. and Berger, B.J. (1999), "Tyrosine aminotransferase catalyzes the final step of methionine recycling in Klebsiella pneumoniae", *Journal of Bacteriology*, American Society for Microbiology, Vol. 181 No. 6, pp. 1739–1747.
Henry, B., Laitala, K. and Klepp, I.G. (2019), "Microfibres from apparel and home textiles: Prospects for including microplastics in environmental sustainability assessment", *Science of the Total Environment*, Elsevier B.V., Vol. 652, pp. 483–494.
Hidalgo-Ruz, V., Gutow, L., Thompson, R.C. and Thiel, M. (2012), "Microplastics

in the marine environment: A review of the methods used for identification and quantification", *Environmental Science and Technology*, Vol. 46 No. 6, pp. 3060–3075.
Holmyard, N. (2019), "Plastic pollution from aquaculture less than that from fishing", *SeafoodSource*, 10 December.
Hu, L., Chernick, M., Lewis, A.M., Lee Ferguson, P. and Hinton, D.E. (2020), "Chronic microfiber exposure in adult Japanese medaka (Oryzias latipes)", *PLoS ONE*, Public Library of Science, Vol. 15 No. 3, available at:https://doi.org/10.1371/journal.pone.0229962.
Hussain, M.G., Barman, B.K., Karim, M. and Keus, E.H.J. (2013), "Progress and the Future for Tilapia Farming and Seed Production in Bangladesh", WorldFish, available at: https://thefishsite.com/articles/green-crabs-coming-to-maryland (accessed 17 February 2021).
Hussain, N., Jaitley, V. and Florence, A.T. (2001), "Recent advances in the understanding of uptake of microparticulates across the gastrointestinal lymphatics", *Advanced Drug Delivery Reviews*, Elsevier, 23 August.
Hwang, J., Choi, D., Han, S., Jung, S.Y., Choi, J. and Hong, J. (2020), "Potential toxicity of polystyrene microplastic particles", *Scientific Reports*, Nature Research, Vol. 10 No. 1, pp. 1–12.
IUCN. (2018), *IUCN (International Union for Conservation of Nature)*.
Iwasaki, S., Isobe, A., Kako, S., Uchida, K. and Tokai, T. (2017), "Fate of microplastics and mesoplastics carried by surface currents and wind waves: A numerical model approach in the Sea of Japan", *Marine Pollution Bulletin*, Elsevier Ltd, Vol. 121 No. 1–2, pp. 85–96.
Jambeck, J.R., Geyer, R., Wilcox, C., Siegler, T.R., Perryman, M., Andrady, A., Narayan, R., et al. (2015), "Plastic waste inputs from land into the ocean", *Science*, American Association for the Advancement of Science, Vol. 347 No. 6223, pp. 768–771.
Jenke, D.R., Story, J. and Lalani, R. (2006), "Extractables/leachables from plastic tubing used in product manufacturing", *International Journal of Pharmaceutics*, Elsevier, Vol. 315 No. 1–2, pp. 75–92.
Jennies Foods. (2021), "Tilapia Fish - Jenniesfoods", *Jennies Cash & Carry*, available at: https://jenniesfoods.co.uk/product/tilapia-fish/ (accessed 17 February 2021).
Joon Shim, W., Kyoung Song, Y., Hee Hong, S. and Jang, M. (2016), "Identification and quantification of microplastics using Nile Red staining", *MPB*, available at:https://doi.org/10.1016/j.marpolbul.2016.10.049.
Journal, A. and Hydrobiology, T. (2018), "Source Attribution of Salmonella and Escherichia coli Contaminating Lake Victoria fish in Kenya A", Vol. 47, pp. 39–47.
Jovanović, B., Gökdağ, K., Güven, O., Emre, Y., Whitley, E.M. and Kideys, A.E. (2018), "Virgin microplastics are not causing imminent harm to fish after dietary exposure", *Marine Pollution Bulletin*, Elsevier Ltd, Vol. 130, pp. 123–131.
Juma, D.W., Wang, H. and Li, F. (2014), "Impacts of population growth and economic development on water quality of a lake: Case study of Lake Victoria Kenya water", *Environmental Science and Pollution Research*, Springer Verlag, Vol. 21 No. 8, pp. 5737–5746.
Kamanyi, J. (1997), "Plankton identified in Stomach contents of Oreochromis nilotics (Pisces, CICHLIDAE) and the water system of Lakes Edward, George, and Kazinga channel - Uganda", *Fisheries Research Institute* , available at: http://aquaticcommons.org/20614/1/paper 7.pdf (accessed 9 April 2021).

Karami, A., Golieskardi, A., Choo, C.K., Romano, N., Ho, Y. Bin and Salamatinia, B. (2017), "A high-performance protocol for extraction of microplastics in fish", *Science of the Total Environment*, Elsevier B.V., Vol. 578, pp. 485–494.

Kateregga, E. and Sterner, T. (2009), "Lake victoria fish stocks and the effects of water hyacinth", *Journal of Environment and Development*, Vol. 18 No. 1, pp. 62–78.

Kelly, M.G., Trobajo, R., Rovira, L. and Mann, D.G. (2015), "Characterizing the niches of two very similar Nitzschia species and implications for ecological assessment", *Diatom Research*, Taylor and Francis Ltd., Vol. 30 No. 1, pp. 27–33.

Khan, F.R., Mayoma, B.S., Biginagwa, F.J. and Syberg, K. (2018), "Microplastics in Inland African waters: Presence, sources, and fate", *Handbook of Environmental Chemistry*, Vol. 58, Springer Verlag, pp. 101–124.

Khan, F.R., Shashoua, Y., Crawford, A., Drury, A., Sheppard, K., Stewart, K. and Sculthorp, T. (2020), "'The plastic nile': First evidence of microplastic contamination in fish from the nile river (Cairo, Egypt)", *Toxics*, MDPI AG, Vol. 8 No. 2, available at:https://doi.org/10.3390/TOXICS8020022.

Kirstein, I.V., Wichels, A., Gullans, E., Krohne, G. and Gerdts, G. (2019), "The plastisphere – Uncovering tightly attached plastic 'specific' microorganisms", *PLoS ONE*, Vol. 14 No. 4, available at:https://doi.org/10.1371/journal.pone.0215859.

KMFRI. (2018), "Kenya Marine and Fisheries Research Institute - Sagana Aquaculture Centre", available at: https://www.kmfri.co.ke/index.php/about-us/research-centres/sagana-aquaculture-centre (accessed 16 February 2021).

KMFRI. (2020), "Kenya Marine and Fisheries Research Institute - About us", available at: https://www.kmfri.co.ke/index.php/about-us (accessed 13 January 2021).

KNBS. (2019), *2019 Kenya Population and Housing Census Volume 1: Population by County and Sub-County*, *2019 Kenya Population and Housing Census*, Vol. I, available at: http://dc.sourceafrica.net/documents/119746-2019-Kenya-Population-and-Housing-Census-Volume.html (accessed 7 April 2021).

Koelmans, A.A., Bakir, A., Burton, G.A. and Janssen, C.R. (2016a), "Microplastic as a Vector for Chemicals in the Aquatic Environment: Critical Review and Model-Supported Reinterpretation of Empirical Studies", *Environmental Science and Technology*.

Koelmans, A.A., Bakir, A., Burton, G.A. and Janssen, C.R. (2016b), "Microplastic as a Vector for Chemicals in the Aquatic Environment: Critical Review and Model-Supported Reinterpretation of Empirical Studies", *Environmental Science and Technology*.

Koelmans, A.A., Besseling, E. and Foekema, E.M. (2014), "Leaching of plastic additives to marine organisms", *Environmental Pollution*, Elsevier, Vol. 187, pp. 49–54.

Koester, V. (2015), "Plasticizers – Benefits, Trends, Health, and Environmental Issues", *ChemViews*, Wiley-Blackwell, available at:https://doi.org/10.1002/chemv.201500028.

Konikoff, M. (2017), *Introduction to the General Principles of Aquaculture - 1st Edition -*, *CRC Press*, available at: https://www.routledge.com/Introduction-to-the-General-Principles-of-Aquaculture/Ackefors-Huner-Konikoff/p/book/9780367401979 (accessed 11 January 2021).

Kundu, R., Aura, C.M., Nyamweya, C., Agembe, S., Sitoki, L., Lung'ayia, H.B.O., Ongore, C., et al. (2017), "Changes in pollution indicators in Lake Victoria, Kenya and their implications for lake and catchment management", *Lakes & Reservoirs: Research & Management*, Blackwell Publishing, Vol. 22 No. 3, pp. 199–214.
Lalah, J.O., Ochieng, E.Z. and Wandiga, S.O. (2008), "Sources of heavy metal input into Winam Gulf, Kenya", *Bulletin of Environmental Contamination and Toxicology*, Pb, Vol. 81 No. 3, pp. 277–284.
LBDA. (2019), "Background – LBDA", available at: https://lbda.go.ke/?page_id=1815 (accessed 16 February 2021).
Leah, R.T. (2005), "The Biology of Lake Victoria", *University of Liverpool*.
Leigh, J.A., Egan, S.A., Ward, P.N., Field, T.R. and Coffey, T.J. (2010), "Sortase anchored proteins of Streptococcus uberis play major roles in the pathogenesis of bovine mastitis in dairy cattle", *Veterinary Research*, Vet Res, Vol. 41 No. 5, available at:https://doi.org/10.1051/vetres/2010036.
Levin, P.A. and Angert, E.R. (2015), "Small but mighty: Cell size and bacteria", *Cold Spring Harbor Perspectives in Biology*, Cold Spring Harbor Laboratory Press, Vol. 7 No. 7, pp. 1–11.
LifeWithoutPlastic. (2020), "Silicone", *LifeWithoutPlastic*, available at: https://lifewithoutplastic.com/silicone/ (accessed 8 April 2021).
Linton, D., Lawson, A.J., Owen, R.J. and Stanley, J. (1997), *PCR Detection, Identification to Species Level, and Fingerprinting of Campylobacter Jejuni and Campylobacter Coli Direct from Diarrheic Samples*, *JOURNAL OF CLINICAL MICROBIOLOGY*, Vol. 35, available at: http://jcm.asm.org/ (accessed 31 March 2021).
Luo, S., Wu, B., Xiong, X. and Wang, J. (2016), "Effects of total hardness and calcium:magnesium ratio of water during early stages of rare minnows (Gobiocypris rarus)", *Comparative Medicine*, American Association for Laboratory Animal Science, Vol. 66 No. 3, pp. 181–187.
Lusher, A., Hollman, P. and Mendozal, J. (2017), *Microplastics in Fisheries and Aquaculture: Status of Knowledge on Their Occurrence and Implications for Aquatic Organisms and Food Safety*, *FAO Fisheries and Aquaculture Technical Paper 615*, available at:https://doi.org/978-92-5-109882-0.
Lusher, A.L., Welden, N.A., Sobral, P. and Cole, M. (2017), "Sampling, isolating and identifying microplastics ingested by fish and invertebrates", *Analytical Methods*, Royal Society of Chemistry, 7 March.
Maes, T., Jessop, R., Wellner, N., Haupt, K. and Mayes, A.G. (2017), "A rapid-screening approach to detect and quantify microplastics based on fluorescent tagging with Nile Red", *Scientific Reports*, Nature Publishing Group, Vol. 7, available at:https://doi.org/10.1038/srep44501.
Marine Conservation Society. (2019), "Microplastics | Marine Conservation Society", available at: https://www.mcsuk.org/clean-seas/microplastics (accessed 1 October 2019).
Martin, J. (2018), "Tourists' plastic waste ruining idyllic holiday spots | Stuff.co.nz", *Stuff*, available at: https://www.stuff.co.nz/travel/news/102773606/life-in-plastic-not-fantastic (accessed 8 November 2019).
Mato, Y., Isobe, T., Takada, H., Kanehiro, H., Ohtake, C. and Kaminuma, T. (2001), "Plastic resin pellets as a transport medium for toxic chemicals in the marine environment", *Environmental Science and Technology*, ACS, Vol. 35 No. 2, pp. 318–324.
Mattsson, K., Johnson, E. V., Malmendal, A., Linse, S., Hansson, L.A. and

Cedervall, T. (2017), "Brain damage and behavioural disorders in fish induced by plastic nanoparticles delivered through the food chain", *Scientific Reports*, Nature Publishing Group, Vol. 7 No. 1, pp. 1–7.
Matxinandiarena, E., Múgica, A., Zubitur, M., Yus, C., Sebastián, V., Irusta, S., Loaeza, A.D., et al. (2019), "The effect of titanium dioxide surface modification on the dispersion, morphology, and mechanical properties of recycled PP/PET/TiO2 PBNANOs", *Polymers*, Vol. 11 No. 10, available at:https://doi.org/10.3390/polym11101692.
Mayes, A.G. (2018), *Rapid Detection of Microplastics Using Fluorescent Tagging*.
McCarthy, N. (2020), "• Chart: Almost Half of World Fish Supply Now Comes From Aquaculture | Statista", *Statista*, available at: https://www.statista.com/chart/2280/the-global-fish-farming-industry-is-booming/ (accessed 26 February 2021).
McGrath, M. (2018), "Plastic microbead ban: What impact will it have? - BBC News", *BBC News*, available at: https://www.bbc.co.uk/news/science-environment-42621388 (accessed 18 November 2019).
McKeen, L. (2019), "Stabilizer (Agent) - an overview | ScienceDirect Topics", *The Effect of UV Light and Weather on Plastics and Elastomers (Fourth Edition)*, available at: https://www.sciencedirect.com/topics/materials-science/stabilizer-agent (accessed 18 February 2021).
Merrington, A. (2015), "New study reveals the global impact of debris on marine life - University of Plymouth", *University of Plymouth*, available at: https://www.plymouth.ac.uk/news/new-study-reveals-the-global-impact-of-debris-on-marine-life (accessed 23 October 2019).
Michael, W. (2015), "Climate Change Shrinking Uganda's Lakes and Fish | Inter Press Service", *IPS*, available at: http://www.ipsnews.net/2015/08/climate-change-shrinking-ugandas-lakes-and-fish/ (accessed 4 March 2021).
Mitchell, C.J., Palumbo-Roe, B. and Bide, T. (2020), "Artisanal & small-scale gold mining research field work, Migori County, Kenya", British Geological Survey.
Mogoathle, L. (2019), "How Companies Are Turning the Tide of Plastic Pollution in Kenya", *Global Cititzen*, available at: https://www.globalcitizen.org/en/content/coca-cola-fighting-plastic-pollution-in-kenya/ (accessed 22 February 2021).
Moore, G. (2019), "Study finds salmon fillets free from microplastics - FishFarmingExpert.com", *Fish Farming Expert*, available at: https://www.fishfarmingexpert.com/article/more-microplastic-found-in-wild-salmon-than-farmed/ (accessed 19 November 2019).
Mosely, T. and McMahon, S. (2020), "COVID-19 Pandemic Has Led To More Ocean Plastic Pollution | Here & Now", *Wbur*.
Mraz, S. (2015), "Mineral Fillers Improve Plastics | Machine Design", *MachineDesign*, available at: https://www.machinedesign.com/materials/article/21834429/mineral-fillers-improve-plastics (accessed 19 March 2021).
Munguti, J.M., Kim, J.-D. and Ogello, E.O. (2014), "An Overview of Kenyan Aquaculture: Current Status, Challenges, and Opportunities for Future Development", *Fisheries and Aquatic Sciences*, Vol. 17 No. 1, pp. 1–11.
Mwamburi, J. (2019), "Lake Sedimentary Environments and Roles of Accumulating Organic Matter in Biogeochemical Cycling Processes and Contaminants Loading Are Invasions of Water Hyacinth in Lake Victoria from 1989 a Concern?", *Persistent Organic Pollutants*, IntechOpen, available at:https://doi.org/10.5772/intechopen.79395.

Naqash, N., Prakash, S., Kapoor, D. and Singh, R. (2020), "Interaction of freshwater microplastics with biota and heavy metals: a review", *Environmental Chemistry Letters*, Springer Science and Business Media Deutschland GmbH, 1 November.
Nations, U. (2017), *Fishery Exports and the Economic Developement of Least Developed Countries: Bangladesh, Cambodia, The Comoros, Mozambique, Myanmar and Uganda*.
Nelms, S.E., Duncan, E.M., Patel, S., Badola, R., Bhola, S., Chakma, S., Chowdhury, G.W., et al. (2021), "Riverine plastic pollution from fisheries: Insights from the Ganges River system", *Science of the Total Environment*, Elsevier B.V., Vol. 756, p. 143305.
Nerín, C., Tornés, A.R., Domeño, C. and Cacho, J. (1996), "Absorption of Pesticides on Plastic Films Used as Agricultural Soil Covers", *Journal of Agricultural and Food Chemistry*, Vol. 44 No. 12, pp. 4009–4014.
Neto, J.G.B., Rodrigues, F.L., Ortega, I., Rodrigues, L. dos S., Lacerda, A.L. d. F., Coletto, J.L., Kessler, F., et al. (2020), "Ingestion of plastic debris by commercially important marine fish in southeast-south Brazil", *Environmental Pollution*, Elsevier Ltd, Vol. 267, p. 115508.
Neves, D., Sobral, P., Ferreira, J.L. and Pereira, T. (2015), "Ingestion of microplastics by commercial fish off the Portuguese coast", *Marine Pollution Bulletin*, Elsevier Ltd, Vol. 101 No. 1, pp. 119–126.
Ngure, V., Davies, T., Kinuthia, G., Sitati, N., Shisia, S. and Oyoo-Okoth, E. (2014), "Concentration levels of potentially harmful elements from gold mining in Lake Victoria Region, Kenya: Environmental and health implications", *Journal of Geochemical Exploration*, Elsevier B.V., Vol. 144 No. PC, pp. 511–516.
NikoMag. (2021), "Rubber and Plastics - NikoMag", *NikoMag*, available at: https://nikomag-europe.com/index.php/markets/rubber-and-plastics (accessed 18 March 2021).
Njiru, J., van der Knaap, M., Kundu, R. and Nyamweya, C. (2018), "Lake Victoria fisheries: Outlook and management", *Lakes & Reservoirs: Research & Management*, Blackwell Publishing, Vol. 23 No. 2, pp. 152–162.
Njiru, M., Kazungu, J., Ngugi, C.C., Gichuki, J. and Muhoozi, L. (2008), "An overview of the current status of Lake Victoria fishery: Opportunities, challenges and management strategies", *Lakes and Reservoirs: Research and Management*, March.
Njiru, M., Okeyo-Owuor, J.B., Muchiri, M. and Cowx, I.G. (2004a), "Shifts in the food of Nile tilapia, Oreochromis niloticus (L.) in Lake Victoria, Kenya", *African Journal of Ecology*, Vol. 42 No. 3, pp. 163–170.
Njiru, M., Okeyo-Owuor, J.B., Muchiri, M. and Cowx, I.G. (2004b), "Shifts in the food of Nile tilapia, Oreochromis niloticus (L.) in Lake Victoria, Kenya", *African Journal of Ecology*, Vol. 42 No. 3, pp. 163–170.
Nyamweya, C., Desjardins, C., Sigurdsson, S., Tomasson, T., Taabu-Munyaho, A., Sitoki, L. and Stefansson, G. (2016a), "Simulation of Lake Victoria circulation patterns using the regional ocean Modeling system (ROMS)", *PLoS ONE*, Public Library of Science, Vol. 11 No. 3, available at:https://doi.org/10.1371/journal.pone.0151272.
Nyamweya, C., Desjardins, C., Sigurdsson, S., Tomasson, T., Taabu-Munyaho, A., Sitoki, L. and Stefansson, G. (2016b), "Simulation of Lake Victoria Circulation Patterns Using the Regional Ocean Modeling System (ROMS)", edited by Xie, S.-P.*PLOS ONE*, Vol. 11 No. 3, p. e0151272.
O'Sullivan, A. and Sheffrin, S.M. (2003), *Economics : Principles in Action*,

Prentice Hall, Needham Mass., available at: https://www.worldcat.org/title/economics-principles-in-action/oclc/50237774 (accessed 11 January 2021).
Obbard, R.W., Sadri, S., Wong, Y.Q., Khitun, A.A., Baker, I. and Thompson, R.C. (2014), "Global warming releases microplastic legacy frozen in Arctic Sea ice", *Earth's Future*, American Geophysical Union (AGU), Vol. 2 No. 6, pp. 315–320.
Oberbeckmann, S., Loeder, M.G.J., Gerdts, G. and Osborn, M.A. (2014), "Spatial and seasonal variation in diversity and structure of microbial biofilms on marine plastics in Northern European waters", *FEMS Microbiology Ecology*, Oxford University Press, Vol. 90 No. 2, pp. 478–492.
Oberbeckmann, S., Osborn, A.M. and Duhaime, M.B. (2016), "Microbes on a bottle: Substrate, season and geography influence community composition of microbes colonizing marine plastic debris", edited by Carter, D.A.*PLoS ONE*, Public Library of Science, Vol. 11 No. 8, p. e0159289.
OECD. (2017), "Wild fisheries landings decline while aquaculture surges - OECD", *OECD*, available at: https://www.oecd.org/newsroom/wild-fisheries-landings-decline-while-aquaculture-surges.htm (accessed 25 February 2021).
OECD. (2020), *OECD-FAO Agricultural Outlook 2020-2029*, OECD, available at:https://doi.org/10.1787/1112c23b-en.
Ogola, J.S., Mitullah, W. V. and Omulo, M.A. (2002), "Impact of gold mining on the environment and human health: A case study in the Migori Gold Belt, Kenya", *Environmental Geochemistry and Health*, Springer Netherlands, Vol. 24 No. 2, pp. 141–157.
Ogonowski, M., Motiei, A., Ininbergs, K., Hell, E., Gerdes, Z., Udekwu, K.I., Bacsik, Z., et al. (2018), "Evidence for selective bacterial community structuring on microplastics", *Environmental Microbiology*, Blackwell Publishing Ltd, Vol. 20 No. 8, pp. 2796–2808.
Oguttu, H.W., Wb Bugenyi, F., Leuenberger, H., Wolf, M. and Bachofen, R. (2008), "Pollution menacing Lake Victoria: Quantification of point sources around Jinja Town, Uganda", available at: http://www.wrc.org.za (accessed 21 November 2019).
Ogutu-Ohwayo, R. (1990), "The decline of the native fishes of lakes Victoria and Kyoga (East Africa) and the impact of introduced species, especially the Nile perch, Lates niloticus, and the Nile tilapia, Oreochromis niloticus", *Environmental Biology of Fishes*, Kluwer Academic Publishers, Vol. 27 No. 2, pp. 81–96.
Onjong, H.A., Ngayo, M.O., Mwaniki, M., Wambui, J. and Njage, P.M.K. (2018), "Microbiological safety of fresh tilapia (Oreochromis niloticus) from kenyan fresh water fish value chains", *Journal of Food Protection*, International Association for Food Protection, Vol. 81 No. 12, pp. 1973–1981.
Outa, J.O., Kowenje, C.O., Avenant-Oldewage, A. and Jirsa, F. (2020), "Trace Elements in Crustaceans, Mollusks and Fish in the Kenyan Part of Lake Victoria: Bioaccumulation, Bioindication and Health Risk Analysis", *Archives of Environmental Contamination and Toxicology*, Springer, Vol. 78 No. 4, pp. 589–603.
Outa, N.O., Yongo, E.O., Keyombe, J.L.A., Ogello, E.O. and Namwaya Wanjala, D. (2020), "A review on the status of some major fish species in Lake Victoria and possible conservation strategies", *Lakes & Reservoirs: Research & Management*, Blackwell Publishing, Vol. 25 No. 1, pp. 105–111.
Papagiannis, I., Kagalou, I., Leonardos, J., Petridis, D. and Kalfakakou, V.

(2004), "Copper and zinc in four freshwater fish species from Lake Pamvotis (Greece)", *Environment International*, Elsevier Ltd, Vol. 30 No. 3, pp. 357–362.
Pearson, G., Barratt, C., Seeley, J., Ssetaala, A., Nabbagala, G. and Asiki, G. (2013), "Making a livelihood at the fish-landing site", available at:https://doi.org/10.1080/17531055.2013.841026.
Pennington, J. (2016), "Every minute, one garbage truck of plastic is dumped into our oceans. This has to stop | World Economic Forum", *World Economic Forum*, available at: https://www.weforum.org/agenda/2016/10/every-minute-one-garbage-truck-of-plastic-is-dumped-into-our-oceans/ (accessed 7 October 2019).
Phys.org. (2020), "Coronavirus masks, gloves polluting Europe's rivers", *Phys.Org*, available at: https://phys.org/news/2020-07-coronavirus-masks-gloves-polluting-europe.html (accessed 3 March 2021).
Picó, Y. and Barceló, D. (2019), "Analysis and prevention of microplastics pollution in water: Current perspectives and future directions", *ACS Omega*, American Chemical Society, Vol. 4 No. 4, pp. 6709–6719.
Pinheiro, C. (2017), "Occurrence and Impacts of Microplastics in Freshwater Fish", *Journal of Aquaculture & Marine Biology*, MedCrave Group, LLC, Vol. 5 No. 6, available at:https://doi.org/10.15406/jamb.2017.05.00138.
Pinto, M., Langer, T.M., Hüffer, T., Hofmann, T. and Herndl, G.J. (2019), "The composition of bacterial communities associated with plastic biofilms differs between different polymers and stages of biofilm succession", edited by Kelly, J.J.*PLoS ONE*, Public Library of Science, Vol. 14 No. 6, p. e0217165.
PlasticEurope. (2008), "PlasticEurope - What are plastics", *Association of Plastics Manufactures*, available at: https://www.plasticseurope.org/en/about-plastics/what-are-plastics (accessed 17 February 2021).
Popma, T. and Masser, M. (1999), "Tilapia Life History and Biology", *South Regional Aquaculture Center*, No. 283, pp. 1–4.
Poulíčková, A. and Manoylov, K. (2019), "Ecology of Freshwater Diatoms – Current Trends and Applications", *Diatoms: Fundamentals and Applications*, Wiley, pp. 289–309.
Powell, J.J., Thoree, V. and Pele, L.C. (2007), "Dietary microparticles and their impact on tolerance and immune responsiveness of the gastrointestinal tract", *British Journal of Nutrition*, Vol. 98, Europe PMC Funders, p. S59.
Prata, J.C., Silva, A.L.P., Walker, T.R., Duarte, A.C. and Rocha-Santos, T. (2020), "COVID-19 Pandemic Repercussions on the Use and Management of Plastics", *Environmental Science and Technology*, American Chemical Society, Vol. 54 No. 13, pp. 7760–7765.
Priester, J.H., Horst, A.M., Van De Werfhorst, L.C., Saleta, J.L., Mertes, L.A.K. and Holden, P.A. (2007), "Enhanced visualization of microbial biofilms by staining and environmental scanning electron microscopy", *Journal of Microbiological Methods*, Elsevier, Vol. 68 No. 3, pp. 577–587.
Pro, L. (2017), "Global Ban on Microbeads in Personal Care Products", *ChemSafetyPro*, available at: https://www.chemsafetypro.com/Topics/Restriction/Latest_Status_of_Global_Ban_on_Microbeads_in_Personal_Care_Products.html (accessed 19 November 2019).
Qi, R., Jones, D.L., Li, Z., Liu, Q. and Yan, C. (2020), "Behavior of microplastics and plastic film residues in the soil environment: A critical review", *Science of the Total Environment*, Elsevier B.V., 10 February.
Reisser, J., Shaw, J., Hallegraeff, G., Proietti, M., Barnes, D.K.A., Thums, M.,

Wilcox, C., et al. (2014), "Millimeter-Sized Marine Plastics: A New Pelagic Habitat for Microorganisms and Invertebrates", edited by Ianora, A.*PLoS ONE*, Public Library of Science, Vol. 9 No. 6, p. e100289.
Roberts, G. (2018), "174,000 tonnes of plastic packaging lost annually in Kenyan environment | Resource Magazine", *Resource*, available at: https://resource.co/article/174000-tonnes-plastic-packaging-lost-annually-kenyan-environment-12693 (accessed 22 February 2021).
Roch, S., Friedrich, C. and Brinker, A. (2020), "Uptake routes of microplastics in fishes: practical and theoretical approaches to test existing theories", *Scientific Reports*, Nature Research, Vol. 10 No. 1, available at:https://doi.org/10.1038/s41598-020-60630-1.
Rochman, C.M., Hoh, E., Kurobe, T. and Teh, S.J. (2013), "Ingested plastic transfers hazardous chemicals to fish and induces hepatic stress", *Scientific Reports*, Nature Publishing Group, Vol. 3 No. 1, pp. 1–7.
Roman Lehner. (2015), "Macro-, Meso-, Micro-, but What About Nanoplastic? - Planet Experts", pp. 1–4.
Rosato, D. and Rosato, M. (2004), "Reinforced Plastics - an overview | ScienceDirect Topics", *Plastic Product Material and Process Selection Handbook*, available at: https://www.sciencedirect.com/topics/materials-science/reinforced-plastics (accessed 18 February 2021).
Ruiz-Grossman, S. and Dahlen, D. (2017), "Heartbreaking Photos Show What Your Trash Does To Animals | HuffPost UK", *HuffPost US*, available at: https://www.huffingtonpost.co.uk/entry/plastic-trash-animals-photos_n_58ee9ec1e4b0b9e984891ddf?ri18n=true (accessed 17 February 2021).
Rummel, C.D., Jahnke, A., Gorokhova, E., Kühnel, D. and Schmitt-Jansen, M. (2017), "Impacts of biofilm formation on the fate and potential effects of microplastic in the aquatic environment", *Environmental Science and Technology Letters*, American Chemical Society, 1 July.
De Sales-Ribeiro, C., Brito-Casillas, Y., Fernandez, A. and Caballero, M.J. (2020), "An end to the controversy over the microscopic detection and effects of pristine microplastics in fish organs", *Scientific Reports*, Nature Research, Vol. 10 No. 1, p. 12434.
Sastri, V. (2014), "Heat Stabiliser - an overview | ScienceDirect Topics", *Plastics in Medical Devices (Second Edition)*, available at: https://www.sciencedirect.com/topics/engineering/heat-stabiliser (accessed 18 February 2021).
Savoca, M.S., Tyson, C.W., McGill, M. and Slager, C.J. (2017), "Odours from marine plastic debris induce food search behaviours in a forage fish", *Proceedings of the Royal Society B: Biological Sciences*, Royal Society Publishing, Vol. 284 No. 1860, p. 20171000.
Scheren, P.A.G.M., Zanting, H.A. and Lemmens, A.M.C. (2000), "Estimation of water pollution sources in Lake Victoria, East Africa: Application and elaboration of the rapid assessment methodology", *Journal of Environmental Management*, Academic Press, Vol. 58 No. 4, pp. 235–248.
Schlundt, C., Mark Welch, J.L., Knochel, A.M., Zettler, E.R. and Amaral-Zettler, L.A. (2019), "Spatial structure in the 'Plastisphere': Molecular resources for imaging microscopic communities on plastic marine debris", *Molecular Ecology Resources*, Blackwell Publishing Ltd, Vol. 20 No. 3, pp. 620–634.
Schneeberger, P.H.H., Fuhrimann, S., Becker, S.L., Pothier, J.F., Duffy, B., Beuret, C., Frey, J.E., et al. (2019), "Qualitative microbiome profiling along a wastewater system in Kampala, Uganda", *Scientific Reports*, Nature

Research, Vol. 9 No. 1, available at:https://doi.org/10.1038/s41598-019-53569-5.
Sewage, S.A. (2019), "Plastic Pollution - Facts and Figures • Surfers Against Sewage", available at: https://www.sas.org.uk/our-work/plastic-pollution/plastic-pollution-facts-figures/ (accessed 7 October 2019).
Shah, S.N.A., Shah, Z., Hussain, M. and Khan, M. (2017), "Hazardous Effects of Titanium Dioxide Nanoparticles in Ecosystem", *Bioinorganic Chemistry and Applications*, available at:https://doi.org/10.1155/2017/4101735.
Shahbandeh, M. (2020), "• Global seafood market value forecast, 2019-2027 | Statista", *Statista*, available at: https://www.statista.com/statistics/821023/global-seafood-market-value/ (accessed 19 March 2021).
Shamseer Mambra. (2019), "How Is Plastic Totally Ruining The Oceans In The Worst Way Possible?", *Marine Insight*, available at: https://www.marineinsight.com/environment/how-is-plastic-ruining-the-ocean/ (accessed 5 November 2019).
Sibanda, L.K., Obange, N. and Awuor, F.O. (2017), "Challenges of Solid Waste Management in Kisumu, Kenya", *Urban Forum*, Springer Netherlands, Vol. 28 No. 4, pp. 387–402.
Sifuna, A. and Onyango, D. (2018), "Source Attribution of Salmonella and Escherichia coli Contaminating Lake Victoria fish in Kenya", *Researchgate*, available at: https://www.researchgate.net/publication/324803765_Source_Attribution_of_Salmonella_and_Escherichia_coli_Contaminating_Lake_Victoria_fish_in_Kenya (accessed 19 March 2021).
Sigma-Aldrich. (2020), "Whatman® glass microfiber filters, Grade GF/B Grade GF/B circles, 25 mm, 100/pk | glass fiber filters | Sigma-Aldrich", available at: https://www.sigmaaldrich.com/catalog/product/aldrich/wha1820047?lang=en&region=GB (accessed 23 March 2021).
Sireyjol Trucost, A., Georgieva Trucost, A., Wainwright Trucost, S., Haridwaj Trucost, A., Joshi Trucost, S., Bullock Trucost, S., Huang Trucost, C., et al. (2014), *Valuing Plastics: The Business Case for Measuring, Managing and Disclosing Plastic Use in the Consumer Goods Industry*, available at: www.gpa.unep.org (accessed 23 February 2021).
Sitoki, L., Kurmayer, R. and Rott, E. (2012), "Spatial variation of phytoplankton composition, biovolume, and resulting microcystin concentrations in the Nyanza Gulf (Lake Victoria, Kenya)", *Hydrobiologia*, Springer, Vol. 691 No. 1, pp. 109–122.
SPC. (2020), "Plating on Plastics | Plastic Electroplating Process | SPC", *SPC*, available at: https://www.sharrettsplating.com/base-materials/plastics (accessed 19 March 2021).
SpecialChem. (2018), "Pigments for Plastic Colorants: Types, Properties & Processing Guide", available at: https://polymer-additives.specialchem.com/selection-guide/pigments-for-plastics (accessed 18 February 2021).
Stager, J.C., Hecky, R.E., Grzesik, D., Cumming, B.F. and Kling, H. (2009), "Diatom evidence for the timing and causes of eutrophication in lake victoria, east africa", *Hydrobiologia*, Kluwer Academic Publishers, Vol. 636 No. 1, pp. 463–478.
Stanton, T., Johnson, M., Nathanail, P., Gomes, R.L., Needham, T. and Burson, A. (2019), "Exploring the Efficacy of Nile Red in Microplastic Quantification:

A Costaining Approach", available at:https://doi.org/10.1021/acs.estlett.9b00499.
Steinberg, R.M., Walker, D.M., Juenger, T.E., Woller, M.J. and Gore, A.C. (2008), "Effects of perinatal polychlorinated biphenyls on adult female rat reproduction: Development, reproductive physiology, and second generational effects", *Biology of Reproduction*, NIH Public Access, Vol. 78 No. 6, pp. 1091–1101.
Tabor, S. and Richardson, C.C. (1987), *DNA Sequence Analysis with a Modified Bacteriophage T7 DNA Polymerase (DNA Polymerase I/Reverse Transcriptase/Chain-Terminating Inhibitors/2'-Deoxyinosine 5'-Triphosphate/Processivity)*, *Biochemistry*, Vol. 84.
Tall, A. (2015), "Fish trade in Africa an update GLOBEFISH Food and Agriculture Organization of the United Nations", available at: http://www.fao.org/in-action/globefish/fishery-information/resource-detail/en/c/338418/ (accessed 1 March 2021).
Tanaka, K. and Takada, H. (2016), "Microplastic fragments and microbeads in digestive tracts of planktivorous fish from urban coastal waters", *Scientific Reports*, Nature Publishing Group, Vol. 6 No. 1, pp. 1–8.
De Tender, C., Schlundt, C., Devriese, L.I., Mincer, T.J., Zettler, E.R. and Amaral-Zettler, L.A. (2017), "A review of microscopy and comparative molecular-based methods to characterize 'Plastisphere' communities", *Analytical Methods*.
The Guardian. (2019), "Dumped fishing gear is biggest plastic polluter in ocean, finds report | Environment | The Guardian", *The Guardian*, available at: https://www.theguardian.com/environment/2019/nov/06/dumped-fishing-gear-is-biggest-plastic-polluter-in-ocean-finds-report (accessed 7 April 2021).
Thiele, C.J., Hudson, M.D. and Russell, A.E. (2019), "Evaluation of existing methods to extract microplastics from bivalve tissue: Adapted KOH digestion protocol improves filtration at single-digit pore size", *Marine Pollution Bulletin*, Elsevier Ltd, pp. 384–393.
Thompson, R.C., Olson, Y., Mitchell, R.P., Davis, A., Rowland, S.J., John, A.W.G., McGonigle, D., et al. (2004), "Lost at Sea: Where Is All the Plastic?", *Science*, Vol. 304 No. 5672, p. 838.
Tolinski, M. (2015), "Colourants - an overview | ScienceDirect Topics", *Additives for Polyolefins (Second Edition)*, available at: https://www.sciencedirect.com/topics/engineering/colourants (accessed 18 February 2021).
Triest, L., Lung'ayia, H., Ndiritu, G. and Beyene, A. (2012), "Epilithic diatoms as indicators in tropical African rivers (Lake Victoria catchment)", *Hydrobiologia*, Springer, Vol. 695 No. 1, pp. 343–360.
Turner, A. and Filella, M. (2020a), "The influence of additives on the fate of plastics in the marine environment, exemplified with barium sulphate", *Marine Pollution Bulletin*, Elsevier Ltd, Vol. 158, p. 111352.
Turner, A. and Filella, M. (2020b), "The influence of additives on the fate of plastics in the marine environment, exemplified with barium sulphate", *Marine Pollution Bulletin*, Elsevier Ltd, Vol. 158, available at:https://doi.org/10.1016/j.marpolbul.2020.111352.
US Department of Commerce, N.O. and A.A. (2020), "What is aquaculture?", *National Ocean Service*.
Volkheimer, G. (1975), "HEMATOGENOUS DISSEMINATION OF INGESTED POLYVINYL CHLORIDE PARTICLES", *Annals of the New York Academy of*

Sciences, Ann N Y Acad Sci, Vol. 246 No. 1, pp. 164–171.
Vrede, K., Heldal, M., Norland, S. and Bratbak, G. (2002), "Elemental composition (C, N, P) and cell volume of exponentially growing and nutrient-limited bacterioplankton", *Applied and Environmental Microbiology*, American Society for Microbiology (ASM), Vol. 68 No. 6, pp. 2965–2971.
Wagner, J., Wang, Z.M., Ghosal, S., Rochman, C., Gassel, M. and Wall, S. (2017), "Novel method for the extraction and identification of microplastics in ocean trawl and fish gut matrices", *Analytical Methods*, Royal Society of Chemistry, Vol. 9 No. 9, pp. 1479–1490.
Waiganjo, C. (2020), "Implementation and Enforcement of the Single-Use Plastic Ban in Kenya | Africa Up Close", *Africa Up Close*, available at: https://africaupclose.wilsoncenter.org/implementation-and-enforcement-of-the-single-use-plastic-ban-in-kenya/ (accessed 19 March 2021).
Wang, Z.M., Wagner, J., Ghosal, S., Bedi, G. and Wall, S. (2017a), "SEM/EDS and optical microscopy analyses of microplastics in ocean trawl and fish guts", *Science of the Total Environment*, Elsevier B.V., Vol. 603–604, pp. 616–626.
Wang, Z.M., Wagner, J., Ghosal, S., Bedi, G. and Wall, S. (2017b), "SEM/EDS and optical microscopy analyses of microplastics in ocean trawl and fish guts", *Science of the Total Environment*, Elsevier B.V., Vol. 603–604, pp. 616–626.
Watts, A.J.R., Urbina, M.A., Goodhead, R., Moger, J., Lewis, C. and Galloway, T.S. (2016), "Effect of Microplastic on the Gills of the Shore Crab Carcinus maenas", *Environmental Science and Technology*, American Chemical Society, Vol. 50 No. 10, pp. 5364–5369.
Welcomme, R. and Lymer, D. (2012), "AN AUDIT OF INLAND CAPTURE FISHERY STATISTICS-AFRICA", *FAO*, available at: www.fao.org/icatalog/inter-e.htm (accessed 25 February 2021).
WHO. (215AD), *Healthy Diet*, available at: http://www.who.int/mediacentre/factsheets/fs394/en/ (accessed 9 April 2021).
WHO. (2019), "WHO | Information sheet: Microplastics in drinking-water", *WHO*, World Health Organization, available at: http://www.who.int/water_sanitation_health/water-quality/guidelines/microplastics-in-dw-information-sheet/en/ (accessed 25 February 2021).
Williams, A.E., Hecky, R.E. and Duthie, H.C. (2007), "Water hyacinth decline across Lake Victoria-Was it caused by climatic perturbation or biological control? A reply", *Aquatic Botany*, Vol. 87 No. 1, pp. 94–96.
Williams, L. (2019), "Everything you need to know about microplastics - Discover Wildlife", *Discover Wildlife*, available at: https://www.discoverwildlife.com/people/facts-about-microplastics/ (accessed 7 November 2019).
World Animal Protection. (2018), "To stop the deaths of countless marine animals, we need to tag fishing gear | World Animal Protection International", *World Animal Protection*, available at: https://www.worldanimalprotection.org/news/stop-deaths-countless-marine-animals-we-need-tag-fishing-gear (accessed 19 November 2019).
Wright, R.J., Langille, M.G.I. and Walker, T.R. (2020), "Food or just a free ride? A meta-analysis reveals the global diversity of the Plastisphere", *ISME Journal*, Springer Nature, Vol. 15 No. 3, pp. 789–806.
Wright, S.L. and Kelly, F.J. (2017), "Plastic and Human Health: A Micro Issue?",

Environmental Science and Technology, American Chemical Society, Vol. 51 No. 12, pp. 6634–6647.
WWF. (2020), "Sustainable Seafood | Industries | WWF", *WWF*, available at: https://www.worldwildlife.org/industries/sustainable-seafood (accessed 4 March 2021).
Xanthos, D. and Walker, T.R. (2017), "International policies to reduce plastic marine pollution from single-use plastics (plastic bags and microbeads): A review", *Marine Pollution Bulletin*, Elsevier Ltd, 15 May.
Xue, B., Zhang, L., Li, R., Wang, Y., Guo, J., Yu, K. and Wang, S. (2020), "Underestimated Microplastic Pollution Derived from Fishery Activities and 'Hidden' in Deep Sediment", *Environmental Science and Technology*, American Chemical Society, Vol. 54 No. 4, pp. 2210–2217.
Yang, Y., Liu, G., Song, W., Ye, C., Lin, H., Li, Z. and Liu, W. (2019), "Plastics in the marine environment are reservoirs for antibiotic and metal resistance genes", *Environment International*, Elsevier Ltd, Vol. 123, pp. 79–86.
Yoo, J.W., Doshi, N. and Mitragotri, S. (2011), "Adaptive micro and nanoparticles: Temporal control over carrier properties to facilitate drug delivery", *Advanced Drug Delivery Reviews*, Elsevier, 1 November.
Yue, G.H., Jiale, L. and Jiale, J. (2016), "Tilapia is the Fish for Next-Generation Aquaculture Molecular Breeding of Sugarcane View project graphene fabrication View project", available at:https://doi.org/10.19070/2577-4395-160003.
Zettler, E.R., Mincer, T.J. and Amaral-Zettler, L.A. (2013), "Life in the 'plastisphere': Microbial communities on plastic marine debris", *Environmental Science and Technology*, Vol. 47 No. 13, pp. 7137–7146.
Zubris, K.A. V. and Richards, B.K. (2005), "Synthetic fibers as an indicator of land application of sludge", *Environmental Pollution*, Elsevier, Vol. 138 No. 2, pp. 201–211.

6.0 Appendix

MUSCLE ID	WHOLE WEIGHT (g)	SAMPLE WEIGHT (g)
Ta1	3.07	1.53
Ta2	7.59	0.98
Ta3	12.85	2.27
Ta4	37.53	1.44
Ta5	29.23	2.8
Ta6	18.92	2.04
Ta7	7.92	2.16
Ta8	3.23	0.77
Ta9	28.71	1.7
Ta10	32.06	2.03
Ta11	12.8	2.59
Ta12	54.17	1.88
Ta13	62.56	2.4
Ta14	25.18	2.24
Ta15	19.2	2.61
Ta16	14.49	1.76
Ta17	40.23	1.65
Ta18	17.74	2.37
Ta19	33.37	1.8
Ta20	6.44	1.73
Ta21	10.61	1.52
Ta22	12.6	1.4
Ta23	38.89	1.9
Ta24	17.38	2.09
Ta25	21.49	1.72
Ta26	28.58	2.15
Ta27	28.19	2.91
Ta28	5.42	1.03
Ta29	18.81	1.68
Ta30	37.71	2.86
Ta31	35.71	1.82
Ta32	35.97	2.52

Table 1 Tilapia muscle sample weights. This table shows all the sample weights (g) of the tilapia muscle samples used in this study, as well as the whole weight (g) of the muscle fillet. The sample ID of the muscle is shown (Ta).

Ta33	17.29	2.44
Ta34	12.91	2.3
Ta35	16.73	2.04
Ta36	19.67	2.41
Ta37	43.27	2.12
Ta38	9.71	1.56
Ta39	12.4	1.96
Ta40	15.37	2.32
Ta41	17.7	1.04
Ta42	12.22	1.86
Ta43	14.8	1.52
Ta44	16.58	2.68
Ta45	16.02	1.65
Ta46	15.03	1.93
Ta47	4.05	1.22
Ta48	3.91	1.08
Ta49	5.06	0.83
Ta50	5.97	2
Ta51	2.31	1.16
Ta52	14.11	2
Ta53	19.64	1.52
Ta54	15.92	1.26
Ta55	6.2	1.24
Ta56	8.39	2.5
Ta57	3.66	1.19
Ta58	4.53	1.08
Ta59	7.52	2.29
Ta60	1.56	0.81
Ta61	33.45	2.65
Ta62	45.59	1.5
Ta63	49	2.51
Ta64	33.85	3.05
Ta65	34.37	3.05
Ta66	34.8	2.98
Ta67	29.35	2.6

Table 1 (continued) Tilapia muscle sample weights. This table shows all the sample weights (g) of the tilapia muscle samples used in this study, as well as the whole weight (g) of the muscle fillet. The sample ID of the muscle is shown (Ta).

Ta68	26.25	2.14
Ta69	39.49	2.71
Ta70	29.98	2.62
Ta71	31.94	5.36
Ta72	51.33	3.48
Ta73	38.47	3.32
Ta74	15.58	2.81
Ta75	15.65	2.31
Ta76	42.83	2.51
Ta77	32.62	3.57
Ta78	32.07	3.2
Ta79	62.45	3.2
Ta80	63.2	2.13

Table 1 (continued) Tilapia muscle sample weights. This table shows all the sample weights (g) of the tilapia muscle samples used in this study, as well as the whole weight (g) of the muscle fillet. The sample ID of the muscle is shown (Ta).

GIT ID	1st WEIGHT (g)	2nd WEIGHT (g)	SAMPLE WEIGHT (g)
GI1	6.24	2.23	**4.01**
GI2	5.26	2.22	**3.04**
GI3	5.18	2.07	**3.11**
GI4	4.20	2.44	**1.76**
GI5	2.28	2.55	**0.27**
GIT6	4.14	0.78	**3.36**
GIT7	4.10	0.94	**3.16**
GIT10	5.90	0.85	**5.05**
GIT13	4.50	0.79	**3.71**
GIT15	7.51	0.64	**6.87**
GIT19	14.05	0.74	**13.31**

Table 2 Tilapia gastrointestinal tract and contents weights. This table shows all the sample weights (g) of the tilapia gastrointestinal tract contents (GI) and intact gastrointestinal tracts (GIT) used in this study. The 1st weight (g) represents the weight of the sample and the bag it was contained in and the 2nd weight (g) represents the empty bag. The final sample weight was determined by subtracting the two recorded weights.

MACROPLASTIC TYPE	SAMPLE LENGTH (mm)	SAMPLE WEIGHT (g)
NET - BLUE	60	0.17
NET - YELLOW	48	0.13
NET - GREEN	Mixture of lengths	0.13
NET - WHITE	42	0.01
FACEWASH BEADS	2	0.03

Table 3 Macroplastic litter and facewash beads weights. This table shows all the sample lengths (mm) and sample weights (g) for the different coloured macroplastic net strands found in Lake Victoria and the microbeads extracted from the facewash, used as positive controls in this study.